

Caractérisation des mécanismes d'ADP- ribosylation de l'ADN et son rôle dans la signalisation des dommages à l'ADN

Thèse de doctorat de l'université Paris-Saclay

École doctorale n°582 CBMS
Cancérologie: Biologie Médecine – Santé
Aspects moléculaires et cellulaires de la biologie
Université Paris-Saclay, Institut Gustave Roussy, CNRS, Stabilité
génétique et oncogenèse, 94805, Villejuif, France.
Faculté de médecine

**Thèse présentée et soutenue à Villejuif,
le 06/03/2020, par**

M. Elie MATTA

Composition du Jury

Mme. Svetlana DOKUDOVSKAYA DR, IGR (UMR8126 CNRS)	Présidente
M. Sébastien HUET MCU, HDR (UMR6290 CNRS)	Rapporteur
M. Didier GASPARUTTO DR, INAC – SyMMES, CEA Grenoble (UMR 5819 CEA CNRS UGA)	Rapporteur
M. Jean-Baptiste CHARBONNIER DR, IBiTec, CEA Saclay (UMR9198)	Examineur
Mme. Mounira AMOR-GUERET DR, UPMC (UMR 3348 CNRS)	Examinatrice
M. Alexander ISHCENKO DR, IGR (UMR8200 CNRS)	Directeur de thèse
Mme. Mira MAALOUF PhD, ULFS2 (LIT)	Co-directrice de thèse

AKNOWLEDGEMENT

This work was carried out between January 2017 and January 2020 within the team 'DNA repair'-CNRS-UMR8200 'Genetic stability and oncogenesis, University of Paris-Sud, under the supervision of Dr. Alexander ISHCENKO.

I would like to convey my extreme gratitude to Dr. Alexander ISHCENKO for the great opportunity he gave me to work in his group on an extremely challenging and interesting project, for giving me the opportunity of independent working, for his advices and guidance throughout my research work. Thank you for trusting me; this experience has incredibly enriched me as a scientist as well as a person. As well, to my co-director Dr. MAALOUF Mira for her advices and support.

I have been a member of the DNA repair team for over three years. My time in this lab has provided me with knowledge and experience that will serve me in both professional and personal endeavors. I would like to thank all past and present members of the DNA repair team for their continuous support, help and teachings. I would like to express a special thanks to Gabriella ZARKOVIC, Caroline ZUTTERLING, Milena BAZLEKOWA, Murat SAPARBAEV (kuchet at 11:30), Regina GROISMAN, Peter MARTIN, Sabira TAIPAKOVA who greeted me on my arrival, to my big brother Haser SUTCU (for all the alcohol we drunk together), to Umit ALIYASKAROVA, Aigerim KUNBAI, Aibek MURSALIMOV, Zhiger AKISHEV and Assel KIRIBAYEVA.

In addition, I acknowledge the members of my thesis committee, Dr. DOKUDOVSKEYA Svetlana, Dr. AMOR-GUERET Mounira, Dr. CHARBONNIER Jean-Baptiste, Dr. GASPARUTTO Didier and Dr. HUET Sébastien for supporting this work with productive input, discussions and ideas.

I will never forget to thank our small Lebanese IGR community, especially Tracy DAGHER, Desiree TANNOUS, Huissein GHAMLOUCH, Carla DIB, Rawan AI AMINE, Johnny FAKHRY, and my big family in Fondation Maison du Liban.

Finally, I want to make it clear that I would not have gotten this far without the unconditional support of my family. Since the start of my schooling, I have been able to benefit from their assistance and encouragement which enabled me to advance and grow, and I thank them with love for that. And to my love and support Vanessa BOU MALHAM.

To all of you and all those I may have forgotten: Thank you !



ABSTRACT

DNA-dependent poly(ADP-ribose) polymerases (PARPs) PARP1, PARP2 and PARP3 act as DNA break sensors signaling DNA damage. Upon detecting DNA damage, these PARPs use nicotine adenine dinucleotide as a substrate to synthesize a monomer or polymer of ADP-ribose (MAR or PAR, respectively) covalently attached to the acceptor residue of target proteins. Recently, it was demonstrated that PARP1–3 proteins can directly ADP-ribosylate DNA breaks by attaching MAR and PAR moieties to terminal phosphates. Nevertheless, little is still known about the mechanisms governing substrate recognition and specificity of PARP1, which accounts for most of cellular PARylation activity, as well, about proteins responsible for detection and removal of ADP-ribosylated DNA adducts and its role in multitude of cellular processes. In this study we provide a detailed characterization of PARP1 DNA substrate specificity and mechanisms of DNA PARylation. We showed that the 3'-terminal phosphate residue at double-strand DNA break ends served as a major acceptor site for PARP1-catalysed PARylation depending on the orientation and distance between DNA strand breaks in a single DNA molecule. Moreover, a preference for ADP-ribosylation of DNA molecules containing 3'-terminal phosphate over PARP1 auto-ADP-ribosylation was observed, and a model of DNA modification by PARP1 was proposed. Similar results were obtained with purified recombinant PARP1 and HeLa cell-free extracts. Thus, the biological effects of PARP-mediated ADP-ribosylation may strongly depend on the configuration of complex DNA strand breaks. Furthermore, we elaborated a new research technique to identify and validate proteins responsible for ADP-ribose-DNA adducts detection ("readers") or removal ("erasers"). Our proteomic data revealed that MARylated DNA adducts selectively modulated DNA recognition of a large number of proteins involved in different cellular pathways. About 90 proteins including protein complexes were selected as potential MAR-DNA adduct readers. The role of DNA ADP-ribosylation in non-homologous end-joining (NHEJ) was partially characterized in an *in vitro* study. We demonstrated that ADP-ribosylation of DSB terminus can lead to inhibition of blunt DSB repair by canonical NHEJ if not removed by PARG glycohydrolase. Contrary, presence of a proximal nick with a stabilized apurinic/apyrimidinic site leads to increased NHEJ efficiency, apparently in ADP-ribosylation-independent manner. Finally we searched for novel PARP1, PARP2 and PARP3 inhibitors among derivatives of 1,4-dihydropyridine with DNA binding capacity. Our results revealed that some of NAD⁺ analogues analogs could be used by PARPs for DNA modification leading to stabilization of corresponding MARylated and PARylated adducts due to their PARG hydrolysis activity resistance. Taking together, these data highlight the physiological relevance and possible biological outcomes of PARP-catalyzed DNA-ADP-ribosylation such as providing a stable benchmark of the location of a DNA strand break on a chromatin map, recruitment of DNA repair proteins and inhibition of the toxic NHEJ.



RESUME

Les poly (ADP-ribose) polymérasés dépendants de l'ADN (PARPs) PARP1, PARP2 et PARP3 agissent comme des détecteurs de cassures d'ADN signalant des dommages à l'ADN. Lors de la détection des dommages à l'ADN, ces PARPs utilisent le nicotinamide adénine dinucléotide comme substrat pour synthétiser un monomère ou un polymère d'ADP-ribose (MAR ou PAR, respectivement) attaché de manière covalente au résidu accepteur des protéines cibles. Récemment, il a été démontré que les protéines PARP1–3 peuvent directement ADP-ribosyler les cassures d'ADN en attachant les oligomères MAR et PAR aux phosphates terminaux.

Néanmoins, peu de choses sont connues sur les mécanismes régissant la reconnaissance et la spécificité du substrat de PARP1, qui représente la majeure partie de l'activité de PARylation cellulaire, ainsi que sur les protéines responsables de la détection et de l'élimination des adduits d'ADN ADP-ribosylés et son rôle dans une multitude de processus cellulaires. Dans cette étude, nous avons caractérisé de manière détaillée la spécificité du substrat (ADN) de PARP1 et des mécanismes de la PARylation de l'ADN. Nous avons montré que le résidu phosphate 3'-terminal aux extrémités des cassures de l'ADN double brin servait de site accepteur majeur pour la PARylation catalysée par PARP1 en fonction de l'orientation et de la distance entre les cassures du brin d'ADN dans une seule molécule d'ADN. De plus, une préférence pour l'ADP-ribosylation des molécules d'ADN contenant du phosphate 3'-terminal a été observée par rapport à l'auto-ADP-ribosylation de PARP1, et un modèle de modification de l'ADN par PARP1 a été proposé. Des résultats similaires ont été observés avec l'enzyme PARP1 recombinante purifiée et des extraits provenant des cellules HeLa. Ainsi, les effets biologiques de l'ADP-ribosylation médiée par PARP peuvent dépendre fortement de la configuration des cassures complexes des brins d'ADN. De plus, nous avons élaboré une nouvelle approche permettant d'identifier et valider les protéines responsables de la détection («readers») ou de l'élimination («erasers») des adduits ADN-ADP-ribose. Nos données protéomiques ont révélé que les adduits de l'ADN MARylé modulaient sélectivement la reconnaissance de l'ADN par un grand nombre de protéines impliquées dans différentes voies de signalisation cellulaire. Environ 90 protéines, y compris des complexes protéiques, ont été sélectionnées comme lecteurs («readers») potentiels d'adduits ADN-MARylé. Le rôle de l'ADP-ribosylation de l'ADN dans la jonction d'extrémités non homologues (NHEJ) a été partiellement caractérisé dans une étude *in vitro*. Nous avons démontré que l'ADP-ribosylation de l'extrémité de la cassure double brin («DSB») peut conduire à l'inhibition de la réparation de la DSB bout franc par la voie NHEJ canonique si elle n'est pas éliminée par la glycohydrolase PARG. Au contraire, la présence d'une coupure («nick») proximale avec un site apurinique / apyrimidinique stabilisé conduit à une efficacité NHEJ accrue, apparemment de manière indépendante de l'ADP-ribosylation. Enfin, nous avons recherché de nouveaux inhibiteurs de PARP1, PARP2 et PARP3 parmi les dérivés de 1,4-dihydropyridine, ayant une capacité de liaison à l'ADN. Nos résultats ont révélé que certains analogues de NAD⁺ pourraient être utilisés par les PARPs pour la modification de l'ADN conduisant à la stabilisation des adduits MARylés et PARylés correspondants, en raison de leur résistance à l'activité d'hydrolyse des PARG. Ensemble, ces données mettent en évidence la pertinence physiologique et les résultats biologiques possibles de l'ADP-ribosylation de l'ADN catalysée par les protéines PARPs, tels que la fourniture d'une référence stable de l'emplacement d'une cassure du brin d'ADN sur une carte de chromatine, le recrutement de protéines de réparation de l'ADN et l'inhibition du mécanisme NHEJ toxique.



SUMMARY

ACKNOWLEDGEMENT	2
ABSTRACT	3
RESUME	4
SUMMARY	5
LIST OF FIGURES	7
LIST OF TABLES	9
ABBREVIATIONS	10
INTRODUCTION	14
I. CONTEXT	14
II. DNA DAMAGE RESPONSE AND GENOMIC INSTABILITY	16
III. SYNTHESIS OF POLY(ADP-RIBOSE) POLYMER AND ADP-RIBOSYLTRANSFERASES	24
IV. THE POLY(ADP-RIBOSE) POLYMERASE (PARP) FAMILY	28
V. PROTEIN ACCEPTORS FOR (ADP-RIBOSYL)ATION	36
VI. ACTIVATION OF DNA DEPENDENT PARPs	37
VII. PARPs ACTIVATION AND INHIBITION VIA DNA INDEPENDENT PATHWAYS	38
VIII. READERS OF (ADP-RIBOSYL)ATED TARGETS	40
IX. REVERSIBLE (ADP-RIBOSYL)ATION OF DNA STRAND BREAKS	45
X. (ADP-RIBOSE) removal from PROTEINS AND DNA BREAKS	49
GOALS	57
MATERIALS AND METHODS	58
RESULTS	71
Chapter I: Insight into DNA substrate specificity of PARP1-catalysed DNA poly(ADP-ribose)ation	71
Chapter II: Identification of MAR Readers in Cell-free Extracts	83
Chapter III: Impact of DNA ADP-ribosylation on NHEJ	99
Chapter IV: Search for novel PARP1 and PARP2 inhibitors among derivatives of 1,4-dihydropyridine with DNA binding capacity	105
CONCLUSION	109
DISCUSSION AND PERSPECTIVES	110
REFERENCES	119
APENDIX	130





LIST OF FIGURES

Figure 1: An overview of substrates, sites and products of ADP-ribosyltransferases.	15
Figure 2: Schematic of various DNA damage-induced DNA repair pathways	18
Figure 3: Five DNA repair pathways.....	23
Figure 4: Possible patterns of ADP-ribosylation on target proteins.	24
Figure 5: ADP-ribose moieties synthesis and attachment on acceptor sites of target proteins by PARPs enzymes.	25
Figure 6: Ribbon representation of the conserved NAD ⁺ binding core of ARTs.	27
Figure 7: Schematic domain architecture of the seventeen members of human PARP superfamily. Adapted from <i>E.Barkauskaite et. al., 2005</i>	32
Figure 8: Schematic representation of the PARP family localization and function. PARPs have been linked to nearly all major cellular processes.	35
Figure 9: Schematic of protein ADP-ribosylation and binding specificities of the various domains that recognize the different parts of the modification.	44
Figure 10: The mechanism of DNA-ADP-ribosylation and DNA substrate specificity of the PARP2 and PARP3 proteins.	48
Figure 11: Reversal of protein ADP-ribosylation by MAR and PAR erasers.	51
Figure 12: Schematic domain architecture of human ADP-Ribosylation removing enzymes.	55
Figure 13: Biotinylated unmodified or MARYlated ss/ds oligonucleotides and peptides bounded to Streptavidin Mag sepharose beads.	66
Figure 14: NHEJ reconstitution of DSB repair using different oligonucleotides structures and purified proteins. B: biotin, PAGE: Polyacrylamide gel electrophoresis.	67
Figure 15: Series of NAD analogues structures (<i>BIOLOG Life Science Institute</i>).	67
Figure 16: Effects of the type and size of protruding ends in Dbait-based DNA structures containing a 1-nt gap on the PARP1-catalysed formation of PAR–DNA adducts.	72
Figure 17: ADP-ribosylation of S1 ⁿ DNA duplexes containing 5'-otherhangs by PARP1 at a non-saturating concentration of NAD ⁺	73
Figure 18: PARP1 DNA PARylation activity in presence of HPF1.	74
Figure 19: PARP1-catalysed PARylation of S2 ⁿ DNA structures with a 3'-phosphate terminus at the DSB end.	75
Figure 20: Gap–DSB distance dependence of PARP1-catalysed PARylation of the 3' phosphate at a DSB end of DNA duplexes.....	77
Figure 21: Validation of PARP1-dependent PARylation of 3'-phosphorylated DSB termini of DNA substrates S2 and S10-13 by CIP-induced dephosphorylation.....	78
Figure 22: The monomeric mode of PARP1 binding to DNA molecules prone to PARylation.....	79
Figure 23: Comparison of the efficiency of PARP1-catalysed auto- and DNA ADP-ribosylation. ..	80
Figure 24: Formation of PAR–3' phosphate–DNA adducts in nuclear extracts from HeLa PARGKD cells.	82
Figure 25: Verification of the presence of bound proteins on MARYlated ssDNA and dsDNA substrates by Silver Staining after SDS PAGE.	84
Figure 26: Volcano plot illustrates significantly differentially abundant proteins in samples purified on MAR-dsDNA beads.....	85
Figure 27: Protein–protein interaction network of 77 proteins enriched on MAR-dsDNA as compared to unmodified dsDNA based on “String v.11” database.....	86



Figure 28: Volcano plots illustrates significantly differentially abundant proteins in P[MAR-ssDNA] versus P[ssDNA].	87
Figure 29: Interaction network of proteins enriched on MAR-ssDNA as compared to unmodified ssDNA.	87
Figure 30: Verification of the MAR presence in used peptides by blotting technic.	88
Figure 31: A. Verification of the presence of bound proteins on MARYlated-peptide samples SDS PAGE. B. Volcano plots illustrates significantly differentially abundant proteins in P[MAR-peptide] versus P[peptide]. The fold change is determined by the P[MAR-peptide]/P[peptide] ratio.	89
Figure 32: Interaction network of proteins enriched on MAR-peptide as compared to unmodified-peptide.	89
Figure 33: CLPB domain organization according to SMART.	91
Figure 34: IMPDH2 domain organization according to SMART.	91
Figure 35: Enrichment of IMPDH2 40 times on MARYlated versus unmodified single-stranded DNA.	96
Figure 36: Enrichment of RPA (1.35 times) on MARYlated versus unmodified single-stranded DNA.	97
Figure 37: EMSA test of MAR-DNA binding potential candidates.	98
Figure 38: PARP3-mediated DNA MARYlation inhibits.	100
Figure 39: PARP3-mediated DNA MARYlation inhibits NHEJ of blunt DSBs.	101
Figure 40: Qualitative representation of the nick stabilization effect on DSB ligation via NHEJ actors and PARPs interaction.	102
Figure 41: Quantitative representation of the DSBs ligation products shown in Figure 38.	104
Figure 42: Endogenous PARPs effect on NHEJ efficiency in presence or not of NAD ⁺ .	105
Figure 43: Denaturing PAGE analysis of A. PARP1 and B. PARP3 generated products of DNA PAR/MARYlation in presence of NAD ⁺ derivatives.	107
Figure 44: PARP2-dependent formation of PAR-DNA adduct in presence of NAD ⁺ derivatives and test of theirs hydrolysis by PARG treatment.	107
Figure 45: Schematic representation of the putative model of DNA modification by PARP1 activated on a 1-nt gap.	113
Figure 46: ADP-ribosylation of S1nDNA duplexes containing 5'-otherhangs by PARP2 and PARP3.	113



LIST OF TABLES

Table 1: Distinct ART genes in distantly related speciesa.....	26
Table 2: Localization and Function of PARP Enzymes. <i>Adapted from Peter Bai, 2015.</i>	34
Table 3: DNA dependent and independent activation pathways of the PARP family masters (PARP1-3).....	39
Table 4: Writers and erasers of nucleic acids ADP-ribosylation in different species.	47
Table 5: Human ADP-ribose erasers. <i>Adapted from Julia O’Sullivan et. al., 2019.</i>	49
Table 6: Primary and secondary antibodies specifications; (H: Human, M: Mouse and R: Rabbit).	65
Table 7: Sequences of the oligonucleotides and their duplexes used in this study.	68
Table 8: List of selected ds/ssDNA MAR-readers.	90
Table 9: Proteomics data for P[MAR-dsDNA] and control samples showing the list of selected proteins with $-\log_{10}(\text{p-value}) \geq 1.3$ (at least for one of three conditions). In green: enriched proteins, in blue: unchanged and in red: depleted proteins for MARYlated dsDNA versus dsDNA along.	93



ABBREVIATIONS

alt-NHEJ: Alternative NHEJ

•O₂⁻: Superoxide radicals

•OH: Hydroxyl radical

Ado: Adenosine

ADP: Adenosine diphosphate

ADPr: ADP-ribose

AID: Activation-induced deaminase

AIF: Apoptosis inducing factor

AMP: Adenosine monophosphate

AP: Apurinic or apyrimidinic

APE1: AP endonuclease

APLF: Aprataxin and PNK-like factor

APOBEC1: Apolipoprotein B mRNA editing enzyme catalytic polypeptide 1

APTX: Apartaxin

ARH: ADP-ribosyl hydrolase

ART: ADP-ribosyltransferase

Art: Artemis

ARTD: ADP-ribosyl transferases diphtheria toxin-like

ATP: Adenosine triphosphate

BER: Base excision repair

bp: Base pair

BSA: Bovine serum albumin

C: Carbon

CARP-1: Cell division cycle and apoptosis regulator protein 1

CCCH: Cys–Cys–Cys–His

CD: Catalytic domain

CIP: Calf-intestinal alkaline phosphatase

c-NHEJ: Canonical NHEJ



CTIP: DNA endonuclease RBBP8

Cys: Cysteine

Da: Dalton

DarG: DNA ADP-ribosyl glycohydrolase

DarT: DNA ADP-ribosyl transferase

DBB: DNA damage-binding protein

DDR: DNA damage response

DMEM: Dulbecco's modified Eagle's medium

DNA: Deoxyribonucleic acid

DNA-PKc: DNA dependent kinase

DNMT1: DNA-methyltransferase 1

dRP: deoxyribose phosphate

DSB: Double-strand break

dsDNA: Double stranded Deoxyribonucleic acid

DTT: Dithiothreitol

EMSA: Electrophoretic mobility shift assay

ENPP1: Ectonucleotide pyrophosphatase/phosphodiesterase 1

ER: Endoplasmic reticulum

FEN-1: Flap endonuclease 1

GGR: Global genome repair

Glu: Glutamate

H1: Histone

H2B: Histone

H2O2: Hydrogen peroxide

HD: Helical regulatory domain

His: Histidine

HR: Homologous recombination

IDL: Insertion/ deletion loop

IPTG: Isopropyl D-galactopyranoside

Ku70: X-ray repair cross-complementing protein 6

Université Paris-Saclay

Espace Technologique / Immeuble Discovery

Route de l'Orme aux Merisiers RD 128 / 91190 Saint-Aubin, France



Ku80: ATP-dependent DNA helicase 2 subunit
LC-MS: Liquid chromatography-mass spectrometry
LIG3: DNA ligase III
LIG4: DNA ligase IV
MacroD1/2: Macrodomain-containing proteins 1 and 2
MAR: Mono(ADP-ribose) polymer
MMR: Mismatch repair
MRE11: Meiotic recombination 11 homolog 1 protein
Mut: DNA mismatch repair protein
NAD: Nicotinamide adenine dinucleotide
Neil1/2: Endonuclease VIII-like 1 and 2
NER: Nucleotide excision repair
NHEJ: Non-homologous end joining
NMN: Nicotinamide mononucleotide
nt: Nucleotide
NUDIX: Nucleoside diphosphates linked to moiety-X
P: Phosphate
PAGE : Polyacrylamide gel electrophoresis
PAR : Poly(ADP-ribose) polymer
PARG: Poly(ADP-ribose) glycohydrolase
PARGi: PARG inhibitor
PARP: poly(ADP-ribose) polymerase
PAXX: Paralog of XRCC4 and XLF
PBS: Phosphate-buffered saline
PBZ: PAR-binding zinc-finger
PEG: Polyethylene glycol
PK: Proteinase K
PNKP: Polynucleotide kinase phosphate
Pol θ : DNA polymerase theta
RAD51: DNA repair protein RAD51 homolog 1



Rib: Ribose
RNA: Ribonucleic acid
ROS: Reactive oxygen species
RPA: Replication protein A
SDS: Sodium dodecyl sulfate
SSB: Single-strand break
ssDNA: Single stranded Deoxyribonucleic acid
SVP: Snake venom phosphodiesterase
TA: Toxin-antitoxin
TARG1: Terminal ADPr protein glycohydrolase 1
TBS: Tris-buffered saline
TCR: Transcription-coupled repair
TDG: Thymine DNA glycosylase
TdP-1: Tyrosyl-DNA-phosphodiesterase
TDP2: Tyrosyl-DNA phosphodiesterase 2
Tdt: DNA nucleotidylexotransferase
Tdt: Terminal deoxynucleotidyl transferase
tRNA: Transfer RNA
Trp: Tryptophan
TRPT1: tRNA 2'-phosphotransferase 1
UV: UltraViolet
WB: Western Blot
WT: Wild type
WWE: Trp-Trp-Glu
XLF: XRCC4-like factor
XPA: DNA repair protein complementing XP-A cells
XRCC2: X-ray repair cross-complementing protein 2
XRCC3: X-ray repair cross-complementing protein 3
XRCC4: X-ray repair cross-complementing protein 4
ZAP: Zinc finger antiviral protein



HEG: Hexaethylene glycol

INTRODUCTION

I. CONTEXT

In response to chemical or physical alterations, cascades of molecular events are induced in most of living organisms, involving specific changes in the cell's crucial macromolecules, such as proteins, nucleic acids and lipids. These modifications are a variety set of transformations that help to diversify the limited genome of organisms by addition of chemical moieties, such as phosphate, acyl (methyl and acetate), small proteins or sugars on proteins and 5-methyl-uracil or 5-hydroxymethyl-uracil on DNA acceptor groups [1, 2]. DNA damage exposes genome integrity to serious threat. Highly dynamic post-translational/replicative modifications of proteins/DNA are critical for DNA damage recognition, signaling and repair [3]. Poly-ADP-ribosylation is a highly conserved post-translational modification of proteins involved in regulation of cell division, transcriptional regulation and regulation of protein degradation. Poly(ADP-ribose) polymer (PAR) also functions during cell stress responses such as DNA damage, heat shock and the cytoplasmic stress response [4, 5]. ADP-ribose (ADPr) modifications onto target nuclear proteins including histones provide an efficient chromatin remodeling mechanism to enable the efficient repair of DNA strand breaks or in case of severe genotoxic stress, poly(ADP-ribose) polymerase (PARP)-dependent pathways may direct the cell-initiated programmed cell death. The PARPs family of proteins, of which there are eighteen known members, catalyzes the synthesis of monomers or polymers of ADP-ribose (MAR or PAR, respectively) covalently attached to acceptor proteins using nicotinamide adenine dinucleotide as substrate [5, 6]. Furthermore, it was shown that Poly-ADP-ribosylation can interact, modify and regulate "Epigenetic Remodeling proteins" like chromatin insulator proteins such as the transcriptional repressor (CTCF) and DNA-methyltransferase 1 (DNMT1) affecting DNA methylation machinery, so the right balance between PARP and poly(ADP-ribose) glycohydrolase (PARG) activities is crucial for maintaining the DNA methylation patterns in normal cells [7-9]. Interestingly, years ago, specific arthropods and bacterium toxins, were shown to transfer an ADPr moiety to double and single stranded DNA nucleobases in a reversible way [10, 11]. Later on, it has been demonstrated that mammalian PARP1, 2 and 3 act as "DNA Break modifiers", having the ability to bind to DNA damage sites and modify not only nuclear proteins but ss and ds DNA breaks termini [12, 13]. Recently RNA was identified as a novel target of reversible mono-ADP-ribosylation [14].

At present, the role of PARP-mediated ADP-ribosylation of DNA strand break termini remains unclear and different from that of proteins. It would be important to examine in this work ADP-ribosylated DNA breaks role not only in protecting DNA termini from non-specific degrada-



tion or aberrant error-prone end joining but also in precise recruitment and assembly of PAR/MAR-guided readers and to focus on the interplay between DNA-ADP-ribosylation and other DNA epigenetic signature marks. As well, to characterize the full mechanism of the PARP1 DNA-ADP-ribosylation; the most abundant PARP in the cell (Figure 1).

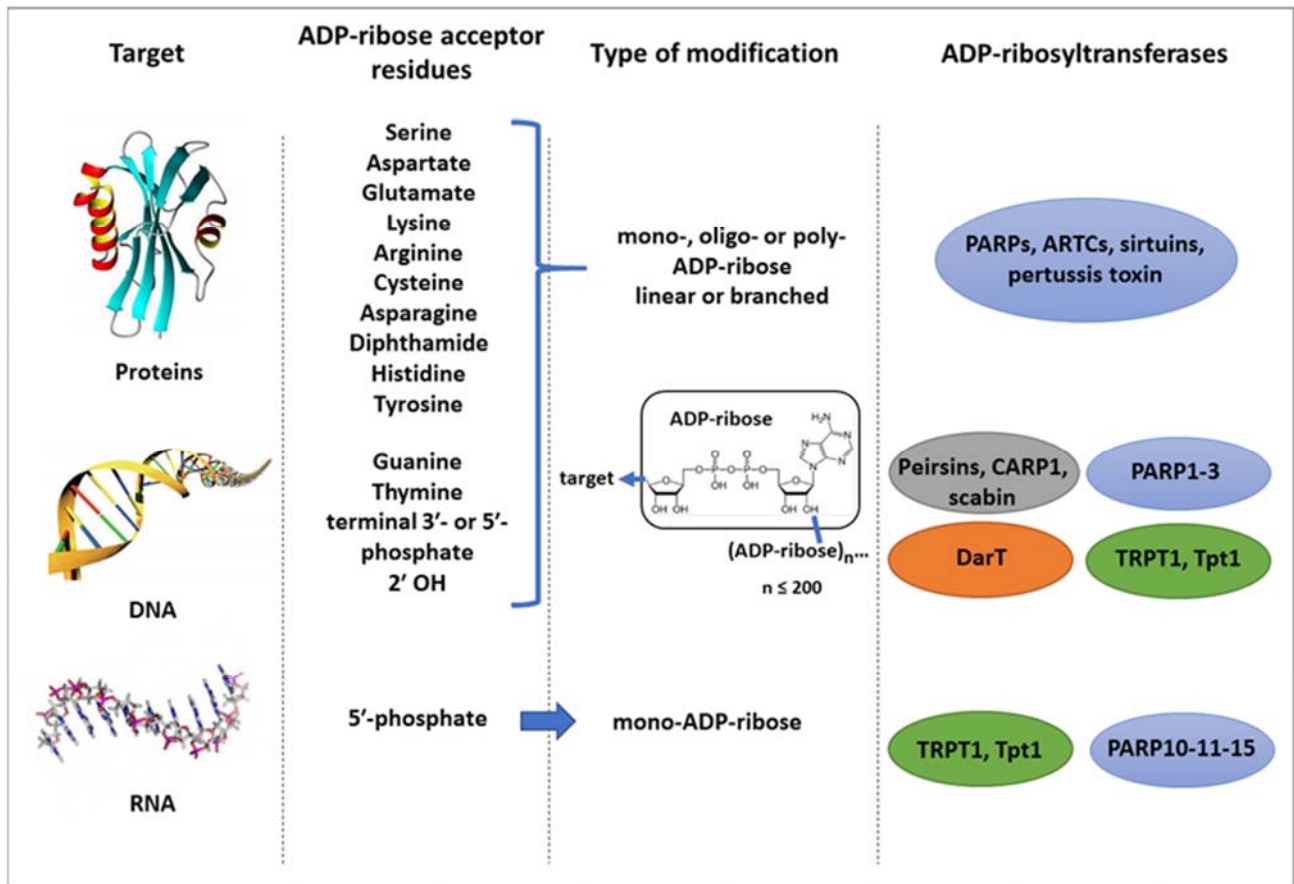


Figure 1: An overview of substrates, sites and products of ADP-ribosyltransferases.

II. DNA DAMAGE RESPONSE AND GENOMIC INSTABILITY

Genome instability defined as higher than normal rates of mutation caused by an enormous category of DNA-damaging agents would be a massive issue for the cell proliferation, viability and survival. The human genome, like other genomes, encodes information to protect its own integrity. DNA damage can be repaired by the robust the DNA Damage Response (DDR) pathways otherwise the cell may trigger apoptosis. Unfortunately, errors may occur. Failure, defect or inactivation of specific DNA repair and/or checkpoint pathways or DNA editing enzymes may cause dysregulation in the cell-cycle progression and lead to mutations accumulation and to DNA damage being permanently passed through cell division. This phenomenon can have catastrophic consequences for age-related diseases such as cancer. Moreover, polymorphisms in DNA repair genes and capacity may affect cancer development. Thus, the maintenance of genetic stability by acquired enzymes that repair DNA anomalies is critical for viability [15-19].

2.1 DNA damage

Human cell is subject to a huge number of heterogeneous lesions per day. Exposition to exogenous agents 'Carcinogens', such as X-rays, ultraviolet (UV) light, and various genotoxic chemicals (alkylating and crosslinking agents), as well to reactive endogenous sources during normal metabolism [hydrolytic and oxidative reactions with water and reactive oxygen species (ROS)], or in DNA repair defectiveness, can cause genetic changes that can promote cancer (Figure 2) [17, 18].

Exogenous agents

Nucleophilic base ring nitrogens/oxygens of guanine, adenine, cytosine, thymine and phosphates in the DNA backbone are targets for exogenous alkylating agents such as tobacco smoke, biomass burning, industrial processing, chemotherapeutic agents (cyclophosphamide), methyl methanesulfonate, ethyl methanesulfonate, N-methyl -N' -nitro-N-nitrosoguanidine, methylnitrosourea, sulfur and the nitrogen mustards. Monofunctional alkylating agents generates mainly N7-methylguanine and N3-methyladenine, leading to apurinic or apyrimidinic (AP) sites; on the other hand, bifunctional reactions result in intra- and inter-strand crosslinks, along with the DNA-protein crosslinks, which block DNA metabolic activity. Converted into ester and sulfate, aromatic amines attack the C8 position of guanine which creates persistent lesions that ultimately give rise to base substitutions and frameshift mutations. As well as aromatic amines, Polycyclic aromatic hydrocarbon such as naphthalene, anthracene, and pyrene depend on the P-450 system of the liver to activate and generate reactive intermediates (dibenzo[a,i]pyrene, etc.) that react with DNA and poses a major cancer risk to humans. In addition to N-nitrosamines and 4-nitroquinoline 1-oxide, causing the 8-hydroxyguanine lesion, hydroxylated estrogen at position, produces reactive catechol



estrogens generating AP sites and strand breakages. After passive diffusion into cells, Toxins (afatoxin B1), generates 8,9-dihydro-8-(N7-guanyl)-9-hydroafatoxin B1, which weakens the glycosidic bond resulting in depurination. Finally cosmetics, pharmaceuticals, food-products/preservatives/additives (bisphenol A, citric acid, brilliant blue, etc.,) are considered chemicals that have health risks, by causing mutagenesis at trinucleotide repeats, which are implicated in the development of neurodegenerative disorders via the alternative non homologous end joining (alt-NHEJ) DNA repair pathway as well promoting cancer development [15-18].

Endogenous sources

Despite the importance of exogenous agents as the major source of DNA damage, novel techniques had elucidated and characterized diverse and abundant types of endogenous DNA mutational signatures. Replication errors, DNA base mismatches and topoisomerase-DNA complexes can occur due to the error prone DNA polymerases α , β , σ , γ , λ , REV1, ζ , η , ι , κ , θ , ν , μ , Terminal deoxynucleotidyl transferase (Tdt) and PrimPol (that can carry out lower fidelity DNA synthesis during DNA replication or repair), strand slippage events (at repetitive sequences) and topoisomerase -DNA cleavage complexes stabilization during replication and transcription. Another source of spontaneous endogenous mutagenesis occurring mainly in single stranded DNA, is known by 'Spontaneous base deamination' where cytosine (C), adenine (A), guanine (G), and 5-methyl cytosine (5mC) in DNA lose their exocyclic amine to become uracil (U), hypoxanthine, xanthine and thymine (T), respectively. Deaminated cytosine is a double-edged sword, while removed from DNA by uracil-DNA glycosylase, it become a substrate for thymine DNA glycosylase (TDG) and relatively slow the mismatch repair (MMR) process but on the other hand, deaminated cytosine can be generated during antibody development during the defense against reteroviruses by the deaminase enzymes such as the activation-induced deaminase (AID) and the Apolipoprotein B mRNA editing enzyme catalytic polypeptide 1 (APOBEC1). The cleavage of the N-glycosyl bond between the nitrogenous base and the sugar phosphate backbone is a highly produced DNA mutation that results in the creation of abasic or AP sites by uracil-DNA glycosylase. Next to their important roles in multiple cellular functions (cellular respiration and redox signaling reactions), the overabundance of superoxide radicals ($\bullet\text{O}_2^-$), hydrogen peroxide (H_2O_2), and the hydroxyl radical ($\bullet\text{OH}$), the most conspicuous of the ROS species, leads to the generation of approximately 100 different oxidative bases lesions (by bases attack) such as thymine glycol residues, or-mamidopyrimidine, 7,8 dihydro-8-oxoguanine (8-oxo-G) as well as 2300 single strand breaks per cell per hour in mammalian cells (by DNA backbone attack). All during Oxidative DNA damage, lipid peroxidation by hydroxyl radicals generates two aldehyde products, the malondialdehyde and 4-hydroxynonenal, capable of reacting with adenine, guanine and cytosine. Some post-translational modification can be, in specific conditions, harmful for the cell. Methylated residues formed essentially by the S-adenosylmethionine (SAM), such as N7-methylguanine, N3-



methyladenine, O6-methylguanine, O4-methylthymine, O4-ethylthymine, N3-methylthymine and N3-methylcytosine are highly mutagenic. Altogether, if left unrepaired, incorrectly paired/incorrectly incorporated nucleotides, abasic sites or deaminated/oxidized/methylated bases, can become mutations in the next round of replication and convert into DNA breaks, thus become implicated in human diseases and cancers [15-18].

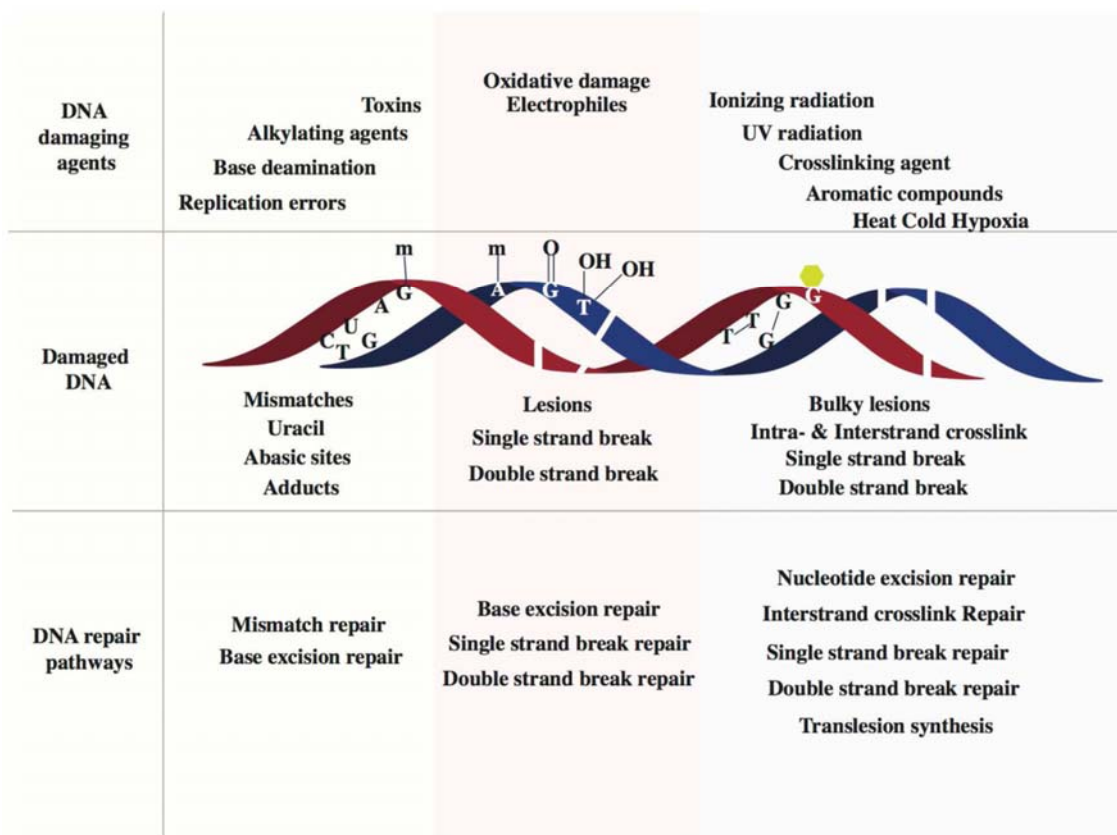


Figure 2: Schematic of various DNA damage-induced DNA repair pathways. *Adapted from Chatterjee et. al., 2017.*

2.2 DNA repair

Multiple DNA repair and damage tolerance pathways involve more than 450 DDR proteins participating into the removal and toleration of the lesions, thus allowing cell survival. Removal of DNA lesions are performed by one of two fundamental mechanisms that involve either the reversal of DNA damage or the excision of damaged elements. In the following section we will represent briefly the main DDR trails as well as the PARP related DNA repair mechanisms (Figure 3).

Base excision repair

Base excision repair (BER), repairs modified bases, by recognizing non-bulky DNA base lesions, as well as abasic sites and single strand breaks (SSBs). In this repair mechanism



the DNA helix or the backbone of DNA is not cut out, only the base is cut from the target site [20]. Complementary strand serves as a repair template for BER which is initiated by several glycosylases (formamidopyrimidine) that produce AP lesions that recruit PARP1, followed by abasic site cleavage and strand nicking by the AP endonuclease (APE1) [21]. The processing of the nicked product containing a blocking end by some glycolases such as the Endonuclease VIII-like 1 and 2 (Neil1/2) or by an AP endonuclease will lead to a 1 nucleotide (nt) gapped product containing 3' phosphate [22]. A DNA strand break must have a hydroxyl on its 3' end and a phosphate on its 5' end for ligation to occur. The Polynucleotide Kinase Phosphate (PNKP) is responsible for these ends during BER. The protein having a kinase domain phosphorylates 5' ends and phosphate domain which removes phosphate from 3' end. Many enzymes that repair the single strand interruptions are: Tyrosyl-DNA-phosphodiesterase (Tdp-1) repairs several 3' blocking termini, Apartaxin (APTX) end process enzyme which specially repair 5'-adenylate intermediate of DNA ligase activity after that strand break through DNA synthesis and ligation [23].

This step includes two different types of pathways which are short patch BER and long patch BER induced respectively by the mono or bifunctional glycosylases. When a single nucleotide is repaired, it is called as Short patch and when bulks of nucleotides are repaired, it is called as Long patch repair. Short patch single nucleotide (80-90% of BER) consist of 1nt gap filling and removal of 5'-deoxyribosephosphate (5'-drp) by lyases activity of the DNA polymerase β and successive ligation of the DNA bases by the DNA ligase 1 or complex of DNA ligase 3 and XPC-HHR23F. In long patch it is only initiated when a 5' blocking lesions occur. The enzyme FEN-1 (Flap endonuclease 1) removes 5' Flap formed during long patch BER. These endonucleases show a great preference for a long 5' Flap adjacent to 1-nt, 3'-Flap. DNA ligase-1 ligates the break in long patch BER. Other proteins included in BER are poly(ADP-ribose) polymerase 1 involved in X-Ray repair. PARP1 is released by dense negative charge of PARP, responsible for repair of proteins to the damaged DNA sites [23].

Nucleotide excision repair

NER removes a variety of forms of DNA damage, including photoproducts induced by UV and other bulky lesions by excising precise nombre of nt oligonucleotides containing the lesion by a multi-step process. In the NER mechanism of mammalian DNA, more than 30 proteins are required. During NER damaged DNA is recognized by the following binding proteins such as the Replication protein A (RPA), DNA repair protein complementing XP-A cells (XPA) and DNA repair protein complementing XP-C cells-Transcription factor II H (XPC-HHR23F), which assemble at the damaged site randomly [21].

NER consists of two sub-pathways: global genome repair (GGR), which removes damage in the genome overall and transcription-coupled repair (TCR), which specifically repairs the



transcribed strand of active genes. The main difference between GGR and TCR is the requirement for different factors during the initial recognition steps. UV-DBB consisting of DNA damage-binding protein 1 and 2 (DDB1 and DDB2), and XPC- human Rad23 homolog (hHR23B) are involved in the recognition step of GGR, while TCR is thought to be initiated by RNA polymerase II stalled at a lesion. Additional factors required for TCR are CSA and CSB a DCX (DDB1-CUL4-X-box)-ERCC-8/6 E3 (DNA excision repair protein) complex. The proteins acting further downstream in GGR and TCR are likely to be identical. First, TFIIH, a complex consisting of nine subunits, is recruited to the damaged site. At this step the initial recognition factors are probably released from the damaged DNA. Two subunits of TFIIH, XPB and XPD, exhibit helicase activity of opposite polarity, and unwind the DNA around the lesion. The next factors that bind to the damaged site are DNA repair protein complementing XP-G cells (XPG) and XPA-RPA. XPA-RPA verifies whether the NER complex is correctly assembled and ensures proper incision of the damaged strand. After binding of DNA repair endonuclease XPF- DNA excision repair protein ERCC-1 (XPF-ERCC1), dual incision occurs by XPG and XPF-ERCC1, which cut 3' and 5' to the damage, respectively. In this way, the damage is released in a 24-32 nucleotide long oligonucleotide. Repair is completed by DNA synthesis and ligation by DNA polymerase 1 and ligase I. Such step requires numerous energies and utilizes ATP by forming ADP and Pi [18, 24].

Mismatch repair

MMR is also an excision-based repair system involving mismatch and small insertion/ deletion loops (IDLs) recognition, excision directed from induced or existing nicks, and synthesis/ligation [21]. In *Escherichia coli*, the main players in MMR are DNA mismatch repair protein (MutS, MutL and MutH). MutH nicks the non-methylated strand and thereby enables discrimination between the newly synthesized strand and the template. MMR is bidirectional, for example nicking and degradation can occur from either the 5' or 3' side of the mismatch [24]. In eukaryotes, several MutS and MutL homologues are involved in MMR. Humans employ the MutS α heterodimer (MSH2/MSH6) to recognize base mismatches and one-to-two nucleotide IDLs, and the MutS β heterodimer (MSH2/MSH3) to recognize large IDLs. The previously accepted model was that after the lesion recognition step, the MutS complex translocates along the DNA in an ATP-dependent manner to make way for the downstream MMR components. Recently, it was shown that MutL can trap MutS at the mismatch before it forms a sliding clamp. Next, the MutL complexes are recruited on to DNA and among the 4-known human MutL homologs; the MutL α heterodimer (MLH1/PMS2 heterodimer) plays a major role in MMR. MutL α regulates termination of mismatch-provoked excision, and its endonuclease activity plays a role in the 3' nick-directed digestion by the exonuclease 1(EXO1) in a PCNA-associated factor- Replication factor C subunit (PCNA/RFC) dependent manner. EXO1 also carries out the 5' directed mismatch excision creating a gap that is stabilized by RPA. POL δ , RFC, HMGB1 (high mobility group box 1 protein) and LIG1 (ligase 1) orchestrate



the final steps of new DNA synthesis and ligation. PCNA plays an important role in both the initiation step of MMR and in the subsequent DNA synthesis by interacting and localizing MutS α / β and MutL α complexes at the lesion site [18].

Homologous recombination

Double-strand breaks (DSBs) can be repaired by either HR or NHEJ. HR uses a homologous DNA template and is highly accurate, whereas NHEJ rejoins the broken ends without using a template and is often accompanied by loss of some nucleotides [24]. The relative contribution of each pathway depends on the cell-cycle stage, with NHEJ being more active in G1 and HR dominating during S and G2 phases. During HR DSBs are converted to 3' single-stranded DNA (ssDNA) tails, which are bound by RPA. Processing of DSBs probably requires a complex of double-strand break repair protein and telomere maintenance protein MRE11-RAD50-NBS1. RAD52 interacts with RPA and promotes binding of RAD51 to the ssDNA, which may be stabilized by RAD51 paralogues [RAD51B, RAD51C, RAD51D, XRCC2 and XRCC3 (X-ray repair cross-complementing protein 2 and 3) in human, RAD55 and RAD57 in yeast]. Subsequently, the RAD51-bound ssDNA invades a homologous molecule in a reaction stimulated by RAD54. After DNA synthesis and ligation, two Holliday junctions are formed and branch migration can occur. The Holliday junctions are finally resolved by resolvases. HR also represents an error-free subpathway of damage tolerance, allowing replicational bypass of lesions through a template switch. Alternatively, damage tolerance can be achieved by error-free and error-prone translesion synthesis carried out by specialized DNA polymerases. HR-dependent lesion bypass may sometimes produce a 3' flap that can be cleaved by a complex of crossover junction endonuclease (MUS81-EME1) or resolved by DNA topoisomerase 3- α -ATP-dependent DNA helicase Q (TOP3-RECQ) [24].

Non-homologous end joining

While HR is the higher fidelity pathway because it utilizes a homologous sister chromatid for repair it can only be performed during the S and G2 phases due to sister chromatid availability, and thus NHEJ is the predominant DSB pathway in cells. NHEJ is more error prone and functions to ligate the two ends together but it is also important for physiological processes such as V(D)J recombination in lymphocyte during T and B cell maturation [18, 21, 24, 25]. NHEJ is divided in two subpathways: canonical NHEJ (c-NHEJ) and alternative NHEJ (alt-NHEJ).

It relies on recognition of the DSB by the heterodimer of X-ray repair cross-complementing protein 6 (Ku70) and the ATP-dependent DNA helicase 2 subunit (Ku80) in the case of c-NHEJ. This Ku70/Ku80 heterodimer forms a ring structure completely encircling DNA duplex. Structurally, this complex also acts as scaffold for the recruitment of XRCC4 (X-ray repair cross-complementing protein 4) and DNA ligase IV. The three proteins complex Ku-XRCC4-ligase IV is the mini-



mal complex required for NHEJ as shown by reconstitution in vitro. The DNA dependent kinase (DNA-PKcs) is activated after binding DNA and Ku complex, phosphorylates several target proteins such as Ku70, Ku80, XRCC4, XLF (XRCC4-like factor), Artemis and DNA ligase IV, and activates the nuclease Artemis, which plays an important role in processing of DSB ends by the DNA-PKcs-Artemis complex, resulting in the creation of appropriate ends that can be ligated by a complex containing XRCC4, DNA ligase IV and XLF [18, 21, 24, 25].

The a-NHEJ also known as microhomology-mediated end joining is distinguished from the other DSB repair mechanisms, by its use of 2-5 base pair microhomologous sequences to align the broken strands before joining. A-NHEJ occurs during the S-phase of the cell cycle in contrast to the NHEJ pathway in G0/G1 and early S-phases and HR in late S to G2-phase. It is a Ku- and DNA-PKcs-independent mechanism which is considered to be initiated by the recognition and binding of poly(ADPr) polymerase 1 to the DSB site. PARP1 facilitates the recruitment and loading of the meiotic recombination 11 homolog 1 protein (MRE11), and has been suggested to stimulate a-NHEJ via the ADP-ribosylation of histone H1. The DSB recognition step is followed by the resection of DNA ends mediated by DNA endonuclease RBBP8 (CtIP) and the MRN complex (MRE11-Rad50-Nbs1), where the nuclease activity of MRE11 is essential. Recessed DNA ends can anneal to each other via microhomology regions as short as 2nt. Pol θ has been shown to stabilize the annealing of two long 3' ssDNA overhangs with a little as 2 base pair (bp) of homology, extending one 3' DNA end by using the annealing partner as a template. Nicks are then sealed by DNA ligase III. Finally, the DNA ends are rejoined by XRCC4-DNA ligase IV. Defective repair of DSBs can result in chromosomal instability, which is characterized by rearrangements and loss of chromosomes. A number of human syndromes, such as Ataxia telangiectasia (AT) and related disorders, Nijmegen breakage syndrome (NBS), as well as breast and ovarian cancer caused by mutation of BRCA1 or BRCA2, are associated with defects in DSB repair. However, these syndromes are a consequence of defects in regulation of DSB repair (e.g. in checkpoint activation) rather than due to a direct inactivation of HR or NHEJ [18, 25].

A few specific lesions can also be removed by direct chemical reversal and interstrand crosslink repair. These repair processes are keys to maintaining genetic stability in cells. Each of the DNA repair pathways needs to be coordinated with a series of signaling responses that arrest cell division or trigger cell death in case the lesions are irreparable.



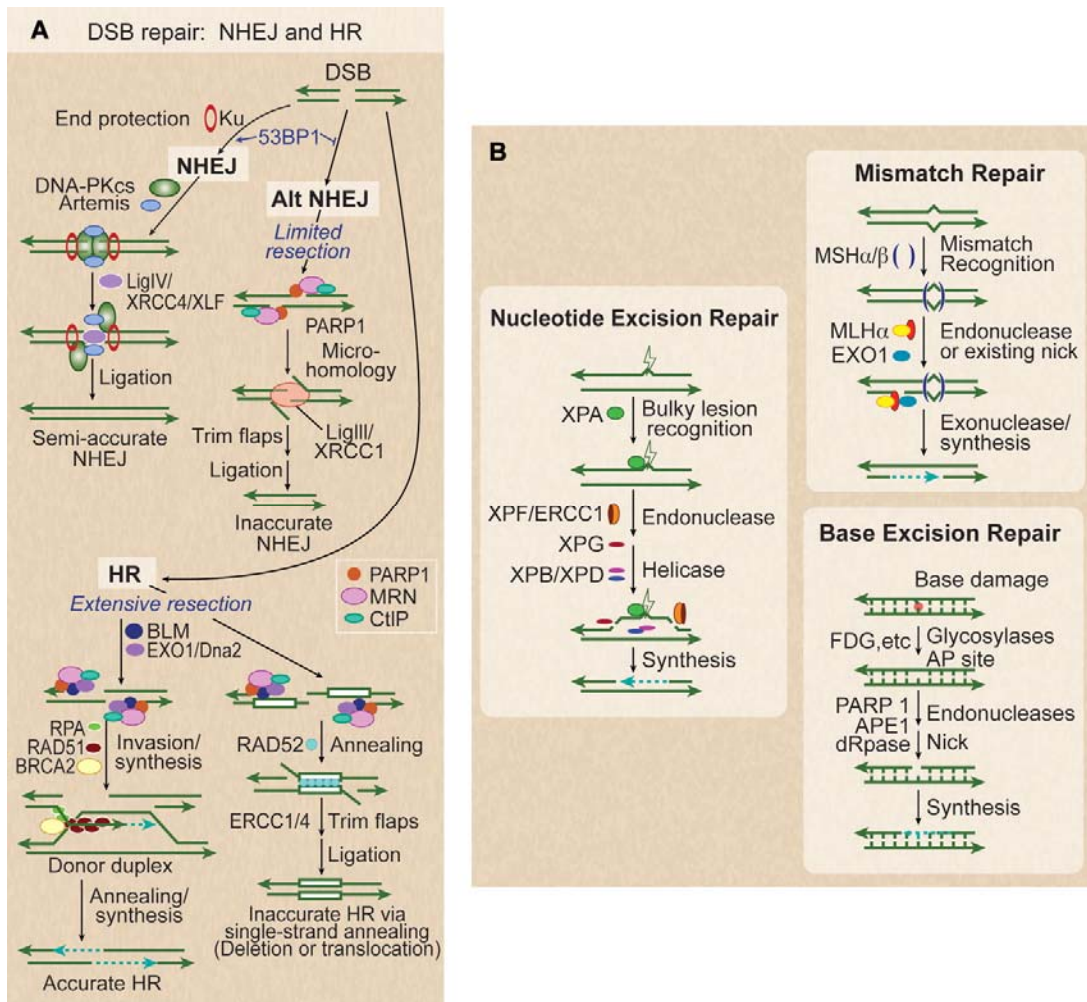


Figure 3: Five DNA repair pathways. (A) DSBs are repaired by 2 NHEJ and 2 HR subpathways. Classic NHEJ initiates with broken ends bound by Ku, which protects ends, leading to accurate or semi-accurate repair. Mutations in classic NHEJ factors shunt DSBs toward alternative NHEJ, which involves limited resection by MRN/CtIP and annealing via microhomology, yielding inaccurate repair. 53BP1 also serves to increase NHEJ accuracy by blocking MRN/CtIP resection. PARP1 promotes more extensive end-resection by EXO1 and BLM to reveal ssDNA and promote HR. RPA binds to ssDNA, BRCA2 mediates replacement of RPA with RAD51, the RAD51 nucleoprotein filament invades a homologous donor sequence (typically the sister chromatid in S/G2 phase), and repair synthesis extends the invading 3' end, which then anneals with resected end to provide accurate repair. If long homologous repeats flank the DSB (white boxes), extensive resection can reveal complementary ssDNA that is annealed in a reaction promoted by RAD52, leading to deletion of one repeat and DNA between repeats, or translocations if DSBs occur on different chromosomes. (B) Base damage, often from oxidation, triggers BER. This results in a short repaired single-strand segment, also called a patch. Bulky nucleotide lesions, such as thymidine dimers from ultraviolet light, are repaired by NER. These involve a long repaired single-strand patch. Mismatch repair (MMR), used to replace nucleotides mistakenly placed opposite a non-paired template nucleotide during DNAsynthesis, and involves long excision of single strands and resynthesis repair patches initiated from existing or induced nicks. *Adapted from Shaheen et. al., 2011.*



III. SYNTHESIS OF POLY(ADP-RIBOSE) POLYMER AND ADP-RIBOSYLTRANSFERASES

Nicotinamide adenine dinucleotide (NAD) is a redox agent that can exist in two forms, the NAD⁺ oxidizing agent and the NADH reducing agent. The NAD is composed of two nucleotides containing adenine and nicotinamide. ADP-ribosylation refers to the transfer of the ADP-ribose group from NAD⁺ to target proteins post-translationally [26]. The synthesis of PAR was first reported in the 1960s. It was detected as the incorporation of (¹⁴C-adenine)-labeled ATP into the acid-insoluble fraction by a nuclear preparation from chicken liver. This activity is greatly enhanced by nicotinamide mononucleotide (NMN). Soon after its discovery, it was demonstrated that the acid insoluble product is a homopolymer of (ADP-ribose) [27], which is synthesized by a class of enzymes known as ADP-ribosyltransferases (ARTs). The addition of ADPr units results in the formation of a chain where ADPr units are linked together through glycosidic ribose-ribose 1''→2' bonds [28]. The ADPr can vary in length from a few to 200 – 400 units in vivo and in vitro [29]. The poly(ADPr) polymer (PAR) can be branched at a frequency of 1 branch per 20-50 subunits of the linear polymer. Branched polymer can have a very complex structure, including helicoidal secondary structures which are, at some extent, similar to RNA or DNA [30, 31]. The branching site of PAR was determined as O-D-ribofuranosyl-(1'''→2'')-O-D-ribofuranosyl-(1'''→2'')-adenosine-5',5'',5'''-tri(phosphate), also known as Ado (P)-Rib (P)-Rib-P. This site is the sale for the linear and the branched region of PAR (Figure 4-5) [32].

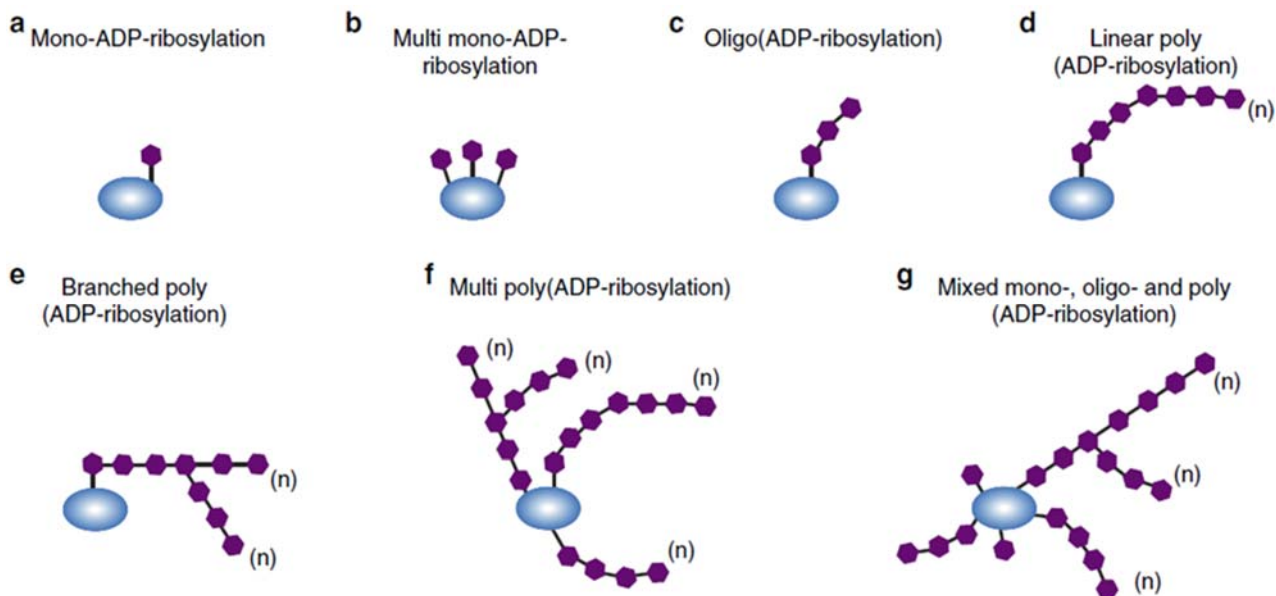


Figure 4: Possible patterns of ADP-ribosylation on target proteins. a Mono-ADP-ribosylation; a single ADP-ribose molecule is attached to the protein. b Multi mono-ADP-ribosylation; multiple single ADP-ribose units are bound along the protein. c Oligo-ADP-ribosylation; short linear chains of ADPr are transferred to the protein. d Linear poly-ADP-ribosylation; ADPr moieties forming a long linear chain up to 200 units in length. e Branched poly-ADP-ribosylation; complex



molecules composed of large and branched polymers of ADPr. Multi poly-ADP-ribosylation; multiple PAR chains either linear or branched on the same protein. g Mixed ADP-ribosylation; a mixture of the previously described ADP-ribose patterns on the same protein, generated either by the combined action of MAR- and PAR transferases or by the degradative action of erasers. Adapted from Julia O'Sullivan et. al., 2019.

PAR (rather free or attached to proteins) synthesized upon genotoxic stress may undergo biphasic decay, the most (~85%) of PAR have a half-life of about 40 s and the remaining is catabolized within approximately 6 min. In contrast, the constitutive fraction of PAR have a much longer half-life (~7,7 h) [33]. A tight regulation of the level of the polymer in the cell by ADPr-protein hydrolases, that reverse the reaction by hydrolyzing the protein-ADPr bond and/ or the bonds between different ADPr units of pADPr is important, since its accumulation can have cytotoxic effects [34].

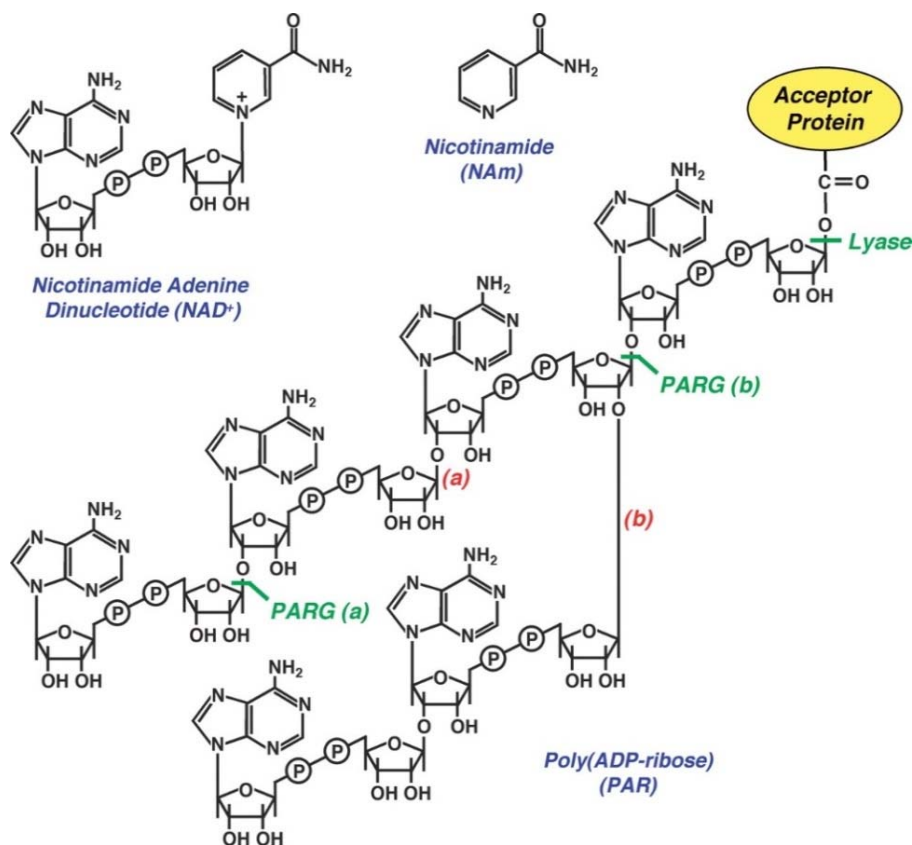


Figure 5: ADP-ribose moieties synthesis and attachment on acceptor sites of target proteins by PARPs enzymes using NAD⁺ as a donor of ADP-ribose units and their cleavage by PAR/MAR hydrolases. Adapted from Kim et. al., 2005.

ADP-ribosylation is a widespread reversible post-translational modification that occurs on proteins but also on other macromolecules such as DNA, or small chemical groups and controls a



vast number of cellular processes [35]. Mono-ADP-ribosylation reactions were originally identified as an important aspect of bacterial pathophysiology, catalyzed by several toxins including diphtheria (Box 1), pertussis, cholera, and certain clostridial toxins. Subsequently, mono-ADP-ribosylation was also discovered in bacteriophages and in eukaryotic cells. Poly-ADP-ribosylation was discovered in multicellular eukaryotes and appears to be less widely used compared to mono-ADP-ribosylation. However recent evidence suggests that it also exists in dinoflagellates and archaeobacteria. ART encoding genes are found in many eukaryotic species of the animal, plant, fungi, and protist kingdoms (Table 1) [29].

Table 1: Distinct ART genes in distantly related species. a Summary of the matches of ART genes found in model organisms with complete or near-complete genome sequences. b,c ART genes were identified by BLAST searches of the genome and cDNA databases using as queries the DNA sequences of each catalytic domains of the 17 human poly-ADP-ribose polymerases (PARP1-17) and each of the 6 mouse ecto-mono-ADP-ribosyltransferases (ART1-5). d Note: the exact number will most likely change as genome sequences are being fully validated. e >: at least. f Ciliates possess two nuclei, a germinal nucleus (micronucleus) and a somatic nucleus (macronucleus). Adapted from Hottiger et. al., 2010.

Species	Genome size (Mbp)	Gene count	Haploid chromosome count	<i>Trpt</i> gene count	<i>Parp</i> gene count ^{b,d}	<i>e-Mart</i> gene count ^{c,d}
<i>Homo sapiens</i>	3038	~ 30000	23	1	17	4 (5)
<i>Pan troglodytes</i>	3300	~ 30000	24	1	17	4 (5)
<i>Equus caballus</i>	2200	~ 21000	32	1	17	>3 ^e
<i>Bos taurus</i>	3000	~ 22000	30	1	16	>4 ^e
<i>Canis familiaris</i>	2400	~ 20000	39	1	17	>4 ^e
<i>Felis catus</i>	3000	~ 20000	14	1	>16 ^e	>4 ^e
<i>Mus musculus</i>	3000	~ 25000	20	1	16	6
<i>Rattus norvegicus</i>	2750	~ 21000	21	1	16	5
<i>Gallus gallus</i>	1200	~ 22000	40	1	>15 ^e	>5 ^e
<i>Xenopus laevis</i>	3100	~ 20000	18	1	15	>2 ^e
<i>Danio rerio</i>	1700	~ 25000	25	1	16	>3 ^e
<i>Oryzias latipes</i>	700	~ 21000	24	1	16	>3 ^e
<i>Anopheles gambiae</i>	278	~ 14000	3	1	>3 ^e	none
<i>Drosophila melanogaster</i>	170	~ 15000	4	1	2	none
<i>Caenorhabditis elegans</i>	97	~ 21000	6	1	3	none
<i>Arabidopsis thaliana</i>	119.2	~ 28000	5	1	>10 ^e	none
<i>Oryza sativa</i>	450	~ 45000	12	1	>3 ^e	none
<i>Trypanosoma brucei</i>	26	~ 10000	11	1	>1 ^e	none
<i>Paramecium tetraurelia</i>	120 and 100 ^f	~ 40000	50 and 350 ^f	1	>7 ^e	none
<i>Dictyostelium discoideum</i>	34	~ 12500	6	1	>9 ^e	none
<i>Entamoeba histolytica</i>	23.8	~ 10000	14	1	>6 ^e	none
<i>Schizosaccharomyces pombe</i>	14	~ 5000	3	1	none	none
<i>Saccharomyces cerevisiae</i>	12.8	~ 6500	16	1	none	none
<i>Aspergillus fumigatus</i>	30	~ 10000	8	1	>1 ^e	none
<i>Magnaporthe grisea</i>	40	~ 12000	7	1	>1 ^e	none
<i>Neurospora crassa</i>	39.23	~ 10000	7	1	>1 ^e	none

Lower eukaryotes generally contain fewer ART genes, and based on their sequence similarity and conserved domain structures, all vertebrate ART genes can be assigned to a particular orthologue. It should be noted that there is no correlation between genome size, chromosome or gene numbers and the total number of ART genes in a genome. Sequence and structure homology searches have identified 22 human genes encoding proteins that encompass an ADP-ribosyl transferase fold and are thus potentially associated with distinct ADP-ribosylation activities.



These proteins have been grouped into three major families: (i) the extracellular membrane-associated ADP-ribosyl transferases (ecto-ARTs); (ii) a single member family of NAD⁺-dependent tRNA 2'-phosphotransferases; and (iii) the mammalian poly-ADP-ribose polymerases (PARPs) [29].

Structurally, prokaryotic and eukaryotic ARTs are characterized by a conserved NAD⁺ binding core (Figure 6) with a central 6-stranded β -sheet [36-39], which include three evolutionary conserved motifs: (i) The R/H-G-T/S motif, which is located in the first β -strand and is involved in NAD⁺ binding, (ii) The S-T-S motif, which is located in the second β -strand, is involved in NAD⁺ binding and is partially or entirely modified (Y-X-T/S or Y-F/X-A/X) in ATRDs, and (iii) The ARTT loop (also known as ADP-ribosylating turn-turn), probably involved in substrate recognition, followed by the β -strand 5. Diphtheria toxin, exotoxin A, cholix toxin and all eukaryotic ARTs catalyzing poly-ADP-ribosylation, the NAD⁺ binding core contains three evolutionary conserved amino acids known as the H-Y-E triad, where histidine residue is in β -strand 1, tyrosine residue in β -strand 3 and the catalytic glutamic acid residue at the front edge of β -strand 5 [36]. In contrast to the turn-turn motif, the catalytic glutamate is highly conserved across the kingdoms of life. Nevertheless, in bacterial transferases and some human mono ADP-ribosyl transferases, the H-Y-E is not conserved.

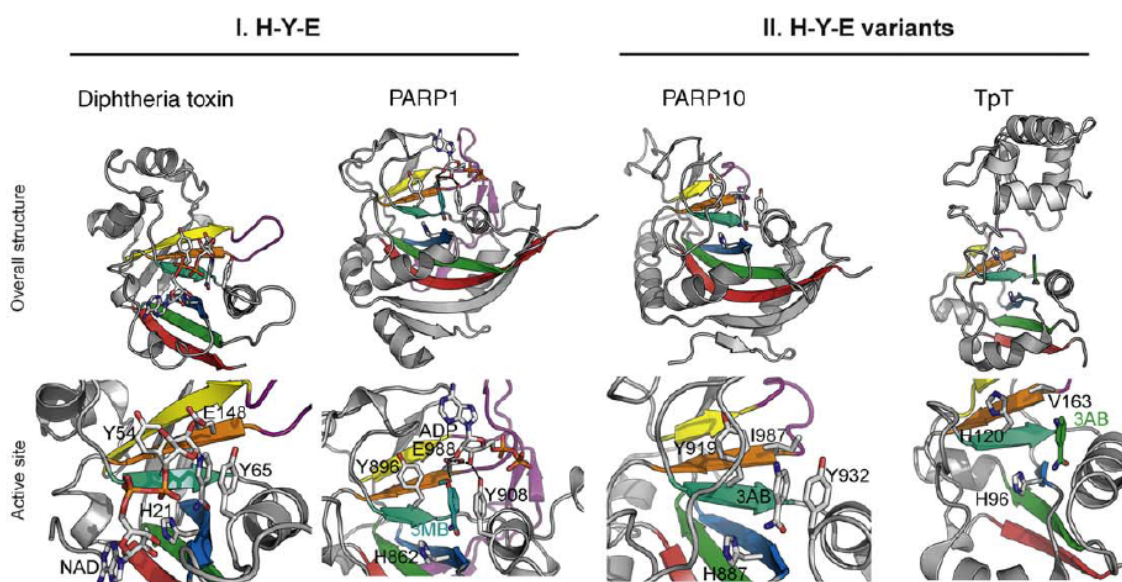


Figure 6: Ribbon representation of the conserved NAD⁺ binding core of ARTs containing the H-Y-E triad (bacterial toxins and bona fide PARPs) or H-Y-E variant (bacterial transferases and novel “mono PARP” enzymes). The six consecutive strands of the central β -sheet are shown in rainbow colors from the first N-terminal strand in blue to the 6th strand in red. Ligands and conserved residues/motifs discussed in the text are shown as sticks. TpT = *Saccharomyces cerevisiae* 2'-phosphotransferase. Adapted from Hottiger et. al., 2010.



For the sake of simplicity, we limit our discussion to poly(ADP-ribose) polymerases (PARPs, also known as ADP-ribosyl transferases diphtheria toxin-like, whose functions are better understood than other ARTs. Furthermore, we focus on DNA dependent PARPs subfamily.

IV. THE POLY(ADP-RIBOSE) POLYMERASE (PARP) FAMILY

The PARP family includes 17 known members (Figure 7) [29, 40]. Highly divergent PARP homolog tRNA 2'-phosphotransferase 1 (TRPT1) is sometimes referred to as the eighteenth PARP family member [41]. According to their structures, PARPs can be subdivided into four subfamilies: DNA-dependent PARPs (PARP1, PARP2, and PARP3), tankyrases (PARP5a and PARP5b), CCCH (Cys–Cys–Cys–His) zinc finger and WWE (Trp–Trp–Glu) domain-containing PARPs (PARP7, PARP12, PARP13.1, and PARP13.2) and macrodomain-containing PARPs (PARP9, PARP14, and PARP15). Although PARP13 is not yet shown to have a catalytic activity [5], most of PARPs have the function of transferring mono or poly(ADPr) moieties onto their target proteins [42], DNA [12, 13, 43], or RNA termini [14]. PARPs play a role in a wide range of biological structures and processes, including DNA repair and maintenance of genomic stability, transcriptional regulation, centromere function, mitotic spindle formation, centrosomal function, the structure and function of vault particles, telomere dynamics, trafficking of endosomal vesicles, inflammation, apoptosis, and necrosis [42, 44] (Table 2 and Figure 8).

PARP1:

The founding member of the PARP family as well as the most ubiquitous and abundant PARP, PARP1 was the most studied. This 110 kDa nuclear protein is composed of six domains essential for DNA-binding, nuclear homing, automodification, protein–protein interactions, and catalytic activity. PARP1 is responsible for 80% to 90% of the PARylation activity in the cell [45]. Based on the structure–function relationship studies, PARP1 was initially characterized as a critical player in the DNA damage response and repair processes under stressful conditions. PARylation can lead to accelerated dissociation of modified proteins from DNA owing to the negative charge of the PARylated protein and steric hindrance. The best example of this dissociation is PARP1-mediated PARylation of histone H1 and PARP2-mediated PARylation of histone H2B; these modifications cause the dissociation of these histones from DNA and eventually chromatin relaxation required for replication, transcription, DNA repair [46–48]. Later on, the list of known biological functions of PARP1 has been expanded: regulation of chromatin structure, transcription, stress responses, and involvement in various physiological processes [49]. Moreover, the roles of PARP1 under normal physiological conditions have been further substantiated, e.g., the regulation of gene expression, RNA biology, and processes in cytoplasm. Recently, PARP1 has been identified as a sensor of unligated Okazaki fragments—during DNA replication in normal S phase cells—which facilitates their maturation [50]. The remaining ADP-ribosylation activity in the cell lacking



PARP1 (in embryonic fibroblasts derived from PARP1^{-/-} knockout mice) falls to other active PARP members, which may or may not share structural similarities or localization with PARP1 but certainly share a highly conserved catalytic (CD) domain (PARP signature). The latter consists of a helical regulatory domain (HD) and an ADP-ribosyl transferase domain (ART) responsible for the catalytic activity, present in PARP2 and PARP3.

PARP2:

PARP2 was discovered as the enzyme responsible for the basal PARylation activity in PARP1-deficient cells [51] and accounts for ~10% of the PARylation activity in the cell. Just as PARP1, PARP2 recognizes and binds a DSB or SSB. The binding of PARP2 to damaged DNA structures triggers its PARylation activity. PARP2 has partially redundant functions with PARP1 that are essential for normal embryogenesis. Double-knockout *Parp1^{-/-}Parp2^{-/-}* mice show early embryonic mortality [52]. PARP2 has function, independent of its PAR synthesis activity, which limits the accumulation of the resection barrier factor 53BP1 at DNA damage sites and directs DSBs toward resection-dependent repair pathways [53]. Aside from DNA repair, cell cycle regulation and inflammation and metabolic regulation, PARP2 acts as a cofactor in transcription and can regulate the expression of 600 to 1,000 genes by facilitating transcription or via attraction of cofactors promoting chromatin compaction and the consequent inhibition of transcription [54-57].

PARP3:

PARP3 is related to PARP1 and PARP2 and its domain organization is similar to that of PARP2, but PARP3 catalyzes MARYlation instead of PARylation [40]. Similar to PARP1 and PARP2, PARP3 is an important player in cell cycle regulation and DNA repair [58]. This PARP interacts with PARP1, DNA ligase III, Ku70/80 other NHEJ proteins and promotes processing DSBs in the canonical NHEJ pathway [59]. Other than its role on the DNA damage response and repair, PARP3 has also been reported to associate with Polycomb group proteins involved in transcriptional silencing and chromatin-remodelling [60].

Besides the PARP1–3 proteins, which become active upon binding to DNA breaks, other PARP family members also play significant roles in the maintenance of genomic stability, transcriptional regulation, centromere function, mitotic spindle formation, centrosomal function, the structure and function of vault particles, telomere dynamics, trafficking of endosomal vesicles, inflammation, apoptosis, and necrosis [35].

PARP4:



PARP4 (also called VPARP or ARTD4) is a component of the cytosolic ribonucleoprotein vault complex [35] and is also present in cytoplasmic clusters (VPARP rods) as well as in the nuclear matrix [6]. The conserved glutamate residue in PARP1 is replaced with isoleucine, leucine, or tyrosine in PARP4, which is associated with the absence of polymerase activity [61]. It was proposed that PARP4 may be involved in an antiviral response [28].

PARP5:

PARPs 5a and 5b (tankyrases) were initially identified as a part of a telomeric complex but are also located in the cytoplasm as peripheral membrane proteins localized to the Golgi complex and are associated with transport vesicles [6]. They are best known for their participation in mitosis and WNT signaling, but they also have functions in telomere and DNA damage repair [35]. Recently, a possible link between tankyrases and the DNA damage response has been proposed. On the one hand, tankyrases associate with DSBs to facilitate the recruitment of the CtIP–BRCA1 complex to damaged chromatin and to promote DNA end resection during homologous recombination (HR); on the other hand, tankyrases associate with DSBs to stimulate the recruitment of the BRCA1A complex (consisting of RAP80–BRCA1–BRCC36–CCDC98) mediated by MERIT40 and activate the G2–M checkpoint for promoting DNA repair before mitosis [62].

Other PARPs (6-16)

PARP6 has been found to be involved in hippocampus neuronal development [35]. Moreover, it plays a role in cell cycle progression and has been associated with the progression of colorectal cancer [28]. Of note, the biological activity of PARP6 depends on its catalytic activity as well as its N-terminal cysteine-rich domain [61]. Several PARPs (PARP7, PARP10, PARP12, and PARP13) are involved in the mechanisms of post-transcriptional regulation of mRNA; the latter process is mediated either by RNA-binding domains or by ADP-ribosylation of RNA-binding proteins [35]. PARP7, present in stress granules [6], is involved in antiviral effects, cytosolic RNA processing, and transcription [54]. PARP10 is a binding protein and an inhibitor of MYC [28] and has been implicated in the regulation of NF- κ B, GSK3B, and transcription [35]. PARP10 directly ADP-ribosylates NEMO. These events lead to the inhibition of nuclear localization of the p65 subunit of NF- κ B and to subsequent attenuation of NF- κ B–dependent gene expression [61]. PARP12 is a catalytically active cytosolic monoenzyme [62], which preferentially associates with the Golgi apparatus and regulates stress granule assembly, microRNA activity, and an antiviral response [28]. Intracellular expression of PARP12 increases upon stimulation by type II interferons, thereby leading to increased NF- κ B signaling, implicating PARP12 in cellular immune responses [61]. PARP13,



also referred as ZAP (zinc finger antiviral protein), has been so far regarded as a catalytically inactive ART with the roles in the assembly of stress granules and regulation of microRNAs, with consequent implications in innate antiviral defense and cancer [28, 62].

PARP9 and PARP14 are believed to act on transcription, especially the transcription of genes required for macrophage activation [35]. PARP9 possesses a unique MARYlating activity specifically targeting the ubiquitin peptides and participates in the DNA damage response, transcription in lymphocytes, and an antiviral response [28]. PARP14 has been implicated in multiple cellular functions such as survival of B cells, cell migration, assembly of stress granules, transcription during inflammation processes, the DNA damage response, and an antiviral response [28]. PARP14 regulates the class distribution, affinity repertoire, and recall capacity of antibody responses, which require efficient differentiation and interactions among B cells, T helper cells, and dendritic cells [61]. Concurrently with its nuclear pore localization, PARP11 modifies targets involved in the coordination of the nuclear envelope and organization of nuclear pores and nuclear envelope biology [28, 35]. PARP15 is a centrosomal PARP involved in stress granule formation, an antiviral response, cytosolic RNA processing, and tumor formation [28, 61]. PARP16 is located in the endoplasmic reticulum (ER) and regulates the unfolded protein response [28, 35]. Researchers found that PARP16 is a tail-anchored ER protein that is inserted into the ER membrane through a C-terminal transmembrane domain, whereas, the N-terminus of PARP16, which contains the catalytic domain, faces the cytoplasm. Moreover, both the PARP16 protein and its catalytic activity are required for the ER stress response because they regulate the unfolded protein response signaling pathway [61]. Cellular localization of other PARPs (PARP8 and PARP17) and their involvement in biological processes remain unknown.



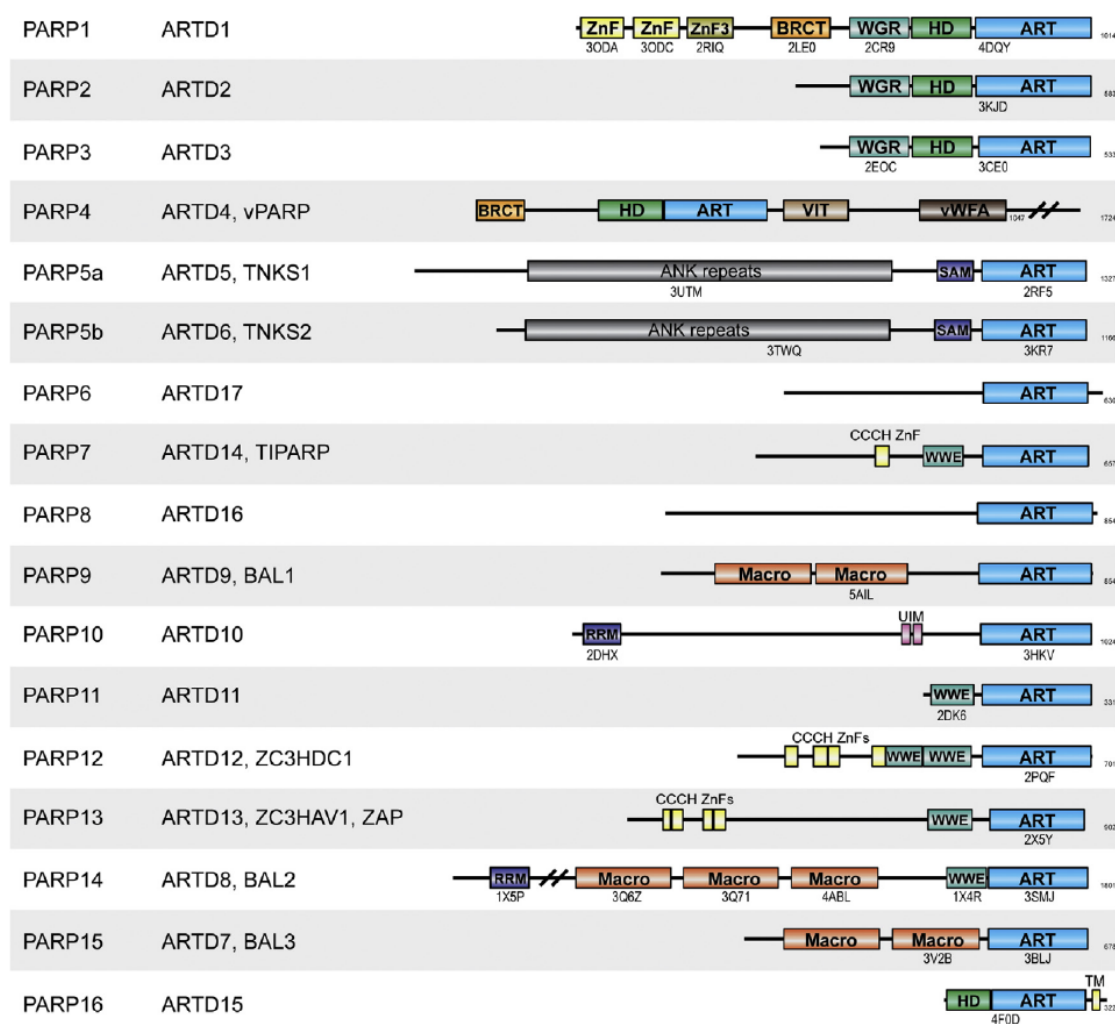


Figure 7: Schematic domain architecture of the seventeen members of human PARP superfamily. Adapted from *E.Barkauskaite et. al., 2005*.

Moreover, some PARP family members can interact with each other, e.g., PARP1 with PARP2 or PARP3 as well as tankyrase 1 with tankyrase 2 [47]. This type of heterodimers may occur in different subcellular compartments and act on different substrates, which monomeric PARPs could not otherwise target individually. This observation may highlight a new organizational order for PARPs that may greatly diversify their biological responses, via combinatorial interactions.

Excessive ADP-ribosylation can lead to the activation of cell death pathways, including parthanatos, a unique form of programmed cell death that occurs independently of caspases and is distinct from necrosis and apoptosis [63]. Due to its manifold role in cell survival, the protein PARylation process is finely regulated. PAR is rapidly degraded by PAR glycohydrolase (PARG), the main enzyme that specifically hydrolyses ribose-ribose bonds that is encoded by a single gene



in mammals [64]. Disruption of the *PARG* gene in mice causes embryonic lethality and studies of PARG-deficient cells have shown that accumulation of PARylated macromolecules is highly toxic to the cell [65, 66]. Nevertheless, PARG has rather limited processivity on short PAR polymers and unable to remove PARylation marks from proteins [67]. A complete reversal of PARylation is performed in human cells by amino acid-specific ADPr-acceptor hydrolases, such as macrodomain-containing proteins MacroD1 and MacroD2, terminal ADPr protein glycohydrolase 1 ((TARG1), and ADP-ribosyl hydrolase (ARH) family members ARH1 and ARH3 (reviewed in [68]).

Although the field was initially focused primarily on the biochemistry and molecular biology of PARPs in DNA damage detection and repair [59, 62, 69-77], the mechanistic and functional understanding of the role of PARPs in different biological processes has grown considerably of late. This has been accompanied by a shift of focus from enzymology to a search for substrates as well as the first attempts to determine the functional consequences of site-specific ADP-ribosylation on those substrates. Supporting these advances is a host of methodological approaches from chemical biology, proteomics, genomics, cell biology, and genetics that have propelled new discoveries in the field. New findings on the diverse roles of PARPs in chromatin regulation, transcription, RNA biology, and DNA repair have been complemented by recent advances that link ADP-ribosylation to stress responses, metabolism, viral infections, and cancer. These studies have begun to reveal the promising ways in which PARPs may be targeted therapeutically for the treatment of disease [61]. For a more detailed description of PARPs biological role, reader is referred to following reviews ([6, 26, 49, 54, 58, 61])



Table 2: Localization and Function of PARP Enzymes. *Adapted from Peter Bai, 2015.*

PARP Enzyme	Cellular Localization	Biological Process
PARP-1	Nucleus	Aging; antiviral effects; cell cycle regulation; chromosome structure; differentiation; DNA repair; inflammation; metabolic regulation; proteasomal degradation; RNA processing; transcription
PARP-2	Nucleus	Chromosome structure; DNA repair; cell cycle regulation; inflammation; metabolic regulation; transcription
PARP-3	Nucleus	Cell cycle regulation; DNA repair
PARP-4 (vPARP)	Nucleus; exosomes; cell membrane; spindle	cancer biology; vault biology
PARP-5a (TNK1)	Nucleus; telomeres; Golgi; cytoplasm	Antiviral effects; cell cycle regulation; cytosolic RNA processing; inflammation; metabolic regulation; mitotic spindle formation; telomere maintenance
PARP-5b (TNK2)	Nucleus; telomeres; Golgi; cytoplasm	Inflammation; metabolic regulation; telomere maintenance?
PARP-6	Cytoplasmic?	cell proliferation
PARP-7 (TiPARP)	Nucleus (?); cytoplasm (?)	Antiviral effects; cytosolic RNA processing; transcription
PARP-8	Unknown	Unknown
PARP-9	Nucleus; cell membrane; cytoplasm (?)	Cell migration; tumor formation
PARP-10	Nucleus; cytoplasm	Cell proliferation; transcription; cytosolic RNA processing; antiviral
PARP-11	Unknown	Unknown
PARP-12	Cytoplasm	Antiviral effects ; cytosolic RNA processing
PARP-13	Cytoplasm	Cytosolic RNA processing
PARP-14	Nucleus; cell membrane	Inflammation; metabolic regulation; nuclear RNA processing; transcription; tumor formation
PARP-15	Cytoplasm	Cytosolic RNA processing; tumor formation
PARP-16	Cell membrane; endoplasmic reticulum	Unfolded protein response



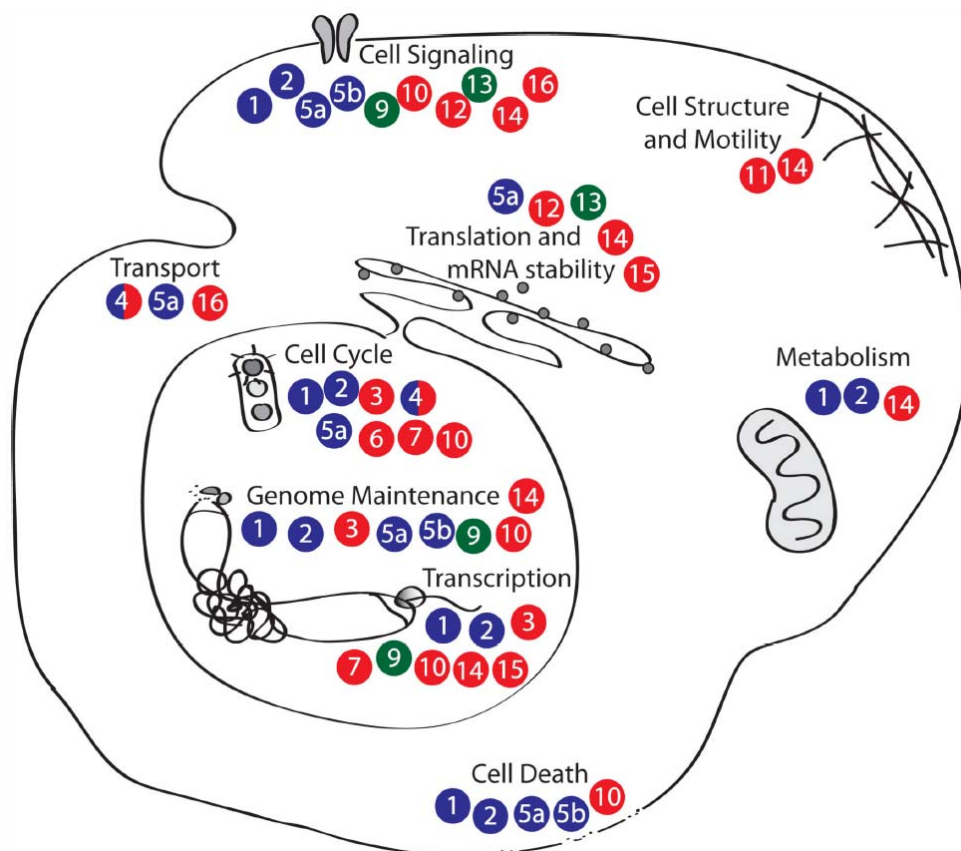


Figure 8: Schematic representation of the PARP family localization and function. PARPs have been linked to nearly all major cellular processes. Juxtaposition of protein identifiers (e.g. 1 = PARP-1) indicates the involvement of the protein in the regulation or execution of the cellular process. Enzymatic activity is indicated by the bubble color: blue = poly(ADP-ribose)transferase, red = mono(ADP-ribose)transferase, green = no transferase activity. *Adapted from Casey M. Daniels et al., 2015.*

V. PROTEIN ACCEPTORS FOR (ADP-RIBOSYL)ATION

Despite PARPs' different biological functions, over decades, little has been known about ADPr acceptors. Starting from the protein PARylation discovery, for ADP-ribosylated proteome analysis, researchers have applied chemical (high pH, hydroxylamine) or enzymatic sensitive methods (based on ARH1, PARG, ARH3, SVP, or NudT16) to quickly release the ADPr groups from modified residues. Hayaishi's group provided one of the first mechanistic insights into PAR synthesis. They demonstrated that in the rat liver, ADPr binds to histone H1 through an ester linkage with either a γ -carboxyl group of glutamic acid residue 2 or 14 or with an α -carboxyl group of C-terminal lysine residue 213 [78]. Linker histones H1 and H5 are known to be primary targets for PARP1-catalyzed PARylation, whereas PARP2 and PARP3 preferentially ADP-ribosylate core histone H2B [79-81]. PARP3 preferentially adds a mono ADPr moiety on Glu2 of histone H2B after DNA damage [80]. Until 2017, it had been generally thought that PARP-catalyzed auto-PARylation and ADP-ribosylation of other proteins occur predominantly on aspartates, glutamates, and lysines [82-84]. Nonetheless, conventional approaches have to overcome many limitations, such as the dynamic heterogeneous nature of protein ADP-ribosylation, low abundance, lability of some sites, and chemical or enzymatic resistance of other ADPr acceptor sites. The evolution of methods for the detection of MAR/PAR attachment sites has led to the use of mutagenesis assays as well as NAD⁺ analogs, unbiased enrichment strategies, chemotherapeutic PARP inhibitors, advanced mass spectrometry (particularly based on electron-transfer higher-energy collisional dissociation), and quantitative proteomic techniques [85-88]. Investigators have uncovered modification of more than 7000 ADP-ribosylation sites across more than 2000 ADP-ribosylation target proteins covering over one-third of the nuclear proteome under genotoxic stress conditions [88]. Upon DNA damage, serine (Ser) becomes the major ($\approx 90\%$) ADPr acceptor residue with the most easily identifiable signals related to the modification of histone proteins as well as PARP automodification [86, 88]. Histones are MARYlated selectively on serine residues of histone H3 (Ser10 and Ser28) and Ser6 of H2B unless the neighboring lysine residues are acetylated [86, 89]. Notably, Ser ADP-ribosylation sites strongly overlap with known kinase-regulated sites (Aurora B and others) [88]. ADP-ribosylation and phosphorylation of these serine residues are considered mutually exclusive [89], suggesting a complex interplay between histone marks. The major hydrolase responsible for the reversal of the Ser-ADPr modification is ARH3 [90, 91]. ARH3-deficient cells show a dramatic increase of PAR content in response to hydrogen peroxide exposure with induction of an AIF release from mitochondria and parthanatos [91, 92]. Moreover, the specificity of ADP-ribosylation is regulated by different factors. HPF1 (histone PARylation factor 1) interacts with PARP1 and PARP2 and guides the ADP-ribosylation of PARP1 and high-mobility group proteins



through a serine residue [85]. In HPF1's absence, acidic residues (Asp and Glu) become the main target sites for ADPr in proteins. Hundreds of ADP-ribosylation sites are also located on histidine, arginine, lysine, cysteine, and tyrosine residues [88, 89, 93]. It is still possible that further development of proteomic tools will allow researchers to detect new types of modifications, such as an acid-labile ADPr adduct of phosphoserine residues. This chimeric modification was noted in histones from the rat liver more than 40 years ago [94], but the enzymes responsible for its formation are still unknown. The diversity of ADPr substrate amino acids has revealed the importance of this PTM in cell signaling and survival and thus the necessity of its regulation.

VI. ACTIVATION OF DNA DEPENDENT PARPs

DNA is the template for the basic processes of replication and transcription. Human cell is subject to approximately 70,000 lesions per day, making the maintenance of genetic stability critical for viability [95, 96]. DNA damage can be categorized into two main classes based on its origin: endogenous (Oxygen radicals, Hydrolysis, Alkylating agents) and exogenous (Ionizing radiation, X-rays, Anti-tumor drugs, UV-light and chemicals). DNA damage is rapidly sensed and activates evolutionarily conserved signaling pathways, known collectively as the DNA-damage response (DDR), whose components can be separated into four functional groups: damage sensors, signal transducers, repair effectors, and arrest or death effectors [97]. DNA dependent PARPs subfamily is recruited to nicks and DSBs in genomic DNA in response to DNA damage and is a critical mediator of DNA damage repair [98, 99]. Majority of PARP proteins consist of multiple independent domains connected by flexible linkers [100]. PARP1 uses the two zinc finger domains ZnF1 and ZnF2 to bind with exposed bases at the DNA damage site [101], while PARP2 binding to damaged DNA consist on a short N-terminal domain that compensate the lack of zinc fingers [57]. DNA breaks sites binding and recognition induces the reorganization of PARPs domains structures, promoting extensive inter-domain contacts and allosteric activation, by unfolding of an auto-inhibitory helical domain (HD), which then allows NAD⁺ binding necessary for ADP-ribosylation activity [99, 100, 102, 103]. Notably, PARP-2 and PARP-3 require 5' phosphorylation at the DNA breaks for activation [56]. Contradictory hypothesis interprets the abundance of PARP1 enzyme in single macromolecule or in complex, taking into account the auto-ADP-ribosylation activity in presence or absence of DNA. One hypothesis claims that the auto-modification activity requires dimerization of PARP1 molecules, on the other hand, some researchers opposing views proposed monomeric recognition of the damaged DNA and cis(self)-PARylation reaction of PARP1 [104]. A study of Liu, L., et al indicates that PARP1 binds to DNA damage sites as a monomer; activated and in presence of NAD, PARP1 undergoes auto-PARylation [105], paradoxically a 2019 study of Kouyama, K., et al. provided data for the first structural evidence of dimeric full-length h-PARP1 with-



out DNA molecule. The tentative model suggested the dimer would represent a DNA-unbound configuration [104], moreover PARP1 has been shown to be able to dimerize and be activated at DNA breaks via formation of an intermolecular complex involving a protein-protein interaction between ZnF1 and ZnF2 domains from separate molecules [106].

VII. PARPs ACTIVATION AND INHIBITION VIA DNA INDEPENDENT PATHWAYS

As shown previously, PARP1-3 can be activated by specific DNA damages or particular types of DNA structure (hairpins, cruciforms and supercoiled DNA) [107, 108] (Table 3). Starting in the 2000, the role and physiological functions of PARPs had been enlarged by different studies showing that these proteins can act independently of the presence of DNA and can be activated by protein-protein interaction, post-translational modifications and also specific type of RNA structures [6, 54, 58, 109, 110]. In vitro, PARP1 was shown to be activated by its C-terminal domain association to nucleosome core histones (H1, H3 and H4) octamers lacking DNA [107, 111]. As well PARP1 has been shown to be activated by physical interactions with phosphorylated ERK an extracellular signal-regulated kinase that mediates growth and differentiation, CTCF a transcriptional repressor, known as CCCTC-binding factor, also with the nicotinamide mononucleotide adenylyltransferase1 (NMNAT 1) one of the PARPs substrate provider, with topoisomerase II during transcription or adipogenesis, with transcription termination factor (TTF) I-interacting protein 5 (TIP5 and BAZ2A) and recently with human tyrosyl tRNA synthetase (TyrRS) [8, 112-116]. Over and above physical interactions, PARP1 can be activated by different post-translational modification, such as its phosphorylation by ERK1/2 at Ser 372 and Thr 373 [117], by JNK1 at undetermined sites [118], and Cyclin-dependent kinase CDK2 [119] as well tankyrase can also bind IRAP (insulin responsive amino peptidase); phosphorylation by MAPK enhances the poly(ADPr) polymerase activity of tankyrase [120]. Moreover p300/CBP (histone acetyl transferases) or PCAF acetylation at Lys 498, Lys 505, Lys 508, Lys 521, and Lys 524 activates PARP1 [121, 122] as well as its SUMOylation by SUMO E3 ligase PIASg at Lys 203 and Lys 486 and ubiquitylation by ubiquitin E3 ligase RNF146 (Iduna) [110]. Recently it was shown that in addition to their physically association with PARP1, PARP3 and SIRT6 can both activate PARP1 by its mono-ADP-ribosylation at specific sites (Lysine 521) [123, 124]. The well-known methyltransferase SET7/9 was able to activate ARTD1 by its methylation at K508 in vitro and in vivo upon cellular stress [125]. In addition to PARP1 and Tankyrase, a new PARPs family member has been shown to be activated by a DNA damage independent way. By its SAP domain, ARTD2 bind RNA in nucleoli during genotoxic stress, activates and stimulates PAR formation [126].

Affecting different cellular pathways, most of these types of DNA independent PARPs activation are also finely regulated by the binding to specific loci or in reversible way. PARP 1 inacti-



vation was observed upon binding to the histone variant macroH2A1.1 [127] as well PARP-1 is inhibited by self-PARylation, deacetylase or sumoylation [54].

Table 3: DNA dependent and independent activation pathways of the PARP family masters (PARP1-3).

Type of activation	Activator	Activated PARP	References
Nucleic acids binding	non-B DNA structures (hairpins, cruciforms, and loops)	PARP1	[107, 108]
	DNA breaks: nicks, gaps, flaps, DSB	PARP1-3	[56, 98-100, 102, 103]
	small nucleolar RNA	PARP1	[128]
	Short rRNA and other single-stranded RNAs	PARP2	[126]
	PAR polymer	PARP2	[129]
Protein-Protein interactions	Nucleosomes and histones	PARP1	[130, 131]
	Phosphorylated extracellular signal-regulated kinases, ERK		[112]
	Nicotinamide mononucleotide adenylyltransferase 1, NMNAT1		[113]
	CTCF		[8]
	TET1		[132]
	TOPO2		[114]
	Bromodomain adjacent to zinc finger domain 2A, BAZ2A/TIP5		[115]
	Human tyrosyl tRNA synthetase, TyrRS		[116]
Post-translational modifications	phosphorylation at Ser372 and Thr373 (by extracellular signal-regulated kinases, ERK1/2)	PARP1	[117]
	phosphorylation at Tyr907 (by c-Jun N-terminal kinase, JNK1/ MAPK8)		[118]
	phosphorylation at Ser782, Ser785, and Ser786 (by cyclin-dependent kinase, CDK2)		[119]
	acetylation at Lys498, Lys505, Lys508, Lys521, and Lys524 (by E1A binding protein, p300/ CREB-binding protein CBP)		[121]
	acetylation of 1-214 and 477-525 aa regions (by P300/CBP-associated factor, PCAF)		[122]
	MARylation by PARP3		[123]
	MARylation at Lys 521 (by Sirtuin 6, SIRT6)		[124]
	phosphorylation at Thr420, Thr622, Thr656 (by checkpoint kinase 2, CHK2)		[133]
	methylation at K508 (by Histone-lysine N-methyltransferase, SET7/9)		[125]



VIII. READERS OF (ADP-RIBOSYL)ATED TARGETS

ADP-ribosylation is a PTM of proteins: it induces the recruitment of the protein (such as TET [134], p53 [135], NF- κ B [136]) or modulates its activity by covalent or noncovalent binding. Aside from protein modification, ADP-ribosylation is also involved in signaling as well as protein–protein or protein–DNA interactions [137]. PARylation as a PTM directly regulates many cellular pathways such as transcription, chromatin modification, and DNA damage and oxidative-stress signaling. Proteins may have a PAR- or MAR-recognizing domains that bind to PAR polymers or MAR moieties [49]. Depending on the nature of recognition, different proteins have different motifs. For instance, a PAR-binding motif (PBM) is believed to engage in an electrostatic interaction with negatively charged PAR chains [137, 138], whereas a PAR-binding zinc finger (PBZ) recognizes two consecutive ADPr moieties although some can also recognize only one ADPr of a PAR chain [139–141]. Similarly to PBZ, WWE requires two consecutive ADPr units for its successful binding; hence, it interacts with iso-ADPr formed by both ADPr units [142]. FHA (fork head–associated) and BRCT (BRCA1 C-terminal) are protein domains that are mostly known to interact with phosphorylated peptides but also have affinity for PAR chains [143]. The latter interaction seems to be similar to that of WWE domain or PBM, respectively. Another class of ADPr-recognizing domains is macrodomains. Unlike other domains, macrodomains interact with mono-ADPr or the terminal ADPr of PAR chains in the case of H2A1.1 [144]. There are also RNA- and DNA-binding motifs that unexpectedly recognize PAR ADPr moieties (Figure 9) [145].

8.1 The PBM

The consensus sequence of a PBM is ([HKR]-X-X-[AIQVY]-[KR]-[KR]-[AILV]-[FILPV]), i.e., approximately 20 residues. The positively-charged–amino acid content of a PBM allows for an electrostatic interaction with highly negatively charged PAR polymers. PBMs have been detected in more than 800 proteins *in silico*, and >500 hits have been obtained in proteomic analysis [137, 138]. PBMs are often found in many DNA damage response proteins and other proteins that are included in the ADPrDB database of ADP-ribosylated proteins [146], suggesting that PAR binding promotes PARylation. For example, tumor protein p53 (p53, TP53) can bind to PAR polymers both in a covalent or noncovalent manner. TP53 contains multiple PBMs. Hence, Fishbach *et al.* suggest that TP53 gets covalently PARylated upon a noncovalent interaction between a PBM located in a C-terminal domain of TP53 and PARylated PARP1 [135]. They demonstrated that noncovalent PAR binding diminishes the sequence-independent DNA-binding capacity of TP53. Nevertheless, simply having a PBM seems to be insufficient for PAR binding. Thus, the entire BRCT domain of



XRCC1—rather than a short PBM—is required for its affinity for PAR [143].

8.2 The PBZ

The PBZ is a C2H2 zinc finger domain consisting of approximately 30 amino acid residues. The PBZ domain has a consensus sequence of [K/R]-X-X-C-X-[F/Y]-G-X-X-C-X-[K/R]-[K/R]-X-X-X-X-H-X-X-X-[F/Y]-X-H and so far has been discovered in three proteins: APLF (aprataxin and PNK-like factor), CHFR (checkpoint with forkhead-associated and ring domain), and CTCF [145]. Unlike CHFR, APLF contains two PBZ domains. Accordingly, one of the two PBZ domains identified in the APLF protein interacts with two consecutive ADPr units, whereas the second PBZ domain is thought to bind to the 3rd ADPr unit likely on a branched PAR polymer or terminal poly-ADPr. The PAR recognition by APLF induces its histone chaperone activity for the release of histones H3 and H4 and chromatin relaxation [129, 147].

8.3 Macrodomains

Macrodomains are mono-ADPr-recognizing domains [144]. One of the well-studied macrodomains is histone variant macroH2A1.1. In addition to MAR, macroH2A1.1 can recognize PAR polymers via their terminal ADPr unit. MacroH2A1.1 participates in metabolic regulation and energy production by inhibiting PARP1 activity and decreasing its nuclear NAD⁺ consumption [148]. MacroH2A1.1–PARP1 interaction is also involved in gene regulation, for instance, in the response to heat shock stress and during expression regulation of senescence-associated secretory phenotype genes or genes participating in adipocyte differentiation and metabolic regulation during muscle differentiation [149]. Another macrodomain-dependent chromatin-remodeling factor is ALC1. This is an inactive ATPase and one of the chromatin remodelers that activates upon DNA damage. During DSB repair, MacroH2A1.1 [150] and ALC1 [151] take part in chromatin remodeling in a macrodomain-dependent manner. PARP family members PARP9, PARP14, and PARP15 have both the MARYlation activity and a macrodomain interacting with MAR [144, 152, 153]. PARG, TARG1, and MACROD1–3 ADPr-hydrolases also contain macrodomains [154].

8.4 The WWE domain

This domain contains two conserved tryptophans and a glutamic acid residue, hence its name, and in total is approximately 80–100 residues long [155, 156]. It recognizes iso-ADPr moieties between two consecutive ADPr units. For instance, E3 ubiquitin-protein ligase RNF146 (a.k.a. Iduna) is one of the first proteins found to have a WWE PAR-binding domain [142]. It has been clearly demonstrated that the WWE domain specifically recognizes ribose–ribose glycosidic bonds within a PAR polymer, not a single ADPr unit [142]. The WWE domain is reported to be present mostly in E3 ubiquitin-protein ligases (DELTEX1, DELTEX2, DELTEX4, and HUWE1) and in two PARPs (PARP11 and PARP14) [142].



8.5 FHA and BRCT domains

These domains play a huge part in cellular responses to DNA damage by recognizing phosphorylated peptides [157, 158]. It has also been discovered that FHA and BRCT domains can recognize PAR polymers. Similarly to the WWE domain, the FHA domain binds iso-ADPr of PAR chains by recognizing the two phosphate groups on ADPr moieties, whereas the BRCT domain directly recognizes ADPr of a PAR chain [143]. The latter phenomenon is possibly due to the phosphate groups on ADPr, which mimics the phosphorylated serine residue recognized by the BRCT domain [159]. ADPr recognition by an FHA or BRCT domain facilitates rapid recruitment of DNA damage response proteins: PNKP and aprataxin by the FHA domain and ligase IV, XRCC1, and the BRCA1–BARD1 complex by the BRCT domain [143, 159-161]. For example, aprataxin contains three domains, which are all necessary for its DNA adduct detection and catalytic activity: the FHA, PAR-binding and protein–protein interaction domain; the HIT (histidine triad) catalytic domain; and the C2H2-type zinc finger DNA-binding domain [143, 162]. Aprataxin catalyzes the release of adenylate groups covalently linked to 5'-phosphate termini, resulting in the formation of 5'-phosphate termini that can be efficiently ligated [163]. Aprataxin interacts with XRCC1 and XRCC4, which are needed for ligases III and IV, respectively, to finalize the repair of DNA damage (BER and NHEJ, respectively) by ligation [163]. In addition to XRCC1, aprataxin interacts with PARP1, which promotes the recruitment of aprataxin to the sites of DNA breaks [164, 165].

8.6 RNA- and DNA-binding motifs (RRM, SR repeat- and KR-rich motif, OB fold, PIN domain, and GAR domain)

Of note, RNA- and DNA-binding motifs can also bind to PAR. Although this is not very surprising because PAR chains have a structure similar to that of oligonucleotides. NONO, an RNA-binding protein, is believed to increase survival during DSB repair although its function is not yet clear; its recruitment is PARP1 dependent. RRM (RNA recognition motif) of NONO recognizes PAR, thereby facilitating the recruitment of NONO to a DNA damage site [166].

It has been shown that splice factors ASF/SF2, SF3A1, SF3B1, and SF3B2 can recognize PAR chains via their SR (serine/arginine) repeats [167, 168]. PAR binding to splicing factor ASF/SF2 inhibits its phosphorylation by TOPOI (DNA topoisomerase I) and activity [167], indicating the involvement of PARPs and PAR chains in RNA stability and metabolism [169]. In a similar context, upon heat shock, KR (lysine/arginine)-rich repeats of the *Drosophila* Mi-2 protein bind PAR chains thus leading to Mi-2 recruitment to heat shock–responsive genes [170]. Recently, it was also proven that a homolog of Mi-2, human chromodomain helicase DNA binding protein 4 (CHD4), which is a component of chromatin-remodeling complex NuRD (nucleosome remodeling deacetylase), has PAR-binding properties. Of note, the PAR-recognizing domain is in the N-



terminal region of CHD4 that has structural similarities to a DNA-binding module called the high-mobility group (HMG) box [171, 172].

Oligonucleotide/oligosaccharide-binding fold (OB fold) is an ssDNA- and RNA-binding motif. The OB fold in human ssDNA-binding protein 1 (hSSB1) is reported to also serve as a PAR-binding motif (in addition to its ssDNA-binding ability), mediating this protein's translocation to a DNA damage site and an interaction with other DNA damage repair proteins. Just as WWE and FHA domains, the OB fold recognizes iso-ADPr of PAR chains [173].

Proteins with PIN (PiIT N terminus) domains are mostly nucleases cleaving ssDNA or ssRNA [174]. Exo1 is one of PIN domain-containing exonucleases in eukaryotes and cleaves ssDNA in the 5'-to-3' direction [174]. Exo1 is an enzyme essential for cellular responses to DNA damage and DNA replication [175]. In particular, during DNA damage repair, the PIN domain of Exo1 was found to recognize DNA damage-induced PARs, and this even is rather sufficient for its recruitment to the DNA damage site [176].

GAR (or RG/RGG box) is another PAR-binding domain and consists of a sequence enriched in arginine and glycine. Cold-inducible RNA-binding protein (CIRBP) has both a C-terminal GAR domain and an N-terminal RRM motif. Although CIRBP belongs to the family of RNA-binding proteins, it performs an important function in genomic stability and DNA repair. It has been suggested that upon DNA damage, the GAR domain recognizes DNA damage-dependent PARs and mediates the association of the ATM-MRN complex with chromatin [177]. There are several other RNA-binding proteins with GAR domains known to recognize PAR chains during DNA damage responses, e.g., FUS/TLS, EWS/EWSR1, and TAF15 [145].



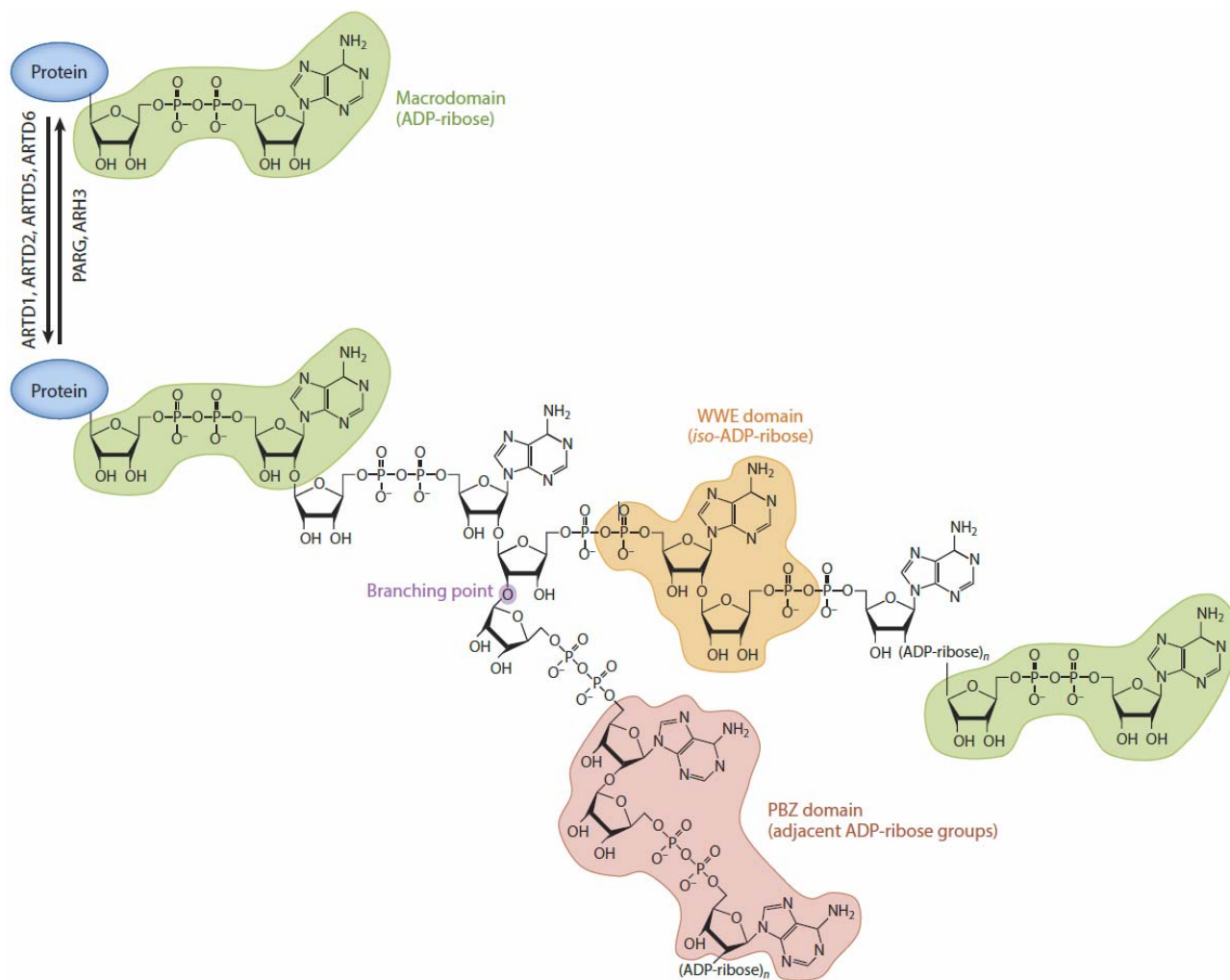


Figure 9: Schematic of protein ADP-ribosylation and binding specificities of the various domains that recognize the different parts of the modification. Abbreviations: ARTD, diphtheria toxin-like ADP-ribosyltransferase; PARG, poly-ADP-ribose (PAR) glycohydrolase; PBZ, PAR-binding zinc-finger; WWE, tryptophan–tryptophan–glutamate. *Adapted from Michael O. Hottiger, 2015.*

IX. REVERSIBLE (ADP-RIBOSYL)ATION OF DNA STRAND BREAKS

The first evidence of DNA ADP-ribosylation was obtained 20 years ago. Watanabe's group demonstrated that a cabbage butterfly toxin, pierisin, induces apoptosis via irreversible MARylation of a guanine base in DNA [178, 179]. Later, other examples of DNA MARylation have been demonstrated for different families of toxins: guanine MARylation by CARP-1 from shellfish [10] and by scabin from *Streptomyces scabies* [180] as well as thymine MARylation by DarT from bacterial toxin–antitoxin system DarTG [11].

Recently, *in vitro* studies in our laboratory have uncovered that mammalian DNA-dependent PARPs catalyze reversible modification of DNA via ADP-ribosylation of terminal phosphates at DNA strand breaks [12]. This finding provides novel molecular insights into PARPs' functions in mammalian cells. Taking into account an unsolved challenge (how to distinguish ADPr adducts on proteins and DNA in the cell), DNA ADP-ribosylation studies have been focused on *in vitro* approaches to gain knowledge about the mechanisms and specific requirements for this unusual substrate specificity of PARPs. It has been found that PARP1 preferentially PARylates DSBs containing 5'- and 3'-terminal phosphates in gapped recessed DNA duplexes, whereas PARP2 and PARP3 preferentially act on 5'-terminal phosphates at DSB and SSB termini of DNA containing multiple proximal breaks [12, 13, 43]. Similarly to protein modification, PARP3 produces a MAR not PAR adduct on DNA substrates, in contrast to PARP1 and PARP2 [13, 43]. In addition to phosphate groups, PARP1 can PARylate 2'-OH groups of 3'-deoxynucleotide and ribonucleotides incorporated at the 3' terminus of oligodeoxyribonucleotides [12]. A recent study by Zarkovic G. et al. revealed ADP-ribosylation of ~3 kb plasmid-based DNA constructs, thus indicating DNA size limitlessness of PARP-mediated modifications of DNA break termini [13]. Moreover, PARP2 and PARP3 switch their substrate preference to DNA from protein when acting upon certain configuration of closely spaced DNA strand breaks, preferentially ADP-ribosylating DNA rather than catalyzing auto-ADP-ribosylation. Effectiveness of PARP3- and PARP2-catalyzed DNA ADP-ribosylation depends on the orientation and a distance between DNA strand breaks in a single DNA molecule [13]. According to a proposed mechanistic model (Figure 10), binding of a PARP to one DNA break activates the CAT domain, which in turn targets and ADP-ribosylates an acceptor group at the second breakage site of the same DNA molecule [12, 13]. This process necessitates the presence of at least two DNA strand breaks separated by a distance from 1 to 2 helix turns [13]. In a DNA-bound PARP complex, this distance determines the accessibility of the DNA acceptor groups for the activated CAT domain directing ADP-ribosylation to a 5'- or 3'-terminal phosphate. At present, little is known about the mechanisms governing substrate interaction and specificity of PARP1, which accounts for most of cellular PARylation activity. Moreover, it remains unclear how can PARPs adopt the conformation which predisposes to DNA ADP-ribosylation activity. According to existing structural data on PARP1 and PARP2 bound to DNA breaks, the



PARP's DNA-binding domain is far from its CAT domain, which is not oriented along the DNA helix [55, 100, 102]. Nevertheless, broad substrate specificity in *trans*, including also auto-modification of different amino acid residues in *cis*, and the multidomain structure of PARPs imply high flexibility of the CAT domain position in DNA–PARP complexes. Therefore, there may be some unexplored abilities to target substrates including formation of oligomeric protein complexes on DNA.

Effective DNA-PAR/MARylation occurs on DNA substrates that mimic intermediate products occurring in various DNA excision repair pathways such as base excision repair (BER), nucleotide excision repair (NER), mismatch repair (MMR), HR and nonhomologous end joining (NHEJ). For example, DNA strand break acceptor sites containing 5'-phosphates can be generated by the action of various DNA exo- and endonucleases, tyrosyl-DNA phosphodiesterase 2 (TDP2) and dRP (5'-deoxyribose phosphate) lyase activity of bifunctional DNA polymerases, whereas 3'-terminal phosphates are produced by certain bifunctional DNA glycosylases, TDP1 and MRE11 [181, 182]. DNA duplexes containing a DSB and a proximal SSB can form in HR and NHEJ repair pathways. It has been reported that a stably blocked replication fork can switch the endonuclease activity of MRN–CtIP complex on and produces an internal nick located ~20 nt downstream of 5'-termini of a DSB [183], thus ensuring proximity of activating and acceptor sites required for DNA ADP-ribosylation activity of PARPs.

At present, the physiological relevance of PARP-dependent DNA ADP-ribosylation is a debated issue. Nevertheless, a dramatic substrate switch of PARPs observed *in vitro* assays, the highly efficient PARP1-catalyzed DNA PARylation in human cell-free extracts and the presence of a PAR signal in purified genomic DNA after genotoxic treatment provide the strong albeit indirect evidence of the presence of PAR–DNA adducts in live cells [13, 184]. Furthermore, it has been shown that 1 nt gapped DNA containing a MARylated 5'-phosphate residue is recognized as a 5'-adenylated DNA substrate by DNA ligase I or IIIa or by other DNA ligases and ligated in the absence of ATP, resulting in the sealed unbroken double-stranded DNA with an aberrant abasic (AP) site-like residue [184]. Such residue can be processed further by apurinic/apyrimidinic endonuclease 1 (APE1) in BER pathway. In line with these results, it has been proposed that PARP2 and PARP3 are involved in the final ligation step of NHEJ, judging by the finding that 5'-phosphorylated nicks are especially efficient activators of the auto-ADP-ribosylation activity of PARP2 and PARP3 but not that of PARP1 [56]. We can hypothesize that DNA ADP-ribosylation can promote retention of the DSB ends either until a complete repair complex is formed or until the ATP concentration required for DNA ligation is restored. Similarly, in case of SSB repair, PARP-mediated ADP-ribosylation can promote the ligation of a gap without polymerase synthesis and ATP. Of note, extensive PARP-mediated PAR synthesis leads to inhibition of hexokinase 1 activity, blockage of glycolysis, and



ATP loss [185]. Thus, one of the functions of DNA ADP-ribosylation can be the patching of DNA breaks during bioenergetic collapse avoiding formation or degradation of toxic DSBs.

Recent advances in RNA biology took the phenomenon of ADP-ribosylation to another level. Studies by Shuman's group have revealed that PARP-like tRNA splicing enzymes Tpt1 (KptA) from bacteria and fungi can ADP-ribosylate RNA and DNA at 5'-monophosphate termini [186, 187]. Further studies by Ahel's laboratory have shown that Tpt1 homologs in higher organisms TRPT1 (PARP18) as well as human PARP10, PARP11, and PARP15 can MARylate phosphorylated ends of RNA [14]. This 5'-phospho-ADPr modification or "capping" of RNA termini may protect RNA substrates from degradation or dephosphorylation and mediate ADP-ribosylation signaling via recruitment of specific cellular factors. Overall, these RNA related studies provide additional evidence that the phenomenon of ADP-ribosylation of nucleic acids at terminal phosphates is more widespread than previously thought (Table 4).

Table 4: Writers and erasers of nucleic acids ADP-ribosylation in different species.

ADP-ribosyl transferases	Species	Substrate	Acceptor groups	Type of modification	Erasers
Pierisins and CARP-1	Cabbage Butterfly and shellfish	dsDNA	guanine nucleobase	MAR	-----
DarT	Bacteria	ssDNA	2nd thymidine in TNTC motif	MAR	DarG
PARP1	Human	dsDNA and ssDNA	terminal 5'- and 3'-phosphates, 2'OH	PAR	PARG, TARG1, ARH3, MACROD1, MACROD2 and MACROD-like hydrolases
PARP2	Mouse	dsDNA	terminal 5'- and 3'-phosphates	PAR	
PARP3	Human	dsDNA	terminal 5'- and 3'-phosphates	MAR	
TRPT1 (Tpt1)	Human, fungi and bacteria	RNA and ssDNA	terminal 5'-phosphate	MAR	
PARP10, PARP11 and PARP15	Human	RNA	terminal 5'-phosphate	MAR	



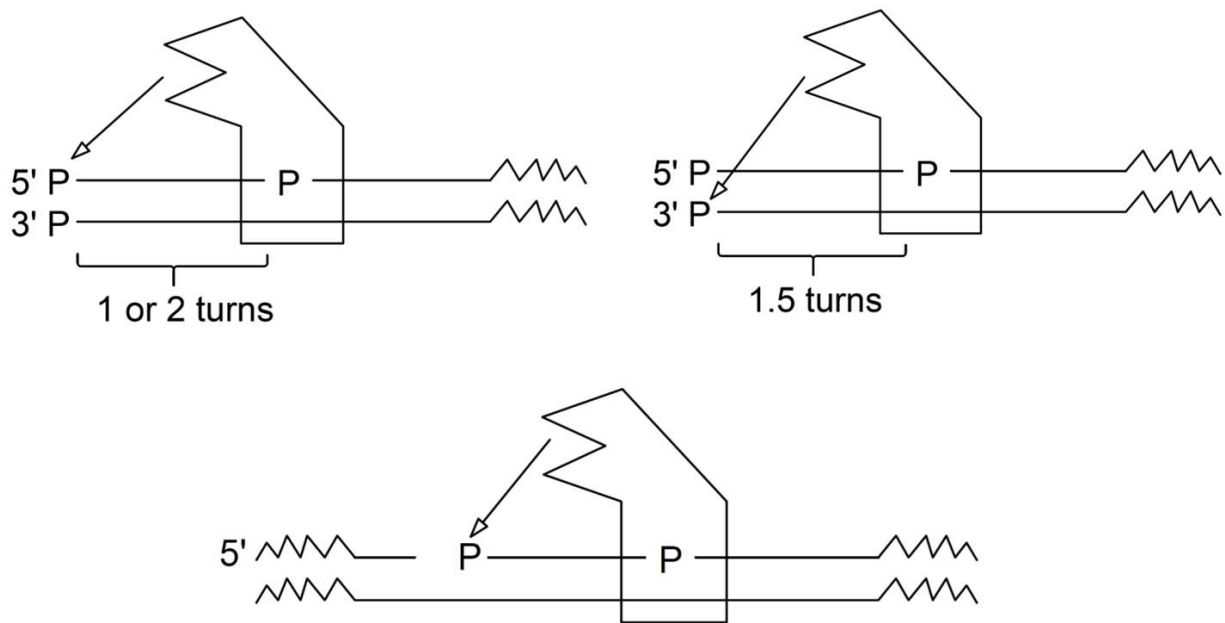


Figure 10: The mechanism of DNA-ADP-ribosylation and DNA substrate specificity of the PARP2 and PARP3 proteins.

X. (ADP-RIBOSE) removal from PROTEINS AND DNA BREAKS

Like any other post-translational modification, PAR levels are tightly controlled in the cell, and after the suitable cellular response has been achieved, ADP-ribosylation signaling has to be quenched appropriately and in a timely manner, and the ADP-ribose building blocks subsequently recycled. Such regulation is achieved not only by directly regulating PARPs (as discussed below), but also by the timely degradation of ADP-ribosylation by specialized ADPr processing enzymes (Table 5) [188].

Due to the presence of different ADP-ribose acceptor sites, different “eraser” activities (with different subcellular localizations) have been shown to contribute to the dynamic turnover of ADPr [6, 61], shifting the attention towards the biological roles of ADPr erasers. Recent advances in defining ADPr metabolism suggest that the balance between ADPr writers and erasers is crucial for the coordination of multiple cellular response pathways such as PAR-binding proteins recruitment and release, as well as transient signaling and the formation of transient sub-organellar structures in the cytoplasm and nucleus [58, 68].

The inability of PARG, the main de PARylating enzyme, to remove MARYlation marks and its limited processivity on short PAR polymers, leaves room for the involvement of other erasers (Table 5). A complete reversal of MARYlation is performed in human cells by amino-acid-specific ADPr-acceptor hydrolases, such as the macrodomain-containing proteins MacroD1 and MacroD2, the terminal ADPr protein glycohydrolase 1 (TARG1), and the ADP-ribose hydrolase (ARH) family members ARH1 and ARH3 [68].

Table 5: Human ADP-ribose erasers. *Adapted from Julia O’Sullivan et. al., 2019.*

Eraser	Classification	Substrate	Targeted bond	ADP-ribosylation reversal	Protein adduct	Amino acid selectivity
PARG	Macrodomain	PAR	O-glycosidic	Partial	ADP-ribose	Linkage-independent
MacroD1	Macrodomain	MAR	Carboxyl ester	Complete	None	D/E
MacroD2	Macrodomain	MAR	Carboxyl ester	Complete	None	D/E
TARG1	Macrodomain	MAR/PAR	Carboxyl ester	Complete	None	D/E
ARH1	ARH fold	MAR	N-glycosidic	Complete	None	R
ARH3	ARH fold	MAR/PAR	O-glycosidic	Complete	None	S
NUDT9	NUDIX	PAR	Phosphodiester	Partial	Phosphoribose	Linkage-independent
NUDT16	NUDIX	MAR/PAR	Phosphodiester	Partial	Phosphoribose	Linkage-independent
ENPP1	ENPP (PDNP)	MAR/PAR	Phosphodiester	Partial	Phosphoribose	Linkage-independent

Moreover, several phosphodiesterases have been shown to possess ADPr processing activity [68]. In this section, we provide an overview of these different ADPr erasing enzymes. ADPr chain can be degraded by different enzymes at different levels of the chain (Figure 11-12). The main group of enzymes with PAR-degrading activity is described below.



10.1 Poly(ADP-ribose) glycohydrolase (PARG)

PARG is the major de-PARylating enzyme, and is primarily responsible for hydrolyzing the glycosidic linkages (2'-1" glycosidic ribose-ribose bonds) between ADPr units of PAR polymers to generate free ADPr monomers but does not hydrolyze the protein-bound ADPr, leaving a MARYlated protein [68]. [189-191]. Despite the lower abundance of cellular PARG compared to PARPs, higher specific activity of PARG allow for rapid turnover of PAR, ensuring tight control of this modification [188]. Human PARG is a constitutively active and possesses both exoglycosidase and endoglycosidase activities. PARGs preferably bind PAR at the chain termini and primarily act as exoglycohydrolases, sequentially digesting glycosidic linkages from the protein-distal end of the polymer similar to carbohydrate glycosyl hydrolases. This processivity improves the catalytic activity of PARG but is strongly chain-length dependent [68, 188]. While binding along the PAR chain and endo-glycohydrolytic cleavage of PAR is structurally possible, it appears to be less efficient. The endoglycohydrolytic activity may have co-evolved with Human PARP1 enzymes that catalyse more complex branched polymers, but is markedly slower than that of elongated ADPr units [58, 188]. Human PARG is composed of three domains: two of these domains, namely macrodomain and the PARG accessory domain, make up the minimal PARG catalytic region, while the third domain, which shows significantly less sequence conservation, is the putative PARG regulatory region (not important for PAR hydrolysis in vitro) The key difference between PARG and the non-catalytic macrodomains, is the "insertion" of a PARG unique catalytic loop in the otherwise conserved globular macrodomain fold. This loop bears the highly conserved GGG-X6-8-QEE PARG signature sequence, which contains the catalytic residues essential for PAR degradation activity [188]. Only a single PARG gene has been identified in mammals and its sequence is highly conserved [68]. PARG isoforms can be obtained by alternative splicing of that single gene: the nuclear full-length isoform (110 kDa), two shorter isoforms (102 and 99 kDa) which are mainly cytoplasmic, a PARG isoform of ~59 kDa, which is probably constitutively active, and a mitochondrial 55-kDa protein [64, 192, 193]. Interestingly, the cytoplasmic 102-kDa PARG isoform translocates to the nucleus, whereas the full-length isoform relocalizes to the cytoplasm in response to DNA damage [194]. PARG mRNA also undergoes additional alternative splicing that generates small isoforms of 55 and 60 kDa. Both hPARG55 and hPARG60 isoforms have been found to be catalytically inactive due to the absence of exon 5-encoded amino-acids. Therefore, these small human PARG isoforms are not involved in general PAR turnover in cells [68].

Nuclear and cytoplasmic compartmentalization, and the shuttling of PARG isoforms between the nucleus and cytoplasm have been proposed as a mechanism to regulate cellular PAR levels [68]. PARG participates in a number of biological processes, including the repair of DNA damage,



chromatin dynamics, transcriptional regulation, cell death, and tumorigenesis, but its specific roles in biological systems remains to be determined (better reviewed in [68]).

Overall, these examples show that the dynamic equilibria established between PARP-1 and PARG activities, and therefore PAR levels, are key for controlling cell fate, suggesting that PAR erasers are as important as PAR writers for cellular homeostasis.

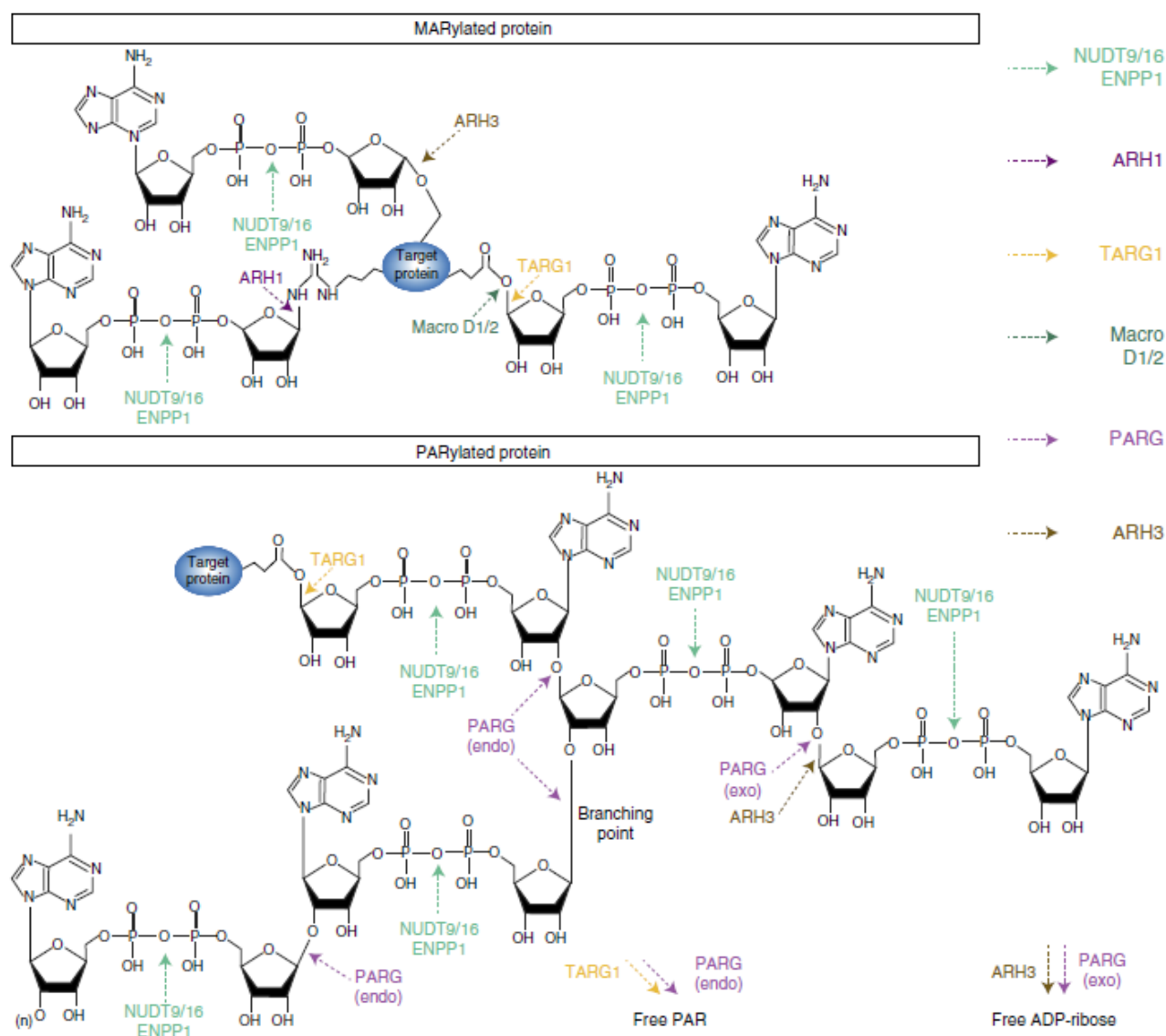


Figure 11: Reversal of protein ADP-ribosylation by MAR and PAR erasers. The diagrams represent MARylated (upper panel) and PARylated proteins (lower panel) with bond-specific chemical cleavage sites for each eraser. A subgroup of erasers that comprises MacroD1, MacroD2, and ARH1 are MAR-specific erasers involved in the removal of single ADPr adducts. MacroD1 and MacroD2 are macrodomain-containing enzymes that release ADPr from ADP-ribosylated acidic residues (aspartate and glutamate). ARH1 is currently the only known MAR hydrolase that specifically removes MAR from arginine residues. A second subgroup that includes

TARG1, ARH3, NUDT9, NUDT16, and ENPP1 can target both MAR and PAR modifications. The TARG1 macroprotein hydrolyzes glutamate-ADP-ribose bonds and releases ADPr from MARYlated proteins. TARG1 has also the unique ability to remove entire PAR chains from acidic residues of PARYlated proteins. ARH3 is limited to exoglycosidic activity toward PAR chains and releases free ADPr. In addition, it possesses MAR hydrolase activity specifically targeting the O-linked ADP-ribosylation. NUDT9 and NUDT16 have nucleoside diphosphatelinked moiety-X (NUDIX) domains, which cleave pyrophosphate bonds and release phospho-ribosyl-AMP from PAR chains or AMP from MARYlated proteins as major reaction products. ENPP1 is a pyrophosphatase lacking a NUDIX domain but with the capability of digesting PAR and MAR modifications similar to NUDIX enzymes. PARG is the main PAR-degrading enzyme but shows no activity towards MARYlated proteins. Human PARG is unable to cleave the proximal ADPr groups from a modified protein but possesses exo- and endoglycosidic activities to hydrolyze the glycosidic bonds between ribose units of PAR. The exoglycosidic activity of PARG generates free ADPr from the processive degradation of PAR from the distal to the proximal end while its in-chain cleavage activity (endoglycosidic) produces protein-free PAR. The endoglycosidic degradation of PAR by of PARG is also responsible for the hydrolysis of the branching points formed when non-adenine riboses are linked together (branching point). *Adapted from Julia O'Sullivan et. al., 2019.*

10.2 ADP-ribose hydrolases (ARHs)

The ADPr hydrolase (ARH) family consists of three related proteins ARH1, ARH2 and ARH3. The three members of the ARH family are related to dinitrogenase-activating glycohydrolase (DRAG). Protein sequence alignment revealed that human ARH1 and ARH2 are 45–47% identical but only ~22% identical to ARH3. Overall, ARH3 is closer to the catalytic region of the 110-kDa PARG (19% identity) than to ARH1 or ARH2 (10% and 13% identity respectively) [68, 195]. Substrate specificity also varies among ARHs. While ARH2 substrates are yet to be discovered, ARH1 is a highly active (ADP-ribosyl)-arginine hydrolase (cleaves the N-glycosidic bond linking ADPr to the guanidino group of arginine) and ARH3 is an (ADP-ribosyl)-serine hydrolase (hydrolysis of the O-glycosidic bond in PAR) [68, 196, 197].

ARHs have different cellular localization: ARH1 and ARH2 are localized in the cytoplasm, ARH3 is located mainly in the cytoplasm, but is also found in the mitochondria and the nucleus [196]. They both recognize the ADPr moiety of the substrate and are competitively inhibited by ADPr, but not ribose 5-phosphate, AMP, ADP or NAD⁺. On the other hand, nor ARH1 nor ARH3 hydrolyze ADP-ribosylated cysteine, asparagine, and diphthamide, synthesized by bacterial toxins [195-197]. In addition to PAR chains, ARH3 also can remove the O-acetyl group from the NAD⁺ metabolite O-acetyl-ADP-ribose [198] and can remove ADP-ribosylation in the mitochondrial matrix [199]. Although ARH2 binds ADPr, it has not been shown to act on neither any of these ADP-ribosylated residues nor on poly-ADPr.

In contrast to ARH1, ARH3 also possesses activity toward the O-glycosidic bond of PAR, similar to the exoglycosidic activity of PARG. However, ARH3 does not rescue *Drosophila* or mouse genetic knockouts of PARG from cell death or PAR accumulation, suggesting that it cannot compensate for the loss of PARG [68].



ARH1-mediated mono-ADP-ribosyl arginine hydrolase activity is involved in intracellular signal transduction, has a crucial role in cell proliferation and cancer suppression (loss of function of ARH1 was strongly correlated with tumorigenesis) and also seems to be involved in estrogen-stimulated tumorigenesis [196]. ARH3 also participates in nuclear and cytoplasmic PAR degradation under oxidative stress conditions induced by hydrogen peroxide [92], which avoids PAR accumulation in the cytoplasm, release of AIF from mitochondria and the consequent AIF-mediated cell death. Thus, ARH3 serves as a suppressor of PARP-1-dependent cell death, parthanatos, under oxidative stress [68, 92].

10.3 Macrodomain-containing ADP-ribose erasers.

The macrodomain fold is an evolutionarily conserved, compact globular shaped structure of ~25 kDa present throughout all of the biological kingdoms. It can be found as a stand-alone module or integrated into multi-domain proteins. The macrodomain was the first characterized ADP-ribose-binding module. It can bind terminal ADPr structures with nanomolar affinity. There is functional diversity related to structural variation in the macrodomain protein family. In addition to their ability to recognize and bind PAR/MAR attached to ADP-ribosylated proteins, a subset of macrodomains exhibit enzymatic activity. The enzymatically active macrodomain proteins are involved in different processes such as transcriptional regulation, cellular signaling, or neurodegeneration [68, 200].

Three human macrodomain-containing proteins: macrodomain-containing protein 1 (MacroD1), macrodomain-containing protein 2 (MacroD2), as well as C6orf130 (TARG1), are known to hydrolyse o-acetyl-ADPr. Studies on the enzymatic activities of their macrodomains have shown that all three can also hydrolyze ADPr attached to target proteins, and that this activity is dependent on macrodomains. Further studies led to the characterization of MacroD1, MacroD2, C6orf130, as well as bacterial Af1521, as glutamate-specific mono-ADP-ribosyl hydrolases and MDO2 have been reported to revert ARTD10-catalyzed MARYlation on histones and GSK3 β [152, 154, 201, 202]. The ability of TARG1 to remove whole PAR chains from the substrate most proximal attachment point is unique among the known erasers, adding another putative regulatory layer to PAR cellular functions [68]. Similarly to TARG1, the mono-ADP-ribose hydrolase activities of MacroD1 and MacroD2 are also selectively directed toward ester bonds established by ADP-ribosylated aspartate and glutamate residues, although with different catalytic modes. Current experimental data suggest that ester-type ADPr bonds in protein substrates are specific targets of the macrodomain erasers.

MDO1, MDO2 and C6orf130 preferentially localize to the mitochondria, cytoplasm, and nucleus, respectively, and are recruited to DNA damage sites via their biochemical capacity to bind ADPr [203]. In vivo, MacroD2, has been implicated in the recycling of automodified PARP1. The removal of the autoinhibitory MAR moieties from PARP1 by MacroD2 has been suggested



to explain the accumulation of MARylated PARP1 in the context of MacroD2 gene deletion in human colorectal cancer cells. The underlying MacroD2- dependent PARP1 recycling model proposed by Sakthianandeswaren et al. involves a biphasic erasing of PARP1 automodification, which implicates PARG as the primary PAR trimming enzyme responsible for the generation of MAR adducts that can subsequently be targeted by MacroD2. As mentioned above, PARG is a member of the macrodomain eraser family, although there is no similarity between the amino acid sequence of PARG and other macrodomain-containing proteins. However, there is a close structural and evolutionary relationship between macrodomains and PARG, and its catalytic center is essentially a macrodomain fold [68].

10.4 Phosphodiester ADP-ribose hydrolases.

Homopolymers of PAR are composed of successive ADPr moieties linked together by alternating phosphodiester and O-glycosidic linkages. The phosphodiester bond is also central to the ADPr monomer itself as it links the adenosine structure to the ribose. The activity of snake venom phosphodiesterases was instrumental in the elucidation of PAR structure in the early studies of PARylation, as it was used to determine chain length and PAR branching frequency [204]. Only recently, a role of phosphodiesterases in the reversal of ADP-ribosylation has been proposed, following the discovery of a group of ADPr processing phosphodiesterases that includes NUDIX (nucleoside diphosphates linked to moiety-X) superfamily members NUDT9 and NUDT16 as well as ectonucleotide pyrophosphatase/phosphodiesterase 1 (ENPP1) [191, 205, 206]. NUDIX is a very vast and diverse family of proteins [68]. NUDIX hydrolases are broadly distributed among the different kingdoms of life. Up to now, 24 genes and 5 pseudogenes coding for NUDIX hydrolases have been identified in human genome. Those genes contain multiple transcriptional and translational initiation sites. As a result, human NUDIX family counts with different isoforms. Four isoforms of 26, 22, 21 and 18 kDa have been detected in human cells [207]. NUDIX proteins are characterized by a highly conserved 23-amino-acid motif or Nudix box, GX5EX7REUXEEXGU, where U is an aliphatic or hydrophobic residue and X is any residue [207, 208]. The Nudix motif residues, folded as a loop-helix-loop, compose the catalytic center [209].

These erasers target the phosphodiester bound in ADPr moieties independently of the type of ADPr linkage established with the substrate protein. However, these enzymes should be classified as partial erasers since they leave a phosphoribose remnant attached to the target protein. It is still unclear whether these phosphoribose remnants are correlated with specific biological outcomes but a pathological accumulation of phosphoribose on glutamate residues has been described [210]. Furthermore, the phosphodiesterase-catalyzed removal of the distal adenine in PAR polymers through cleavage of the terminal AMP likely prevents digestion by PARG, as it was observed with etheno-PAR, a derivatized PAR with modified adenine moieties [211]. In vivo, NUDIX hydrolases seem to fulfil 'housekeeping' functions, facilitating the detoxification of



potentially deleterious endogenous metabolites [212]. Furthermore, they have been proposed to be involved in replenishing the cellular AMP pool from ADP-ribose monomer products of PARG/ARH3-mediated PAR depolymerization. This metabolic response is consistent with the AMP-dependent mitochondrial energy failure observed following DNA damage and PARP-1 activation [213]. The accumulation of PAR-derived AMP has also been implicated in the modulation of mTOR signalling through AMPK activation [214]. These examples show that ADPr erasing reactions can have diverse effects on metabolism by generating free ADPr monomers and related molecules such as AMP. Interestingly, the hydrolase activity of a third NUDIX, NUDT5, diverges from the other ADPr-processing NUDIX hydrolases because it cannot hydrolyze protein-conjugated ADPr. However, NUDT5 generates ATP from free ADPr and pyrophosphate in a recycling-like process to quickly replenish nuclear ATP levels. While NUDT5 cannot be classified as an ADPr eraser because of its inability to remove protein ADP-ribosylation, it certainly deserves attention as it can influence the level of energetic substrates following PAR catabolism. The extracellular ENPP1 phosphodiesterase, which lacks a NUDIX and a macrodomain, is yet to be characterized regarding its involvement in ADPr processing. ENPP1 shows considerable phosphodiesterase activity *in vitro* against MAR and PAR, exceeding that observed for NUDT16 in a cell free system. The high conversion rate of ADP-ribosylation modifications to phosphoribose adducts by ENPP1 has been suggested as a key feature for the generation of phosphoribose signatures for analysis by liquid chromatography-mass spectrometry (LC-MS) [68].

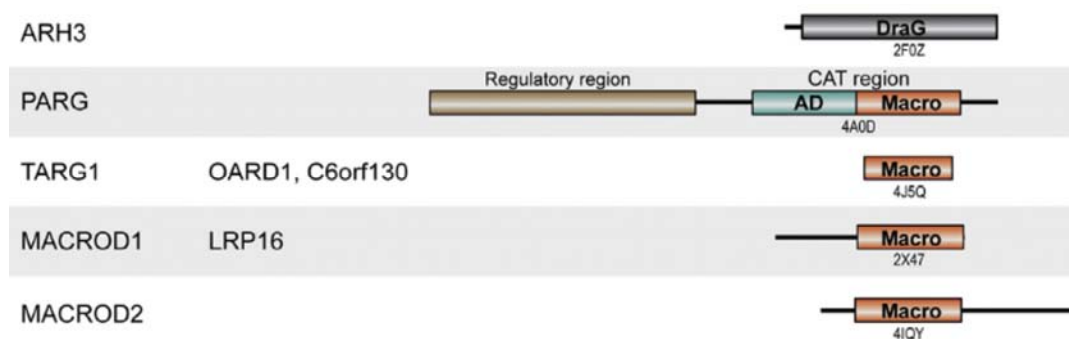


Figure 12: Schematic domain architecture of human ADP-Ribosylation removing enzymes. Adapted from *E.Barkauskaite et. al., 2005*.



10.5 ADPr removal from DNA breaks

Incapable to ignore the novel DNA signature and its role in controlling the functional state of DNA/RNA, this modification should be also finely regulated. From bacterial toxins to human proteins, this DNA-ADP-ribosylation was shown to be reversible. PARG, a PAR glycohydrolase, efficiently restores native DNA structure by hydrolysing PAR/MAR-DNA adducts generated by PARP1, PARP2 and PARP3. Biochemical and mass spectrometry analyses of the adducts demonstrated that PARPs can utilise DNA termini as an alternative to 2'-hydroxyl of ADP-ribose and protein acceptor residues to catalyse PAR/MAR chain initiation either via the 2',1''-O-glycosidic ribose-ribose bond or via phosphodiester bond formation between C1' of ADP-ribose and the phosphate of a terminal nucleotide in a DNA duplex. In addition to many ADP-ribose glycohydrolasesas DarG, PARG,MACROD2, TARG1 and ARH3 that were able to remove ADP-ribose adducts from DNA ends (with variable efficiencies) [11-13, 43]. Munnur, D., et al., showed that MACROD1 and MACROD-like hydrolases can restore RNA initial structure after RNA ADP-ribosylation [14]. Interestingly, ADP-ribosylation of 5-terminal thiophosphates at DSB termini makes MAR–DNA adducts resistant to PARG hydrolysis [13].

The presence of multiple human ADP-ribose oligomers hydrolyzes, leaves open the question of their specificity and functional overlap. A better understanding of PARG's catalytic activity and regulation, and of the roles played by PARG, ARH3, and other hydrolases in the turnover of PAR is needed, in order to broaden our knowledge of the ADP-ribosylation life cycle [6].



GOALS

At present, a slew of critical questions concerning the molecular mechanisms and the role of PARP-mediated ADP-ribosylation of DNA strand break termini remain unclear. For instance, what are the DNA substrate requirements for efficient DNA PARylation by PARP1, which activity is responsible for 80–90% of measurable PAR synthesis following DNA damage? What are the consequences of DSB ends MARylation or PARylation for processing of breaks termini, for interaction with NHEJ and HR proteins and subsequent DSB repair? Are there specific proteins responsible for ADP-ribosylated DNA adducts detection, signaling or removal? Can PAR/MAR-DNA adducts stabilization in the cell be used as an anticancer drug by increasing cell toxicity in cancer cells? Finally, what is their major biological function of ADP-ribosylated DNA adducts? In this regard, the main aim of my thesis was to characterize the molecular mechanisms and the role of PARP-mediated ADP-ribosylation of DNA strand break termini in DNA damage response and in coordination of DNA strand break repair.

The main goals during my thesis were:

- Identification of the substrate specificity and mechanisms of PARP1-dependent DNA ADP-ribosylation.
- Identification of novel MAR-DNA readers in cell-free extracts.
- Characterization of the impact of DNA ADP-ribosylation on NHEJ.
- Search for analogs of NAD⁺ that can lead to stabilization of PAR-DNA adducts in the cell.

The new knowledge about the role and mechanisms of PARPs actions in double strand break repair will identify novel therapeutic or diagnostic targets in cancer and other age-related diseases.



MATERIALS AND METHODS

Proteins, chemicals and reagents

Proteinase K from *Tritirachium album*, Deoxyribonuclease I from bovine pancreas (DNase I) and Streptavidin Mag Sepharose beads (GE healthcare) were purchased from Sigma–Aldrich (France). PRONASE® Protease, *Streptomyces griseus* and hydrogen peroxide were purchased from Merck (Darmstadt, Germany). CIP (alkaline phosphatase, calf intestinal), TdT (terminal deoxynucleotidyl transferase), BSA (Bovine serum albumin) and PmlI and Nb. BsmI endonucleases were purchased from New England Biolabs France (Evry, France). T4 polynucleotide kinase was purchased from Thermo Scientific. Human PARP1 (EC 2.4.2.30) and bovine PARG were purchased from Trevigen (Gaithersburg, USA). The plasmids coding for murine PARP2 and human PARP3 were kindly provided by Dr V. Schreiber (ESBS, Illkirch, France), moreover, NHEJ proteins such as Ku70/80 complex, XRCC4/L4 complex, Artemis, PAXX, XLF and APLF (Aprataxin and PNK-like factor) were provided by Dr J-B. Charbonnier. DNA-PK (DNA-Dependent Protein Kinase) was purchased from Promega (France). Olaparib (AZD2281, Ku-0059436) was acquired from Selleck Chemicals (Houston, USA) and NAD⁺ analogues such as 6-Biotin-17-NAD⁺, 6-Fluo-10-NAD⁺, 8-Br-7-CH-NAD⁺, 8-Br-NAD⁺, ara-2'-F-NAD⁺, dAP2(Nic), epsilon-NAD⁺ from BIOLOG (Bremen, Germany). Antibodies used in western blot were described in [Table 6](#).

Purification of PARP3 and CLPB

Human PARP3 was cloned into the pETHSUL vector using the overlap extension polymerase chain reaction cloning approach [215]. N-terminal His₆-tagged SUMO-PARP3 fusion was expressed in *Escherichia coli* Rosetta 2 (DE3) electrocompetent cells (Novagen). The bacterial culture was grown at 37° C in a LB medium (supplemented with 100 g/ml ampicillin) to OD₆₀₀ = 0.6–0.8. The protein expression was induced by 0.5 mM isopropyl D-galactopyranoside (IPTG; Sigma-Aldrich) during overnight incubation at 18° C. The bacteria were harvested by centrifugation, and cell pellets were lysed using a French press at 18 000 psi in a buffer consisting of 20 mM HEPES-KOH pH 7.6, 40 mM NaCl and 0.1 % (w/v) NP-40 supplemented with the cComplete™ Protease Inhibitor Cocktail (Roche Diagnostics, Switzerland). Lysates were cleared by centrifugation at 40 000 × g for 30 min at 4° C, and the resulting supernatant was adjusted to 500 mM NaCl and 20 mM imidazole and loaded onto a HiTrap Chelating HP column (Amersham Biosciences, GE Healthcare). The column was washed with buffer A (20 mM HEPES-KOH pH 7.6, 500 mM NaCl, 40 mM imidazole) and the bound PARP3 fusion was eluted with a linear 20–500 mM gradient of imidazole in buffer A on Akta Purifier (GE Healthcare). Eluted fractions of the PARP3 fusion were diluted in glycerol (50 % final concentration). PARP3 protein was stored at – 80° C. The concentration of the purified proteins was determined by the method of Bradford and the activity of PARP3 was tested with labeled oligonucleotide in the presence of NAD⁺ on PAGE gel. Same pro-



protocol was used to purify N- and C-terminal of CLPB, using pET28c vector and Rosetta 2 (DE3) PlyS cells (chemically competent cells).

Oligonucleotides and Dbait molecules

Sequences of the oligonucleotides, their duplexes and Dbait molecules used in the present work are shown in [Table 7](#). Regular oligonucleotides, oligonucleotides with thiophosphates and Dbait molecules, containing a hexaethyleneglycol linker [(CH₂-CH₂-O)₆] tethering two complementary DNA strands, were purchased from Eurogentec (Seraing, Belgium). Prior to enzymatic assays, the oligonucleotides were labeled at the 5'OH end using normal or 3' phosphatase minus T4 polynucleotide kinase (Thermo Scientific in the presence of [³²P] ATP (3000 Ci·mmol⁻¹) (PerkinElmer) or at the 3'OH end by means of TdT in the presence of [³²P]-3-dATP (cordycepin 5' triphosphate, 5,000 Ci·mmol⁻¹; PerkinElmer). Cold ATP at 1 mM was added to phosphorylate the remaining non-labeled oligonucleotides. After labeling reactions, the radioactively labeled oligonucleotides were desalted on a Sephadex G-25 column, equilibrated with water and then annealed with a corresponding complementary strand for 3 min at 65°C in the following buffer: 20 mM HEPES/KOH (pH 7.6) and 50 mM KCl. Radioactive labeling of duplex DNA was also performed using radioactive [adenylate-³²P] NAD⁺ (800 Ci·mmol⁻¹) (PerkinElmer) in the presence of PARPs.

An assay for PARP-dependent DNA ADP-ribosylation

This assay was carried out as described previously [13]. Briefly, 20 nM [³²P] labeled oligonucleotide duplexes were combined with 20 nM PARP1 in the presence of 1 mM NAD⁺ in ADPR buffer [20 mM HEPES/KOH pH 7.6, 50 mM KCl, 2 mM MgCl₂, 1 mM 1,4- dithiothreitol (DTT) and 100 g/ml bovine serum albumin (BSA)]. The mixture was incubated for 30 min at 37° C, unless otherwise stated. After the reaction, the samples were incubated in the presence of 50 ng/l proteinase K and 0.15 % SDS for 30 min at 50° C followed by addition of 4 M urea and incubation for 10 s at 95°C. The reaction products were analyzed by electrophoresis in denaturing 20 % (w/v) polyacrylamide gels (PAGE; 7 M Urea, 0.5 × Tris-Borate-EDTA buffer, 42° C). The gels were used to expose a Fuji FLA-3000 Phosphor Screen, which was then scanned with Typhoon FLA-9500 and analyzed using the Image Gauge 4.0 software. The same experiment was performed also using 2,5 µg/µl of HeLa extracts with 50 nM [³²P] labeled oligonucleotide duplexes for 20 min at 37° C, under standard reaction conditions for a PARP-dependent DNA ADP-ribosylation assay [500µM NAD⁺, 1X BER buffer, 3 µM PARG inhibitor (PARGi)]. PAR-DNA adducts were treated with 0,02 pg/µl of PARG or with 5 U of CIP after phenol chloroform extraction and acetone, 0,2 % perchlorate precipitation of PARylated DNA. The reaction products were analyzed by denaturing PAGE.

Analysis of the efficiency of PARP1-catalyzed auto- and DNA ADP-ribosylation

Université Paris-Saclay

Espace Technologique / Immeuble Discovery

Route de l'Orme aux Merisiers RD 128 / 91190 Saint-Aubin, France



The efficiency of PARP1-catalyzed auto- and DNA (ADP-ribosyl)ation was measured using a PARP1 specific cold duplex phosphorylated at the 5' end of the nick and on the 3' end of the DSB, (with or without a thiophosphate at the DSB terminus). The assay was performed in ADPR buffer but without BSA. 320 nM of PARP1 was added to 1 μ M oligonucleotide cold duplex and incubated in the presence of 0.5 μ M [adenylate- 32P] NAD⁺ for 30 min. The reaction products were treated with PARG at 50 pg/l for 30 min at 30°C and then with 10.5 U DNase I for 30 min at 37° C in the presence of 0.5 mM CaCl₂ or treated with 50 ng/l proteinase K for 30 min at 50° C in the presence of 0.1 % SDS. The reactions were terminated by the addition of a stop solution (7.5 M Urea, 0.33 % SDS, 10 mM ethylenediaminetetraacetic acid (EDTA), bromophenol blue) at 1:1 (v/v), heated at 95° C for 10 s, and the products of the reactions were analyzed by denaturing PAGE as described in our previous work [13].

The cell line, culture conditions and cell extracts preparation

Stable PARG knockdown (shPARG/PARG^{KD}) and control (shCTL/BD650) HeLa cell lines have been described elsewhere [216]. The cells were grown in DMEM (Dulbecco's modified Eagle's medium) supplemented with penicillin/streptomycin (Gibco, Gaithersburg, USA) and 10 % of fetal bovine serum in a humidified atmosphere containing 5 % of CO₂. After harvesting, the cells were washed twice in cold phosphate-buffered saline (PBS). All the procedures were conducted at 4° C.

i. Whole cell extract preparation for DNA-MAR reader identification:

The cell pellets were resuspended in 3 volumes (w/v) of lysis buffer (20 mM HEPES-KOH, 5 mM EDTA, 1 mM EGTA, 300 mM NaCl, 0.2 μ M olaparib and 0.3 % NP-40 (nonyl phenoxypolyethoxyethanol) + 1 X cOmplete protease inhibitors [Roche]). The cells were ground by mixture pipetting with 200 μ l pipet and then incubated 30 min on ice. After a 20 min centrifugation at 16000 g / 4° C, the lysate was collected and the proteins concentration was measured by Bradford method.

ii. Nuclear cell extract preparation for DNA-(ADP-ribosyl)ation and NHEJ reconstitution :

The cell pellets were resuspended in 3 volumes (w/v) of cytoplasmic extract buffer (10 mM HEPES-KOH pH 7.6, 10 mM KCl, 0.1 mM EDTA, 0.15 mM spermine, 0.7 mM spermidine, 1 \times cOmplete protease inhibitors EDTA-free [Roche], 1 mM DTT); 0.1 % NP-40 was added immediately after cell resuspension. The cells were allowed to swell on ice for 5 min. Nuclei were collected by centrifugation (500 \times g, 5 min), then resuspended in one volume of nuclear extract buffer (20 mM HEPES-KOH pH 7.6, 0.4 M NaCl, 1 mM EDTA, 25 % glycerol, 1 \times cOmplete protease inhibitors EDTA-free [Roche], 1 mM DTT). After 10 min incubation on ice, the samples were centrifuged at 13 000 \times g for 5 min. The nuclear extracts (supernatants) were stored at - 20° C if not used immediately and the proteins concentration was measure by Bradford method.



Purification of DNA-MAR readers

A nicked duplex S26, containing a 5' P on the DSB was prepared. 10 μ M of S26 substrate was incubated with 5 μ M PARP3 in the presence of ADPR buffer (5 mM $MgCl_2$) and 1 mM NAD^+ for 20 min at 37° C. The MARYlated nicked duplex was then treated with 1 % of PK (10 mg/ml) and SDS (10 %) for 30 min at 50° C and precipitated using 9 V of acetone with 2 % $LiClO_4$. After centrifugation the pellet was resuspended in TE buffer, mixed with 1:1 (v/v) of stop solution (10 M Urea and 10 mM EDTA), heated for 3 min at 65° C and loaded on PAGE 20 %. After migration, the gel was exposed to UV light and bands containing the MARYlated oligonucleotide (S27) were cut (with the minimum of gel) and incubated overnight in 200 μ l of water or TE buffer in a shaker at 4° C. The collected supernatant was mixed with 9 V acetone with 2 % $LiClO_4$ and the precipitated MARYlated-S27 was resuspended with 40 μ l of water and the oligonucleotide concentration was measured by the nandrop (biospec-nano, Shimadzu). Purity of MARYlated-S27 was verified on PAGE 20 % by its 3' labelling with cordycepin in comparison with non MARYlated oligonucleotide. Biotinylated duplexes with and without MAR on 5' terminus were obtained by annealing 10 μ M of MARYlated-S27 or unmodified-S27 with 10 μ M of a 30 nt substrate containing a HEG spacer with subsequent nick ligation by T4 ligase (Thermo Scientific™ ref. EL0011) diluted 1:20 and incubated for 1 hr at 37° C in 1X T4 buffer resulting in S28 or S28 (MAR) duplexes, respectively (Figure 13). MARYlated and unmodified S27 and S28 was then bound to 20 μ l of Streptavidin Mag sepharose beads (Figure 13) and equilibrated with 500 μ l of washing buffer containing 20 mM HEPES, pH 7.6, 100 mM NaCl and 0.1 % NP-40. Beads with ss and ds, MARYlated or unmodified substrates were incubated with 200 μ l of HeLa shPARG cell extracts containing 2 mM DTT, 1 mM $MgCl_2$, 3 μ M PARG inhibitor and 5 % glycerol for 1 hr at 4° C while shaking. The beads alone, containing MARYlated and unmodified substrates were washed 5 times with a low salt concentration buffer (20 mM HEPES-KOH pH=7.6, 100 mM NaCl, 0.1 % NP-40 buffer), then proteins bound were eluted with two successive elutions of 20 μ l of 500 mM and 20 μ l of 350 mM NaCl in buffer containing 20 mM HEPES-KOH pH=7.6, 0.5 % NP-40, respectively. Presence of proteins in eluates was checked by SDS-PAGE and gel staining (SilverQuest™ Silver Staining Kit #LC6070). After short electrophoresis migration (5 - 10 mm) on SDS-PAGE and Commassie Bleu staining, gels were sent to SICaPS platform (I2BC, Gif sur Yvette, France).

i. Nano-LC MS/MS analysis performed by SICaPS platform

Gel regions of interest were excised and in-gel enzymatic digestion was performed with standard conditions. Briefly, protein bands were extensively washed with CH_3CN and 100 mM



NH_4HCO_3 . The excised bands were treated with 10 mM DTT at 56° C for 30 min. After DTT removal, cysteine carbamidomethylation was performed at room temperature for 30 min by addition of 55 mM iodoacetamide. After removal of the supernatant, the washing procedure was repeated, and gel slices were dried. Tryptic digestion was performed overnight at 37°C by addition of 50 μl of 5 ng/ μl Porcine Gold Trypsin (Promega) diluted in 50 mM NH_4HCO_3 . Proteolytic peptides were extracted first by addition of 100 μl of 50% acetonitrile and 0.1% formic acid and second by addition of 100 μl of 100% acetonitrile. Extracted tryptic peptides were vacuum dried and resuspended in 5% acetonitrile and 0.1% TFA prior to Triple TOF nanoLC-MS/MS analyses. For TIMS-TOF PRO nanoLC-MS/MS analyses, tryptic peptides were first desalted off-line using Pierce C18 spin columns and resuspended in 5% acetonitrile and 0.1% TFA after vacuum dried. Depending on sample protein band intensities, nanoLC-MS/MS analyses were performed either with the triple-TOF 4600 mass spectrometer (Absciex, Framingham, MA, USA) coupled to the Nano-RSLC system (Thermo scientific) or with the Tims-TOF-PRO mass spectrometer coupled with the nanoElute (Bruker). Briefly, for the Triple-TOF analysis, peptides were desalted on a C18 reverse phase pre-column (C18 Acclaim Pepmap100, 3 μm , 100 Å, 75 μm i.d.2cm length) using a loading solvent containing $\text{H}_2\text{O}/\text{ACN}/\text{TFA}$ 98%/2%/0.05%) at 5 $\mu\text{L}/\text{min}$ and were then eluted at a flow rate of 300nl/min from the reverse phase analytical C18 column (C18 Acclaim Pepmap100, 2 μm , 100 Å, 75 μm i.d.50cm length) using a 5-35% solvent B gradient for 120 min. Solvent B was 0.1% formic acid in 100% acetonitrile and solvent A was 0.1% formic acid in water. NanoLC-MS/MS experiments were conducted in Data Dependent acquisition method by selecting the 20 most intense precursors for CID fragmentation with Q1 quadrupole set at low resolution for better sensitivity. For TIMS-TOF PRO nano-LC-MS/MS, peptides were directly injected on a Aurora C18 column (C18 1.6 μm , 250mmx75 μm), ION OPTIK) using a solvent containing 2% ACN, 0.1% FA at 800 bars and were then eluted at a constant flow rate of 400nl/min using a 0-35% solvent B gradient for 100 min. Solvent B was 0.1% formic acid in 100% acetonitrile and solvent A was 0.1% FA in 2% ACN, 98% H_2O . NanoLC-MS/MS experiments were conducted using the Data Dependent Acquisition PASEF mode.

ii. Proteomic data analysis

Raw data from Triple-TOF and Tims-TOF Pro were processed respectively using MS data converter tool (Absciex) and Data Analysis software (Bruker). Protein identification was performed using the MASCOT search engine (Matrix science, London, UK) against SwissProt database (release 2018_10, all taxa) with carbamidomethylation of cysteines set as fixed modification. Oxidation of methionines were set as variable modifications. Peptide and fragment tolerance were respectively set at 25 ppm and 0.05 Da for Triple-TOF data and 10 ppm and 0.05 Da for Tims-TOF Pro data. Only PSM peptides with mascot ions scores higher than the identity threshold (15 and 25 for Tims-TOF and Triple-TOF respectively) at less than 1% FDR were considered.



For label-free protein quantification, Triple-TOF and TIMS-TOF Pro raw data were respectively processed with MaxQuant software versions 1.6.3.4 and 1.6.6.0 (Max-Planck-Institute of Biochemistry, MPIB) using defaults parameters and match between runs functionality. All statistical analyses were performed using Perseus software (MPIB). After imputation of missing values with randomly generated numbers following a normal distribution, multiple Welch's tests were performed to discriminate significant interactors. Proteins with p-value <0.05 and fold change >2 were first considered as variants.

iii. Basic Silver Staining Protocol

For a 8 × 8 cm NuPAGE® Novex Bis-Tris mini-gel, 1.0 mm thick. After electrophoresis, remove the gel from the cassette and place the gel in a clean staining tray of the appropriate size. Rinse the gel briefly with ultrapure water. Fix the gel in 100 mL of fixative for 20 min with gentle rotation. Decant the fixative solution and wash the gel in 30 % ethanol for 10 min. Decant the ethanol and add 100 mL of sensitizing solution to the washed gel in the staining container. Incubate the gel in the sensitizing solution for 10 min. Decant the sensitizing solution and wash the gel in 100 mL of 30 % ethanol for 10 min. Wash the gel in 100 mL of ultrapure water for 10 min. Incubate the gel in 100 mL of staining solution for 15 min. After the staining is complete, decant the staining solution and wash the gel with 100 mL of ultrapure water for 20–60 s. Incubate the gel in 100 mL of developing solution for 4–8 min until bands start to appear and the desired band intensity is reached. After the appropriate staining intensity is achieved, immediately add 10 mL of stopper directly to the gel still immersed in developing solution. Gently agitate the gel for 10 min. The color changes from pink to colorless indicating that the development has stopped. Decant the Stopper solution and wash the gel with 100 mL of ultrapure water for 10 min. (For more details check SilverQuest™ Silver Staining Kit - Catalog Number LC6070)

iv. Western Blot

Equal amounts of DNA-MAR readers (eluate) derived from the “Purification of DNA-MAR readers” assay (described above) were boiled in sample buffer (Bolt™ LDS sample buffer and sample reducing agent) for 5 min at 95° C, centrifuged for 1 min at 16 000 g and then loaded into SDS-PAGE Bolt™ precast mini gel (Invitrogen) along with molecular weight marker (SeeBlue™ Plus2 pre-stained protein standard). Electrophoresis was run first at 200 V for 2 min and then at 120 V for 45 min. After running the gel, proteins were transfer on an integrated nitrocellulose transfer membrane for dry blotting (iBlot™ 2 Transfer Stacks: ref. IB23001) using the iBlot 2 gel transfer device (user guide: catalog number ref. IB21001). The blot was then rinsed briefly with water, stained with Ponceau solution. After checking the transfer quality, the blot was blocked for 2 hr (to overnight) with 5 % milk in 1 X TBST at room temperature (RT) while shaking. After blocking, the membrane was incubated with primary antibody (in 5% milk + TBST 1X) against target protein, for



overnight at 4°C while shaking. The blot was then rinsed 3-5 times for 10 mins with TBST 1X, prior to its incubation with HRP-conjugated secondary antibody (in 5% milk + TBST 1X) for 1 hr at RT. Finally, the membrane was rinsed 3-5 times for 10 mins with TBST 1 X and chemiluminescent substrate (WesternBright™ ECL – Advansta F ref.-12045-D20) was applied to the blot according to the manufacture's recommendation. Chemiluminescent signals were captured using a CCD-camera based imager (Amersham Imager 600 imagers - GE Healthcare Life Sciences). Primary and secondary antibodies specifications are described in [Table 6](#).

v. Electrophoretic mobility shift assay (EMSA)

DNA versus MARylated-DNA binding activity of MAR reader's potential candidates was measured by EMSA. Binding reactions were performed by incubating 40 nM of ³²P-labeled S28 and MAR-S28 DNA (unligated nick) respectively with 20 nM of commercial CLPB, 160 nM of PARP1, 200 nM of RPA, 1.75 μM of APTX, 1 μM of purified PARP3 or 1μM of purified N- and C-terminal of CLPB in EMSA buffer containing 20 mM Tris-HCl, pH 7.6, 50 mM KCl (or 50 mM NaCl or 2 mM spermine), 1 mM EDTA, 0.5 % glycerol, 1 mM DTT) for 10 min at RT (or 30 min at 4° C) . Protein was diluted to working concentrations in EMSA buffer and always added last. After incubation, the products of the binding reaction were mixed 1:1 (v/v) with stop solution (10 % glycerol, 6 mM EDTA, 1.66 Tris-HCl pH 7.6, 0.005 % bromophenol blue and 0.005 % Xylene cyanol) on ice, and loaded on 10 % PAGE 1:80 Bis-Acrylamide. Migration was done for 5 hrs (to ON) at 4°C (100-150V, 24 mA, 6W).

In-vitro NHEJ reconstitution assay

NHEJ reconstitution of DSB repair was accomplished using different oligonucleotides structures and NHEJ purified proteins ([Figure 14](#)). 20 nM of S22 a nicked biotinylated blunt end duplex containing a 5' P on its DSB; prone for PARP3 MARylation, and 20 nM of S25 a full-length biotinylated blunt end duplex were incubated with 100 nM KuFL, 200 nM XL4, 25 nM DNA-PK, 25 nM Artemis, 500 nM PAXX, 20 nM XLF, 50 nM APLF and 100 nM PARP3 for 1 hr at 37° C in the presence of 200 nM streptavidine, 0.5 mM ATP and 1 μM BSA in NHEJ buffer [25 mM Tris-HCl (pH=8), 50 mM KCl, 13 mM MgCl₂, 1 mM DTT and 10 % PEG]. Ligation products were then treated with 0.5 μg/μl pronase and 1 % sarcosyl for 30 min at 40° C (for streptavidin elimination), mixed with stop solution (10 M urea and 10 mM EDTA) and heated for 10 s at 90° C. The reaction products were analyzed by denaturing PAGE 8 %. The same experiment was performed also using 0.5 μg/μl of pre-heated (5 min at 37° C) BL2 or or CHO extracts instead of purified NHEJ proteins in NHEJ buffer (10 % PEG, 1 mM MgCl₂, 3 μM PARGi and 1 mM NAD⁺) for 15 min at 37° C.

Search for novel PARP1 and PARP2 inhibitors among derivatives of 1,4-dihydropyridine with DNA binding capacity

Université Paris-Saclay

Espace Technologique / Immeuble Discovery

Route de l'Orme aux Merisiers RD 128 / 91190 Saint-Aubin, France



80 nM of PARP1 or 100nM of PARP2 or PARP3 were incubated with 10 nM of 5'-[³²P] labelled DNA duplex (S30 for PARP1 and S31 for PARP2 and PARP3) in the presence of 8 different NAD⁺ analogs (Figure 15) (0.5 mM): β- Nicotinamide- 2'- deoxyadenine dinucleotide (2'-deoxy-NAD⁺ or **dNAD⁺**), β-Nicotinamide-8-bromoadenine dinucleotide (8-Bromo-NAD⁺ or **Br-NAD⁺**), β- Nicotinamide-1,N⁶-ethenoadenine dinucleotide (1,N⁶-etheno-NAD⁺ or **ε-NAD⁺**), β- Nicotinamide-8-bromo-7-deazaadenine dinucleotide (8-Br-7-CH-NAD⁺ or **CH-NAD⁺**), β-Nicotinamide-N⁶-(2-(6-[fluoresceinyl]amino)hexanoyl)aminoethyl)adenine dinucleotide (6-Fluo-10-NAD⁺ or **flu-NAD⁺**), β- ara-2'-deoxy-2'-fluoro-nicotinamide adenine dinucleotide (ara-2'-F-NAD⁺ or **ara-NAD⁺**), β- Nicotinamide- N⁶- (2- (6- (6 [biotinyl]amino)hexanoyl)amino)hexanoyl)aminoethyl)adenine dinucleotide (6-Biotin-17-NAD⁺ or **bio-NAD⁺**), β- Nicotinamide-8-bromohypoxanthine dinucleotide (8-Br-NHD⁺ or **NHD⁺**) from BIOLOG Life Science Institute (Figure 14). Reaction mixture was incubated for 30 min at 37°C in ADPR buffer and then boiled for 10 sec at 95°C in Urea/EDTA stop solution (as described above), passed through urea G25 sephadex column and loaded on 20 % denaturing PAGE. To assess the influence of the type of NAD⁺ derivatives on stabilization of PAR/MAR-DNA adducts against PARG, reaction product was heated for 5 min at 85°C, treated with 0.1 μM PARG for 30 min at 30°C then boiled 10 sec at 95°C in Urea/EDTA stop solution (described previously), passed through urea G25 sephadex column and loaded on 20 % denaturing PAGE.

Table 6: Primary and secondary antibodies specifications; (H: Human, M: Mouse and R: Rabbit).



Name	Primary	Ref	Company	Clonality	Isotype	Host	Reactivity
Anti-CLPB	Primary	ab76179	abcam	Polyclonal	IgG	rabbit	Human
Anti-CLPB	Primary	HPA039006	Atlas	Polyclonal	IgG	rabbit	Human
Anti-IMPDPH2	Primary	HPA001400	Sigma (Atlas)	Polyclonal	IgG	rabbit	Human
Anti-RPA3	Primary	WH0006119M1	Sigma (Atlas)	Monoclonal	IgG1 λ	mouse	Human
Anti-ERI1	Primary	MA5-25827	Thermo-Invitrog	Monoclonal	IgG2b	mouse	H, M, R
Anti-PARP1	Primary	9532S	Cell signaling	Monoclonal		Rabbit	H, M, R
Anti-PARP3	Primary	PA5-21478	Thermo-Invitrog	Polyclonal	IgG	Rabbit	H, M, R
Anti-PAR	Primary	ALX-804-220-R100	Enzo	mono-10H	IgG3	mouse	H, M, R
Anti-PAN	Primary	MABE1016	Merck millipore	recombinant		rabbit	H, M, R
Anti-MAR	Primary	MABE1076	Merck millipore	recombinant		rabbit	H, M, R
Anti-C1QPB	Primary	5734S	Cell signaling	Polyclonal	IgG	rabbit	H, M, R
Anti-PARP	Primary	9542	Cell signaling	Polyclonal		rabbit	H, M, R

Name	Secondary	Ref	Company	Clonality	Isotype	Host	Reactivity
Rabbit TrueBlot	Secondary	18-8816-31	Rockland	Mono eB182	IgG	mouse	Rabbit
Anti-Rabbit HRP	Secondary	A0545	Sigma-Aldrich	Polyclonal	IgG	Goat	Rabbit
Anti-mouse HRP	Secondary	A0168	Sigma-Aldrich	Polyclonal	IgG-Fc	Goat	Mouse

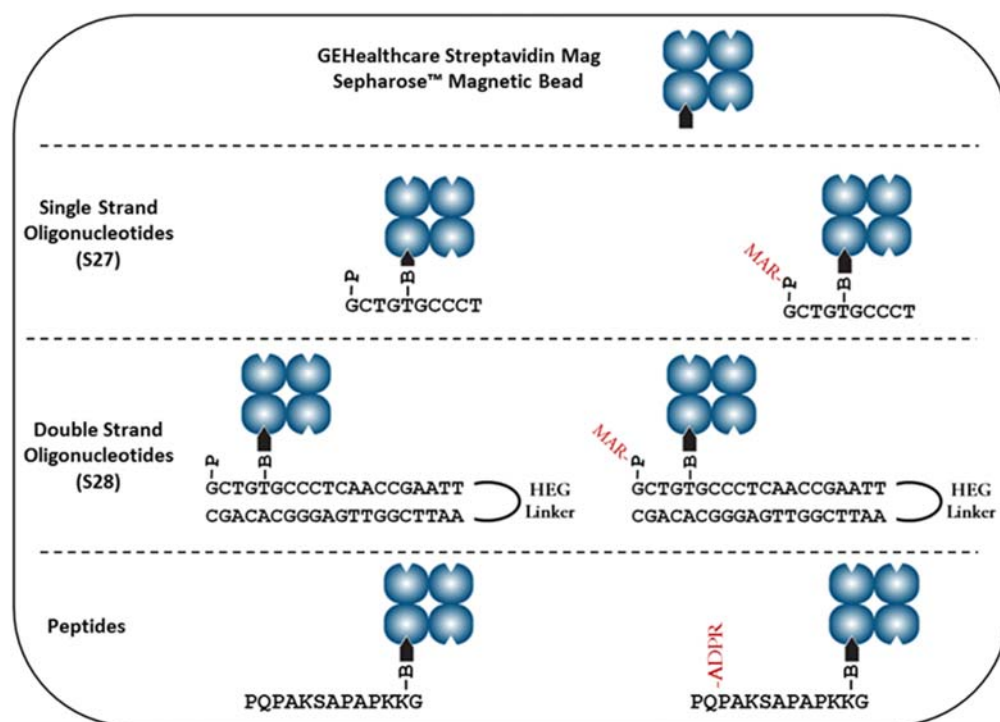


Figure 13: Biotinylated unmodified or MARYlated ss/ds oligonucleotides and peptides bounded to Streptavidin Mag sepharose beads.

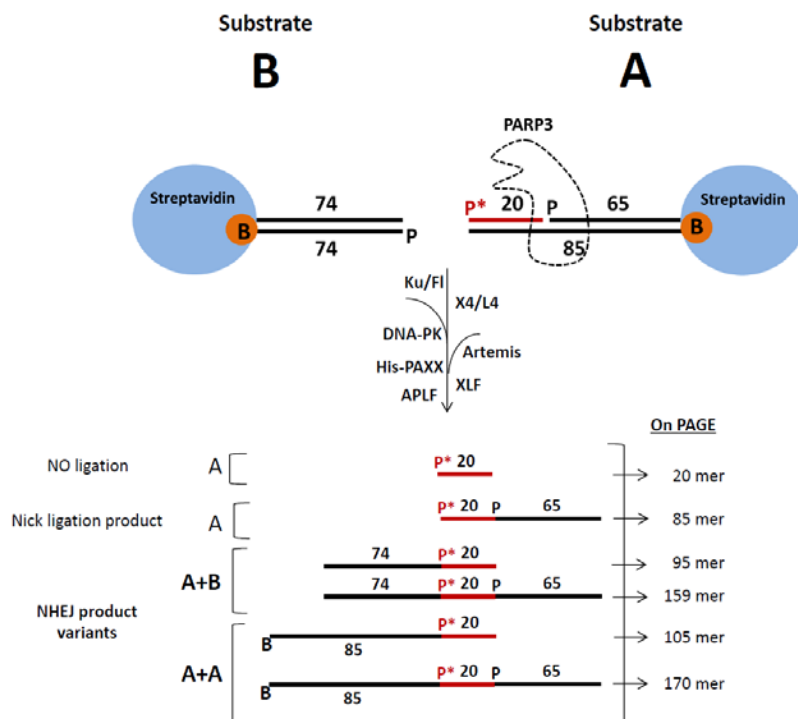


Figure 14: NHEJ reconstitution of DSB repair using different oligonucleotides structures and purified proteins. B: biotin, PAGE: Polyacrylamide gel electrophoresis. In the presence of PARP3 and NAD^+ , MARYlated-20 mer radiolabeled oligonucleotide can be observed.

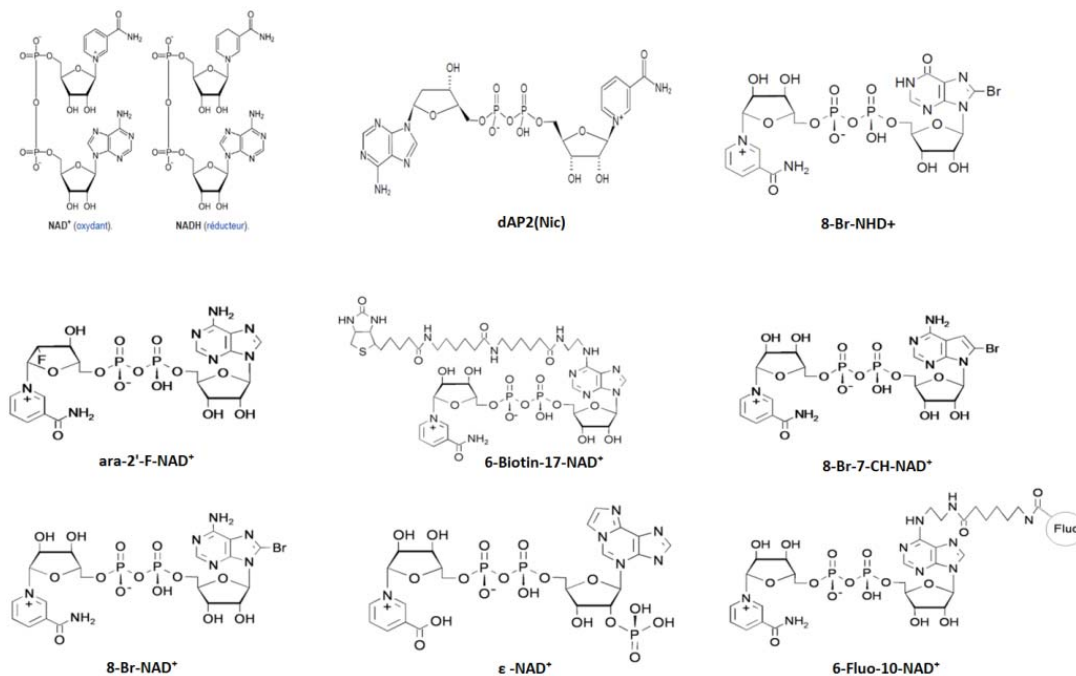


Figure 15: Series of NAD analogues structures (BIOLOG Life Science Institute).





Table 7: Sequences of the oligonucleotides and their duplexes used in this study.

Name	Oligonucleotides sequences and structures
S1 ⁿ	$ \begin{array}{l} \text{5' } \overset{32\text{P}}{\text{TCATAGGCTTAGTCGTCATTC}} \text{GCTGTGCCCTCAA } \overset{\text{P}}{\text{CGAATTCACAAGCCTAGA}} \\ \text{3' } \text{CGACACGGGAGTTGGCTTAAGTGTTCGGATCT} \end{array} $
S2 ⁿ	$ \begin{array}{l} \text{5' } \text{GCTGTGCCCTCAA } \overset{32\text{P}}{\text{CGAATTCACAAGCCTAGA}} \\ \text{3' } \overset{\text{P}}{\text{CTTACTGCTGATTCGGATACT}} \text{CGACACGGGAGTTGGCTTAAGTGTTCGGATCT} \end{array} $
S2 (S2 ⁰)	$ \begin{array}{l} \text{5' } \overset{32\text{P}}{\text{GCTGTGCCCTCAA}} \text{ } \overset{\text{P}}{\text{CGAATTCACAAGCCTAGA}} \\ \text{3' } \text{CGACACGGGAGTTGGCTTAAGTGTTCGGATCT} \end{array} $
S2 ⁻¹	$ \begin{array}{l} \text{5' } \overset{32\text{P}}{\text{GCTGTGCCCTCAA}} \text{ } \overset{\text{P}}{\text{CGAATTCACAAGCCTAGA}} \\ \text{3' } \text{GACACGGGAGTTGGCTTAAGTGTTCGGATCT} \end{array} $
S2 ⁻³	$ \begin{array}{l} \text{5' } \overset{32\text{P}}{\text{GCTGTGCCCTCAA}} \text{ } \overset{\text{P}}{\text{CGAATTCACAAGCCTAGA}} \\ \text{3' } \text{CACGGGAGTTGGCTTAAGTGTTCGGATCT} \end{array} $
S3 ⁿ	$ \begin{array}{l} \text{5' } \text{GCTGTGCCCTCAACCGAATTCACAAGCCTAGA} \\ \text{3' } \overset{\text{P}}{\text{CTTACTGCTGATTCGGATACT}} \text{CGACACGGGAGTT } \overset{32\text{P}}{\text{GCTTAAGTGTTCGGATCT}} \end{array} $
S4	$ \begin{array}{l} \text{5' } \overset{32\text{P}}{\text{GCTGTGCCCTCAACCGAATTCACAAGCCTAGA}} \\ \text{3' } \text{CGACACGGGAGTTGGCTTAAGTGTTCGGATCT} \end{array} $
S5	$ \begin{array}{l} \text{5' } \overset{32\text{P}}{\text{GCTGTGCCCTCAA}} \text{ } \overset{\text{P}}{\text{CGAATTCACAAGCCTAGA}} \\ \text{3' } \text{CGACACGGGAGTTGGCTTAAGTGTTCGGATCT} \end{array} $
S6	$ \begin{array}{l} \text{5' } \overset{32\text{P}}{\text{GCTGTGCCCT}} \text{ } \overset{\text{P}}{\text{AAGCGAATTCACAAGCCTAGA}} \\ \text{3' } \text{CGACACGGGAGTTGGCTTAAGTGTTCGGATCT} \end{array} $
S7	$ \begin{array}{l} \text{5' } \overset{32\text{P}}{\text{GCTGTGCCCTCAAC}} \text{ } \overset{\text{P}}{\text{CGAATTCACAAGCCTAGA}} \\ \text{3' } \text{CGACACGGGAGTTG-GCTTAAGTGTTCGGATCT} \end{array} $
S8	$ \begin{array}{l} \text{5' } \overset{32\text{P}}{\text{GCTGTGCCCTCAACC}} \text{ } \overset{\text{P}}{\text{AATTCACAAGCCTAGA}} \\ \text{3' } \text{CGACACGGGAGTTGGCTTAAGTGTTCGGATCT} \end{array} $
S9	$ \begin{array}{l} \text{5' } \overset{32\text{P}}{\text{GCTGTGCCCTCAACCGAATT}} \text{ } \overset{\text{P}}{\text{ACAAGCCTAGA}} \\ \text{3' } \text{CGACACGGGAGTTGGCTTAAGTGTTCGGATCT} \end{array} $
S10	$ \begin{array}{l} \text{5' } \overset{32\text{P}}{\text{GCTGTGCCCTCAACCGAATTCAC}} \text{ } \overset{\text{P}}{\text{AGCCTAGA}} \\ \text{3' } \text{CGACACGGGAGTTGGCTTAAGTGTTCGGATCT} \end{array} $



S11	$\begin{array}{l} 5' \text{ GCTGTGCCCTCAA } \overset{32\text{P}}{\text{AATCACAAGCCTAGA}} \\ 3' \text{ CGACACGGGAGTTGGCTTAAGTGTTCGGATCT} \end{array}$ <p>HEG Linker</p>
S12	$\begin{array}{l} 5' \text{ GCTGTGCCCTCAA } \overset{32\text{P}}{\text{CACAAGCCTAGA}} \\ 3' \text{ CGACACGGGAGTTGGCTTAAGTGTTCGGATCT} \end{array}$ <p>HEG Linker</p>
S13	$\begin{array}{l} 5' \text{ GCTGTGCCCTCAA } \overset{32\text{P}}{\text{AGCCTAGA}} \\ 3' \text{ CGACACGGGAGTTGGCTTAAGTGTTCGGATCT} \end{array}$ <p>HEG Linker</p>
S14	$\begin{array}{l} 5' \text{ GCTGTGCCCTCAACCGAA } \overset{32\text{P}}{\text{TCACAAGCCTAGA}} \\ 3' \text{ CGACACGGGAGTTGGCTTAAGTGTTCGGATCT} \end{array}$ <p>HEG Linker</p>
S15	$\begin{array}{l} 5' \text{ GCTGTGCCCTCAA } \overset{32\text{P}}{\text{CGAATTCACAAGCCTAGAGTTACATTAGCAGATACG}} \\ 3' \text{ CGACACGGGAGTTGGCTTAAGTGTTCGGATCTCAATGTAATCGTCTATGC} \end{array}$ <p>HEG Linker</p>
S16	$\begin{array}{l} 5' \text{ GCTGTGCCCTCAACCGAAT } \overset{32\text{P}}{\text{CACAAGCCTAGAGTTACATTAGCAGATACG}} \\ 3' \text{ CGACACGGGAGTTGGCTTAAGTGTTCGGATCTCAATGTAATCGTCTATGC} \end{array}$ <p>HEG Linker</p>
S17	$\begin{array}{l} 5' \text{ GCTGTGCCCTCAACCGAATT } \overset{32\text{P}}{\text{CACAAGCCTAGAGTTACATTAGCAGATACG}} \\ 3' \text{ CGACACGGGAGTTGGCTTAA-GTGTTCGGATCTCAATGTAATCGTCTATGC} \end{array}$ <p>HEG Linker</p>
S18	$\begin{array}{l} 5' \text{ GCTGTGCCCTCAACCGAATTCAC } \overset{32\text{P}}{\text{AGCCTAGAGTTACATTAGCAGATACG}} \\ 3' \text{ CGACACGGGAGTTGGCTTAAGTGTTCGGATCTCAATGTAATCGTCTATGC} \end{array}$ <p>HEG Linker</p>
S19	$\begin{array}{l} 5' \overset{32\text{P}}{\text{GCTGTGCCCTCAACCGAATTCACAAGCCTAGA}} \\ 3' \text{ CGACACGGGAGTTGGCTTAAGTGTTCGGATCT} \end{array}$ <p>HEG Linker</p>
S20	$\begin{array}{l} 5' \overset{32\text{P}}{\text{GCTGTGCCCTCAA}} \text{CGAATTCACAAGCCTAGA} \\ 3' \text{ CGACACGGGAGTTGGCTTAAGTGTTCGGATCT} \end{array}$ <p>HEG Linker</p>
S21	$\begin{array}{l} 5' \overset{32\text{P}}{\text{GCTGTGCCCTCAA}} \text{CGAATTCACAAGCCTAGA} \\ 3' \text{ CGACACGGGAGTTGGCTTAAGTGTTCGGATCT} \end{array}$ <p>HEG Linker</p>



S22	³² P- GATGCCTCCAAGGTCGACGA TGCAGACACTGATATATGTACAGATTCGGTTGATCATAGCACAAATGCCTGCTAACCCACTATCG CTACGGAGGTTCCAGCTGCT-ACGTCGTGACTATATACATGTCTAAGCCAAC TAGTATCGTGTTACGGACGATTGGGTGATAGC B
S23	³² P- GATGCCTCCAAGGTCGACGATGCAGACACTGATATATGTACAGATTCGGTTGATCATAGCACAAATGCCTGCTAACCCACTATCG CTACGGAGGTTCCAGCTGCTACGTCGTGACTATATACATGTCTAAGCCAAC TAGTATCGTGTTACGGACGATTGGGTGATAGC B
S24	³² P- GATGCCTCCAAGGTCGACGATGCAGACACTGATATATGTACAGATTCGGTTGATCATAGCACAAATGCCTGCTAACCCACTATCG CTACGGAGGTTCCAGCTGCTACGTCGTGACTATATACATGTCTAAGCCAAC TAGTATCGTGTTACGGACGATTGGGTGATAGC B
S25	CGTTAAGTATCTGCATCTTACTTGATGGAGGATCCTGTGCACGTGCTAGACTACTGGTCAAGCGCATCGAGAACC GCAATTCATAGACGTAGAATGAACTACCTCCTAGGACAGTGCCAGATGTCATGACCAGTTCGCGTAGCTCTTGG B
S26	^P ^M GCTGTGCCCT CAACCGAATTCACAAGCCTAGA CGACACGGGA-GTTGGCTTAAGTGTTCGGATCT
S27	^P ^M GCTGTGCCCT
S27 (MAR)	MAR ^P ^M GCTGTGCCCT
S28	^P ^M GCTGTGCCCTCAACCGAATT CGACACGGGAGTTGGCTTAA  HEG Linker
S28 (MAR)	MAR ^P ^M GCTGTGCCCTCAACCGAATT CGACACGGGAGTTGGCTTAA  HEG Linker



RESULTS

Chapter I: Insight into DNA substrate specificity of PARP1-catalysed DNA poly(ADP-ribosylation)

Preferential PARylation of 3'-terminal phosphate at a DSB site by PARP1

Previously, we have demonstrated that PARP1 preferentially ADP-ribosylates 5'-terminal phosphates of single-stranded (ss) oligonucleotides and of 5'-overhangs of a DSB in recessed DNA duplexes [12, 13]. Notably, the 2'-hydroxyl group of cordycepin at the 3' end of a recessed DNA is also targeted by PARP1 for covalent PARylation [12]. Nevertheless, PARP1-mediated DNA ADP-ribosylation of DNA substrates tested until now is still much less effective than PARP2- or PARP3-catalysed PARylation of their preferred DNA substrates [12, 13]. In the present study, we further characterised PARP1 DNA substrate specificity and the mechanism of its DNA PARylation activity. It has been demonstrated elsewhere that PARP2- and PARP3-catalysed DNA ADP-ribosylation is strongly dependent on the distance between breaks in DNA substrates [13]. Thus, for optimisation of PARP1 DNA PARylation activity we performed an *in vitro* assay at a saturating concentration of NAD⁺ (1 mM) with the human PARP1 enzyme and various ³²P-radiolabelled Dbait-based DNA structures (Table 7) containing a one-nucleotide (nt) gap for PARP1 activation and 5'- or 3'-terminal phosphates as acceptor groups of various overhangs at a unique DSB end (the opposite DSB terminus ended with a hexaethyleneglycol loop). The reaction products were analysed by denaturing PAGE. As shown in Fig. 16, in case of a 1-nt gap situated 13 nt downstream of the 5' DSB terminus, effective PARylation of the 5'-terminal phosphate started when 5'-overhangs were ≥ 7 nt, resulting in a 24–34% yield of PARylated products (S1ⁿ DNA substrates, $n \geq 7$; Fig. 16A, B). Similar results were obtained in the presence of a physiological non-saturating concentration of NAD⁺ (50 μ M) and a 2.5-fold-increased concentration of PARP1 (Figure 17) suggesting that speed of PARP1-catalysed PAR formation does not significantly affect DNA substrate specificity. Notably, HPF1 (histone PARylation factor 1), a PARP1's interacting partner that is known for modulation of target specificity of PARP1 to serine residues, did not affect PARP1 activity towards the S17 substrate or its profile towards S1ⁿ DNA substrates (Figure 18). Substrates S0_n mimicking substrates S1_n but containing a gap on the opposite strand were less effectively PARylated than S1ⁿ were; however, S0_n showed a similar profile of the PARylation dependence on the length of 5' overhangs (Figure 16B). In contrast to S0ⁿ and S1ⁿ, 3'-phosphorylated protruding termini in DNA substrates S2ⁿ and S3ⁿ were not effectively PARylated by PARP1 even at $n = 21$ (Fig. 16C). By contrast, surprisingly, we found that an S2 (S2^o) DNA substrate containing 3'-phosphate at the blunt DSB terminus was PARylated very effectively (72% of the product; Fig. 16C). Notably, we did not observe significant modification of 3'-phosphorylated termini when the 1-nt gap was placed on the



same, 3'-terminus-containing strand of the duplex (S3ⁿ substrates, Fig. 16C). Furthermore, we compared PARP1 activity towards substrates S2, S2¹, S2⁻¹ and S2⁻³ (Fig. 19A) to verify how sensitive PARP1 is towards the position of the 3'-phosphate in S2-based DNA duplexes. The results revealed drastic inhibition of DNA PARylation in case of substrates with a 1-nt 3'-overhang or 3-nt recessed 3' terminus (S2¹ and S2⁻³, respectively; Fig. 19A). Only substrate S2⁻¹ was as effective as substrate S2 was (Fig. 19A, B), suggesting strict necessity of PARP1 for a 3'-phosphorylated blunt or 1-nt recessed DSB terminus when the gap is positioned on the opposite strand of the DNA duplex 13 nt downstream from the 5' terminus of DSB. Modification of an unlabelled 3'-terminal phosphate and not of a 5'-[32P]labelled terminus in the S2 molecule was confirmed by calf intestinal alkaline phosphatase (CIP) treatment of the reaction products (Fig. 19C). PARP1 kinetic experiments uncovered rapid 3'-phosphate modification with a majority of S2 and S2⁻¹ DNA substrates PARylated already after the first minute of the reaction (Fig. 19B) and continued to be effective at low (down to 2 μM) concentrations of NAD⁺ (Fig. 19D).

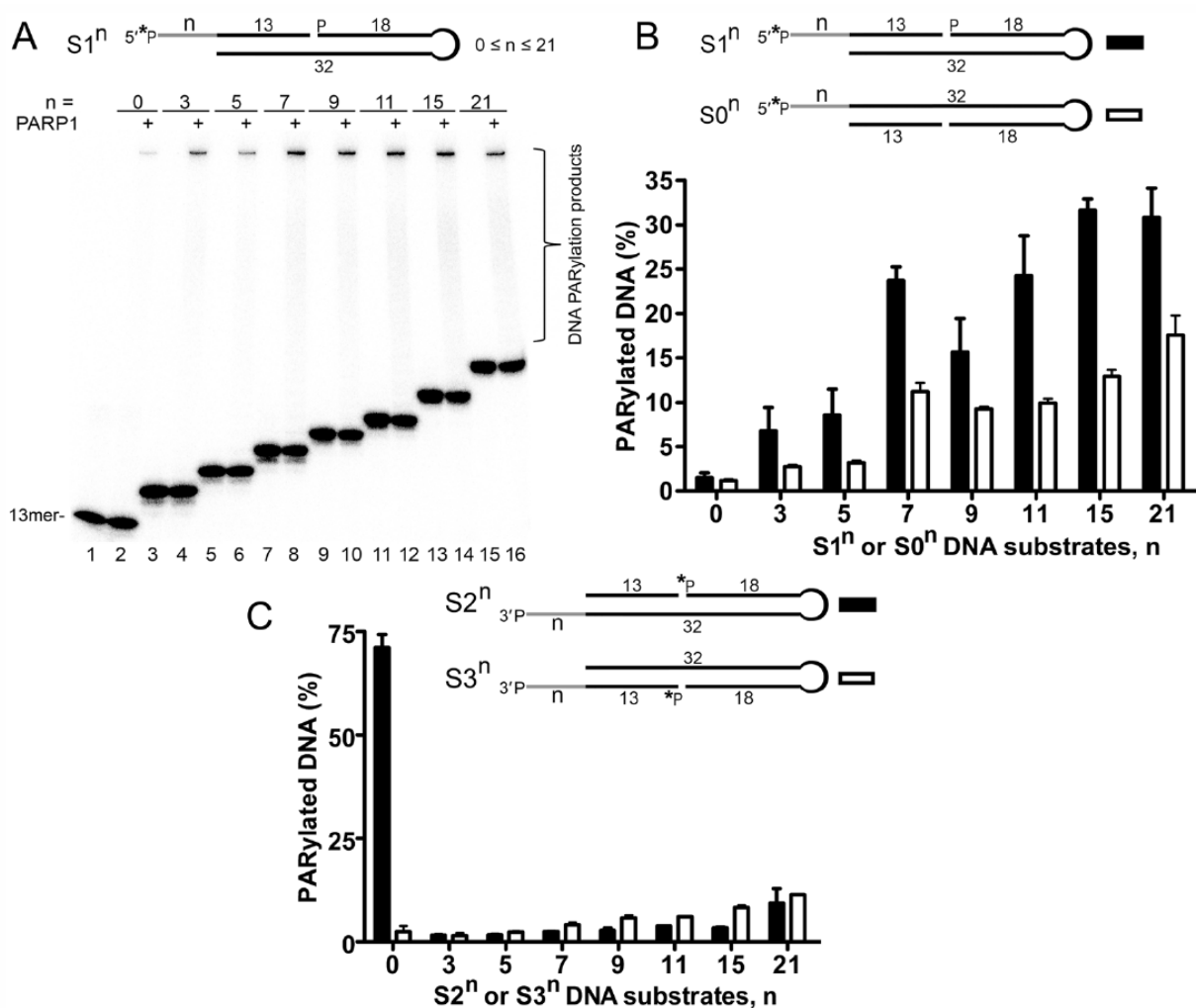


Figure 16: Effects of the type and size of protruding ends in Dbait-based DNA structures containing a 1-nt gap on the PARP1-catalysed formation of PAR-DNA adducts. Twenty-nanomolar PARP1 was incubated with 20 nM 5'-[32P]labelled oligonucleotide and 1 mM



NAD⁺ for 15 min at 37°C under standard reaction conditions. (A) Denaturing PAGE analysis of PARP1-generated products of PARylation of [³²P]labelled DNA substrates S1ⁿ. (B) Comparison of DNA PARylation efficiency among the experiments presented in panel A. (C) Comparison of DNA PARylation activities of PARP1 towards DNA substrates S2ⁿ and S3ⁿ. The data on PARP-catalyzed formation of PAR-DNA products are presented as mean ± SD from three independent experiments.

Furthermore, we compared PARP1 activity towards substrates S2, S2¹, S2⁻¹ and S2⁻³ (Fig. 17 A) to verify how sensitive PARP1 is towards the position of the 3'-phosphate in S2-based DNA duplexes. The results revealed drastic inhibition of DNA PARylation in case of substrates with a 1-nt 3'-overhang or 3-nt recessed 3' terminus (S2¹ and S2⁻³, respectively; Fig. 17 A). Only substrate S2⁻¹ was as effective as substrate S2 was (Fig. 17 A and B), suggesting strict necessity of PARP1 for a 3'-phosphorylated blunt or 1-nt recessed DSB terminus when the gap is positioned on the opposite strand of the DNA duplex 13 nt downstream from the 5' terminus of DSB. Modification of an unlabelled 3'-terminal phosphate and not of a 5'-[³²P]labelled terminus in the S2 molecule was confirmed by calf intestinal alkaline phosphatase (CIP) treatment of the reaction products (Fig. 17 C). PARP1 kinetic experiments uncovered rapid 3'-phosphate modification with a majority of S2 and S2⁻¹ DNA substrates PARylated already after the first minute of the reaction (Fig. 17 B) and continued to be effective at low (down to 2 μM) concentrations of NAD⁺ (Fig. 17 D).

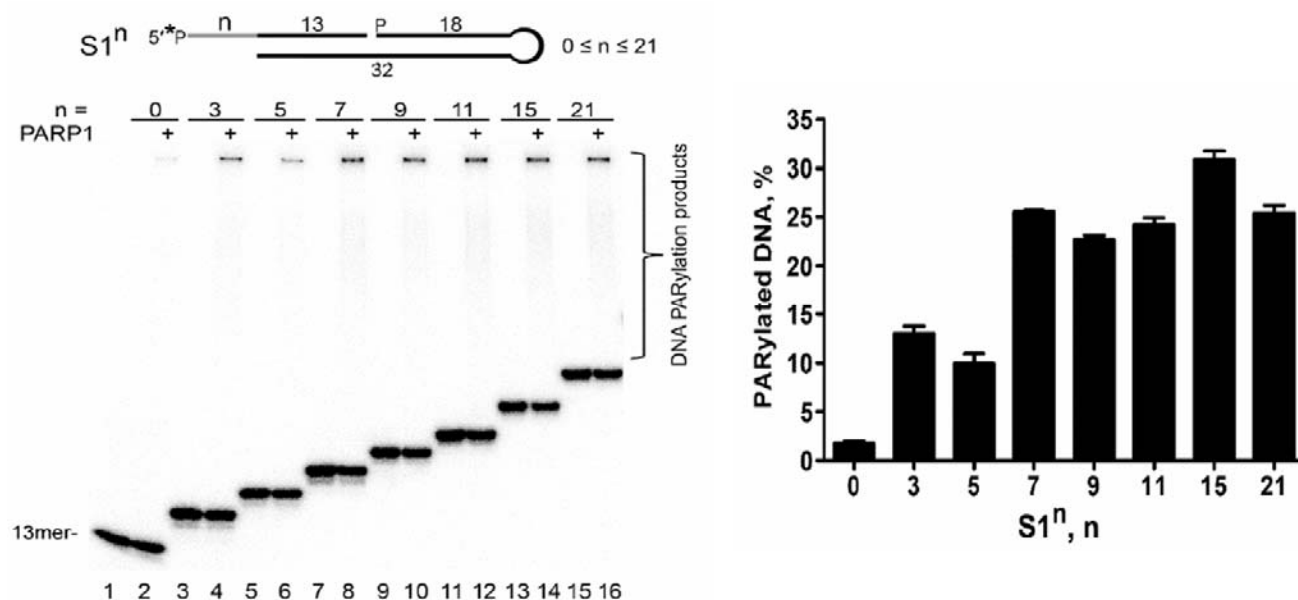


Figure 17: ADP-ribosylation of S1ⁿ DNA duplexes containing 5'-otherhangs by PARP1 at a non-saturating concentration of NAD⁺. [³²P]labelled S1ⁿ DNA duplexes (20 nM) were combined with 50 nM PARP1 in the presence of 50 μM NAD⁺ for 15 min at 37°C under standard reaction conditions. The data on PARP-catalyzed formation of DNA ADP-ribosylation products are presented as mean ± SD from three independent experiments.



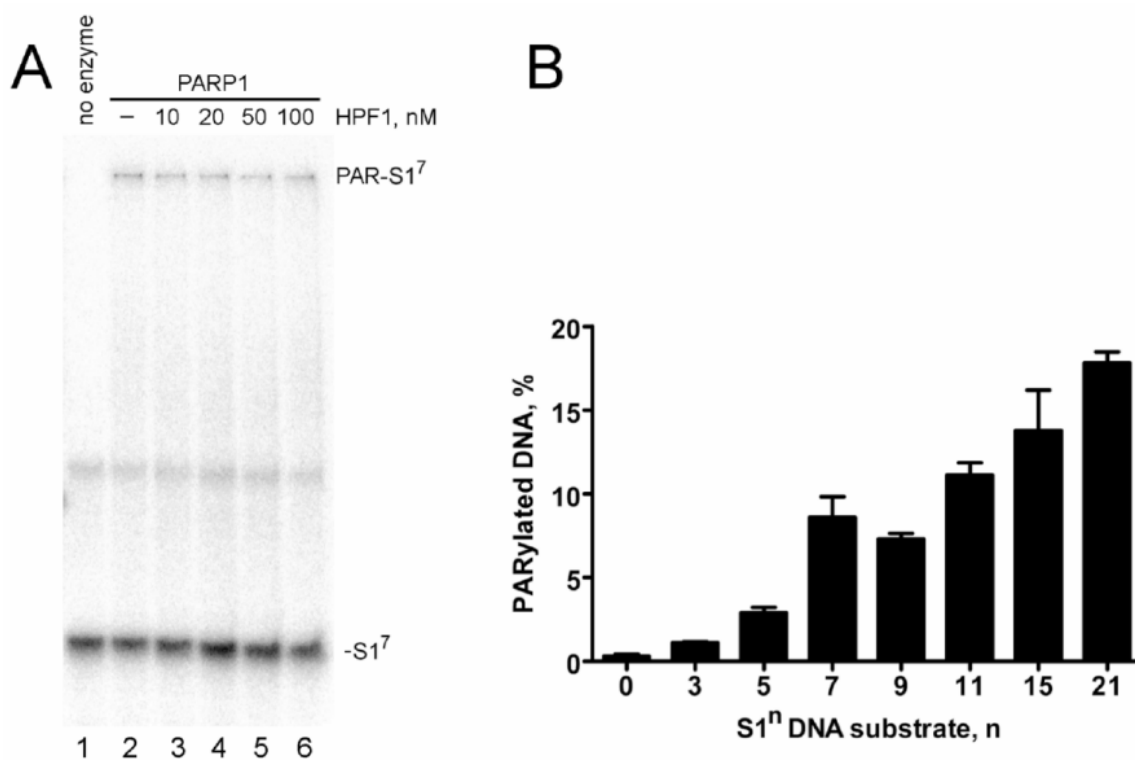


Figure 18: PARP1 DNA PARylation activity in presence of HPF1. (A) The 5'-[³²P]labelled S1⁷ DNA duplex (20 nM) was incubated with PARP1 (10 nM) and varying concentrations of HPF1 under standard reaction conditions. The products of the reaction were separated using denaturing PAGE. (B) Comparison of DNA PARylation activities of PARP1 (10 nM) toward S1ⁿ DNA substrates (20 nM) in presence of 100 nM HPF1 under standard reaction conditions. The purified human HPF1 protein was kindly provided by Dr Ivan Ahel (University of Oxford, U.K.). The error bars represent the standard deviation (n= 3).

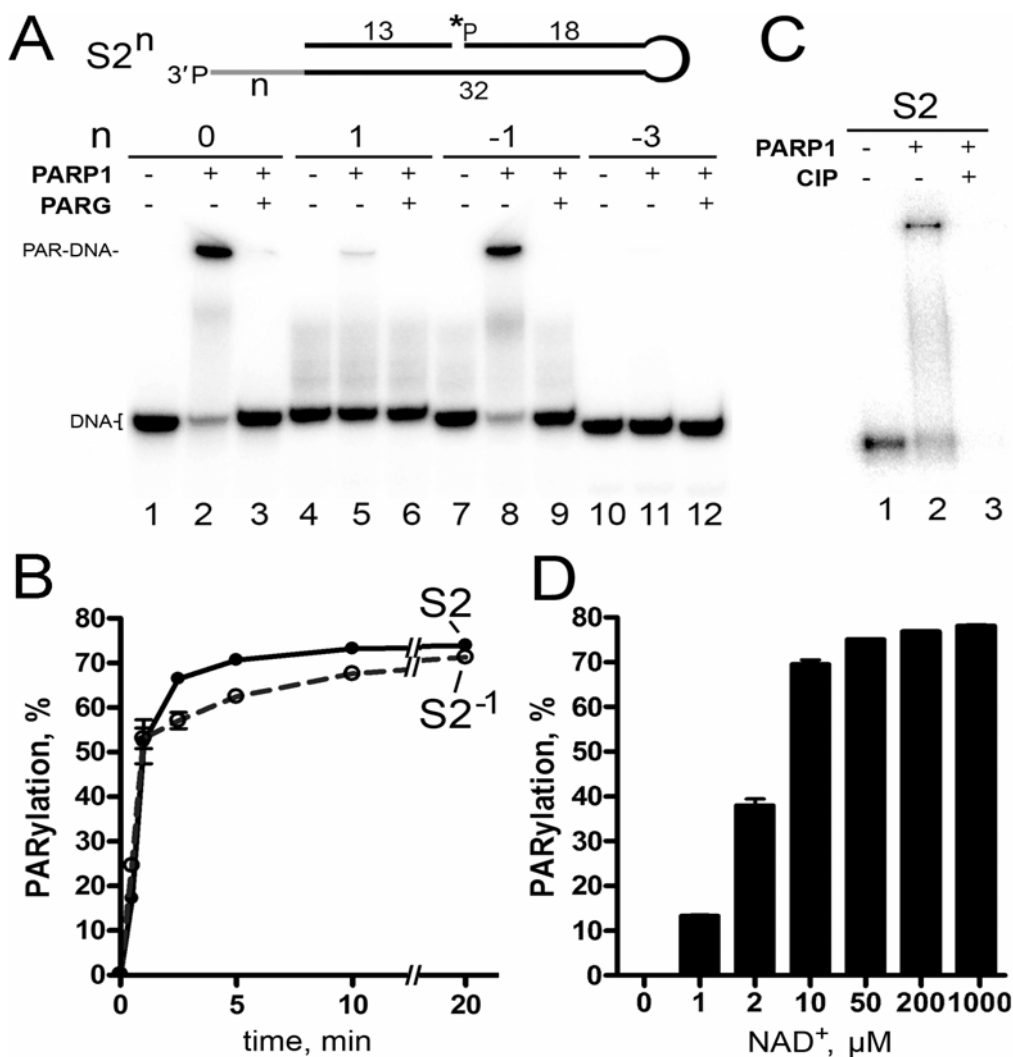


Figure 19: PARP1-catalysed PARylation of S2ⁿ DNA structures with a 3'-phosphate terminus at the DBS end. (A) [³²P] labelled DNA substrates S2ⁿ (50 nM) were incubated with 40 nM PARP1 for 10 min 37°C. (B) Time dependence of PARP1-driven PARylation of substrates S2 and S2⁻¹. DNA substrates (50 nM) were incubated with 20 nM PARP1 for the indicated period under standard reaction conditions. (C) CIP-induced dephosphorylation of 5'-[³²P] labelled PAR-S2ⁿ products. After incubation with PARP1, the S2 samples were heated for 10 min at 85°C, and the resulting [³²P]labelled DNA PARylation products were further incubated with 10 U of CIP for 30 min at 37°C. (D) The dependence of S2 DNA (40 nM) PARylation by PARP1 (20 nM) on NAD⁺ concentration. The data in panels C and D are presented as mean ± SD from three independent experiments.

An SSB-oriented mechanism of PARP DNA PARylation

It has been demonstrated that the accessibility of terminal phosphates of a DSB for PARP2 and PARP3 catalytic sites depends on the distance from a downstream nick [13]. Here, we assessed the dependence of PARP1-catalysed 3'-terminal phosphate PARylation on the distance between a gap and a blunt DSB end in Dbait-based DNA structures of different lengths. As presented in Fig. 20, among substrates tested in columns 1–10, only DNA substrates containing a gap at a 13- or 23-nt distance from DSB termini (substrates S2 and S15 or S10 and S18, respectively) were PARylated effectively. Notably, the extent of DNA-PARylation was very sensitive to the distance between the DSB and the 3' end of the SSB because attachment of a single nucleotide to the S7 substrate resulted in a strong reduction of DNA PARylation in comparison to the S2 substrate. Taking into account that the 10-nt difference in the distance represents one turn of the DNA helix, these data suggest that the position of the acceptor phosphate relative to SSB in the DNA helix plays a discriminating role for PARP1-dependent modification, as observed previously in the case of PARP2 and PARP3 enzymes. This conclusion was confirmed by significant PARylation of a 5'-terminal phosphate observed at a blunt-ended DSB in the S14 substrate (Fig. 20, column 14) but not in the S1⁰ substrate (Fig. 16), which feature a half-DNA helix difference in the positions of their gaps (18 and 13 nt downstream from the DSB end, respectively). The increased size of gaps in substrates S11, S12, and S13 (3, 7 and 11 nt, respectively) resulted in a significantly lower DNA PARylation yield (17–48%) as compared to the S2 substrate (77%) containing a 1-nt gap (Fig. 20, columns 11–13 versus 2). Modification of an unlabelled 3'-terminal phosphate at DSB end in substrates S10–13 was confirmed by CIP treatment of the reaction products (Fig. 21). These results indicated that PARP1-dependent DNA PARylation of the 3'-terminal phosphate at the DSB terminus is not restricted to DNA duplexes with short gaps although the 1-nt gap apparently better coordinates PARP1 binding and activation for subsequent PARylation of such DNA substrates.



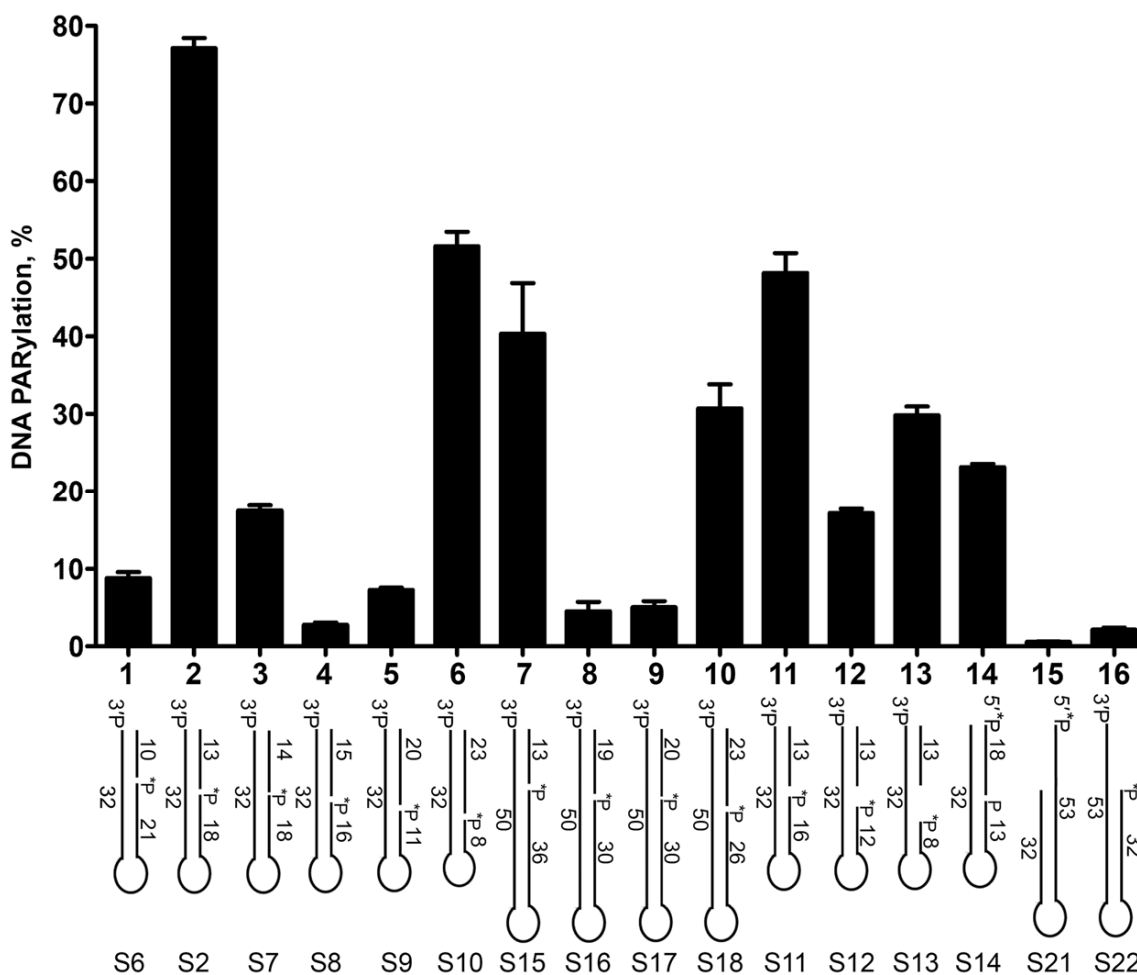


Figure 20: Gap–DSB distance dependence of PARP1-catalysed PARylation of the 3' phosphate at a DSB end of DNA duplexes. The data on PARP-catalyzed formation of PAR-DNA products are presented as mean \pm SD from three independent experiments performed under standard reaction conditions.

respectively) indicating a binding of an additional PARP1 molecule. Previously, formation of 1:1 or 2:1 PARP1–DNA complexes on EMSA gels has been demonstrated with 53-bp blunt-ended DNA duplexes [218]. These data are suggestive of the monomeric mode of PARP1 binding to the S2 DNA substrate (Fig. 22 B). Intramolecular accommodation of the phosphorylated DSB terminus of the S2 substrate in the catalytic site of PARP1 bound to the gap on the same DNA molecule, in our opinion, could explain the observed “hiding” of the DSB terminus of the S2 substrate from the binding of an additional PARP1 molecule and consequently its effective PARylation.

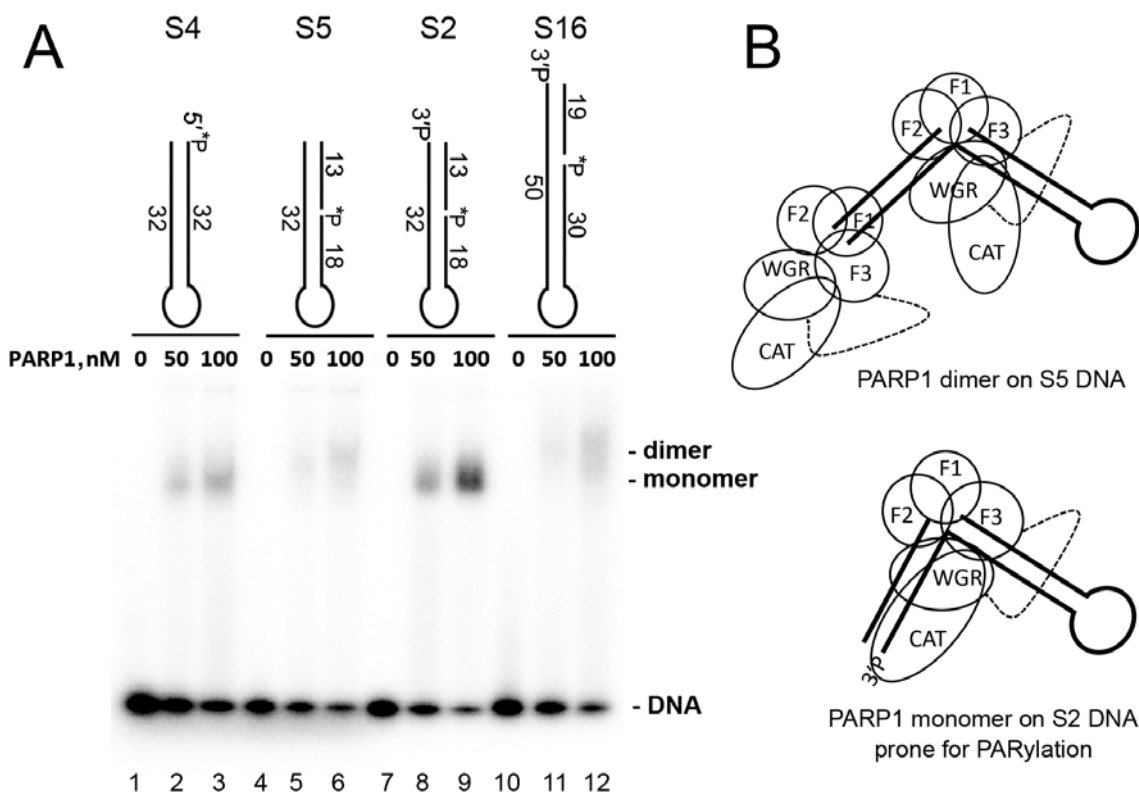


Figure 22: The monomeric mode of PARP1 binding to DNA molecules prone to PARylation. (A) The EMSA. Each of 20 nM DNA duplexes was incubated with 0, 50 or 100 nM PARP1 in a buffer consisting of 20 mM Tris-HCl pH 7.6, 50 mM KCl and 1 mM DTT for 10 min at room temperature. The DNA–protein complexes were analysed by electrophoresis in a 4–12% Tris-Glycine polyacrylamide gel (Novex) under non-denaturing conditions. (B) The putative model of PARP1 complexes with DNA substrates prone (S2) or not prone (S5) to DNA break PARylation.

A 3'-phosphorylated DSB terminus is a major acceptor site of PARylation as compared to PARP1 auto-ADP-ribosylation

Previously, we demonstrated preferential DNA break modifications by enzymes PARP2 (~5-fold) and PARP3 (~50-fold) as compared to their auto-ADP-ribosylation if the DNA substrates are prone to ADP-ribosylation [13]. Nevertheless, PARP1 modification of DNA breaks in our *in vitro* assays has always been at least 10-fold less effective than simultaneous auto-ADP-ribosylation [12, 13]. Here, we incubated unlabelled DNA substrates S2, S4 and S5 with PARP1 in the presence of a low concentration of [adenylate- 32 P]NAD $^{+}$ and separated both types of ADP-ribosylation products by SDS-PAGE (Fig. 23).

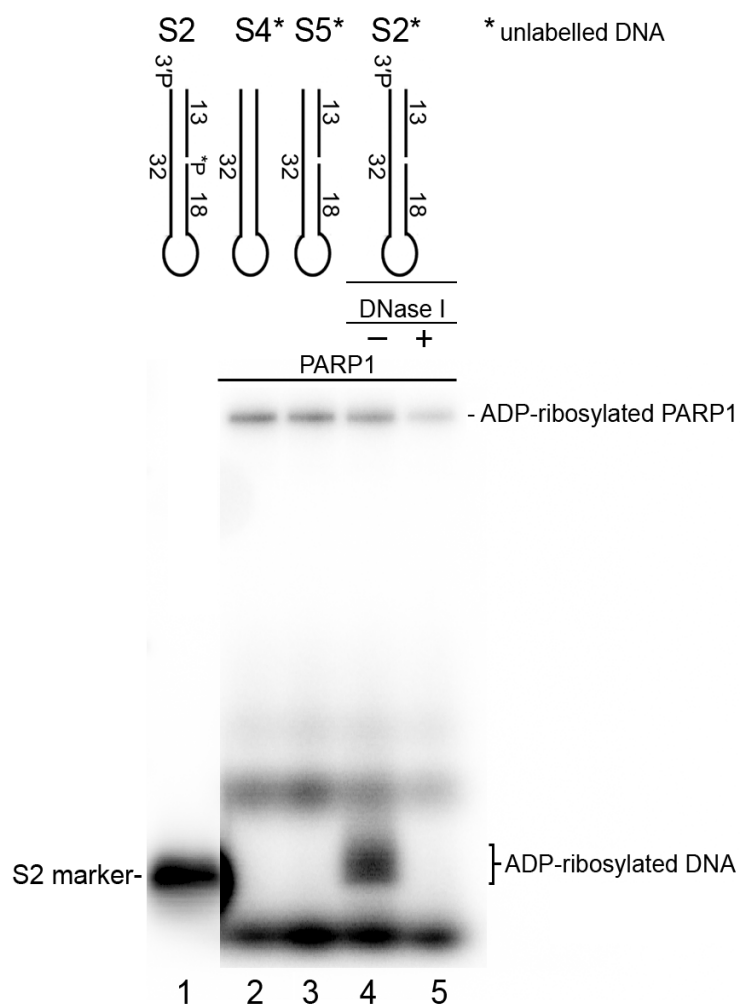


Figure 23: Comparison of the efficiency of PARP1-catalysed auto- and DNA ADP-ribosylation. The denaturing SDS-PAGE analysis of the products of PARP1 incubation with cold oligonucleotide duplexes in the presence of [adenylate- 32 P]NAD $^{+}$. For details see Materials and Methods.



The results indicated that PARP1 was efficiently auto-ADP-ribosylated in the presence of any DNA substrates tested, but a DNA ADR-ribosylation product was observed only in case of the S2 construct containing the 3'-phosphate at the DSB terminus. The yield of S2 DNA ADR-ribosylation was ~5-fold higher as compared to PARP1 auto-ADR-ribosylation in the same reaction mixture (Fig. 23, lane 4), suggesting that PARP1-catalysed DNA ADP-ribosylation can be even more effective than its auto-ADP-ribosylation in case of an optimal configuration of proximal DNA strand breaks.

3'-Phosphorylated DNA substrates are PARylated in human cell-free extracts

To test the possibility of the 3'-terminal phosphate ADP-ribosylation at a DSB site in extracts of human cells, we used DNA substrates S19 and S20 mimicking constructs S4 and S2, respectively, but containing several internucleotide thiophosphate linkages for protection against nuclease degradation (Table 7). As depicted in Figure 23, the 5'-[³²P]labelled S19 control substrate without a gap and 3'-terminal phosphate group was not effectively PARylated in HeLa PARG^{KD} cell-free extracts and partially degraded (lanes 3–5). In contrast, the 5'-[³²P]labelled S20 substrate with a 1-nt gap, 3'-terminal phosphate, and an additional thiophosphate linkage at the site of the hexa-ethyleneglycol loop was effectively PARylated and not degraded in the condition tested (lanes 9, 10 and 15). PARylation of the 3'- but not 5'-[³²P]labelled phosphate in the S20 substrate was confirmed by additional CIP treatment that completely removed the unprotected [³²P]labelled phosphate of PARylated products (lanes 14 and 16). These results are in agreement with the data obtained in our previous work showing effective PARP1-dependent PARylation of a 5'-terminal phosphate in a 5'-overhang of an S1⁷-like DNA molecule in human cell-free extracts[13]. Altogether, these results suggest that the DNA PARylation activity in the HeLa cell-free extracts can be efficient towards both 3'- and 5'-terminal phosphates depending on the structure of DNA breaks.



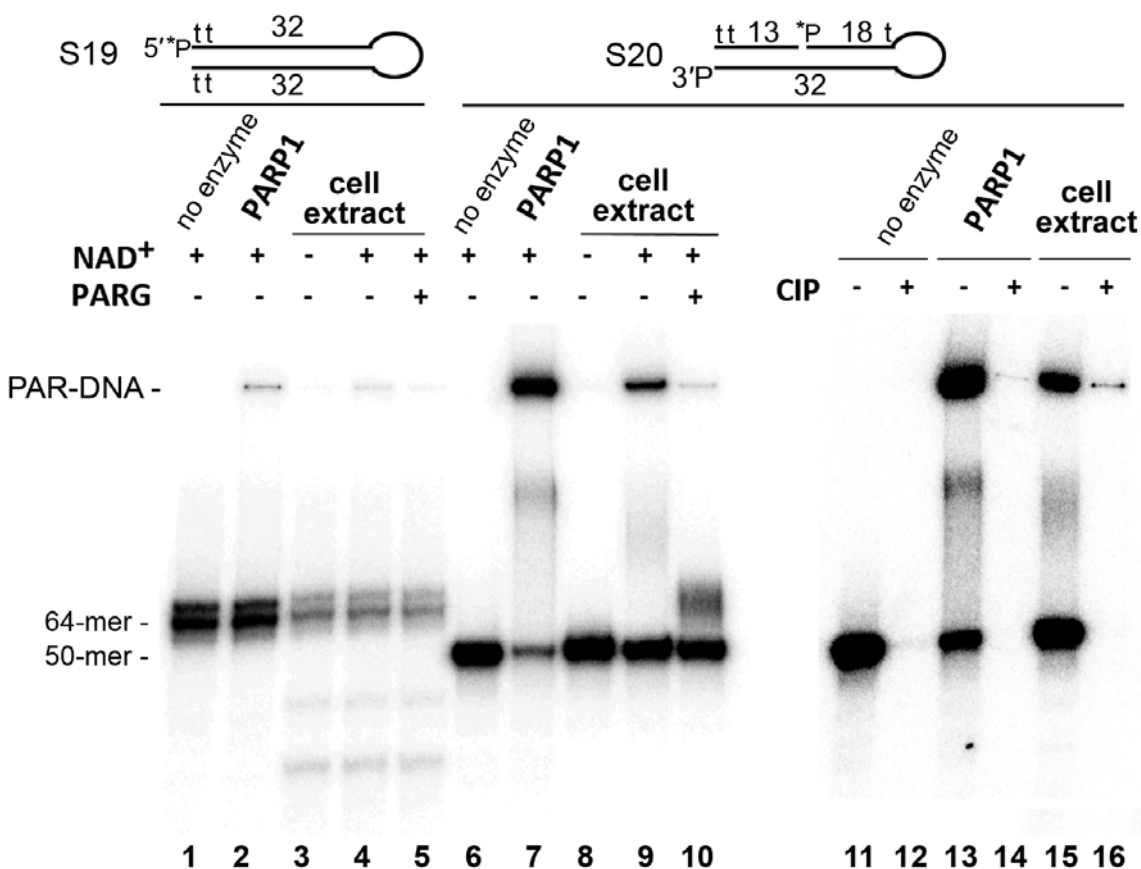


Figure 24: Formation of PAR-3' phosphate-DNA adducts in nuclear extracts from HeLa PARGKD cells. Fifty-nanomolar [³²P]labelled S19 or S20 Dbait-based molecules were incubated with 2.5 µg/µl HeLa extracts or 40 nM PARP1 in the presence of 67 mM KCl, 10 mM HEPES- KOH pH 8.0 and 500 µM NAD⁺ for 20 min at 37°C. The reactions were stopped by heating the samples for 10 min at 80°C, and the resulting DNA PARylation products were next incubated with 20 µg/µl PARG (lanes 5 and 10) or after phenol-chloroform extraction with 10 U of CIP for 30 min at 37°C (lanes 12, 14 and 16). The reaction products were analysed by denaturing PAGE.

Chapter II: Identification of MAR Readers in Cell-free Extracts

Identification of MAR Readers in cell-free extracts: use of proteomics-based approach to purify and identify proteins that specifically bind to MAR-DNA adducts

Still little is known about proteins responsible for detection and removal of ADP-ribosylated DNA adducts. Recently, Ahel's laboratory demonstrated that the MAR moiety that is covalently attached to oligonucleotide termini can be removed not only by PARG but also by other cellular hydrolases, though with much lower efficacy, such as MACROD1, MACROD2, TARG1, and ARH3 [43, 219]. We believe that the half-life of DNA-PAR or DNA-MAR adducts should be similar to that of PARylated proteins and may depend on the recruitment of PARG to the sites of ADP-ribosylation. In the absence of PARG, which is the major glycohydrolase in the nucleus, ADP-ribosylated DNA strand break termini may lead to persistent DNA damage and thus would be highly genotoxic as compared to PARylated PARPs and histones. The inhibition PARG and other related enzymes represents an attractive strategy for developing new inhibitors of the DNA repair pathways, overcoming limitations of existing PARP inhibitors. Here, we used a proteomics-based approach to purify and identify proteins that specifically bind to MAR-DNA adducts. This information will provide insights on the protein interaction network that is modulated by DNA ADP-ribosylation, and potentially on the function of this modification in the regulation and coordination of DNA strand breaks repair, replication and apoptosis.

For affinity purification of readers of ADPr-DNA adducts we used MARylated and not PARylated ss and dsDNA oligonucleotides in order to avoid concomitant purification of PAR-binding proteins. PARP3 MARylated oligonucleotides, synthetic MARylated short peptides and corresponding non-MARylated control oligomers containing biotin were bound to streptavidin coated magnetic beads and incubated with whole cell-free extracts from HeLa PARG^{KD} cells. After extensive wash step and elution with high salt concentration protein samples were loaded on SDS PAGE and the results were visualized by Silver Staining assay after electrophoresis.

As it's shown in [Figure 25](#), MARylated duplexes bound more proteins (P[MAR-dsDNA]) compared to non-MARylated duplexes (P[dsDNA]), in contrast to MARylated ssDNA (P[MAR-ssDNA]), where we notice a depletion of certain proteins compared to control ssDNA (P[ssDNA]). Almost no proteins were bound to the beads alone (P[beads]), which were used here as a "negative control". Similar results were obtained with SDS elution, except for the presence of high levels of streptavidin contamination. For proteomic analysis protein samples were loaded on SDS PAGE and after short migration and fixation were sent to I2BC proteomic Platform.



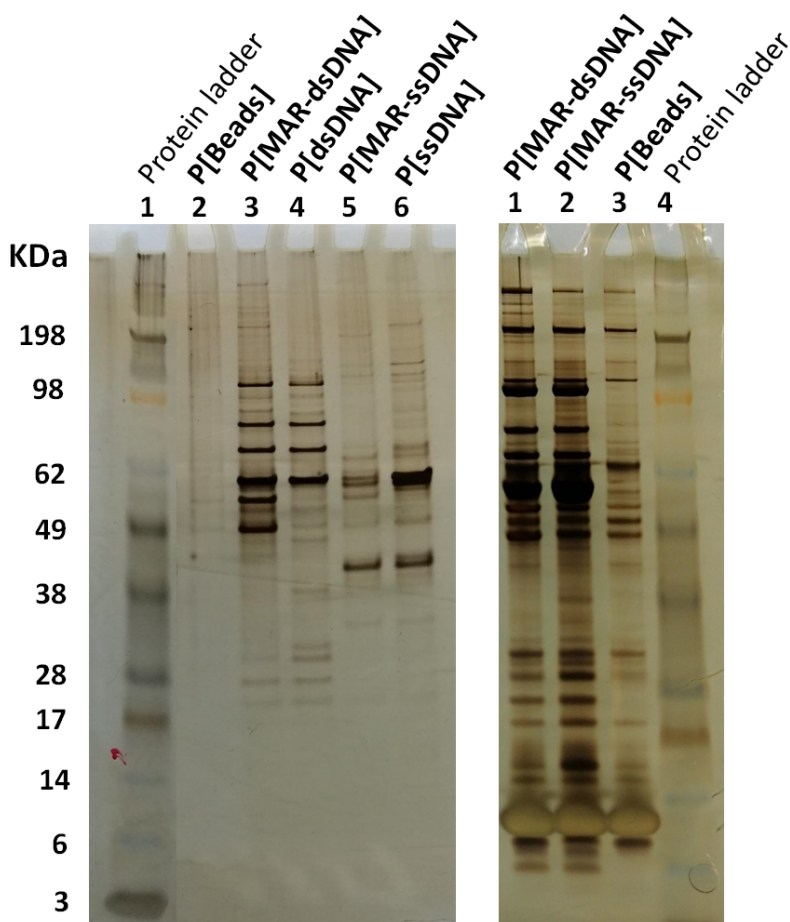


Figure 25: Verification of the presence of bound proteins on MARylated ssDNA and dsDNA substrates by Silver Staining after SDS PAGE.

More than 500 different proteins in P[MAR-dsDNA] and P[ssDNA] samples have been identified. Quantitative and statistical data obtained from proteomic analyses represented in [Figures 26 and 28](#) (for dsDNA and ssDNA-based ligands, respectively) as a volcano plot with $-\log_{10}(\text{p-value})$ versus $\log_2(\text{fold change})$. Selections of 70 depleted, 18 unchanged or 75 enriched proteins out of a total of 526 proteins in case of P[MAR-dsDNA] were made by their $\text{p-value} < 0.05$ ($-\log_{10}(\text{p-value}) \geq 1.3$) and fold change ≥ 2 or ≤ 0.5 ($\log_2(\text{fold change}) \geq |1|$) ([Table 9](#)). Similarly we selected 120 depleted, 3 unchanged or 15 enriched proteins out of a total of 470 proteins in case of P[MAR-ssDNA]. The observed enrichment of PARP14 (known for high affinity to ADPr [220]) and TARG1 (known for ADPr-phosphate bond hydrolysis [43]) in all samples with MARylated ligands serves as a positive control for these experiments and confirms the reliability of the data obtained.

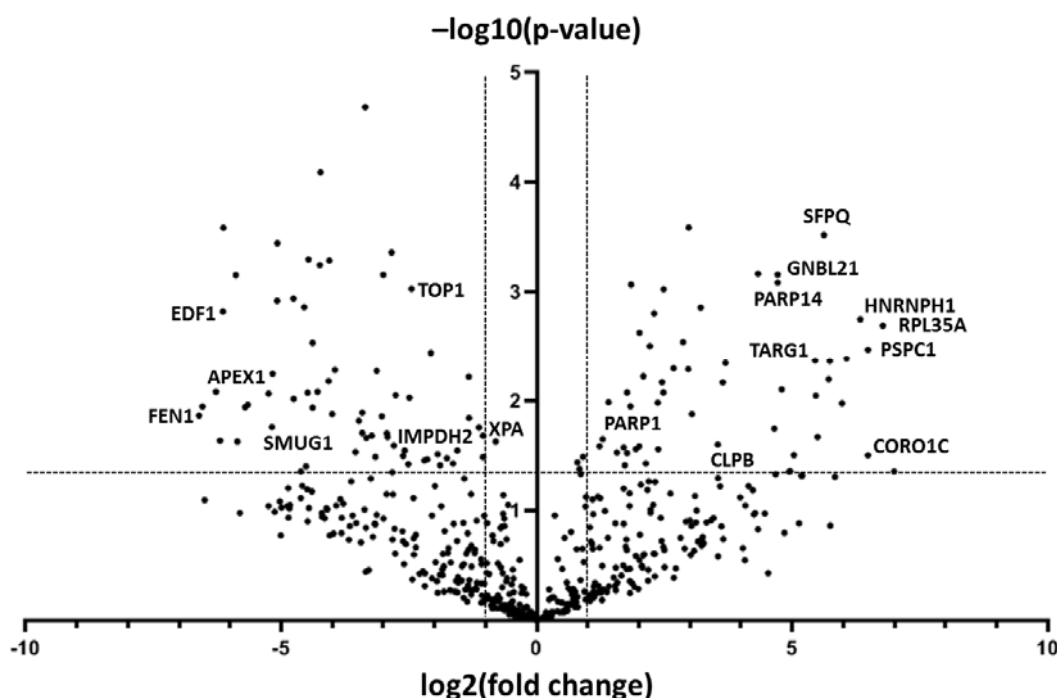


Figure 26: Volcano plot illustrates significantly differentially abundant proteins in samples purified on MAR-dsDNA beads. The fold change is determined by the $P[\text{MAR-dsDNA}]/P[\text{dsDNA}]$ ratio.

Importantly, as the washing conditions used in the purification protocol were not strong enough to dissociate protein complexes present in the cell extracts, it is possible that some proteins, which are found enriched on MARylated ligands, do not interact with these ligands directly but as a part of protein complexes. Analysis of potential protein-protein interactions among identified candidates (Figures 27 and 29) was performed using “String v.11” database (<https://string-db.org>). Thus, the majority of the obtained complexes/clusters such as ribonucleoproteins or cytoskeletal proteins were excluded of the MAR-DNA readers’ candidates list, as the protein(s) in these complexes responsible for direct interaction with the MARylated adducts remains undefined. Notably, some of the DNA repair proteins (NHEJ proteins: NONO, PSC1, PAXX, APTX), cytoskeletal proteins (Filament-forming cytoskeletal GTPase: SEPT9, 2 and 7 and Heteromer forming proteins: NONO, PSC1), PAR synthesis and degradation proteins (PARP1, PARP14, TARG1), ribonucleoproteins (HNRNPH1, HNRNPK-M, SNRPD3, SYNCRIP) were found to be enriched in MARylated versus non MARylated samples, on the other hand some of the DNA repair proteins (BER, NER: APEX1, SMUG1, TDG, NEIL2, RAD54B, XPA) and exonucleases (XNR2, FEN1, NEIL2) were depleted in MARylated samples.



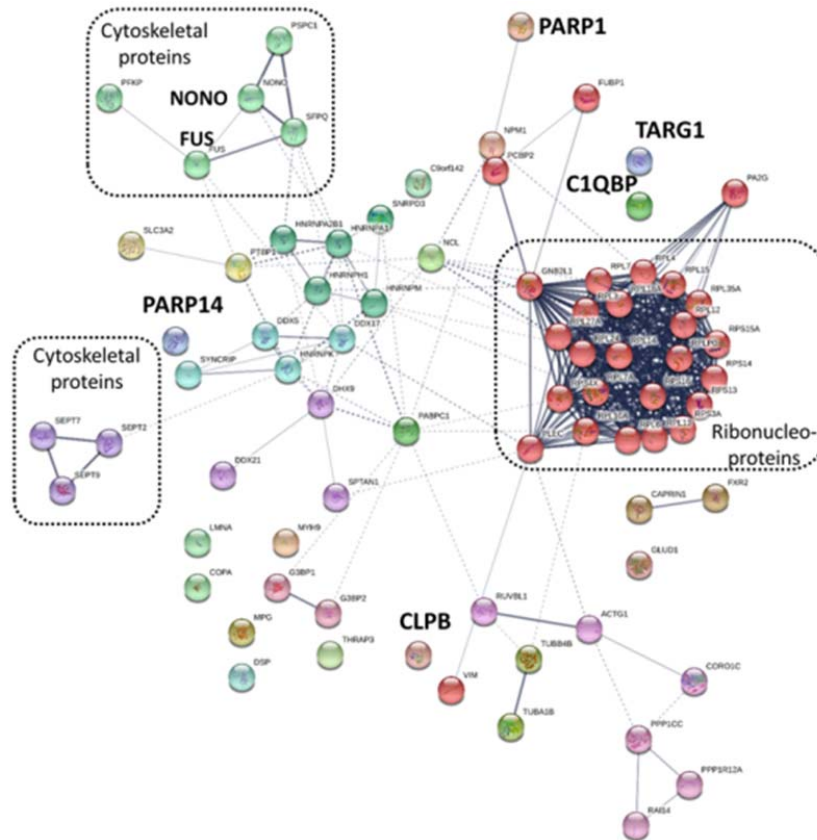


Figure 27: Protein–protein interaction network of 77 proteins enriched on MAR-dsDNA as compared to unmodified dsDNA based on “String v.11” database. Where the thickness of lines between protein nodes indicates the strength of experimental/biochemical data support for their physical interaction (confidence score ≥ 0.4). Network was clustered to the Markov Cluster (MCL) inflation parameter = 3.

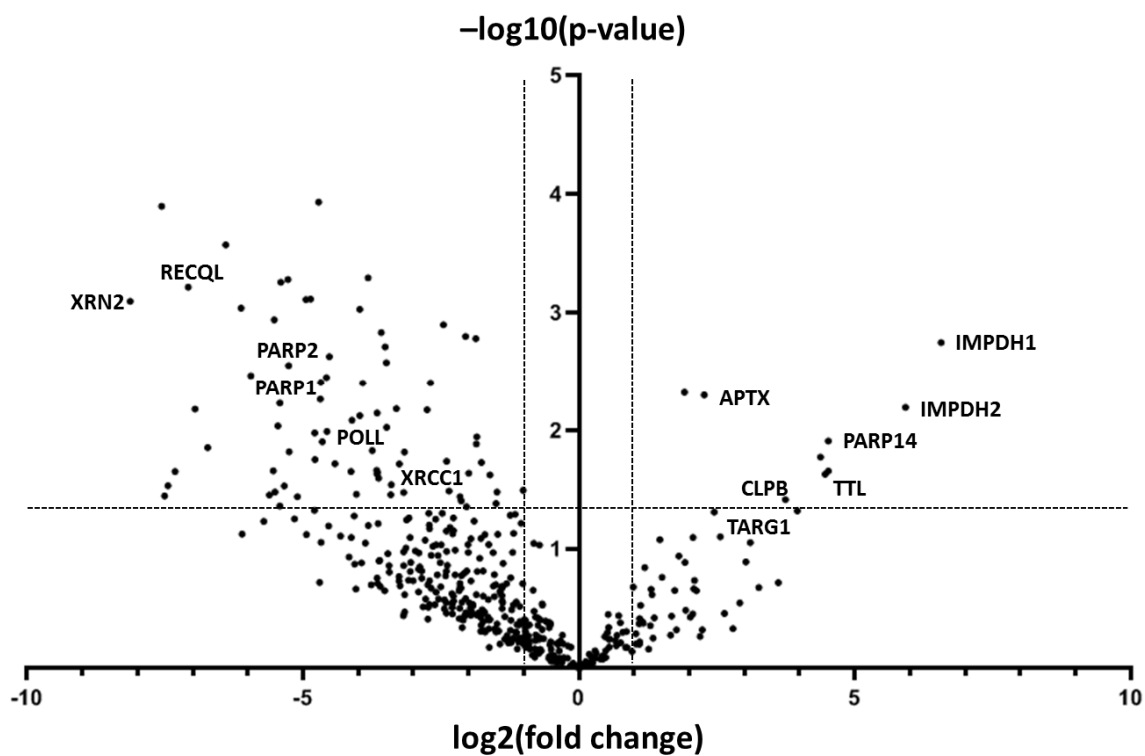


Figure 28: Volcano plots illustrates significantly differentially abundant proteins in P[MAR-ssDNA] versus P[ssDNA]. The fold change is determined by the P[MAR-ssDNA]/P[ssDNA] ratio.

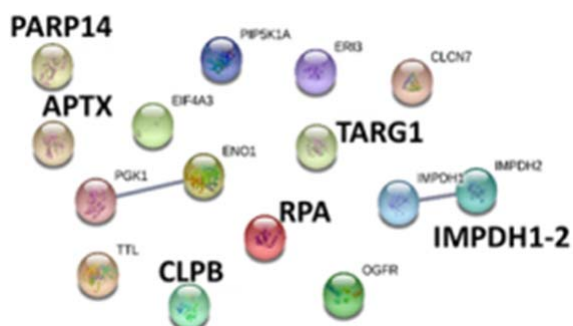


Figure 29: Interaction network of proteins enriched on MAR-ssDNA as compared to unmodified ssDNA (based on “String v.11” database, as described in Figure 25).



In order to distinguish proteins that are able specifically bind MAR-DNA adducts and not just a terminal MAR-residue, we performed purification of proteins from the HeLa PARG^{KD} cell-free extracts bound to the beads with a synthetic MARylated peptide (P[MAR-peptide] samples, [Figure 30](#)) in comparison to control unmodified peptide (P[peptide]) and beads alone ([Figure 31](#)).

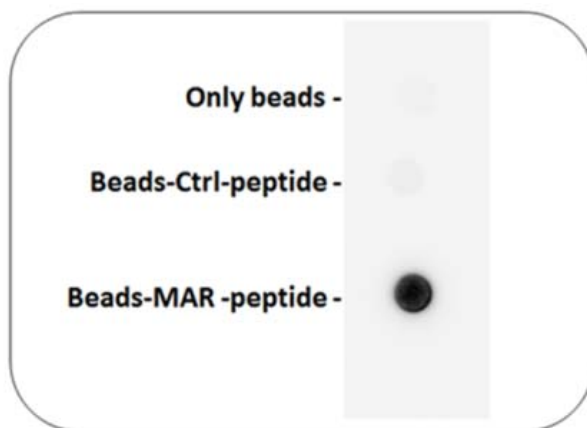


Figure 30: Verification of the MAR presence in used peptides by blotting technic (Anti-MAR antibody ref. MABE1076).

As it is shown corresponding volcano plot ([Figure 31 B](#)), 51 proteins out of total 758 proteins were significantly enriched in P[MAR-peptide] versus P[peptide] samples. Importantly, the majority of these proteins were different from those enriched on MARylated DNA suggesting their specific interaction with MAR-DNA adducts. The enrichment of known ADPr readers PARP14 (-log p value 1.88; fold change log₂ 7.55), PARP9 (-log p value 3.5; fold change log₂ 9.42) and ARH3 [68, 72] (-log p value 2.26; fold change log₂ 3.29) on MARylated versus unmodified peptides validate the obtained data. The strong enrichment of IMPDH1 and IMPDH2 on both MAR-ssDNA and MAR-peptide samples exclude their specific interaction with MAR-DNA adducts but strongly suggest that these proteins are novel ADPr readers.



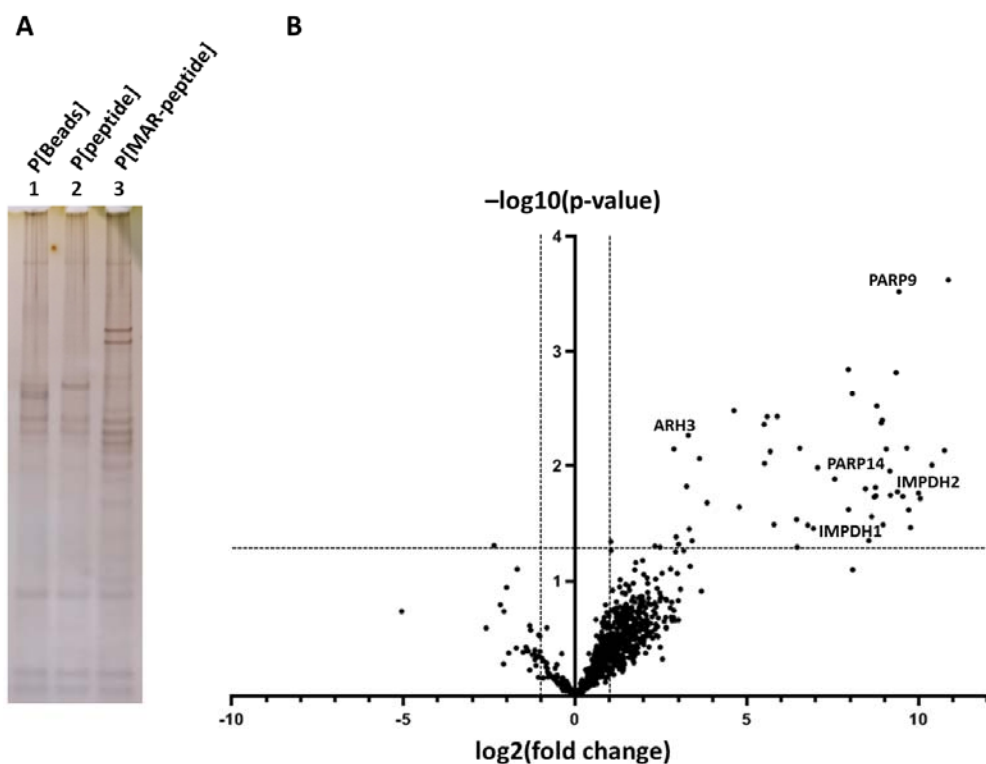


Figure 31: A. Verification of the presence of bound proteins on MARylated-peptide samples SDS PAGE. B. Volcano plots illustrates significantly differentially abundant proteins in P[MAR-peptide] versus P[peptide]. The fold change is determined by the P[MAR-peptide]/P[peptide] ratio.

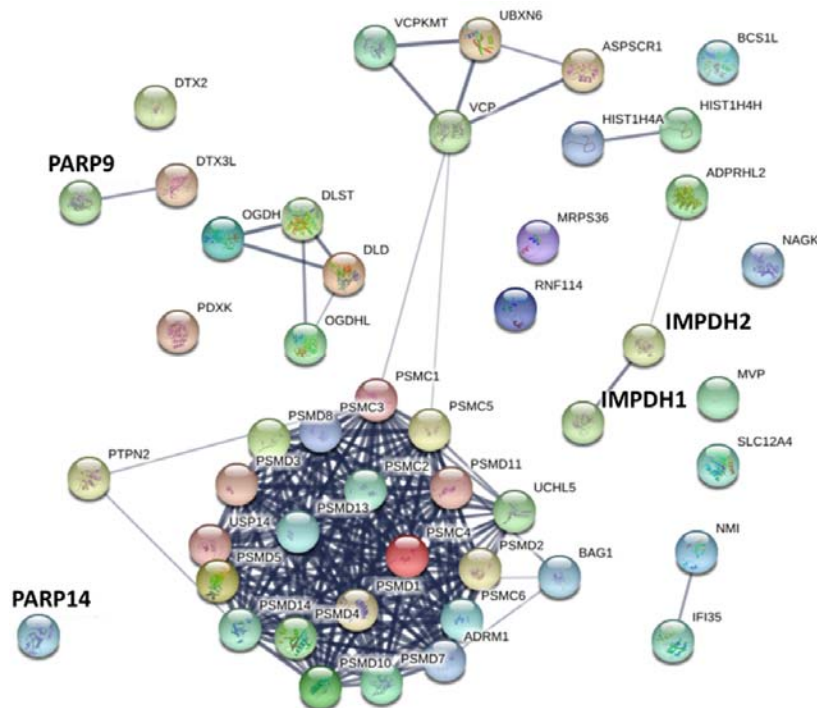


Figure 32: Interaction network of proteins enriched on MAR-peptide as compared to unmodified-peptide (based on “String v.11” database, as described in (Figure 25)).

Finally, after exclusion of ADPr readers enriched on MARylated-peptide from the list of proteins enriched on MAR-dsDNA and MAR-ssDNA (Table 9) the obtained potential DNA-MAR readers were summarized in Table 8.

Table 8: List of selected ds/ssDNA MAR-readers.

Selected enriched proteins on P[MAR-dsDNA] versus P[dsDNA]	Selected enriched proteins on P[MAR-ssDNA] versus P[ssDNA]
NONO, RPL35A, PSPC1, CORO1C, HNRNPH1, SEPT9, PPP1R12A, SEPT2, PPP1CC, FUBP1, SFPQ, SPTAN1, GLUD1-2, OARD1 (TARG1), CAPRIN1, SEPT7, DDX21, PABPC1, PA2G4, MYH9 , GNB2L1, G3BP2, C1QBP , VIM, G3BP1, RUVBL1, PTBP1, SLC3A2, CLPB , DSP, DHX9, RAI14, PFKP, SYNCRIP, DDX17, RPL13, LMNA, C9orf142 (PAXX), HNRNPK, RPS3A, RPL10A, PLEC, FUS , RPL24, HNRNPM, ACTG1-A, NCL, RPL12, HNRNPA2B1, RPS13, RPL18A, HNRNPA1, THRAP3, RPL4, RPL14, RPS15A, TUBA1B, RPS4X, NPM1, RPL3, TUBB4B-A, RPL7A, PCBP2, RPL6, RPL7, RPLP0-6, PARP1, HSPA8, RPL15, MPG, RPS16, RPL27A, APT X, XRCC1	EIF4A3, TTL, CLCN7, OGFR, CLPB , PIP5K1A, APT X, RTCA, RPA3, SEC61A1; OARD1 (TARG1), NFIB, ERI3, ENO1, PGK1.

Notably, CLPB and IMPDH1/2 do not possess known ADPr-binding motifs or domains contrary to majority of the proteins found enriched in MARylated samples. It is possible that their adenosine binding domains: AAA of CLPB and CBS of IMPDH1/2 are responsible for ADPr recognition (Figures 33 and 34).



- **CLPB** (Caseinolytic peptidase B protein homolog) a mitochondrial chaperone protein belonging to the AAA + superfamily of ATPases, The AAA + ATP binding domain can potentially be involved in the recognition of ds and ss DNA-MAR adducts. CLPB scores a $-\log p$ value 1.3 and a fold change $\log_2 3.5$ in MAR versus control ds-DNA, and a $-\log p$ value 1.4 and a fold change $\log_2 3.74$ in MAR versus control ss-DNA.

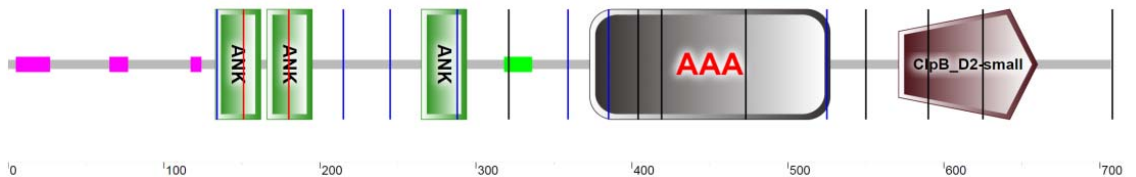


Figure 33: CLPB domain organization according to SMART (Simple Modular Architecture Research Tool, <https://smart.embl.de> protein domain annotation resource. ANK (ankyrin repeat) domain, AAA (ATPases Associated) domain.

- **IMPDH1/2** (inosine-5'-monophosphate dehydrogenase) a protein belonging to the GMPR family. It catalyzes the conversion of inosine 5'-phosphate (IMP) to xanthosine 5'-phosphate (XMP), in the de novo synthesis of guanine nucleotides, and therefore plays an important role in the regulation of cell growth. It could also have single-stranded nucleic acid binding activity and could play a role in the metabolism of RNA and / or DNA; enriched in the case of MARylated ss-DNA versus control ss-DNA, IMPDH1 ($-\log p$ value 2.75; fold change $\log_2 6.56$) and IMPDH2 ($-\log p$ value 2.19 ; fold change $\log_2 5.92$).

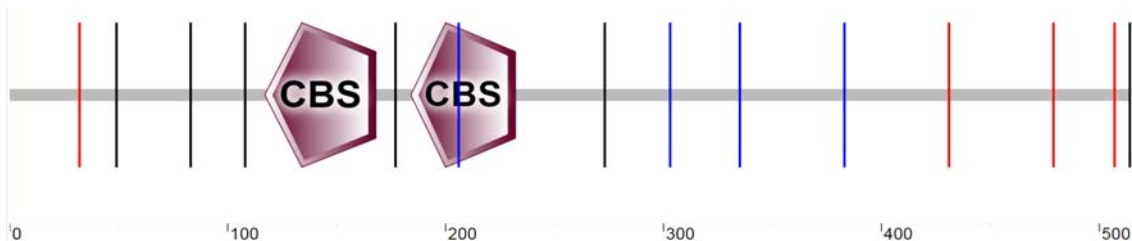


Figure 34: IMPDH2 domain organization according to SMART (Simple Modular Architecture Research Tool, <https://smart.embl.de>) protein domain annotation resource. CBS (cystathionine beta-synthase) domain.





Table 9: Proteomics data for P[MAR-dsDNA] and control samples showing the list of selected proteins with $-\log_{10}(\text{p-value}) \geq 1.3$ (at least for one of three conditions). In green: enriched proteins, in blue: unchanged and in red: depleted proteins for MARYlated dsDNA versus dsDNA along.

Gene names	number of peptides	P[MAR-dsDNA] vs P[dsDNA]		P[dsDNA] vs P[beads]		P[MAR-dsDNA] vs P[beads]	
		(-log 10 p-value)	log2(fold change)	(-log 10 p-value)	log2(fold change)	(-log 10 p-value)	log2(fold change)
NONO	19	1,36	7,00	0,63	3,03	1,73	10,02
RPL35A	4	2,69	6,77	0,23	-0,78	1,77	6,00
PSPC1	6	2,47	6,48	0,16	0,26	4,68	6,74
CORO1C	10	1,50	6,48	0,59	-0,90	1,25	5,58
HNRNPH1	5	2,75	6,33	NaN	0,00	1,60	5,01
SEPT9	9	2,39	6,06	0,15	0,23	3,73	6,29
PPP1R12A	8	1,98	5,97	0,10	0,29	1,78	6,27
(Sept 2)	8	1,31	5,84	0,42	1,52	2,45	7,36
PPP1CC	4	2,36	5,74	NaN	0,00	2,44	5,07
FUBP1	5	2,20	5,71	NaN	0,00	2,64	6,16
SFPQ	24	3,52	5,62	1,42	1,31	3,14	6,93
SPTAN1	10	1,67	5,50	1,72	-3,22	0,83	2,28
GLUD1-2	8	2,05	5,46	0,05	0,14	3,08	5,60
OARD1	7	2,37	5,45	0,93	1,66	2,82	7,11
CAPRIN1	6	1,32	5,20	0,60	2,16	3,06	7,35
(Sept 7)	7	1,32	5,18	0,52	1,67	2,66	6,85
DDX21	6	1,50	5,03	0,08	-0,31	1,86	4,72
PABPC1	15	1,36	4,96	0,23	0,74	3,36	5,70
PA2G4	6	1,35	4,94	0,63	1,79	2,38	6,73
MYH9	43	2,10	4,79	1,14	1,66	2,90	6,46
GNB2L1	4	3,16	4,71	0,73	0,85	3,18	5,57
PARP14	48	3,08	4,71	0,21	0,69	1,42	5,40
G3BP2	5	1,33	4,68	0,41	1,22	3,97	5,90
C1QBP	4	1,75	4,65	0,54	1,36	2,42	6,00
VIM	41	3,17	4,33	0,42	0,77	2,05	5,10
G3BP1	13	1,19	4,23	1,05	3,67	2,93	7,89
RUVBL1	2	2,35	3,70	NaN	0,00	2,94	4,62
PTBP1	19	2,17	3,64	1,50	3,19	2,45	6,83
SLC3A2	3	1,22	3,59	0,35	-1,03	0,95	2,56
CLPB	7	1,29	3,55	0,11	-0,41	1,30	3,14
DSP	36	1,60	3,54	0,09	0,29	1,58	3,83
DHX9	11	2,86	3,21	0,84	2,61	1,53	5,82
RAI14	7	1,00	3,13	0,27	0,88	1,61	4,01
PFKP	7	1,13	3,10	NaN	0,00	1,11	3,32
SYNCRIP	8	1,88	3,04	1,30	2,16	2,03	5,20
DDX17	16	3,58	2,97	0,78	3,37	1,25	6,34
RPL13	6	2,29	2,97	0,92	3,49	1,38	6,46
LMNA	27	2,54	2,86	0,09	-0,13	2,06	2,73
C9orf142	6	2,30	2,68	2,41	2,77	2,61	5,45
HNRNPK	30	1,16	2,62	1,04	2,21	1,90	4,83
RPS3A	15	3,02	2,48	1,36	3,36	1,82	5,84
RPL10A	5	2,08	2,48	0,97	1,03	2,54	3,51
PLEC	122	2,17	2,45	1,59	1,94	2,85	4,39
FUS	5	1,56	2,38	2,38	3,94	2,99	6,32
RPL24	3	1,98	2,37	1,65	3,84	2,48	6,21
HNRNPM	15	1,26	2,31	1,20	4,44	1,58	6,76
ACTG1-A	13	1,05	2,28	0,71	0,40	1,24	2,68
NCL	20	1,01	2,22	0,78	1,66	2,65	3,88
RPL12	6	2,51	2,22	0,89	3,63	1,25	5,85



HNRNPA2B1	9	1,27	2,19	1,69	2,75	2,42	4,94
RPS13	4	1,19	2,17	1,25	3,39	1,85	5,56
RPL18A	4	1,43	2,13	2,87	4,60	3,08	6,73
HNRNPA1	12	2,22	2,08	2,13	4,00	2,72	6,09
THRAP3	2	1,24	2,04	NaN	0,00	1,35	2,47
RPL4	12	2,63	2,01	0,80	3,53	1,14	5,54
RPL14	3	1,59	2,01	0,68	2,26	1,16	4,27
RPS15A	4	1,56	1,94	1,72	4,96	1,82	6,90
TUBA1B	18	3,07	1,84	1,52	1,98	2,24	3,83
RPS4X	10	1,95	1,84	2,53	3,34	3,02	5,18
NPM1	7	1,04	1,82	0,77	1,86	1,44	3,68
RPL3	9	1,16	1,82	3,63	1,93	1,77	3,75
TUBB4B-A	16	1,52	1,77	1,95	2,52	2,89	4,29
RPL7A	10	2,07	1,77	0,80	3,70	1,07	5,46
PCBP2	20	1,41	1,72	2,04	1,71	2,48	3,43
RPL6	8	1,58	1,70	1,09	4,75	1,35	6,45
RPL7	12	1,20	1,70	1,16	2,43	1,85	4,13
RPLP0-6	11	1,53	1,57	1,45	3,67	1,94	5,24
PARP1	60	1,99	1,40	3,77	7,60	4,23	9,00
HSPA8	27	1,00	1,33	1,77	2,42	2,21	3,75
RPL15	5	1,65	1,29	1,07	2,39	1,52	3,68
MPG	12	1,11	1,24	4,68	8,89	3,63	10,14
RPS16	7	1,59	1,23	1,41	5,53	1,63	6,76
RPL27A	2	1,13	1,20	1,31	4,18	1,62	5,37
APTX	9	0,97	1,10	1,61	7,20	1,62	8,30
XRCC1	18	0,70	1,08	3,55	10,08	2,77	11,16
XRCC5	43	1,49	0,90	2,79	10,49	2,90	11,40
HNRNPU	9	1,38	0,84	1,28	4,43	1,46	5,27
XRCC6	47	1,44	0,79	2,30	11,61	2,31	12,41
LIG3	39	0,96	0,36	2,08	10,09	2,14	10,45
DDB1	44	0,28	0,24	4,18	10,04	4,07	10,29
DDB2	16	0,19	0,24	2,91	8,70	3,56	8,94
NMT1	2	0,02	0,14	0,54	2,61	0,81	2,75
RPA3	4	0,02	0,06	1,41	3,33	1,26	3,39
POLD1	52	0,01	0,02	0,96	1,84	1,01	1,86
RPA2	10	0,12	-0,19	2,08	6,57	2,82	6,38
MSH3	48	0,13	-0,20	3,00	7,94	2,82	7,74
PNKP	21	0,25	-0,30	2,45	8,64	3,15	8,34
MSH2	38	0,55	-0,34	2,34	11,09	2,46	10,75
TDP1	14	0,26	-0,45	2,74	6,45	2,17	6,00
UBP1	11	1,05	-0,56	2,63	8,38	3,16	7,82
GTF2I	53	1,63	-0,80	2,30	11,38	2,32	10,58
POLL	6	0,20	-0,83	1,07	3,73	1,11	2,90
IMPDH1	12	0,23	-0,97	1,36	3,78	0,82	2,81
HIST1H1C	9	1,49	-1,05	3,00	5,14	2,19	4,09
XPA	4	1,68	-1,05	2,34	6,38	2,43	5,33
RPS10-P5	7	1,76	-1,13	4,54	9,27	4,31	8,14
POLR3E	18	1,15	-1,29	2,31	7,53	2,75	6,25
RPS25	5	1,84	-1,32	2,26	7,79	2,28	6,47
MYBL2	9	2,22	-1,33	1,51	5,49	1,26	4,16
RBPJ	7	1,29	-1,42	2,07	7,54	2,16	6,12
LIN9	4	1,55	-1,56	3,61	6,21	2,77	4,65
PARP2	6	0,25	-1,56	2,23	5,21	0,63	3,65
HMCES	12	1,43	-1,64	3,88	7,54	3,12	5,90
RPL11	6	1,48	-1,76	3,06	6,01	2,65	4,25
POLE	14	1,04	-1,87	1,95	5,86	1,48	4,00
NTHL1	9	1,41	-1,89	4,26	7,14	2,64	5,25
RMI1	9	1,51	-1,94	2,07	5,71	1,92	3,77
POLR3F	10	1,22	-1,99	2,02	6,68	2,10	4,69



RPS7	7	2,44	-2,07	2,57	6,89	1,97	4,82
SNRPA	1	1,47	-2,14	1,23	2,39	NaN	0,00
IMPDH2	24	1,46	-2,20	2,19	8,42	2,37	6,22
KPRP	3	1,12	-2,41	1,34	2,99	NaN	0,00
XPC	4	0,37	-2,43	0,55	2,94	0,09	0,51
TOP1	12	3,03	-2,45	2,78	6,91	2,10	4,46
SSBP1	8	2,03	-2,49	4,16	9,78	3,15	7,29
PXDN	16	1,42	-2,51	1,79	3,39	1,23	0,88
TOP3A	15	1,55	-2,59	3,09	6,30	1,68	3,71
FAN1	3	0,51	-2,60	0,63	3,18	NaN	0,00
CCDC124	5	1,50	-2,62	2,36	5,91	1,78	3,29
NR2F2	12	2,05	-2,76	3,89	7,67	3,52	4,91
RFX5	3	1,59	-2,80	1,21	2,06	NaN	0,00
RECQL	38	3,36	-2,84	3,01	9,47	2,93	6,62
VRK1	7	1,70	-2,93	1,71	7,45	1,38	4,52
CUL4A	23	3,16	-3,00	3,08	7,49	2,28	4,49
HMGB3	7	1,86	-3,03	4,29	9,46	2,39	6,43
SERBP1	17	2,27	-3,13	2,49	7,55	1,93	4,42
WBSR22	3	1,49	-3,16	3,24	4,69	0,91	1,53
HMGA1	3	1,68	-3,23	1,95	3,72	NaN	0,00
RXR	12	1,29	-3,25	3,67	7,84	1,73	4,60
MLXIP	2	4,68	-3,36	1,80	3,84	NaN	0,00
BUD31	7	1,71	-3,41	2,42	6,63	1,47	3,22
RPN2	7	0,89	-3,53	3,74	6,98	0,87	3,44
DNMT1	19	1,27	-3,63	4,22	7,00	1,22	3,37
ALKBH2	6	0,86	-3,66	2,15	6,74	0,71	3,08
RAD54B	3	1,10	-3,84	0,78	2,93	NaN	0,00
UHRF1	36	2,28	-3,95	3,38	11,01	4,04	7,06
NEIL2	5	1,88	-4,00	1,77	4,67	0,23	0,67
TUBG1-2	20	3,29	-4,06	4,01	10,77	4,06	6,71
TDG	4	1,02	-4,12	3,68	6,34	0,59	2,22
PRC1	12	4,09	-4,23	2,81	7,32	2,21	3,09
KIF22	11	3,24	-4,25	2,92	6,49	1,51	2,25
RPTOR	8	2,08	-4,29	1,88	3,82	NaN	0,00
ELF2	4	2,54	-4,39	3,48	5,02	NaN	0,00
IFI16	34	3,30	-4,47	2,62	11,12	2,03	6,65
TOPBP1	4	2,07	-4,48	1,50	4,42	NaN	0,00
RCC1	7	1,40	-4,51	2,76	6,92	0,80	2,41
YY1	5	2,86	-4,55	3,33	5,49	NaN	0,00
VDR	2	1,22	-4,59	2,84	5,06	NaN	0,00
ESRRA	4	1,11	-4,62	2,08	5,72	0,27	1,10
KIF4A	40	2,02	-4,76	2,47	9,02	2,36	4,26
SAFB-2	2	2,94	-4,76	1,53	2,57	NaN	0,00
NFIC	9	1,20	-4,86	2,33	8,21	0,98	3,34
CKAP5	3	3,44	-5,08	3,39	4,26	1,55	-0,81
RREB1	9	2,92	-5,08	3,14	6,00	NaN	0,00
SMUG1	4	1,76	-5,18	1,70	4,95	NaN	0,00
APEX1	21	2,06	-5,25	3,66	11,33	2,72	6,08
CMAS	16	1,63	-5,86	5,49	8,33	0,91	2,47
HIST2H3A	2	3,15	-5,89	4,11	5,65	NaN	0,00
UTS2	1	3,58	-6,13	2,50	2,76	2,31	-3,37
EDF1	2	2,82	-6,14	2,17	5,71	NaN	0,00
HMGB2	9	1,64	-6,20	4,15	8,59	0,84	2,40
MNT	5	1,95	-6,54	2,35	5,75	NaN	0,00
FEN1	17	1,86	-6,61	5,78	12,53	1,79	5,93



Validation of proteomics data by other methods

In order to test the reliability of the quantitative data obtained in the proteomic approach, we compared the amount of RPA3 and IMPDH2 in samples used for proteomics. The results obtained by western blot assay (Figures 35 and 36), are consistent with those obtained from proteomics, showing respectively the enrichment of IMPDH2 and RPA (40 and 1.35 times) on MARYlated versus unmodified ssDNA. IMPDH2 possess two CSB domains (Figure 34) which have been shown to be critical for binding of RNA, DNA and ligands with an adenosyl group such as ATP and S-adenosyl methionine [221, 222]). Evidently, CSB domains are also involved in MAR recognition via its adenosyl group. It is possible, that the observed absence of higher IMPDH2 enrichment on the MAR-dsDNA in comparison to dsDNA containing beads in proteomics data is explained by very strong IMPDH2 recognition of unmodified dsDNA (Figure 35 – Gel lane 5 and 6) leading to a saturation effect. RPA3, on the other hand, binds weakly to double-stranded DNA, which generates low intensity bands, preventing good statistical studies (Figure 36).

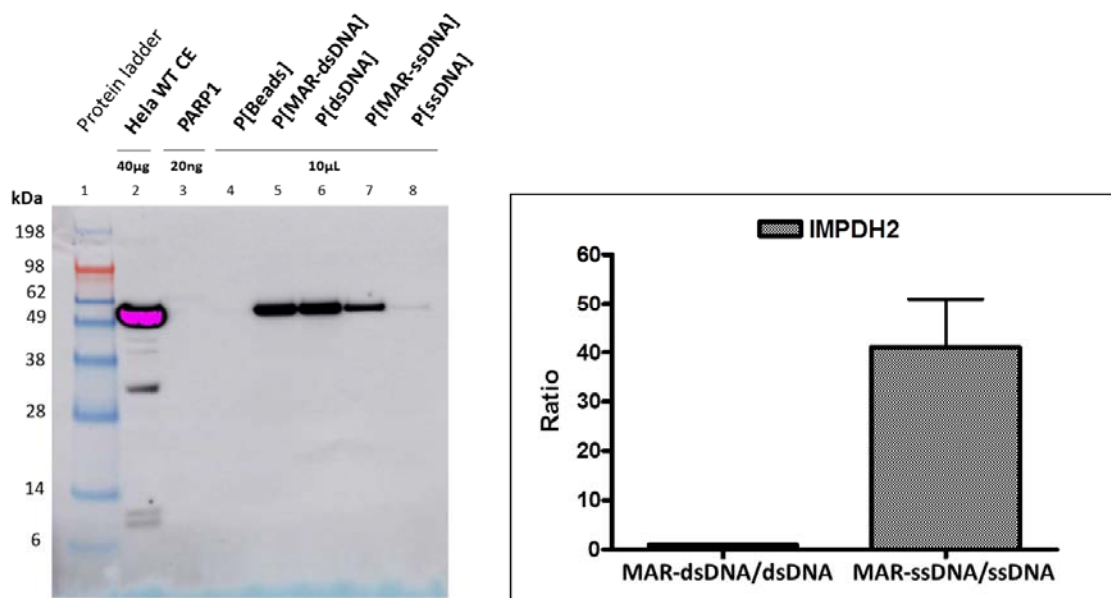


Figure 35: Enrichment of IMPDH2 40 times on MARYlated versus unmodified single-stranded DNA. IMPDH2, possessing double-stranded DNA binding domains, it strongly recognizes unmodified ds-DNA which prevents a good comparison of specificity between the MARYlated and unmodified ds-oligonucleotide (saturated bands).



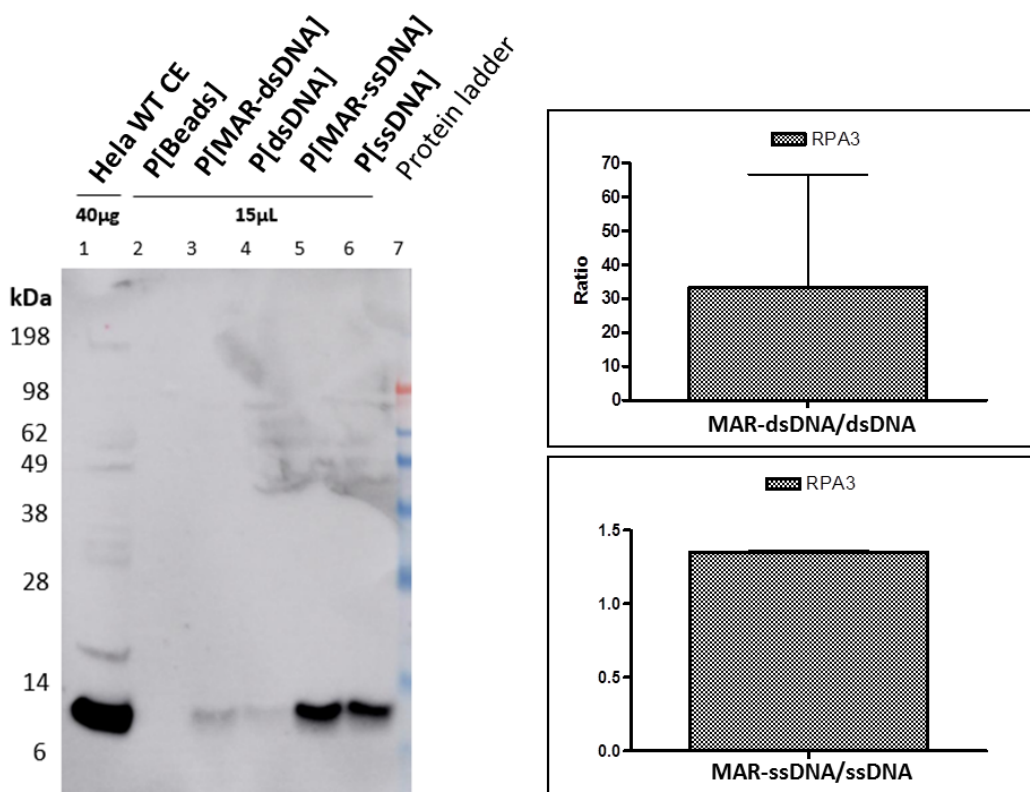


Figure 36: Enrichment of RPA (1.35 times) on MARylated versus unmodified single-stranded DNA. RPA3 binds weakly to double-stranded DNA, which generates low intensity bands, preventing good statistical studies.

Western blotting and proteomics remain qualitative methods. Thus, we used the quantitative EMSA "Electrophoretic Mobility Shift Assay" to test the binding affinity of some of our available proteins (RPA3, PARP1, PARP3 and commercial CLPB) on MARylated versus unmodified dsDNA. Our preliminary EMSA data were in agreement with Western blott and proteomic results. For example, nonselective PARP1 and RPA complex (RPA1-3 proteins) binding to MARylated dsDNA was confirmed (Figure 37). Furthermore, promising preliminary data were obtained by testing different mutated isoforms of CLPB protein (data not shown).

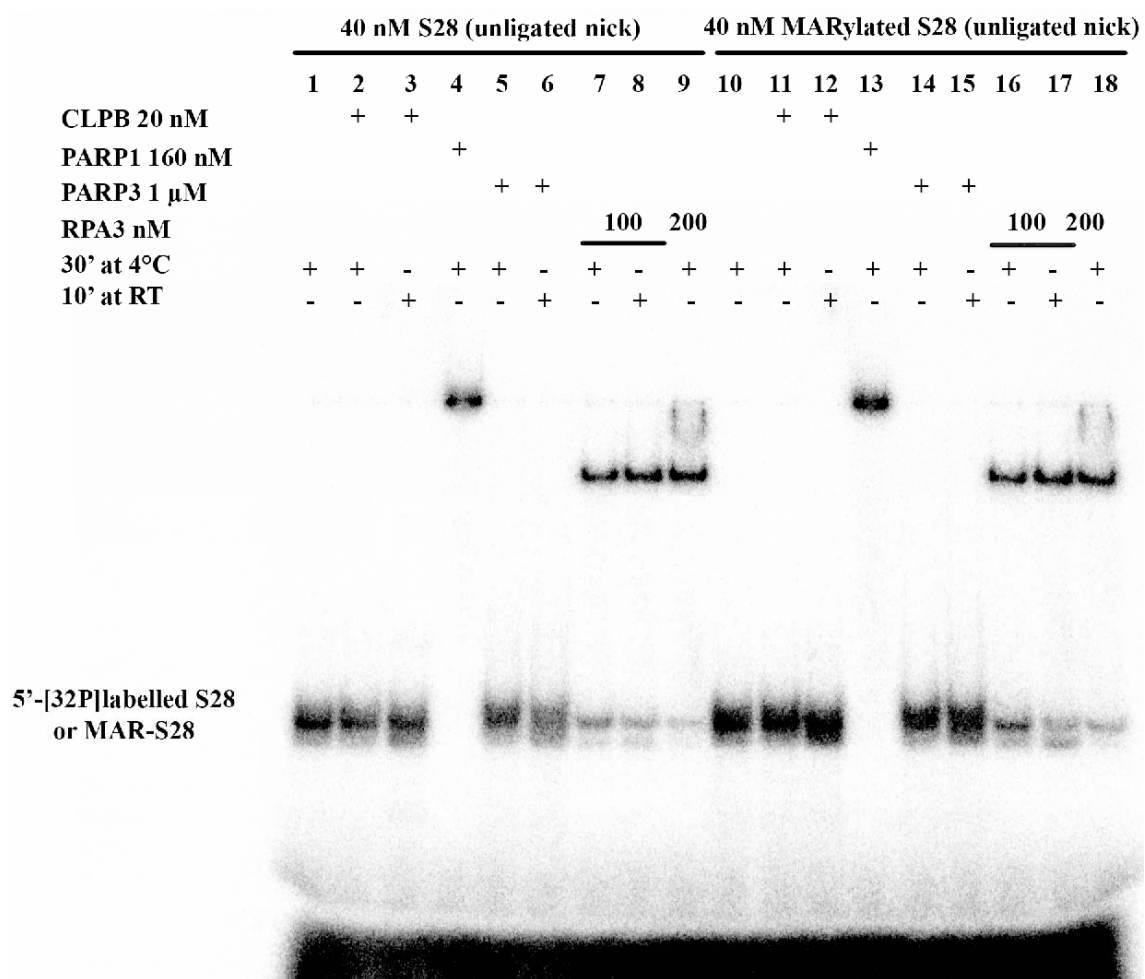


Figure 37: EMSA test of MAR-DNA binding potential candidates.

Chapter III: Impact of DNA ADP-ribosylation on NHEJ

DNA duplexes containing DSB and proximal SSB can form in HR and NHEJ repair pathways. It has been reported that the MRN–CtIP complex generates an internal nick located 20 nt downstream of 5'-termini of a DSB [183] which is suitable for initiation of DSB termini ADP-ribosylation. Notably, PARP1-3 differently influence the relative contribution of canonical and alternative NHEJ (c-NHEJ and a-NHEJ, respectively) and HR pathways in DSB repair [74, 223]. PARP1 is recognized as a key component of a-NHEJ, acting at the initiation step of DSB repair in cooperation with the DSB sensors MRE11 and NBS1 (as a part of MRN complex) [224]. It has been reported that PARP3 interacts with proteins of c-NHEJ pathway, including DNA-PKcs, DNA ligase IV, Ku70/80 and APLF; ADP-ribosylates some of them (Ku70/80 and others); facilitates their recruitment to a DSB and consequently stimulates both earlier and later steps of accurate c-NHEJ [74]. Here, we used nicked DNA duplexes to address the effect of DNA termini MARylation on interaction with purified NHEJ proteins and on repair of DSBs *in vitro* NHEJ reconstitution assay.

PARP3-mediated DNA MARylation inhibits NHEJ of blunt DSBs

In our NHEJ reconstitution assay we used two duplexes of 74- and 85-nt length (DNA substrates S25 and S22, respectively), where S22 substrate contained a nick 20 nt downstream from its 5'-^[32P]labelled blunt end making it prone for PARP3-catalysed MARylation. The opposite 5'-DSB end in S22 and one of 3'-DSB ends in S25 duplex were biotinylated. Formation of corresponding biotin-streptavidin complexes in the assay was expected to exclude them from the ligation and facilitate reaction product analysis.

To carry out the NHEJ reactions, we added Ku, XRCC4, DNA ligase IV complex (X4L4), Artémis, PAXX, DNA-PK, XLF, APLF and PARP3 proteins. We incubated reactions in presence of streptavidin, ATP and NAD⁺, deproteinized and analysed with denaturing PAGE. As shown in [Figures 38 and 39 A](#), Ku and X4L4 complex are able to effectively ligate nick of S22 substrate (^[32P]labelled 85-mer band) and blunt DSB ends of duplexes S22 and S25 producing two bands: 170-mer (S22+S22) and 155-mer (S22+S25) ([Figure 38, lane 2](#)). Position of the ligation bands was validated by control T4 ligase treatment (data not shown). Treatment of X4L4 with 1/30 dilution of commercial lambda phosphatase combined with MnCl₂ for 5 min at 30°C did not ameliorate NHEJ ligation product percentage (data not shown). The percentage of the NHEJ product, doubled by adding 50 nM APLF or a mixture of 25 nM artemis, 500 nM His-PAXX, 25 nM DNA-PK and 20 nM XLF (NHEJ proteins). In order to address the role of DNA (ADP-ribosylation) in repair of DSBs via NHEJ, 100 nM of PARP3 was added to the reaction mixture in the presence or not of 1 mM NAD⁺. The addition of NAD⁺ or PARP3 alone didn't affect significantly the NHEJ product yield (PARP3 bind to nick site; DSB end remains accessible for Ku and for NHEJ proteins). Otherwise, the addition of PARP3 and NAD⁺ together, decreases significantly (≈ 40%) the NHEJ ligation



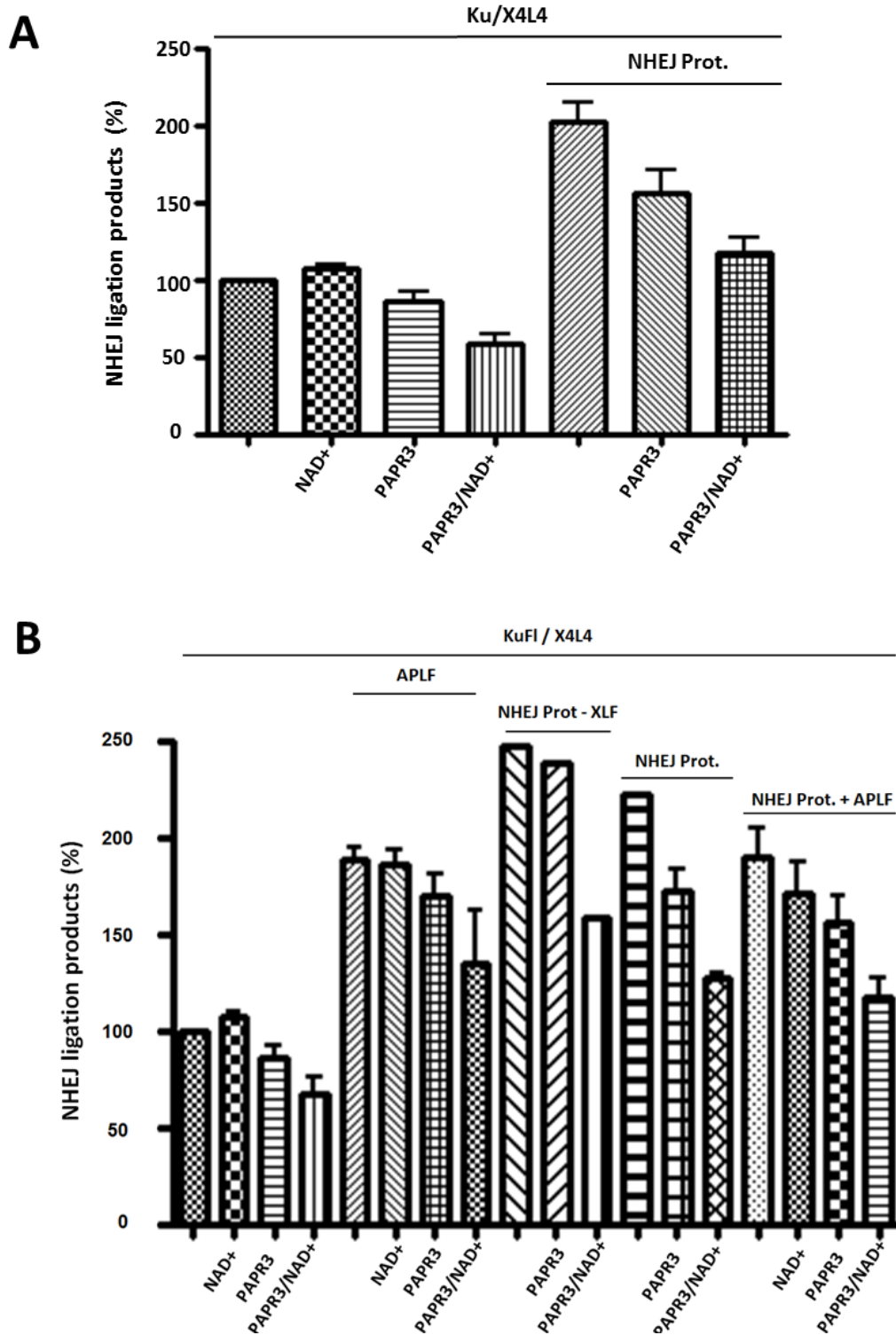


Figure 39: PARP3-mediated DNA MARYlation inhibits NHEJ of blunt DSBs. NHEJ prot.: mixture of Artémis, His-PAXX, DNA-PK and XLF.

Nick stabilization with 5'-THF leads to increased NHEJ efficiency (in-vitro study)

Effect of the nick in proximity to DSB end, which make 5'-phosphorylated DSB-end prone for MARYlation, on NHEJ was verified by using different hamster CHO cell-free extracts (CE). Wild type (KA8 WT), deficient in Ku80 (XDS Ku80-) or XRCC4/Ligase 4 (X4V XRCC4-), and supplemented with XRCC4/Ligase 4 (X4V XRCC4+) CHO cell were kindly provided by Bernard Lopez [225].

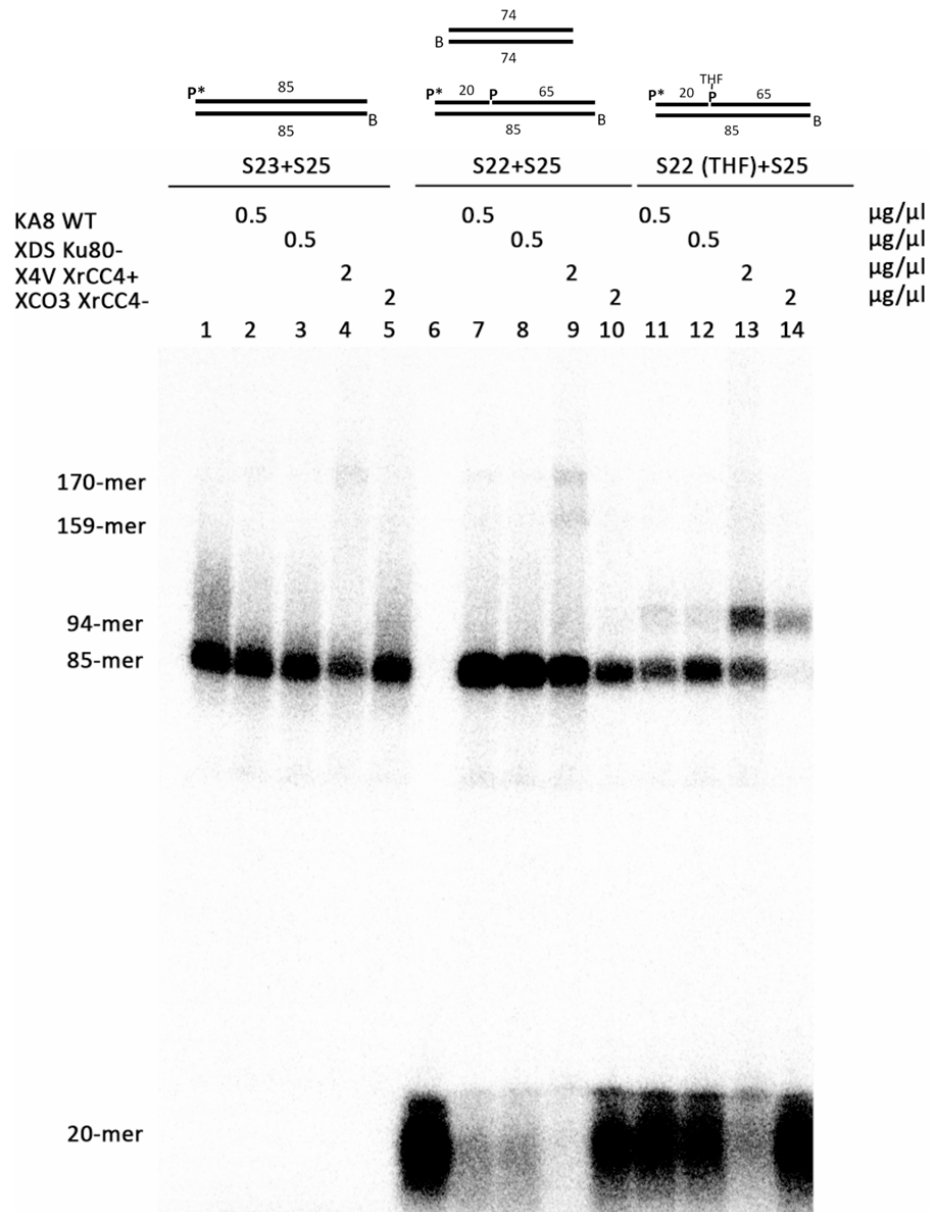


Figure 40: Qualitative representation of the nick stabilization effect on DSB ligation via NHEJ ac-



tors and PARPs interaction (experiments conditions described in [Figure 41](#)). Nick stabilisation with 5'-THF leads to increased NHEJ efficiency (in-vitro study).

S22 and S25 DNA substrates were incubated in the presence of 0.5 µg/µl of different CHO CE. At first, we managed to ligate DSB ends of these two duplexes using X4V XRCC4⁺ CE (supplemented in Ligase 4) [Figure 40](#). But S22's nick was ligated very efficiently (85-mer product) making S22 not prone to MARYlation. Knowing that PARP3 activity require DNA duplexes containing DSB and proximal SSB, we tried to inhibit the nick ligation. We synthesized a new version of S22 substrate containing a 5'-tetrahydrofuran (THF) residue (modeling a stabilized apurinic/apyrimidinic site) at the nick site [S22(THF)]. Blocking of ligation with THF residue led to “stabilization” of the nick and to an increase in NHEJ efficiency ([Figure 40, lane 13](#)). As expected, in absence of X4L4 (X4V XRCC4- CE), nick ligation was totally inhibited in the presence of THF residue at the nick site ([Figure 40 – Lane 14](#)), but surprisingly we observed an increase in NHEJ repair activity of blunt DSB (these results will be discussed later on). To better interpret these obtained results, full length, nicked and ‘stabilized nicked’ duplexes were incubated with different CHO cell free extracts. As shown in [Figures 40 and 41](#), duplexes containing a nick (S22) and considered as structures prone to ADP-ribosylation did not increase the NHEJ effectiveness compared to full length duplexes (S23+S25) but slightly inhibits the DSB ligation process.



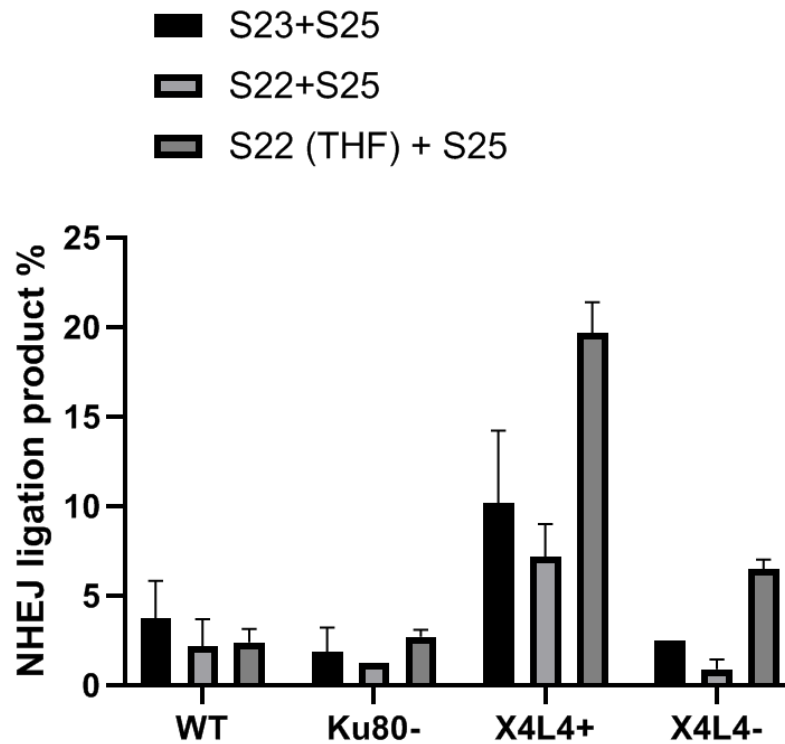


Figure 41: Quantitative representation of the DSBs ligation products shown in Figure 38.

Contrary, S22(THF) structure increases the NHEJ-DSB ligation product in a prominent way (2-4 fold) in comparison with S23 and S22 in X4L4+ and X4L4- CHO cell-free extracts. As expected, X4L4+ CE achieved the best DSB ligation product percentage. Surprisingly, in the case of stabilized-nicked duplexes S22(THF), DSB was ligated more efficiently in the absence of XRCC4/Ligase 4 complex than in WT and Ku80- CE. Finally, in absence of Ku80- DSB ligation percentage was not significantly affected as compared with WT CHO CE under condition used in this experimental system (Figure 41). As shown in Figure 42 no remarkable effect was detected by the addition of NAD⁺ (PARP's substrate), suggesting that the increase in NHEJ efficiency was independent of the PAR/MARylation activity of the endogenous PARPs.



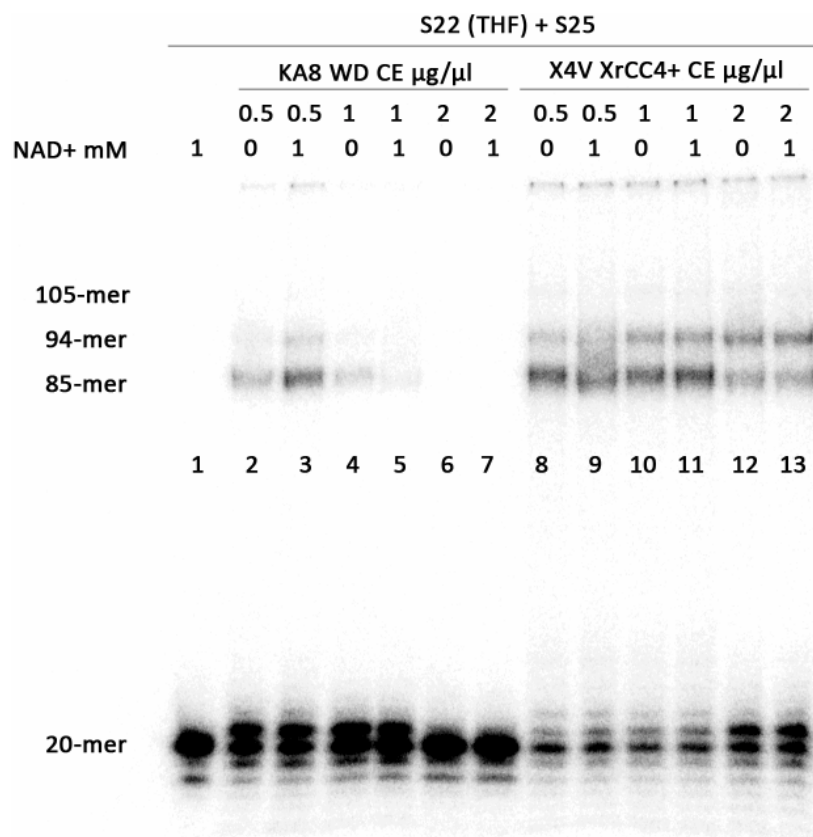


Figure 42: Endogenous PARPs effect on NHEJ efficiency in presence or not of NAD⁺. 20 nM of [³²P]-S22 (THF) and S25, were incubated with KA8 WD (0.1% NP-40) or X4V XrCC4+ (0.3% NP-40) CE in NHEJ buffer (containing 10 % PEG), 200 nM streptavidin, 1 μM BSA, and 0.5 μM ATP for 30 min at 37°C.

Chapter IV: Search for novel PARP1 and PARP2 inhibitors among derivatives of 1,4-dihydropyridine with DNA binding capacity

Check MAR/PARYlation activity of PARP1-3 with commercially available analogs of NAD⁺ *in vitro*, using purified enzymes and standard assays

In the frame of the project, we incubated PARP1-3 proteins with corresponding optimised 5'-[³²P] labelled DNA duplexes (unligated S28 or S28 (MAR)) in the presence of different NAD⁺ analogs: β - Nicotinamide- 2'- deoxyadenine dinucleotide dNAD⁺, Br-NAD⁺, ϵ -NAD⁺, CH-NAD⁺, flu-NAD⁺, ara-NAD⁺, bio-NAD, NHD⁺. These analogues were selected from a current list of 49 products available at BIOLOG Life Science Institute according to two main criteria : i) the capacity to be incorporated into ADPr-oligomers by PARP enzymes (some of NAD⁺ analogues were



excluded according to previous studies); ii) modification(s) in NAD⁺ molecule should be localized on ADPr moiety and not on the nicotinamide residue in order to attempt the PAR/MAR-DNA adducts stabilization against PARG and other cellular glycohydrolases.

The results obtained suggest that each PARP efficiently ADP-ribosylated the 5'-phosphate residue located at the double-strand termini of DNA duplexes in the presence of natural NAD⁺ but their specificity for NAD⁺ derivatives was very different despite high level of homology of their catalytic domains. We showed that PARP1 was able to effectively PARylate DNA termini only with Br-NAD⁺ compound among the eight analogs used. Notably, PARP2 was much less restrictive and was able to incorporate almost all NAD⁺ analogs except ara-NAD⁺ although much less efficiently than natural NAD⁺. Importantly, PARP3 effectively PARylate DNA termini with bio-NAD⁺, flu-NAD⁺ and especially Br-NAD⁺ analog, which incorporation was several times even more effective than that of natural NAD⁺ (Figure 43 A and B).

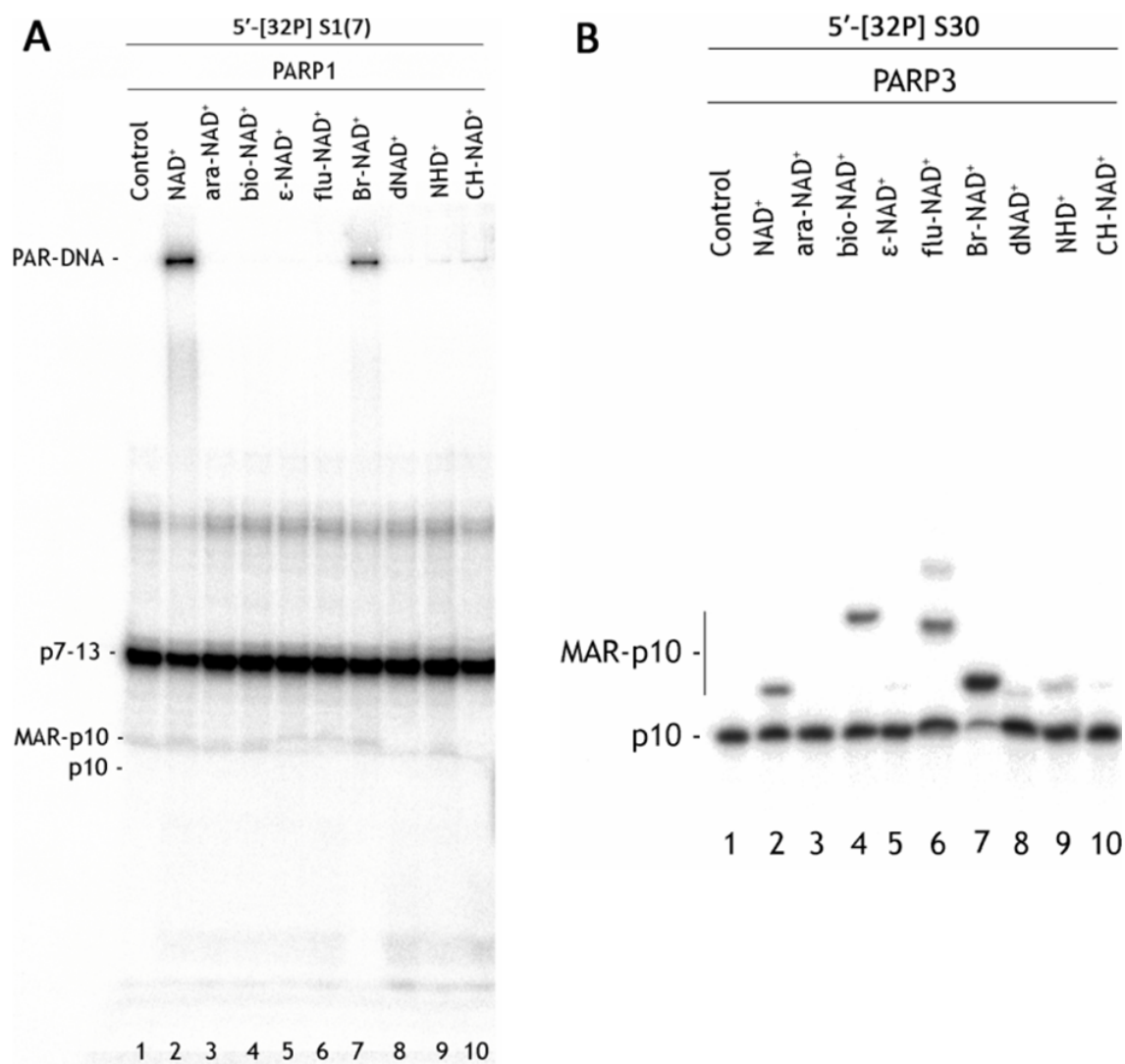


Figure 43: Denaturing PAGE analysis of A. PARP1 and B. PARP3 generated products of DNA PAR/MARylation in presence of NAD⁺ derivatives.

Next, we assessed the influence of the type of NAD⁺ derivatives on stabilization of PAR/MAR-DNA adducts against PARG, which is major of PAR glycohydrolase in the cell. The preliminary results in [Figure 44](#), showed that PARG was active on PARP2 formed polymers/oligomers of CH-NAD⁺, dNAD⁺ and ϵ -NAD⁺ derivatives of NAD⁺ but not of bio-NAD⁺, Br-NAD⁺ and NHD⁺. Similar results were obtained in experiments with PARG hydrolysis of PARP3 produced mono DNA adducts but surprisingly PARG was able to remove mono-Br-ADPr and not 1,N6-etheno- ADPr residue from the terminal 5'-phosphate of the DNA substrate used.

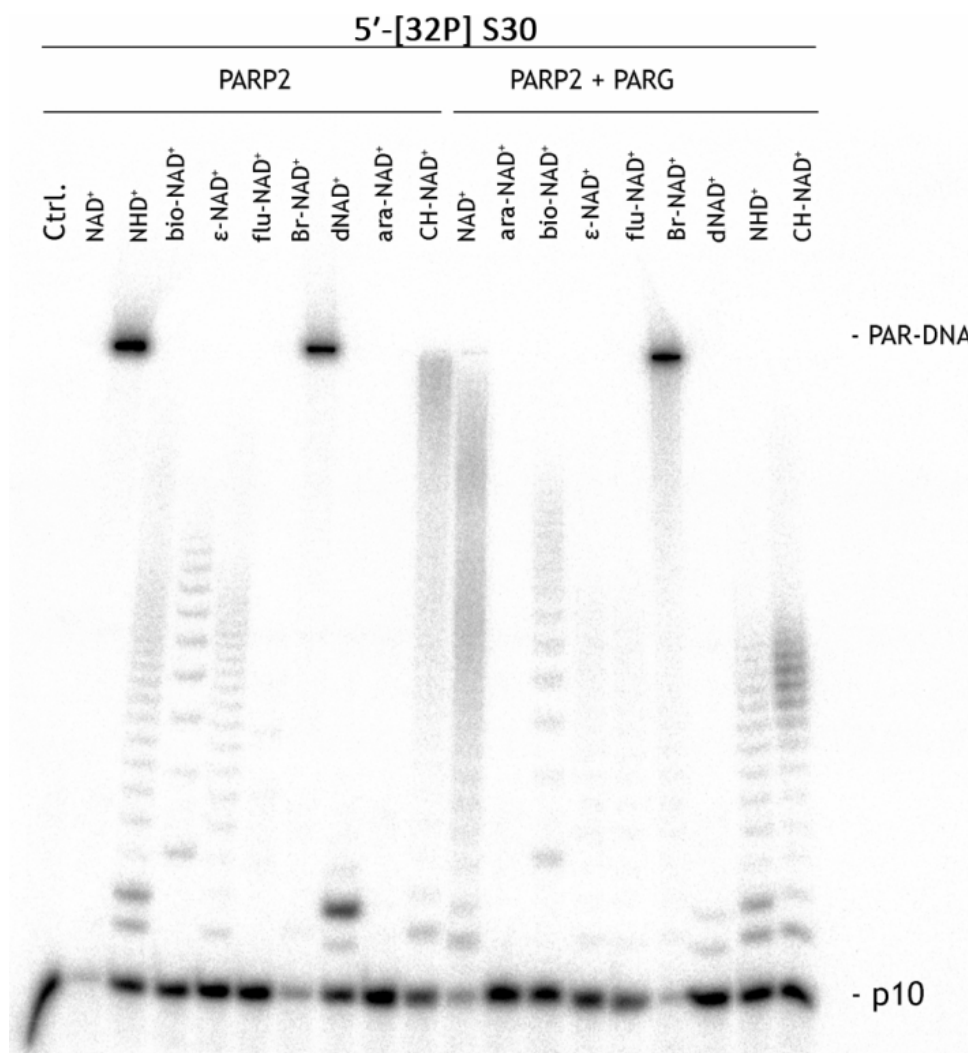


Figure 44: PARP2-dependent formation of PAR-DNA adduct in presence of NAD⁺ derivatives and test of their hydrolysis by PARG treatment.



CONCLUSION

- DNA molecules containing 3'P at a blunt and 1 nt 5'-protruding DSB termini and a proximal SSB on the opposite strand is the most preferred substrate for PARP1 DNA PARylation activity in a wide range (2–1000 μ M) of NAD⁺ concentrations.
- PARP1, in comparison with PARP2 and PARP3, has different DNA substrate requirements for PARylation of terminal phosphates (1.3 or 2.3 and 1.8 helix turns for 3'- and 5'-DSB blunt termini, respectively) but shows similar dependence on DNA helicity and on the orientations of strand breaks.
- Phosphorylated DNA breaks can be preferred acceptors for PAR as compared with PARP1 auto-modification of its own amino acid residues.
- DNA PARylation activity in the HeLa cell-free extracts can be efficient towards both 3'- and 5'-terminal phosphates depending on the structure of DNA breaks.
- With a DNA molecule prone to PARylation, PARP1 form a specific monomeric complex stabilized by interactions with both proximal breaks, apparently including the CAT domain interaction with the phosphorylated acceptor break.
- PARylated DNA adducts are recognized by many different proteins directly involved in different cellular pathways, including DNA repair factors.
- PARylation of ssDNA and DNA duplexes at DSB terminus differently affect binding of hundreds of factors.
- Mitochondrial CLPB protein is specifically enriched on PARylated DNA termini.
- New ADPr recognizing factors (ADPr-readers) like IMPDH1 and IMPDH2 have been identified. It is possible that adenosine binding domains AAA of CLPB and CBS of IMPDH1/2 are responsible for ADPr recognition.
- ADP-ribosylation of blunt DSB termini leads to inhibition of DSB repair by purified enzymes of canonical NHEJ.
- Inhibition of nick ligation with a 5'-THF residue leads to increased NHEJ efficiency on proximal DSB site in X4L4⁺ and X4L4⁻ CHO cell-free extracts in an ADP-ribosylation independent manner.
- Bio-NAD⁺, flu-NAD⁺, Br-NAD⁺ and NHD⁺ analogs could be used (incorporated) by PARP1-3 for DNA ADP-ribosylation leading to stabilization of ADP-ribosylated DNA and protein adducts.
- bio-NAD⁺, Br-NAD⁺ and NHD⁺ PARP2-formed polymers/oligomers and 1,N⁶-etheno-MAR DNA adducts are resistant to PARG hydrolysis activity.



DISCUSSION AND PERSPECTIVES

PARP1 is an abundant, ubiquitously expressed nuclear protein that has long been regarded as a central DNA damage–responsive factor in mammalian cells that is required for the maintenance of genome integrity [173, 244]. It is generally accepted that PARP-dependent PARylation of chromatin results in chromatin remodelling facilitating the assembly of repair complexes at SSBs and DSBs [55, 245]. PARylation and other PARP1-mediated events are critically involved not only in DNA damage repair but also in a wide array of other biological processes, including replication, epigenetic regulation, transcription, apoptosis, inflammation, RNA metabolism, autophagy and proteasomal activation [6, 174-176]. Other DNA-dependent proteins, PARP2 and PARP3, have their specific and partially redundant functions relative to PARP1, and all three enzymes often act synergistically in response to genotoxic stress [43, 236]. The number of known PARP functions in the cell continues to grow. For example, recent work from Caldecott's laboratory indicates that in unperturbed cells, PARP1 is a sensor of unligated Okazaki fragments during DNA replication and facilitates their repair [41]. Other functions still need to be clarified, including roles of reversible ADP-ribosylation of DNA catalysed by PARP1–3 and MARYlation of 5'-phosphorylated termini of RNA molecules by PARP10, PARP11, PARP15 and TRPT1 recently demonstrated in *in vitro* studies [12, 13, 34].

Chapter I: Insight into DNA substrate specificity of PARP1-catalysed DNA poly(ADP-ribosyl)ation

Despite prior insights into PARP1 DNA PARylation activity, there remain key questions regarding the regulation of PARP1 activity, including the mechanism and specific requirements for its unusual substrate specificity towards DNA breaks. PARP1 activity towards previously tested DNA substrates is relatively slow and not very effective as compared to the DNA ADP-ribosylation activity of enzymes PARP2 and PARP3 [12, 13], thus casting a reasonable doubt on the biological relevance of this PARP1 activity.

Here, we show that PARP1 very effectively PARylates a 3'-terminal phosphate at a DSB site of gapped DNA duplexes thereby producing more than 50% of PARylated DNA products already after 1 min of incubation at relatively low (20 nM) enzyme concentrations (Fig. 19B). This activity is effective in a wide range (2–1000 μ M) of NAD⁺ concentrations (Fig. 19D). Taking into account that the NAD⁺ concentrations in the nucleus and cytoplasm are estimated to be ~100 μ M [246], these results support the potency of PARP1-dependent PARylation of specific DNA breaks in the cell. This notion is also supported by the PARylation of 3'-phosphorylated DNA breaks in cell-free extracts (Fig. 24) and by the results of the parallel measurement of PARP1-mediated auto- and DNA PARylation, revealing even more efficient modification of the 3'-phosphate of the S2 DNA



substrate prone to PARylation as compared to simultaneous PARP1 auto-PARylation (Fig. 23). A similar observation has been made previously regarding PARP2-mediated and PARP3-mediated ADP-ribosylation of a 5'-terminal phosphate at a DSB site of nicked DNA duplexes [13], suggesting that all three DNA-dependent PARPs can preferentially target proximal DNA breaks.

PARP1 is a modular protein and has six distinct folded domains, where three N-terminal zinc finger domains and a tryptophan-glycine-arginine (WGR) domain have been reported to be essential for DNA break binding and DNA-dependent activation of the C-terminal catalytic (CAT) domain [82, 84, 86, 247]. Interdomain contacts play a primary role in the allosteric mechanism of catalytic activation of all three DNA-dependent PARPs via local destabilisation of the auto-inhibitory helical subdomain of CAT [85]. In contrast to PARP1, PARP2 and PARP3 do not have zinc finger domains and PARPs 1–3 are differently activated by a variety of damaged DNA structures [47, 248, 249]. Notably, PARP2 and PARP3 are preferentially activated by an SSB harbouring a 5'-terminal phosphate, in contrast to PARP1, which is activated regardless of the phosphorylation status of the DNA ends [47]. Previously, we proposed a mechanistic model where PARP3-catalysed and PARP2-catalysed DNA ADP-ribosylation depends on the orientations and distances between DNA strand breaks in a single DNA molecule [13]. Accordingly, PARP3 and PARP2 ADP-ribosylate the 5' DSB terminus of the same nicked strand if these breaks are separated by a distance of one or two turns of the DNA helix and less effectively ADP-ribosylate the 3'-DSB terminus of opposite strands if the breaks are separated by a distance of 1.5 helix turns [13]. The present study shows that PARP1 has different DNA substrate requirements for PARylation of terminal phosphates (1.3 or 2.3 and 1.8 helix turns for 3'- and 5'-DSB blunt termini, respectively) but shows similar dependence on DNA helicity and on the orientations of strand breaks (Figs. 16 and 20). Taken together, these findings suggest that effective DNA ADP-ribosylation depends on an interplay between the activation of a DNA-bound PARPs and accessibility of the DNA acceptor group for their CAT domain. According to these results, we propose a model of PARP1-mediated DNA ADP-ribosylation (Fig. 45) where the binding of PARP1 to an SSB (1-nt gap) activates its catalytic domain, which in turn starts to ADP-ribosylate all sterically accessible acceptor groups in the same DNA–enzyme complex. This model is supported by the observed monomeric mode of PARP1 binding to the S2 DNA substrate prone to effective PARylation despite the presence of two breaks on the same DNA molecule (Fig. 22B). Structural studies conducted in Pascal's and Neuhaus's laboratories have revealed that PARP1 binds SSBs with directional selectivity, where zinc fingers 1 and 2 bind to 5' and 3' stems, respectively, and the distance between a DNA break (DSB or SSB)-binding site and the catalytic site in PARP1–DNA complexes is $\sim 45 \text{ \AA}$, which corresponds to ~ 1.3 turns ($\approx 13 \text{ bp}$) of a B-DNA helix [99, 100, 226]. This observation may explain the strong preference of PARP1 for the S2 substrate, in which the distance between a protein-binding SSB and the PAR-accepting DSB termini is 13 bp. Nevertheless, it should be stressed that other DNA substrates with a



greater distance between two strand break sites can still be modified by PARP1. We can hypothesise that the efficient ADP-ribosylation of S2, S10, S14 and other DNA substrates is due to (i) the position of their acceptor phosphates, which is on the same side of the DNA helix exposed to the active site of the PARP1 CAT domain; (ii) the highly dynamic nature of the multi-domain proteins and (iii) the flexibility of ss overhangs in substrates S0_n and S1_n (with $n \geq 7$), which might enable 5' termini to reach the CAT site. The latter notion is supported by effective ADP-ribosylation of 5' overhangs in S1ⁿ duplexes (with $n \geq 3$ nt) – but not that of the blunt S10 duplex – catalysed by PARP2 or PARP3 (Fig. 46) relaxing the necessity of a 10 or 20 bp distance between a blunt DSB and an SSB for effective ADP-ribosylation of a 5' DSB terminus [13]. The absence of PARylation of the S21 substrate (Fig. 20), which mimics S1²¹ but lacks a gap, rules out that PARP1 is activated on ds-ssDNA transitions at 5' overhangs when it PARylates S1²¹ and other S1ⁿ structures. The absence of DNA PARylation of substrates S2ⁿ and S3ⁿ with 3' overhangs (Fig. 16) suggests that other structural elements of the acceptor DNA terminus are required for accommodation of the terminal phosphate residue in the active site of the PARP1 CAT domain. The existing 3D structures of PARP1 bound to DNA with a single SSB cannot explain the interaction of the CAT domain of the same PARP1 molecule with a proximal DSB site [82, 85]. Given the strong flexibility of both PARP1 and SSB-containing DNA polymers, it is tempting to speculate that with a DNA molecule prone to PARylation, PARP1 will preferentially form structurally different complexes stabilised by interactions with both proximal breaks including the CAT domain interaction with an upstream phosphorylated terminus. Further studies are needed to test this hypothesis.

According to the evidence collected so far, DNA ADP-ribosylation activity of PARPs strongly depends on the type and position of DNA breaks. Proximal DNA breaks can be generated directly by genotoxic agents or during processing of the initial DNA damage by DNA repair and DNA replication machineries. In this study, we demonstrate that PARP1 preferentially PARylates a 3'-phosphate of DSB sites in proximity to an SSB. It should be noted that 3'-phosphate termini can be generated endogenously as an intermediate of the action of bi-functional DNA glycosylases or as a product of a tyrosyl-DNA phosphodiesterase 1 (TDP1) reaction, which can remove a variety of 3' adducts from an SSB and DSB during DNA repair and leave a 3'-terminal phosphate [250, 251]. It has been reported that PARP1 plays a critical part in TDP1-mediated repair of trapped topoisomerase I (TOP1) cleavage complexes [252]. PARP1 directly binds to the N-terminal domain of TDP1 and PARylates TDP1 without blocking its catalytic activity. Multiple studies show that PARP inhibitors sensitise cells to TOP1 poisoning by camptothecin [253-255]. Moreover, genetic evidence indicates that PARP1 and TDP1 are epistatic for the repair of TOP1-induced DNA damage [252]. We suggest that the PARP1-dependent PARylation of 3'-phosphorylated DNA breaks observed here may further enhance the functional interactions between the PARP1 and TDP1. Addi-



tional studies are warranted to elucidate how PARP1-dependent DNA PARylation can perform its specific function in a cellular response to DNA damage.

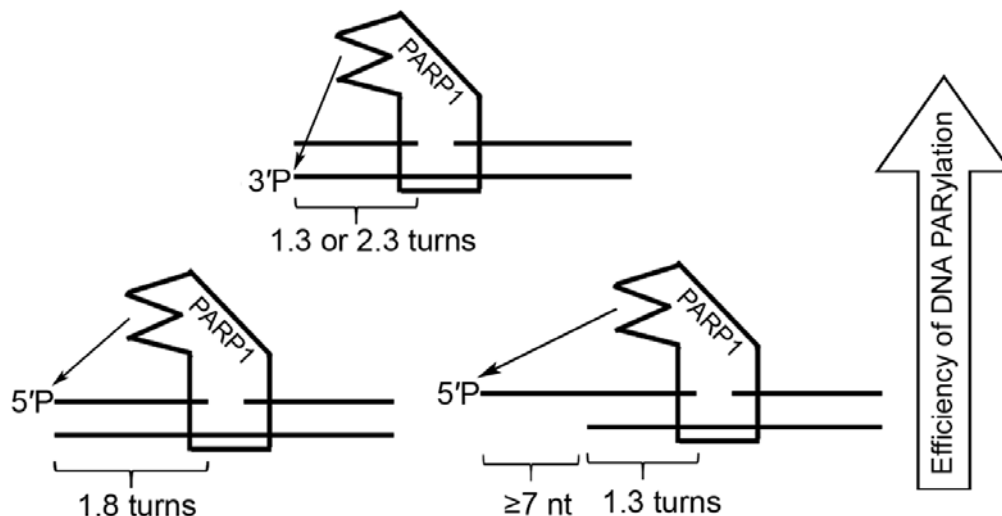


Figure 45: Schematic representation of the putative model of DNA modification by PARP1 activated on a 1-nt gap.

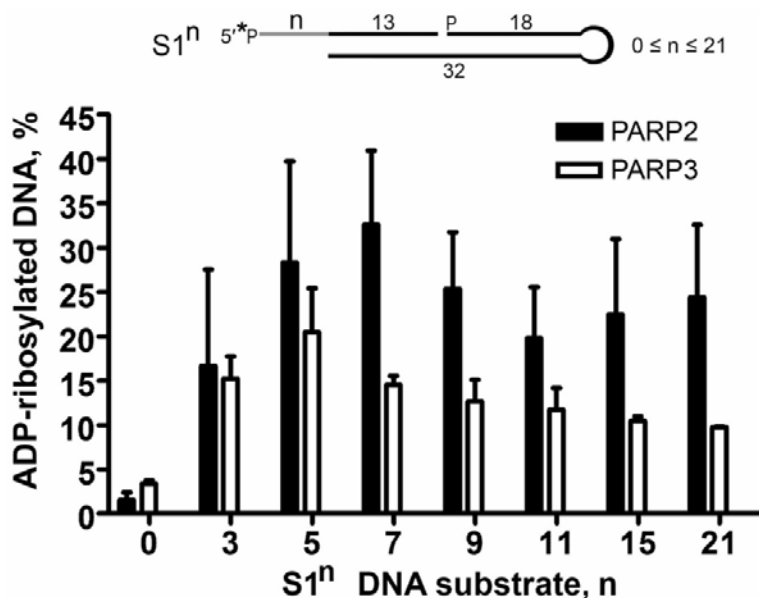


Figure 46: ADP-ribosylation of S1_nDNA duplexes containing 5'-otherhangs by PARP2 and PARP3. [³²P]labelled S1_n DNA duplexes (20 nM) were combined with 50 nM PARP3 or PARP2 in the presence of 1 mM NAD⁺ in ADPR buffer (20 mM HEPES-KOH pH 7.6, 50 mM KCl, 5 mM MgCl₂, 1 mM DTT and 100 μg/mL BSA). The mixture was incubated for 10 min (PARP3) or 30 min (PARP2) at 37°C. The data on PARP-catalyzed formation of DNA ADP-ribosylation products are presented as mean ±SD from three independent experiments.



Chapter II: Identification of MAR-DNA readers in cell-free extracts

Still little is known about proteins responsible for detection and removal of ADP-ribosylated DNA adducts. Recently, Ahel's laboratory demonstrated that the MAR moiety that is covalently attached to oligonucleotide termini can be removed not only by PARG but also by other cellular hydrolases, though with much lower efficacy, such as MACROD1, MACROD2, TARG1, and ARH3 [43, 219]. The time lapse before removal of the ADP-ribosylated adducts from DNA by PARG and other hydrolases could be used to recruit and assemble DNA damage signaling, processing and DNA repair machinery.

One of our major goals was the identification of specific factors that recognize MAR-DNA adducts in order to provide new research tools for identification of ADP-ribosylated DNA adducts in living cells and deciphering their biological role. For affinity purification of readers of ADP-ribose-DNA adducts we used MARYlated and not PARYlated ss/dsDNA oligonucleotides in order to avoid concomitant purification of PAR-binding proteins as well to bypass technical difficulties concerning PARYlated oligonucleotides purification and PARYlated peptides synthesis. Here, we observe simultaneously enrichment with certain factors and loss of similar number of other proteins on MARYlated versus non-MARYlated dsDNA, in contrast to the experiment with ssDNA, where more proteins lost affinity for ssDNA capped with MAR adduct than were enriched (Figure 26 and 28). Depletion of some enzymes possessing DNA exonuclease activities (APEX1, XNR2, FEN1) on MARYlated versus non-MARYlated DNA substrates suggests a protecting role of the ADPr moiety on DNA termini. As shown in Table 9, majority of proteins enriched on MAR-dsDNA also recognize dsDNA alone (P[dsDNA] vs P[beads]) but with a lower affinity as compared to MARYlated dsDNA, suggesting that DNA ADP-ribosylation may serve as a specific tag, enhancing the recruitment of certain DNA repair proteins, cytoskeletal proteins, PAR synthesis/degradation proteins and ribonucleoproteins (showed in Table 8). Notably, MARYlation does not affect enrichment of several DNA breaks binding proteins (Table 9). For example, the unchanged fold of Ku protein on MARYlated versus unmodified dsDNA, suggest that DSB MARYlation do not affect Ku binding. As future perspective, the effective Ku complex binding to ADP-ribosylated DSB termini can be also validated by electrophoretic mobility shift assay (EMSA) and by surface plasmon resonance imaging (SPRI) of DNA-protein complex after immobilization of the modified DNA on surface, as described in [227].

For selection of specific DNA-MAR readers, proteins with known high affinity to ADPr residues alone (PARP1, PARP14, PARP9 and TARG1) were excluded, as well as cytoskeletal proteins and ribonucleoproteins [228] due to their capacity to form clusters, thus, making us unable to identify the protein(s) responsible for the recognition DNA-MAR adduct (Figure 28 and 30). Data analysis and comparison of enriched protein on MARYlated-peptide versus MARYlated ds/ssDNA revealed that majority of proteins enriched on MARYlated DNA ligands were different from those enriched on MARYlated peptide, suggesting that they are not MAR (along) readers. Contrary,



IMPDH1/2 proteins show a very strong enrichment on both MAR-ssDNA and MAR-peptide, suggesting that the IMPDH1/2 are new terminal ADPr-readers. Notably, IMPDH1/2 have high affinity for dsDNA potentially leading to a saturation effect on MAR-dsDNA ligand (Figure 35) that can explain the absence of IMPDH1/2 enrichment on MAR-dsDNA versus dsDNA (Table 9).

Notably, one of the DNA repair protein enriched on ADP-ribosylated DSB is aprataxin (APTX, Tables 8 and 9). Aprataxin recognizes an ADP residue on 5' termini of a DNA break formed during an abortive DNA ligation reaction and catalyzes the release of the AMP group [163]. Thus, the ADP recognition by the catalytic domain together with the PAR-binding affinity of its FHA domain can be responsible for enrichment on MARylated DNA ligands. Hence, due to structural similarities, the MAR unit at a DNA strand break end [13, 184] may also be a good substrate for aprataxin activity along with recruitment of XRCC1 or XRCC4, depending on the nature of the DNA strand break, to finalize the repair of DNA damage via BER or NHEJ, respectively [163].

The only protein that was enriched only on MARylated ds/ssDNA ligands is mitochondrial CLPB protein that can potentially be used in future studies for generation of recombinant antibody-like ADP-ribose-DNA adducts binding protein(s) by fusion of the corresponding binding domain(s) to the Fc region of immunoglobulins (as described in [220]). The obtained results suggest that adenosine binding domains of CLPB (AAA) and of IMPDH1/2 (CBS) are new candidates for the list of MAR-DNA or MAR recognizing domains. More *in vitro* and cellular studies are needed for validation of these hypotheses.

Finally, the acquired data provide new insights on the protein interaction network that is modulated by DNA ADP-ribosylation, and potentially on the function of this modification in the regulation and coordination of DNA strand breaks repair, replication and apoptosis. In perspective, the development and validation the specific antibody for identification of DNA-ADP-ribose adducts in living cells could be used for identification of DNA damage, DNA repair, oxidative stress and inflammatory markers and for characterization of cellular response to DNA damage. Analysis of PAR-DNA adducts level in cells or tissues of patients may have diagnostic and therapeutic implications.



Chapter III: Impact of DNA ADP-ribosylation on NHEJ

The role of DNA ADP-ribosylation in repair and processing of DSBs via NHEJ assays was addressed by the use of the ligation test implicating NHEJ proteins (Ku, XRCC4, Ligase 4, DNA-PK, XLF and PAXX) different cell extracts from Hamster CHO [225] and purified proteins, including PARPs, PARG and/or ADP-ribosylated DNA substrates. It was already proposed that PARP2 and PARP3 are involved in the final ligation step of NHEJ, relying on the data that 5' phosphorylated nicks are particularly efficient activators for auto-ADP-ribosylation activity of PARP2 and PARP3 but not PARP1 [56]. Ku and X4L4 complex are able to effectively ligate the nick of S22 substrate and blunt DSB ends of duplexes S22 and S25 (Figure 38). As expected, the addition of other of the NHEJ actors increases the yield of NHEJ ligation products. Addition of PARP3 in the absence of NAD⁺ does not significantly inhibit the DSB ends ligation despite its affinity to DSB termini. This can be explained by stronger DSB binding by XRCC4/LIG4 complex and by the PARP3 preferential binding to the nick site of substrate S22 [13], thus DSB ends remain accessible for Ku and for NHEJ proteins. Contrary, the addition of PARP3 and NAD⁺ together, significantly decreases the yield of NHEJ ligation products, suggesting two possible scenarios, where the MARYlation of the DSB end used by NHEJ enzymes may inhibit the NHEJ repair pathway by: (i) inhibiting the LIG4 DSB ligation activity; (ii) inhibiting the binding of Ku complex essential for the recruitment of NHEJ proteins to blunt DSB end. In the proteomic part of the work (Table 8), we showed an unchanged yield of Ku complex (XRCC5 and XRCC6 proteins) on MARYlated versus unmodified dsDNA ligands, suggesting that DSB MARYlation do not affect Ku binding on DSB ends, thereby supporting the first scenario.

Moreover, we used WT, Ku80⁻, XRCC4⁻, and XRCC4⁺ CHO cell free extracts to test the effect of DSB ADP-ribosylation on NHEJ by introducing a nick in proximity to 5'-phosphorylated DSB end that make the DSB end prone for MARYlation by PARP3 or PARYlation by PARP2 (Figure 40 and 41). Duplexes containing blunt DSB ends a nick (S22+S25) does not increase the NHEJ effectiveness compared to full-length duplexes (S23+S25) but slightly inhibits the DSB ligation process. Clearly, LIG4 in presence of a nick gets partially recruited to this nick site that diminishes its effective concentration for the DSBs ligation. Moreover, the observed quick and full ligation of the nick diminish a potential impact of PARP-mediated DSB ADP-ribosylation on NHEJ. After nick stabilization - with incorporation of 5'-THF residue at the nick site – we observed a significant stimulation of NHEJ repair in the different CHO CE used (Figure 40 and 41). The observed effect does not depend on addition of NAD⁺ suggesting that this is PARP activity independent process. However, one cannot fully exclude involvement of the endogenous NAD⁺ in protein and/or DNA ADP-ribosylation in these reactions. We hypothesize, that this NHEJ stimulation can be due to PARP1 recruitment at the nick site instead of DSB termini, preventing its competition for DSB binding with Ku complex of canonical NHEJ and driving LIG4 to DSB end. Interestingly in ab-



sence of X4L4 (X4V XRCC4⁻ CE), when nick ligation is strongly inhibited (Figure 40, lanes 10 and 14), the NHEJ repair activity on blunt DSB is notably increased in the presence of THF residue at the nick site as compared to S22 substrate or unnicked substrate S23 and all three substrates tested in WT CE. These results suggest that a proximal unligated nick can stimulate DSB ligation via a XRCC4/LIG4 independent pathway. It is possible that LIG1 and/or LIG3 are recruited more effectively to the DSB site when there is a proximal long-living nick site and ensure an alternative NHEJ in the presence of PEG in our NHEJ reconstitution system.

Taking together, these data suggest that ADP-ribosylation of DSB termini which do not need an additional processing prior to ligation will result in inhibition of classical NHEJ. It should be taken into account that the conditions used in our *in vitro* NHEJ reconstitution experiments – presence of PEG, diluted concentration of proteins, including PARPs and NHEJ factors, as compared to cellular conditions – do not take into account the chromatin context and promote a simple DSB ligation with the XRCC4/LIG4 complex. The role of MAR-DNA as a scaffold for the recruitment of DNA damage signaling, chromatin remodeling and DNA repair proteins remains unexplored. More experiments using pre-MARylated-duplexes containing nicks and protruding ends are needed to test the role of DNA-MARylation on alternative NHEJ, as well as a potential interplay between nicking and resection activities of MRN-CtIP complex and DNA ADP-ribosylation. In perspective, it would be important to verify if the aberrant ligation of 5'-MARylated can happen in case of DSB repair as it was shown for 1 nt gapped DNA in absence of ATP [184]. We speculate that DNA ADP-ribosylation can promote retention of the DSB ends until the complete repair complex is formed or until ATP concentration required for DNA ligation will be restored.

Chapter IV: Search for novel PARP1 and PARP2 inhibitors among derivatives of 1,4-dihydropyridine with DNA binding capacity

Université Paris-Saclay

Espace Technologique / Immeuble Discovery

Route de l'Orme aux Merisiers RD 128 / 91190 Saint-Aubin, France



It is generally accepted that covalently attached PAR polymer confers negative charge to PARPs, histones and other PARylated proteins, resulting in decrease in DNA binding and electrostatic repulsion of these proteins from DNA [70]. Thus, PARylated proteins together with PAR-recruited complexes of DNA repair factors should also withdraw from the site of DNA damage. Contrary, PAR attached to DNA termini should stably recruit those factors directly to the sites of DNA damage. Importantly, the PARP catalyzed ADP-ribosylation of DNA is a fully reversible process since PAR and MAR DNA modifications can be entirely and effectively removed by PARG and other ADPr hydrolases. PARP1-3 activity was tested using eight different NAD analogues, on different and specific oligonucleotides substrates. Moreover, the stability of these (ADP-ribose) oligomers was examined with a set of PAR/MAR erasers.

Among DNA-depend PARPs (PARP1-3), PARP3 was the only one to effectively PARylate DNA termini with bio-NAD⁺, flu-NAD⁺ and especially Br-NAD⁺ analog, which incorporation was several times even more effective than that of natural NAD⁺ (Figure 43 A and B). Similar effect was observed with PARP1 incorporating only Br-NAD⁺ and PARP2 incorporating all NAD⁺ analogs except ara-NAD⁺ although much less efficiently than natural NAD⁺. Furthermore, the preliminary results in Figure 44, showed that PARG was active on PARP2 formed polymers/oligomers of CH-NAD⁺, dNAD⁺ and ε-NAD⁺ derivatives of NAD⁺ but not of bio-NAD⁺, Br-NAD⁺ and NHD⁺. Similar results were obtained in experiments with PARG hydrolysis of PARP3 produced mono DNA adducts but surprisingly PARG was able to remove mono-Br-ADPr and not 1,N6-etheno- ADPr residue from the terminal 5'-phosphate of the DNA substrate used.

These results suggest that bio-NAD⁺, flu-NAD⁺, Br-NAD⁺ and NHD⁺ analogs and potentially their derivatives could be used for stabilization of PAR/MAR-DNA and PAR/MAR-proteins adducts, inhibition of PARG and sensibilization of cells to genotoxic/anticancer treatments. Further studies needed to test the compounds selected above in cell culture for ability to modify level of poly(ADPr) synthesis in response to DNA damage.



REFERENCES

1. Boyer, R., *Posttranslational modification of proteins: Expanding nature's inventory*. Christopher T. Walsh, Roberts & Company Publishers, Greenwood Village, CO, 2005, 576 pp., ISBN 0-9747077-3-2, \$98.00. *Biochemistry and Molecular Biology Education*, 2006. **34**(6): p. 461-462.
2. Klungland, A. and A.B. Robertson, *Oxidized C5-methyl cytosine bases in DNA: 5-Hydroxymethylcytosine; 5-formylcytosine; and 5-carboxycytosine*. *Free Radic Biol Med*, 2017. **107**: p. 62-68.
3. Dabin, J., A. Fortuny, and S.E. Polo, *Epigenome Maintenance in Response to DNA Damage*. *Mol Cell*, 2016. **62**(5): p. 712-27.
4. Farres, J., et al., *PARP-2 sustains erythropoiesis in mice by limiting replicative stress in erythroid progenitors*. *Cell Death Differ*, 2015. **22**(7): p. 1144-57.
5. Vyas, S., et al., *Family-wide analysis of poly(ADP-ribose) polymerase activity*. *Nat Commun*, 2014. **5**: p. 4426.
6. Hottiger, M.O., *Nuclear ADP-Ribosylation and Its Role in Chromatin Plasticity, Cell Differentiation, and Epigenetics*. *Annu Rev Biochem*, 2015. **84**: p. 227-63.
7. Yu, W., et al., *Poly(ADP-ribosyl)ation regulates CTCF-dependent chromatin insulation*. *Nat Genet*, 2004. **36**(10): p. 1105-10.
8. Guastafierro, T., et al., *CCCTC-binding factor activates PARP-1 affecting DNA methylation machinery*. *J Biol Chem*, 2008. **283**(32): p. 21873-80.
9. Guetg, C., et al., *Inheritance of silent rDNA chromatin is mediated by PARP1 via noncoding RNA*. *Mol Cell*, 2012. **45**(6): p. 790-800.
10. Nakano, T., et al., *Pierisins and CARP-1: ADP-ribosylation of DNA by ARTCs in butterflies and shellfish*. *Curr Top Microbiol Immunol*, 2015. **384**: p. 127-49.
11. Jankevicius, G., et al., *The Toxin-Antitoxin System DarTG Catalyzes Reversible ADP-Ribosylation of DNA*. *Mol Cell*, 2016. **64**(6): p. 1109-1116.
12. Talhaoui, I., et al., *Poly(ADP-ribose) polymerases covalently modify strand break termini in DNA fragments in vitro*. *Nucleic Acids Res*, 2016. **44**(19): p. 9279-9295.
13. Zarkovic, G., et al., *Characterization of DNA ADP-ribosyltransferase activities of PARP2 and PARP3: new insights into DNA ADP-ribosylation*. *Nucleic Acids Res*, 2018. **46**(5): p. 2417-2431.
14. Munnur, D., et al., *Reversible ADP-ribosylation of RNA*. *Nucleic Acids Res*, 2019. **47**(11): p. 5658-5669.
15. Berwick, M. and P. Vineis, *Markers of DNA repair and susceptibility to cancer in humans: an epidemiologic review*. *J Natl Cancer Inst*, 2000. **92**(11): p. 874-97.
16. Wood, R.D., M. Mitchell, and T. Lindahl, *Human DNA repair genes, 2005*. *Mutat Res*, 2005. **577**(1-2): p. 275-83.
17. Tubbs, A. and A. Nussenzweig, *Endogenous DNA Damage as a Source of Genomic Instability in Cancer*. *Cell*, 2017. **168**(4): p. 644-656.
18. Chatterjee, N. and G.C. Walker, *Mechanisms of DNA damage, repair, and mutagenesis*. *Environ Mol Mutagen*, 2017. **58**(5): p. 235-263.
19. Desai, A., Y. Yan, and S.L. Gerson, *Advances in therapeutic targeting of the DNA damage response in cancer*. *DNA Repair (Amst)*, 2018. **66-67**: p. 24-29.
20. Lantsov, V.A., *[DNA repair and carcinogenesis: universal mechanisms for repair in pro- and eukaryotes and consequences of the damage in humans]*. *Mol Biol (Mosk)*, 1998. **32**(5): p. 757-72.
21. Shaheen, M., et al., *Synthetic lethality: exploiting the addiction of cancer to DNA repair*. *Blood*, 2011. **117**(23): p. 6074-82.



22. Sancar, A., et al., *Molecular mechanisms of mammalian DNA repair and the DNA damage checkpoints*. Annu Rev Biochem, 2004. **73**: p. 39-85.
23. Zharkov, D.O., *Base excision DNA repair*. Cell Mol Life Sci, 2008. **65**(10): p. 1544-65.
24. Fleck, O. and O. Nielsen, *DNA repair*. J Cell Sci, 2004. **117**(Pt 4): p. 515-7.
25. Chang, H.H.Y., et al., *Non-homologous DNA end joining and alternative pathways to double-strand break repair*. Nat Rev Mol Cell Biol, 2017. **18**(8): p. 495-506.
26. Daniels, C.M., S.E. Ong, and A.K. Leung, *The Promise of Proteomics for the Study of ADP-Ribosylation*. Mol Cell, 2015. **58**(6): p. 911-24.
27. Chambon, P., J.D. Weill, and P. Mandel, *Nicotinamide mononucleotide activation of new DNA-dependent polyadenylic acid synthesizing nuclear enzyme*. Biochem Biophys Res Commun, 1963. **11**: p. 39-43.
28. Palazzo, L. and I. Ahel, *PARPs in genome stability and signal transduction: implications for cancer therapy*. Biochem Soc Trans, 2018. **46**(6): p. 1681-1695.
29. Hottiger, M.O., et al., *Toward a unified nomenclature for mammalian ADP-ribosyltransferases*. Trends Biochem Sci, 2010. **35**(4): p. 208-19.
30. Minaga, T. and E. Kun, *Probable helical conformation of poly(ADP-ribose). The effect of cations on spectral properties*. J Biol Chem, 1983. **258**(9): p. 5726-30.
31. Minaga, T. and E. Kun, *Spectral analysis of the conformation of polyadenosine diphosphoribose. Evidence indicating secondary structure*. J Biol Chem, 1983. **258**(2): p. 725-30.
32. Sugimura, T., *Poly(adenosine diphosphate ribose)*. Prog Nucleic Acid Res Mol Biol, 1973. **13**: p. 127-51.
33. Alvarez-Gonzalez, R. and F.R. Althaus, *Poly(ADP-ribose) catabolism in mammalian cells exposed to DNA-damaging agents*. Mutat Res, 1989. **218**(2): p. 67-74.
34. Davidovic, L., et al., *Importance of poly(ADP-ribose) glycohydrolase in the control of poly(ADP-ribose) metabolism*. Exp Cell Res, 2001. **268**(1): p. 7-13.
35. Palazzo, L., A. Mikoc, and I. Ahel, *ADP-ribosylation: new facets of an ancient modification*. FEBS J, 2017. **284**(18): p. 2932-2946.
36. Otto, H., et al., *In silico characterization of the family of PARP-like poly(ADP-ribosyl)transferases (pARTs)*. BMC Genomics, 2005. **6**: p. 139.
37. Domenighini, M. and R. Rappuoli, *Three conserved consensus sequences identify the NAD-binding site of ADP-ribosylating enzymes, expressed by eukaryotes, bacteria and T-even bacteriophages*. Mol Microbiol, 1996. **21**(4): p. 667-74.
38. Glowacki, G., et al., *The family of toxin-related ecto-ADP-ribosyltransferases in humans and the mouse*. Protein Sci, 2002. **11**(7): p. 1657-70.
39. Li, J., et al., *A conserved NAD(+) binding pocket that regulates protein-protein interactions during aging*. Science, 2017. **355**(6331): p. 1312-1317.
40. Ame, J.C., C. Spenlehauer, and G. de Murcia, *The PARP superfamily*. Bioessays, 2004. **26**(8): p. 882-93.
41. Aravind, L., et al., *The natural history of ADP-ribosyltransferases and the ADP-ribosylation system*. Curr Top Microbiol Immunol, 2015. **384**: p. 3-32.
42. Burkle, A., *Poly(ADP-ribose). The most elaborate metabolite of NAD+*. FEBS J, 2005. **272**(18): p. 4576-89.
43. Munnur, D. and I. Ahel, *Reversible mono-ADP-ribosylation of DNA breaks*. FEBS J, 2017. **284**(23): p. 4002-4016.
44. Qi, H., B.D. Price, and T.A. Day, *Multiple Roles for Mono- and Poly(ADP-Ribose) in Regulating Stress Responses*. Trends Genet, 2019. **35**(2): p. 159-172.
45. Shieh, W.M., et al., *Poly(ADP-ribose) polymerase null mouse cells synthesize ADP-ribose polymers*. J. Biol. Chem., 1998. **273**(46): p. 30069-72.
46. Poirier, G.G., et al., *Poly(ADP-ribosyl)ation of polynucleosomes causes relaxation of chromatin structure*. Proc Natl Acad Sci U S A, 1982. **79**(11): p. 3423-7.



47. Krishnakumar, R. and W.L. Kraus, *The PARP side of the nucleus: molecular actions, physiological outcomes, and clinical targets*. Mol Cell, 2010. **39**(1): p. 8-24.
48. Krishnakumar, R. and W.L. Kraus, *PARP-1 regulates chromatin structure and transcription through a KDM5B-dependent pathway*. Mol Cell, 2010. **39**(5): p. 736-49.
49. Kraus, W.L., *PARPs and ADP-Ribosylation: 50 Years ... and Counting*. Mol Cell, 2015. **58**(6): p. 902-10.
50. Hanzlikova, H., et al., *The Importance of Poly(ADP-Ribose) Polymerase as a Sensor of Unligated Okazaki Fragments during DNA Replication*. Mol Cell, 2018. **71**(2): p. 319-331 e3.
51. Ame, J.C., et al., *PARP-2, A novel mammalian DNA damage-dependent poly(ADP-ribose) polymerase*. J Biol Chem, 1999. **274**(25): p. 17860-8.
52. Menissier de Murcia, J., et al., *Functional interaction between PARP-1 and PARP-2 in chromosome stability and embryonic development in mouse*. EMBO J, 2003. **22**(9): p. 2255-63.
53. Fouquin, A., et al., *PARP2 controls double-strand break repair pathway choice by limiting 53BP1 accumulation at DNA damage sites and promoting end-resection*. Nucleic Acids Res, 2017. **45**(21): p. 12325-12339.
54. Bai, P., *Biology of Poly(ADP-Ribose) Polymerases: The Factotums of Cell Maintenance*. Mol Cell, 2015. **58**(6): p. 947-58.
55. Obaji, E., T. Haikarainen, and L. Lehtio, *Characterization of the DNA dependent activation of human ARTD2/PARP2*. Sci Rep, 2016. **6**: p. 34487.
56. Langelier, M.F., A.A. Riccio, and J.M. Pascal, *PARP-2 and PARP-3 are selectively activated by 5' phosphorylated DNA breaks through an allosteric regulatory mechanism shared with PARP-1*. Nucleic Acids Res, 2014. **42**(12): p. 7762-75.
57. Riccio, A.A., G. Cingolani, and J.M. Pascal, *PARP-2 domain requirements for DNA damage-dependent activation and localization to sites of DNA damage*. Nucleic Acids Res, 2016. **44**(4): p. 1691-702.
58. Gibson, B.A. and W.L. Kraus, *New insights into the molecular and cellular functions of poly(ADP-ribose) and PARPs*. Nat Rev Mol Cell Biol, 2012. **13**(7): p. 411-24.
59. Beck, C., et al., *Poly(ADP-ribose) polymerases in double-strand break repair: focus on PARP1, PARP2 and PARP3*. Exp Cell Res, 2014. **329**(1): p. 18-25.
60. Rouleau, M., et al., *PARP-3 associates with polycomb group bodies and with components of the DNA damage repair machinery*. J Cell Biochem, 2007. **100**(2): p. 385-401.
61. Gupte, R., Z. Liu, and W.L. Kraus, *PARPs and ADP-ribosylation: recent advances linking molecular functions to biological outcomes*. Genes Dev, 2017. **31**(2): p. 101-126.
62. Martin-Hernandez, K., et al., *Expanding functions of ADP-ribosylation in the maintenance of genome integrity*. Semin Cell Dev Biol, 2017. **63**: p. 92-101.
63. David, K.K., et al., *Parthanatos, a messenger of death*. Front Biosci (Landmark Ed), 2009. **14**: p. 1116-28.
64. Bonicalzi, M.E., et al., *Regulation of poly(ADP-ribose) metabolism by poly(ADP-ribose) glycohydrolase: where and when?* Cell Mol Life Sci, 2005. **62**(7-8): p. 739-50.
65. Koh, D.W., et al., *Failure to degrade poly(ADP-ribose) causes increased sensitivity to cytotoxicity and early embryonic lethality*. Proc Natl Acad Sci U S A, 2004. **101**(51): p. 17699-704.
66. Tang, J.B., et al., *N-methylpurine DNA glycosylase and DNA polymerase beta modulate BER inhibitor potentiation of glioma cells to temozolomide*. Neuro Oncol, 2011. **13**(5): p. 471-86.
67. Hatakeyama, K., et al., *Purification and characterization of poly(ADP-ribose) glycohydrolase. Different modes of action on large and small poly(ADP-ribose)*. J Biol Chem, 1986. **261**(32): p. 14902-11.



68. O'Sullivan, J., et al., *Emerging roles of eraser enzymes in the dynamic control of protein ADP-ribosylation*. Nat Commun, 2019. **10**(1): p. 1182.
69. Molinete, M., et al., *Overproduction of the poly(ADP-ribose) polymerase DNA-binding domain blocks alkylation-induced DNA repair synthesis in mammalian cells*. EMBO J, 1993. **12**(5): p. 2109-17.
70. Satoh, M.S., G.G. Poirier, and T. Lindahl, *Dual function for poly(ADP-ribose) synthesis in response to DNA strand breakage*. Biochemistry, 1994. **33**(23): p. 7099-106.
71. Rodríguez-Vargas, J.M., F.J. Oliver-Pozo, and F. Dantzer, *PARP1 and Poly(ADP-ribose) Signaling during Autophagy in Response to Nutrient Deprivation*. Oxidative Medicine and Cellular Longevity, 2019. **2019**: p. 1-15.
72. Hou, W.H., S.H. Chen, and X. Yu, *Poly-ADP ribosylation in DNA damage response and cancer therapy*. Mutat Res, 2019. **780**: p. 82-91.
73. Nagy, Z., et al., *Tankyrases Promote Homologous Recombination and Check Point Activation in Response to DSBs*. PLoS Genet, 2016. **12**(2): p. e1005791.
74. Beck, C., et al., *PARP3 affects the relative contribution of homologous recombination and nonhomologous end-joining pathways*. Nucleic Acids Res, 2014. **42**(9): p. 5616-32.
75. Caron, M.C., et al., *Poly(ADP-ribose) polymerase-1 antagonizes DNA resection at double-strand breaks*. Nat Commun, 2019. **10**(1): p. 2954.
76. Boehler, C., et al., *Poly(ADP-ribose) polymerase 3 (PARP3), a newcomer in cellular response to DNA damage and mitotic progression*. Proc Natl Acad Sci U S A, 2011. **108**(7): p. 2783-8.
77. Smith, R., et al., *Poly(ADP-ribose)-dependent chromatin unfolding facilitates the association of DNA-binding proteins with DNA at sites of damage*. Nucleic Acids Res, 2019. **47**(21): p. 11250-11267.
78. Ogata, N., et al., *ADP-ribosylation of histone H1. Identification of glutamic acid residues 2, 14, and the COOH-terminal lysine residue as modification sites*. J Biol Chem, 1980. **255**(16): p. 7616-20.
79. Haenni, S.S., et al., *Identification of lysines 36 and 37 of PARP-2 as targets for acetylation and auto-ADP-ribosylation*. Int J Biochem Cell Biol, 2008. **40**(10): p. 2274-83.
80. Grundy, G.J., et al., *PARP3 is a sensor of nicked nucleosomes and monoribosylates histone H2B(Glu2)*. Nat Commun, 2016. **7**: p. 12404.
81. Messner, S., et al., *PARP1 ADP-ribosylates lysine residues of the core histone tails*. Nucleic Acids Res, 2010. **38**(19): p. 6350-62.
82. Altmeyer, M., et al., *Molecular mechanism of poly(ADP-ribosylation) by PARP1 and identification of lysine residues as ADP-ribose acceptor sites*. Nucleic Acids Res, 2009. **37**(11): p. 3723-38.
83. Zhang, Y., et al., *Site-specific characterization of the Asp- and Glu-ADP-ribosylated proteome*. Nat Methods, 2013. **10**(10): p. 981-4.
84. Martello, R., et al., *Proteome-wide identification of the endogenous ADP-ribosylome of mammalian cells and tissue*. Nat Commun, 2016. **7**: p. 12917.
85. Bonfiglio, J.J., et al., *Serine ADP-Ribosylation Depends on HPP1*. Mol Cell, 2017. **65**(5): p. 932-940 e6.
86. Palazzo, L., et al., *Serine is the major residue for ADP-ribosylation upon DNA damage*. Elife, 2018. **7**: p. e34334.
87. Kalesh, K., et al., *An Integrated Chemical Proteomics Approach for Quantitative Profiling of Intracellular ADP-Ribosylation*. Sci Rep, 2019. **9**(1): p. 6655.
88. Hendriks, I.A., S.C. Larsen, and M.L. Nielsen, *An Advanced Strategy for Comprehensive Profiling of ADP-ribosylation Sites Using Mass Spectrometry-based Proteomics*. Mol Cell Proteomics, 2019. **18**(5): p. 1010-1026.
89. Bartlett, E., et al., *Interplay of Histone Marks with Serine ADP-Ribosylation*. Cell Rep, 2018. **24**(13): p. 3488-3502.e5.



90. Abplanalp, J., et al., *Proteomic analyses identify ARH3 as a serine mono-ADP-ribosylhydrolase*. Nat Commun, 2017. **8**(1): p. 2055.
91. Fontana, P., et al., *Serine ADP-ribosylation reversal by the hydrolase ARH3*. Elife, 2017. **6**: p. e28533.
92. Mashimo, M., J. Kato, and J. Moss, *ADP-ribosyl-acceptor hydrolase 3 regulates poly (ADP-ribose) degradation and cell death during oxidative stress*. Proc Natl Acad Sci U S A, 2013. **110**(47): p. 18964-9.
93. Leslie Pedrioli, D.M., et al., *Comprehensive ADP-ribosylome analysis identifies tyrosine as an ADP-ribose acceptor site*. EMBO Rep, 2018. **19**(8): p. e45310.
94. Ord, M.G. and L.A. Stocken, *Adenosine diphosphate ribosylated histones*. Biochem J, 1977. **161**(3): p. 583-92.
95. Friedberg, E.C., *A brief history of the DNA repair field*. Cell Res, 2008. **18**(1): p. 3-7.
96. Lindahl, T. and D.E. Barnes, *Repair of endogenous DNA damage*. Cold Spring Harb Symp Quant Biol, 2000. **65**: p. 127-33.
97. Blanpain, C., et al., *DNA-damage response in tissue-specific and cancer stem cells*. Cell Stem Cell, 2011. **8**(1): p. 16-29.
98. Audebert, M., B. Salles, and P. Calsou, *Involvement of poly(ADP-ribose) polymerase-1 and XRCC1/DNA ligase III in an alternative route for DNA double-strand breaks rejoining*. J Biol Chem, 2004. **279**(53): p. 55117-26.
99. Langelier, M.F., et al., *Structural basis for DNA damage-dependent poly(ADP-ribosylation) by human PARP-1*. Science, 2012. **336**(6082): p. 728-32.
100. Eustermann, S., et al., *Structural Basis of Detection and Signaling of DNA Single-Strand Breaks by Human PARP-1*. Mol Cell, 2015. **60**(5): p. 742-54.
101. Langelier, M.F., et al., *Crystal structures of poly(ADP-ribose) polymerase-1 (PARP-1) zinc fingers bound to DNA: structural and functional insights into DNA-dependent PARP-1 activity*. J Biol Chem, 2011. **286**(12): p. 10690-701.
102. Dawicki-McKenna, J.M., et al., *PARP-1 Activation Requires Local Unfolding of an Autoinhibitory Domain*. Mol Cell, 2015. **60**(5): p. 755-68.
103. Steffen, J.D., M.M. McCauley, and J.M. Pascal, *Fluorescent sensors of PARP-1 structural dynamics and allosteric regulation in response to DNA damage*. Nucleic Acids Res, 2016. **44**(20): p. 9771-9783.
104. Kouyama, K., et al., *Single-particle analysis of full-length human poly(ADP-ribose) polymerase 1*. Biophys Physicobiol, 2019. **16**: p. 59-67.
105. Liu, L., et al., *PARP1 changes from three-dimensional DNA damage searching to one-dimensional diffusion after auto-PARylation or in the presence of APE1*. Nucleic Acids Res, 2017. **45**(22): p. 12834-12847.
106. Ali, A.A., et al., *Corrigendum: The zinc-finger domains of PARP1 cooperate to recognize DNA strand breaks*. Nat Struct Mol Biol, 2015. **22**(8): p. 645.
107. Kim, M.Y., et al., *NAD⁺-dependent modulation of chromatin structure and transcription by nucleosome binding properties of PARP-1*. Cell, 2004. **119**(6): p. 803-14.
108. Lonskaya, I., et al., *Regulation of poly(ADP-ribose) polymerase-1 by DNA structure-specific binding*. J Biol Chem, 2005. **280**(17): p. 17076-83.
109. Hakme, A., et al., *The expanding field of poly(ADP-ribosylation) reactions. 'Protein Modifications: Beyond the Usual Suspects' Review Series*. EMBO Rep, 2008. **9**(11): p. 1094-100.
110. Luo, X. and W.L. Kraus, *On PAR with PARP: cellular stress signaling through poly(ADP-ribose) and PARP-1*. Genes Dev, 2012. **26**(5): p. 417-32.
111. Pinnola, A., et al., *Nucleosomal core histones mediate dynamic regulation of poly(ADP-ribose) polymerase 1 protein binding to chromatin and induction of its enzymatic activity*. J Biol Chem, 2007. **282**(44): p. 32511-9.



112. Cohen-Armon, M., et al., *DNA-independent PARP-1 activation by phosphorylated ERK2 increases Elk1 activity: a link to histone acetylation*. Mol Cell, 2007. **25**(2): p. 297-308.
113. Berger, F., C. Lau, and M. Ziegler, *Regulation of poly(ADP-ribose) polymerase 1 activity by the phosphorylation state of the nuclear NAD biosynthetic enzyme NMN adenylyl transferase I*. Proc Natl Acad Sci U S A, 2007. **104**(10): p. 3765-70.
114. Erener, S., et al., *Poly(ADP-ribose)polymerase-1 (PARP1) controls adipogenic gene expression and adipocyte function*. Mol Endocrinol, 2012. **26**(1): p. 79-86.
115. Guetg, C. and R. Santoro, *Formation of nuclear heterochromatin: the nucleolar point of view*. Epigenetics, 2012. **7**(8): p. 811-4.
116. Sajish, M. and P. Schimmel, *A human tRNA synthetase is a potent PARP1-activating effector target for resveratrol*. Nature, 2015. **519**(7543): p. 370-3.
117. Kauppinen, T.M., et al., *Direct phosphorylation and regulation of poly(ADP-ribose) polymerase-1 by extracellular signal-regulated kinases 1/2*. Proc Natl Acad Sci U S A, 2006. **103**(18): p. 7136-41.
118. Zhang, S., et al., *c-Jun N-terminal kinase mediates hydrogen peroxide-induced cell death via sustained poly(ADP-ribose) polymerase-1 activation*. Cell Death Differ, 2007. **14**(5): p. 1001-10.
119. Wright, R.H., et al., *CDK2-dependent activation of PARP-1 is required for hormonal gene regulation in breast cancer cells*. Genes Dev, 2012. **26**(17): p. 1972-83.
120. Chi, N.W. and H.F. Lodish, *Tankyrase is a golgi-associated mitogen-activated protein kinase substrate that interacts with IRAP in GLUT4 vesicles*. J Biol Chem, 2000. **275**(49): p. 38437-44.
121. Hassa, P.O., et al., *Acetylation of poly(ADP-ribose) polymerase-1 by p300/CREB-binding protein regulates coactivation of NF-kappaB-dependent transcription*. J Biol Chem, 2005. **280**(49): p. 40450-64.
122. Rajamohan, S.B., et al., *SIRT1 promotes cell survival under stress by deacetylation-dependent deactivation of poly(ADP-ribose) polymerase 1*. Mol Cell Biol, 2009. **29**(15): p. 4116-29.
123. Loseva, O., et al., *PARP-3 is a mono-ADP-ribosylase that activates PARP-1 in the absence of DNA*. J Biol Chem, 2010. **285**(11): p. 8054-60.
124. Mao, Z., et al., *SIRT6 promotes DNA repair under stress by activating PARP1*. Science, 2011. **332**(6036): p. 1443-6.
125. Kassner, I., et al., *SET7/9-dependent methylation of ARTD1 at K508 stimulates poly-ADP-ribose formation after oxidative stress*. Open Biol, 2013. **3**(10): p. 120173.
126. Leger, K., et al., *ARTD2 activity is stimulated by RNA*. Nucleic Acids Res, 2014. **42**(8): p. 5072-82.
127. Ouararhni, K., et al., *The histone variant mH2A1.1 interferes with transcription by down-regulating PARP-1 enzymatic activity*. Genes Dev, 2006. **20**(23): p. 3324-36.
128. Kim, D.S., et al., *Activation of PARP-1 by snoRNAs Controls Ribosome Biogenesis and Cell Growth via the RNA Helicase DDX21*. Mol Cell, 2019. **75**(6): p. 1270-1285 e14.
129. Chen, Q., et al., *PARP2 mediates branched poly ADP-ribosylation in response to DNA damage*. Nat Commun, 2018. **9**(1): p. 3233.
130. Clark, N.J., et al., *Alternative modes of binding of poly(ADP-ribose) polymerase 1 to free DNA and nucleosomes*. J Biol Chem, 2012. **287**(39): p. 32430-9.
131. Thomas, C., et al., *Hit and run versus long-term activation of PARP-1 by its different domains fine-tunes nuclear processes*. Proc Natl Acad Sci U S A, 2019. **116**(20): p. 9941-9946.
132. Ciccarone, F., et al., *5mC-hydroxylase activity is influenced by the PARylation of TET1 enzyme*. Oncotarget, 2015. **6**(27): p. 24333-47.
133. Hsu, P.C., et al., *CHK2-mediated regulation of PARP1 in oxidative DNA damage response*. Oncogene, 2019. **38**(8): p. 1166-1182.



134. Ciccarone, F., M. Zampieri, and P. Caiafa, *PARP1 orchestrates epigenetic events setting up chromatin domains*. *Semin Cell Dev Biol*, 2017. **63**: p. 123-134.
135. Fischbach, A., et al., *The C-terminal domain of p53 orchestrates the interplay between non-covalent and covalent poly(ADP-ribosylation) of p53 by PARP1*. *Nucleic Acids Res*, 2018. **46**(2): p. 804-822.
136. Verheugd, P., et al., *Regulation of NF-kappaB signalling by the mono-ADP-ribosyltransferase ARTD10*. *Nat Commun*, 2013. **4**: p. 1683.
137. Pleschke, J.M., et al., *Poly(ADP-ribose) binds to specific domains in DNA damage checkpoint proteins*. *J Biol Chem*, 2000. **275**(52): p. 40974-80.
138. Gagne, J.P., et al., *Proteome-wide identification of poly(ADP-ribose) binding proteins and poly(ADP-ribose)-associated protein complexes*. *Nucleic Acids Res*, 2008. **36**(22): p. 6959-76.
139. Oberoi, J., et al., *Structural basis of poly(ADP-ribose) recognition by the multizinc binding domain of checkpoint with forkhead-associated and RING Domains (CHFR)*. *J Biol Chem*, 2010. **285**(50): p. 39348-58.
140. Ahel, I., et al., *Poly(ADP-ribose)-binding zinc finger motifs in DNA repair/checkpoint proteins*. *Nature*, 2008. **451**(7174): p. 81-5.
141. Li, G.Y., et al., *Structure and identification of ADP-ribose recognition motifs of APLF and role in the DNA damage response*. *Proc Natl Acad Sci U S A*, 2010. **107**(20): p. 9129-34.
142. Wang, Z., et al., *Recognition of the iso-ADP-ribose moiety in poly(ADP-ribose) by WWE domains suggests a general mechanism for poly(ADP-ribosylation)-dependent ubiquitination*. *Genes Dev*, 2012. **26**(3): p. 235-40.
143. Li, M., et al., *The FHA and BRCT domains recognize ADP-ribosylation during DNA damage response*. *Genes Dev*, 2013. **27**(16): p. 1752-68.
144. Karras, G.I., et al., *The macro domain is an ADP-ribose binding module*. *The EMBO Journal*, 2005. **24**(11): p. 1911-1920.
145. Teloni, F. and M. Altmeyer, *Readers of poly(ADP-ribose): designed to be fit for purpose*. *Nucleic Acids Res*, 2016. **44**(3): p. 993-1006.
146. Vivel, C.A., et al., *ADPriboDB: The database of ADP-ribosylated proteins*. *Nucleic Acids Res*, 2017. **45**(D1): p. D204-D209.
147. Rulten, S.L., et al., *PARP-3 and APLF function together to accelerate nonhomologous end-joining*. *Mol Cell*, 2011. **41**(1): p. 33-45.
148. Posavec Marjanovic, M., et al., *MacroH2A1.1 regulates mitochondrial respiration by limiting nuclear NAD(+) consumption*. *Nat Struct Mol Biol*, 2017. **24**(11): p. 902-910.
149. Hurtado-Bages, S., I. Guberovic, and M. Buschbeck, *The MacroH2A1.1 - PARP1 Axis at the Intersection Between Stress Response and Metabolism*. *Front Genet*, 2018. **9**: p. 417.
150. Xu, C., et al., *The histone variant macroH2A1.1 is recruited to DSBs through a mechanism involving PARP1*. *FEBS Lett*, 2012. **586**(21): p. 3920-5.
151. Singh, H.R., et al., *A Poly-ADP-Ribose Trigger Releases the Auto-Inhibition of a Chromatin Remodeling Oncogene*. *Mol Cell*, 2017. **68**(5): p. 860-871.e7.
152. Feijs, K.L., et al., *Macrodomain-containing proteins: regulating new intracellular functions of mono(ADP-ribosylation)*. *Nat Rev Mol Cell Biol*, 2013. **14**(7): p. 443-51.
153. Forst, A.H., et al., *Recognition of mono-ADP-ribosylated ARTD10 substrates by ARTD8 macrodomains*. *Structure*, 2013. **21**(3): p. 462-75.
154. Rosenthal, F., et al., *Macrodomain-containing proteins are new mono-ADP-ribosylhydrolases*. *Nat Struct Mol Biol*, 2013. **20**(4): p. 502-7.
155. DaRosa, P.A., et al., *Allosteric activation of the RNF146 ubiquitin ligase by a poly(ADP-ribosylation) signal*. *Nature*, 2015. **517**(7533): p. 223-6.
156. Aravind, L., *The WWE domain: a common interaction module in protein ubiquitination and ADP ribosylation*. *Trends Biochem Sci*, 2001. **26**(5): p. 273-5.



157. Durocher, D. and S.P. Jackson, *The FHA domain*. FEBS Lett, 2002. **513**(1): p. 58-66.
158. Yu, X., et al., *The BRCT domain is a phospho-protein binding domain*. Science, 2003. **302**(5645): p. 639-42.
159. Li, M. and X. Yu, *Function of BRCA1 in the DNA damage response is mediated by ADP-ribosylation*. Cancer Cell, 2013. **23**(5): p. 693-704.
160. Breslin, C., et al., *The XRCC1 phosphate-binding pocket binds poly (ADP-ribose) and is required for XRCC1 function*. Nucleic Acids Res, 2015. **43**(14): p. 6934-44.
161. Polo, L.M., et al., *Efficient Single-Strand Break Repair Requires Binding to Both Poly(ADP-Ribose) and DNA by the Central BRCT Domain of XRCC1*. Cell Rep, 2019. **26**(3): p. 573-581.e5.
162. Rass, U., I. Ahel, and S.C. West, *Molecular mechanism of DNA deadenylation by the neurological disease protein aprataxin*. J Biol Chem, 2008. **283**(49): p. 33994-4001.
163. Rass, U., I. Ahel, and S.C. West, *Actions of aprataxin in multiple DNA repair pathways*. J Biol Chem, 2007. **282**(13): p. 9469-74.
164. Harris, J.L., et al., *Aprataxin, poly-ADP ribose polymerase 1 (PARP-1) and apurinic endonuclease 1 (APE1) function together to protect the genome against oxidative damage*. Hum Mol Genet, 2009. **18**(21): p. 4102-17.
165. Gueven, N., et al., *Aprataxin, a novel protein that protects against genotoxic stress*. Hum Mol Genet, 2004. **13**(10): p. 1081-93.
166. Krietsch, J., et al., *PARP activation regulates the RNA-binding protein NONO in the DNA damage response to DNA double-strand breaks*. Nucleic Acids Res, 2012. **40**(20): p. 10287-301.
167. Malanga, M., et al., *Poly(ADP-ribose) binds to the splicing factor ASF/SF2 and regulates its phosphorylation by DNA topoisomerase I*. J Biol Chem, 2008. **283**(29): p. 19991-8.
168. Bock, F.J., T.T. Todorova, and P. Chang, *RNA Regulation by Poly(ADP-Ribose) Polymerases*. Mol Cell, 2015. **58**(6): p. 959-69.
169. Ke, Y., et al., *Novel insights into PARPs in gene expression: regulation of RNA metabolism*. Cell Mol Life Sci, 2019. **76**(17): p. 3283-3299.
170. Murawska, M., et al., *Stress-induced PARP activation mediates recruitment of Drosophila Mi-2 to promote heat shock gene expression*. PLoS Genet, 2011. **7**(7): p. e1002206.
171. Silva, A.P., et al., *The N-terminal Region of Chromodomain Helicase DNA-binding Protein 4 (CHD4) Is Essential for Activity and Contains a High Mobility Group (HMG) Box-like-domain That Can Bind Poly(ADP-ribose)*. J Biol Chem, 2016. **291**(2): p. 924-38.
172. Smith, R., et al., *CHD3 and CHD4 recruitment and chromatin remodeling activity at DNA breaks is promoted by early poly(ADP-ribose)-dependent chromatin relaxation*. Nucleic Acids Res, 2018. **46**(12): p. 6087-6098.
173. Zhang, F., et al., *The oligonucleotide/oligosaccharide-binding fold motif is a poly(ADP-ribose)-binding domain that mediates DNA damage response*. Proc Natl Acad Sci U S A, 2014. **111**(20): p. 7278-83.
174. Senissar, M., M.C. Manav, and D.E. Brodersen, *Structural conservation of the PIN domain active site across all domains of life*. Protein Sci, 2017. **26**(8): p. 1474-1492.
175. Keijzers, G., et al., *Human Exonuclease 1 (EXO1) Regulatory Functions in DNA Replication with Putative Roles in Cancer*. Int J Mol Sci, 2018. **20**(1).
176. Zhang, F., et al., *The PIN domain of EXO1 recognizes poly(ADP-ribose) in DNA damage response*. Nucleic Acids Res, 2015. **43**(22): p. 10782-94.
177. Chen, J.K., et al., *PARP-1-dependent recruitment of cold-inducible RNA-binding protein promotes double-strand break repair and genome stability*. Proc Natl Acad Sci U S A, 2018. **115**(8): p. E1759-e1768.
178. Watanabe, M., et al., *Molecular cloning of an apoptosis-inducing protein, pierisin, from cabbage butterfly: possible involvement of ADP-ribosylation in its activity*. Proc Natl Acad Sci U S A, 1999. **96**(19): p. 10608-13.



179. Takamura-Enya, T., et al., *Mono(ADP-ribosyl)ation of 2'-deoxyguanosine residue in DNA by an apoptosis-inducing protein, pierisin-1, from cabbage butterfly*. Proc Natl Acad Sci U S A, 2001. **98**(22): p. 12414-9.
180. Lyons, B., et al., *Scabin, a Novel DNA-acting ADP-ribosyltransferase from Streptomyces scabies*. J Biol Chem, 2016. **291**(21): p. 11198-215.
181. Sacho, E.J. and N. Maizels, *DNA repair factor MRE11/RAD50 cleaves 3'-phosphotyrosyl bonds and resects DNA to repair damage caused by topoisomerase I poisons*. J Biol Chem, 2011. **286**(52): p. 44945-51.
182. Kawale, A.S. and L.F. Povirk, *Tyrosyl-DNA phosphodiesterases: rescuing the genome from the risks of relaxation*. Nucleic Acids Res, 2018. **46**(2): p. 520-537.
183. Anand, R., et al., *Phosphorylated CtIP Functions as a Co-factor of the MRE11-RAD50-NBS1 Endonuclease in DNA End Resection*. Mol Cell, 2016. **64**(5): p. 940-950.
184. Belousova, E.A., A.A. Ishchenko, and O.I. Lavrik, *DNA is a New Target of PARP3*. Sci Rep, 2018. **8**(1): p. 4176.
185. Fouquerel, E., et al., *ARTD1/PARP1 negatively regulates glycolysis by inhibiting hexokinase I independent of NAD+ depletion*. Cell Rep, 2014. **8**(6): p. 1819-1831.
186. Munir, A., A. Banerjee, and S. Shuman, *NAD+-dependent synthesis of a 5'-phospho-ADP-ribosylated RNA/DNA cap by RNA 2'-phosphotransferase Tpt1*. Nucleic Acids Res, 2018. **46**(18): p. 9617-9624.
187. Banerjee, A., et al., *Structure of tRNA splicing enzyme Tpt1 illuminates the mechanism of RNA 2'-PO4 recognition and ADP-ribosylation*. Nat Commun, 2019. **10**(1): p. 218.
188. Barkauskaite, E., G. Jankevicius, and I. Ahel, *Structures and Mechanisms of Enzymes Employed in the Synthesis and Degradation of PARP-Dependent Protein ADP-Ribosylation*. Mol Cell, 2015. **58**(6): p. 935-46.
189. Slade, D., et al., *The structure and catalytic mechanism of a poly(ADP-ribose) glycohydrolase*. Nature, 2011. **477**(7366): p. 616-20.
190. Pascal, J.M. and T. Ellenberger, *The rise and fall of poly(ADP-ribose): An enzymatic perspective*. DNA Repair (Amst), 2015. **32**: p. 10-6.
191. Palazzo, L., et al., *Processing of protein ADP-ribosylation by Nudix hydrolases*. Biochem J, 2015. **468**(2): p. 293-301.
192. Ame, J.C., E.L. Jacobson, and M.K. Jacobson, *Molecular heterogeneity and regulation of poly(ADP-ribose) glycohydrolase*. Mol Cell Biochem, 1999. **193**(1-2): p. 75-81.
193. Meyer-Ficca, M.L., et al., *Human poly(ADP-ribose) glycohydrolase is expressed in alternative splice variants yielding isoforms that localize to different cell compartments*. Exp Cell Res, 2004. **297**(2): p. 521-32.
194. Haince, J.F., et al., *Dynamic relocation of poly(ADP-ribose) glycohydrolase isoforms during radiation-induced DNA damage*. Biochim Biophys Acta, 2006. **1763**(2): p. 226-37.
195. Oka, S., J. Kato, and J. Moss, *Identification and characterization of a mammalian 39-kDa poly(ADP-ribose) glycohydrolase*. J Biol Chem, 2006. **281**(2): p. 705-13.
196. Mashimo, M., J. Kato, and J. Moss, *Structure and function of the ARH family of ADP-ribosyl-acceptor hydrolases*. DNA Repair (Amst), 2014. **23**: p. 88-94.
197. Mueller-Dieckmann, C., et al., *The structure of human ADP-ribosylhydrolase 3 (ARH3) provides insights into the reversibility of protein ADP-ribosylation*. Proc Natl Acad Sci U S A, 2006. **103**(41): p. 15026-31.
198. Ono, T., et al., *The 39-kDa poly(ADP-ribose) glycohydrolase ARH3 hydrolyzes O-acetyl-ADP-ribose, a product of the Sir2 family of acetyl-histone deacetylases*. Proc Natl Acad Sci U S A, 2006. **103**(45): p. 16687-91.
199. Niere, M., et al., *ADP-ribosylhydrolase 3 (ARH3), not poly(ADP-ribose) glycohydrolase (PARG) isoforms, is responsible for degradation of mitochondrial matrix-associated poly(ADP-ribose)*. J Biol Chem, 2012. **287**(20): p. 16088-102.



200. Han, W., X. Li, and X. Fu, *The macro domain protein family: structure, functions, and their potential therapeutic implications*. *Mutat Res*, 2011. **727**(3): p. 86-103.
201. Jankevicius, G., et al., *A family of macrodomain proteins reverses cellular mono-ADP-ribosylation*. *Nat Struct Mol Biol*, 2013. **20**(4): p. 508-14.
202. Peterson, F.C., et al., *Orphan macrodomain protein (human C6orf130) is an O-acyl-ADP-ribose deacylase: solution structure and catalytic properties*. *J Biol Chem*, 2011. **286**(41): p. 35955-65.
203. Neuvonen, M. and T. Ahola, *Differential activities of cellular and viral macro domain proteins in binding of ADP-ribose metabolites*. *J Mol Biol*, 2009. **385**(1): p. 212-25.
204. Reeder, R.H., et al., *Studies on the polymer of adenosine diphosphate ribose. II. Characterization of the polymer*. *J Biol Chem*, 1967. **242**(13): p. 3172-9.
205. Daniels, C.M., et al., *Nudix hydrolases degrade protein-conjugated ADP-ribose*. *Sci Rep*, 2015. **5**: p. 18271.
206. Palazzo, L., et al., *ENPP1 processes protein ADP-ribosylation in vitro*. *FEBS J*, 2016. **283**(18): p. 3371-88.
207. McLennan, A.G., *The Nudix hydrolase superfamily*. *Cell Mol Life Sci*, 2006. **63**(2): p. 123-43.
208. Mildvan, A.S., et al., *Structures and mechanisms of Nudix hydrolases*. *Arch Biochem Biophys*, 2005. **433**(1): p. 129-43.
209. Gabelli, S.B., et al., *The structure of ADP-ribose pyrophosphatase reveals the structural basis for the versatility of the Nudix family*. *Nat Struct Biol*, 2001. **8**(5): p. 467-72.
210. Williams, J.C., J.P. Chambers, and J.G. Liehr, *Glutamyl ribose 5-phosphate storage disease. A hereditary defect in the degradation of poly(ADP-ribosylated) proteins*. *J Biol Chem*, 1984. **259**(2): p. 1037-42.
211. Shirato, M., et al., *Poly(etheno ADP-ribose) blocks poly(ADP-ribose) glycohydrolase activity*. *Biochem Biophys Res Commun*, 2007. **355**(2): p. 451-6.
212. Bessman, M.J., D.N. Frick, and S.F. O'Handley, *The MutT proteins or "Nudix" hydrolases, a family of versatile, widely distributed, "housecleaning" enzymes*. *J Biol Chem*, 1996. **271**(41): p. 25059-62.
213. Formentini, L., et al., *Poly(ADP-ribose) catabolism triggers AMP-dependent mitochondrial energy failure*. *J Biol Chem*, 2009. **284**(26): p. 17668-76.
214. Ethier, C., et al., *PARP-1 modulation of mTOR signaling in response to a DNA alkylating agent*. *PLoS One*, 2012. **7**(10): p. e47978.
215. Weeks, S.D., M. Drinker, and P.J. Loll, *Ligation independent cloning vectors for expression of SUMO fusions*. *Protein Expr Purif*, 2007. **53**(1): p. 40-50.
216. Bryksin, A. and I. Matsumura, *Overlap extension PCR cloning*. *Methods Mol Biol*, 2013. **1073**: p. 31-42.
217. D'Silva, I., et al., *Relative affinities of poly(ADP-ribose) polymerase and DNA-dependent protein kinase for DNA strand interruptions*. *Biochim Biophys Acta*, 1999. **1430**(1): p. 119-26.
218. Lilyestrom, W., et al., *Structural and biophysical studies of human PARP-1 in complex with damaged DNA*. *J Mol Biol*, 2010. **395**(5): p. 983-94.
219. Agnew, T., et al., *MacroD1 Is a Promiscuous ADP-Ribosyl Hydrolase Localized to Mitochondria*. *Front Microbiol*, 2018. **9**: p. 20.
220. Gibson, B.A., et al., *Generation and Characterization of Recombinant Antibody-like ADP-Ribose Binding Proteins*. *Biochemistry*, 2017. **56**(48): p. 6305-6316.
221. McLean, J.E., et al., *Inosine 5'-monophosphate dehydrogenase binds nucleic acids in vitro and in vivo*. *Biochem J*, 2004. **379**(Pt 2): p. 243-51.
222. Scott, J.W., et al., *CBS domains form energy-sensing modules whose binding of adenosine ligands is disrupted by disease mutations*. *J Clin Invest*, 2004. **113**(2): p. 274-84.



223. Martin-Hernandez, K., et al., *Expanding functions of ADP-ribosylation in the maintenance of genome integrity*. Semin Cell Dev Biol, 2016.
224. Haince, J.F., et al., *PARP1-dependent kinetics of recruitment of MRE11 and NBS1 proteins to multiple DNA damage sites*. J Biol Chem, 2008. **283**(2): p. 1197-208.
225. Guirouilh-Barbat, J., et al., *Defects in XRCC4 and KU80 differentially affect the joining of distal nonhomologous ends*. Proc Natl Acad Sci U S A, 2007. **104**(52): p. 20902-7.
226. Ikejima, M., et al., *The zinc fingers of human poly(ADP-ribose) polymerase are differentially required for the recognition of DNA breaks and nicks and the consequent enzyme activation. Other structures recognize intact DNA*. J Biol Chem, 1990. **265**(35): p. 21907-13.
227. Schreiber, V., et al., *Poly(ADP-ribose): novel functions for an old molecule*. Nat Rev Mol Cell Biol, 2006. **7**(7): p. 517-28.
228. Yang, C., et al., *Ribosomal protein L6 (RPL6) is recruited to DNA damage sites in a poly(ADP-ribose) polymerase-dependent manner and regulates the DNA damage response*. J Biol Chem, 2019. **294**(8): p. 2827-2838.



APENDIX

1. Publication N°1

Haser H. Sutcu*, Elie Matta*, and Alexander A. Ishchenko. (*Co-first authors)

Role of PARP-catalyzed ADP-ribosylation in the Crosstalk Between DNA Strand Breaks and Epigenetic Regulation

Journal of Molecular Biology - Published

<https://doi.org/10.1016/j.jmb.2019.12.019>

(Presented in the PDF version)

2. Publication N°2

Elie Matta, Assel Kiribayeva, Bekbolat Khassenov, Bakhyt T. Matkarimov, Alexander A. Ishchenko.

Insight into DNA substrate specificity of PARP1-catalysed DNA poly(ADP-ribosylation)

Scientific Reports – Accepted

(Presented in the PDF version)



Role of PARP-catalyzed ADP-ribosylation in the crosstalk between DNA strand breaks and epigenetic regulation.

Haser H. Sutcu^{1,2,†}, Elie Matta^{1,2,†}, and Alexander A. Ishchenko^{1,2,*}

¹Groupe «Réparation de l'ADN», Equipe Labellisée par la Ligue Nationale contre le Cancer, CNRS UMR 8200, Univ. Paris-Sud, Université Paris-Saclay, F-94805 Villejuif, France

²Gustave Roussy, Université Paris-Saclay, F-94805 Villejuif, France

[†]H.H.S. and E.M. contributed equally to this work

Correspondence to Alexander A. Ishchenko: Alexander.Ishchenko@gustaveroussy.fr; Tel.: +33 142115405; Fax: +33 142115008

Keywords:

programmed DNA breaks; DNA and RNA ADP-ribosylation; DNA demethylation; readers of ADP-ribosylated targets; regulation of transcription

Abbreviations used:

5caC, 5-carboxyl; 5hmC, 5-hydroxymethyl-cytosine; 5mC, 5-methylcytosine; ADPr, ADP-ribose; AID, activation-induced cytidine deaminase; APOBEC, apolipoprotein B mRNA-editing catalytic polypeptide-like; APLF, aprataxin and PNK-like factor; ARTD, diphtheria toxin-like ADP-ribosyl-transferases; BER, base excision repair; BRCT, BRCA1 C-terminal; CAD, caspase-activated DNase; CDK, cyclin-dependent kinase; CGI, CpG island; CHFR, checkpoint with forkhead-associated and ring domain; CSR, class switch recombination; DNMT, DNA methyltransferase; DSB, double-strand DNA break; FHA, fork head-associated; HR, homologous recombination; MAR, monomer of ADP-ribose; MMR, mismatch repair; NAD⁺, nicotinamide adenine dinucleotide; NF-κB, nuclear factor kappa B; NHEJ, non-homologous end-joining; OB fold, oligonucleotide/oligosaccharide-binding fold; PAR, polymers of ADP-

ribose; PARG, poly(ADP-ribose) glycohydrolase; PARP, Poly(ADP-ribose) polymerases; PBM, poly(ADP-ribose) binding motif; PBZ, poly(ADP-ribose) binding zinc finger; PPAR γ , peroxisome proliferator activated receptor γ ; PTM, posttranslational modification; RRM, RNA recognition motif; SSB, single-strand DNA break; ssDNA, single-stranded DNA; snoRNA, small nucleolar RNA; TET, ten-eleven translocation; UNG, uracil-N-glycosylase; TOP1, DNA topoisomerase I; TOP2, DNA topoisomerase II.

Abstract

Covalent linkage of ADP-ribose units to proteins catalyzed by poly(ADP-ribose) polymerases (PARPs) plays important signaling functions in a plethora of cellular processes including DNA damage response, chromatin organization, and gene transcription. Poly- and mono-ADP-ribosylation of target macromolecules are often responsible both for the initiation and for coordination of these processes in mammalian cells. Currently, the number of cellular targets for ADP-ribosylation is rapidly expanding, and the molecular mechanisms underlying the broad substrate specificity of PARPs present enormous interest. In this review, the roles of PARP-mediated modifications of protein and nucleic acids, the readers of ADP-ribosylated structures, and the origin and function of programmed DNA strand breaks in PARP activation, transcription regulation, and DNA demethylation are discussed.

Introduction

In most of living organisms, in response to environmental stress, cascades of molecular events are induced that involve specific changes in the cell's key macromolecules, such as proteins, nucleic acids, and lipids. These modifications are various chemical and structural transformations that enable to diversify the restrained genetic information encoded in DNA by the addition of chemical moieties, such as phosphate, acyl (methyl and acetate) groups, small peptides, and sugar residues on proteins and methyl group and its oxidized forms on nucleobases in DNA [1,2]. DNA damage poses a serious threat to genome integrity. Highly dynamic posttranslational and postreplicative modifications of proteins and DNA, respectively, are critical for DNA damage recognition and repair and for associated signaling [3]. In eukaryotes, ADP-ribosylation is a highly conserved posttranslational modification (PTM) of

proteins involved in the regulation of stress responses, cell division, transcription, and protein degradation. This reaction is catalyzed by ADP-ribosyltransferases using nicotinamide adenine dinucleotide (NAD⁺) as a source of ADP-ribose (ADPr) moiety. The largest family of ADP-ribosyltransferases in eukaryotes are poly(ADP-ribose) polymerases (PARPs) that catalyze the synthesis of monomers or polymers of ADPr (MARs or PARs, respectively) covalently attached to acceptor targets (Figure 1) [4,5]. Free nonattached PAR can also function in the cell stress responses including DNA damage, heat shock, and cytoplasmic stress response [4,6]. Importantly, the cellular turnover of PAR is regulated by PAR glycohydrolase (PARG), which degrades the polymer by hydrolysis of ribose–ribose bonds [7]. ADP-ribose (ADPr)-based modifications of target nuclear proteins including histones provide an efficient chromatin-remodeling mechanism required for efficient repair of DNA strand breaks, yet—in the case of severe genotoxic stress—PARP-catalyzed modifications of cell content may direct cell-initiated programmed cell death. Furthermore, it has been shown that PARP1 can interact with, modify, and regulate epigenetic remodeling proteins such as chromatin insulator protein CTCF (CCCTC-binding factor) and DNMT1 (DNA methylation maintenance protein); thus, the right balance between PARylation and PAR degradation by PARG is crucial for the maintenance of DNA methylation patterns in normal cells [8-10]. Of note, years ago, specific enzymes in arthropods and bacterial toxins were shown to transfer an ADP-ribosyl moiety to double- and single-stranded DNA nucleobases in a reversible manner [11,12]. Later on, it has been demonstrated that mammalian PARP1, -2, and -3 (having the ability to act as DNA break sensors) modify not only cellular proteins but also terminal phosphate residues at double-strand DNA break (DSB) and single-strand DNA break (SSB) termini [13,14]. Recently, RNA also was identified as a target of reversible mono-ADP-ribosylation [15]. At present, the biological role of PARP-mediated ADP-ribosylation of DNA strand break termini remains unclear, but might be different from that of proteins. This review focuses on the interplays among DNA breaks, ADP-ribosylation, and DNA epigenetic signatures. We also discuss the putative role of ADP-ribosylated DNA breaks in DNA metabolism and in the recruitment of specific PAR–DNA or MAR–DNA adduct–guided factors.

PARPs at the center of stress response pathways

Cellular stress responses are mediated by various sensors and effectors from multiple signaling pathways including phosphorylation, ubiquitylation, SUMOylation, methylation, acetylation, and ADP-ribosylation. PARylation and MARylation [poly- and mono(ADP-ribosyl)ation] catalyzed by PARPs alter the function of the modified proteins and provide a scaffold for the recruitment of other proteins, which in turn can also undergo ADP-ribosylation. The latter regulates a number of biological processes including the DNA damage response, chromatin reorganization, transcription, apoptosis, autophagy, mitosis, and cell metabolism and development (reviewed in [5,16-18]).

The family of PARPs, also known as diphtheria toxin–like ADP-ribosyl-transferases (ARTDs), includes 17 known members [19,20]. Highly divergent PARP homolog tRNA 2'-phosphotransferase 1 (TRPT1) is sometimes referred to as the 18th PARP family member [21]. According to their structures, PARPs can be subdivided into four subfamilies: DNA-dependent PARPs (PARP1, PARP2, and PARP3), tankyrases (PARP5a and PARP5b), CCCH (Cys–Cys–Cys–His) zinc finger and WWE (Trp–Trp–Glu) domain–containing PARPs (PARP7, PARP12, PARP13.1, and PARP13.2), and macrodomain-containing PARPs (PARP9, PARP14, and PARP15). Although PARP13 is not yet shown to have a catalytic activity [4], most of PARPs have the function of transferring PAR or MAR moieties onto their target proteins [22], DNA [13,14,23], or RNA termini [15]. PARPs play a role in a wide range of biological structures and processes, including DNA repair and maintenance of genomic stability, transcriptional regulation, centromere function, mitotic spindle formation, centrosomal function, the structure and function of vault particles, telomere dynamics, trafficking of endosomal vesicles, inflammation, apoptosis, and necrosis [6,22,24].

The founding member of the PARP family as well as the most ubiquitous and abundant PARP, PARP1 was the most studied. This 110 kDa nuclear protein is composed of six domains essential for DNA binding, nuclear homing, automodification, protein–protein interactions, and catalytic activity. PARP1 is responsible for 80% to 90% of the PARylation activity in the cell [25]. Based on the structure–function relationship studies, PARP1 was initially characterized as a critical player in the DNA damage response and repair processes under stressful conditions. PARylation can lead to accelerated dissociation of modified proteins from DNA owing to the negative charge of the PARylated protein and steric hindrance. The best example of this dissociation is PARP1-mediated PARylation of histone H1 and PARP2-mediated PARylation of histone H2B; these modifications cause the dissociation of these histones from DNA and eventually chromatin relaxation required for replication, transcription, DNA repair [26–28]. Later on, the list of known biological functions of PARP1 has been expanded: regulation of chromatin structure, transcription, stress responses, and involvement in various physiological processes [29]. Moreover, the roles of PARP1 under normal physiological conditions have been further substantiated, e.g., the regulation of gene expression, RNA biology, and processes in cytoplasm. Recently, PARP1 has been identified as a sensor of unligated Okazaki fragments—during DNA replication in normal S phase cells—which facilitates their maturation [30]. The remaining ADP-ribosylation activity in the cell lacking PARP1 (in embryonic fibroblasts derived from PARP1^{-/-} knockout mice) falls to other active PARP members, which may or may not share structural similarities or localization with PARP1 but certainly share a highly conserved catalytic (CD) domain (PARP signature). The latter consists of a helical regulatory domain (HD) and an ADP-ribosyl transferase domain (ART) responsible for the catalytic activity, present in PARP2 and PARP3.

PARP2 was discovered as the enzyme responsible for the basal PARylation activity in PARP1-deficient cells [31] and accounts for ~10% of the PARylation activity in the cell. Just as PARP1, PARP2 recognizes and binds a DSB or SSB. The binding of PARP2 to damaged DNA structures triggers its PARylation activity. PARP2 has partially redundant functions with PARP1

that are essential for normal embryogenesis. Double-knockout *Parp1*^{-/-}*Parp2*^{-/-} mice show early embryonic mortality [32]. PARP2 has a function, independent of its PAR synthesis activity, which limits the accumulation of the resection barrier factor 53BP1 at DNA damage sites and directs DSBs toward resection-dependent repair pathways [33]. Aside from DNA repair, cell cycle regulation, and inflammation and metabolic regulation, PARP2 acts as a cofactor in transcription and can regulate the expression of 600 to 1,000 genes by facilitating transcription or via attraction of cofactors promoting chromatin compaction and the consequent inhibition of transcription [34-37].

PARP3 is related to PARP1 and PARP2 and its domain organization is similar to that of PARP2, but PARP3 catalyzes MARYlation instead of PARylation [20]. Similar to PARP1 and PARP2, PARP3 is an important player in cell cycle regulation and DNA repair [38]. This PARP interacts with PARP1, DNA ligase III, Ku70/80, other nonhomologous end-joining (NHEJ) proteins and promotes processing DSBs in the canonical NHEJ pathway [39]. Other than its role on the DNA damage response and repair, PARP3 has also been reported to associate with Polycomb group proteins involved in transcriptional silencing and chromatin-remodeling [40].

PARP4 (also called VPARP or ARTD4) is a component of the cytosolic ribonucleoprotein vault complex [24] and is also present in cytoplasmic clusters (vPARP rods) as well as in the nuclear matrix [5]. The conserved glutamate residue in PARP1 is replaced with isoleucine, leucine, or tyrosine in PARP4, which is associated with the absence of polymerase activity [41]. It was proposed that PARP4 may be involved in an antiviral response [42].

PARPs 5a and 5b (tankyrases) were initially identified as a part of a telomeric complex but are also located in the cytoplasm as peripheral membrane proteins localized at the Golgi complex and are associated with transport vesicles [5]. They are best known for their participation in mitosis and WNT signaling, but they also have functions in telomere and DNA damage repair [24]. Recently, a possible link between tankyrases and the DNA damage response has been proposed. On the one hand, tankyrases associate with DSBs to facilitate the recruitment of the

CtIP–BRCA1 complex to damaged chromatin and to promote DNA end resection during homologous recombination (HR); on the other hand, tankyrases associate with DSBs to stimulate the recruitment of the BRCA1A complex (consisting of RAP80–BRCA1–BRCC36–CCDC98) mediated by MERIT40 and activate the G2–M checkpoint for promoting DNA repair before mitosis [43].

PARP6 has been found to be involved in hippocampus neuronal development [24]. Moreover, it plays a role in cell cycle progression and has been associated with the progression of colorectal cancer [42]. Of note, the biological activity of PARP6 depends on its catalytic activity as well as its N-terminal cysteine-rich domain [41].

Several PARPs (PARP7, PARP10, PARP12, and PARP13) are involved in the mechanisms of posttranscriptional regulation of mRNA; the latter process is mediated either by RNA-binding domains or by ADP-ribosylation of RNA-binding proteins [24]. PARP7, present in stress granules [5], is involved in antiviral responses, cytosolic RNA processing, and transcription [34]. PARP10 is a binding protein and an inhibitor of MYC [42] and has been implicated in the regulation of nuclear factor kappa B (NF- κ B), GSK3B, and transcription [24]. PARP10 directly ADP-ribosylates NEMO. These events lead to the inhibition of nuclear localization of the p65 subunit of NF- κ B and to subsequent attenuation of NF- κ B-dependent gene expression [41]. PARP12 is a catalytically active cytosolic monoenzyme [43], which preferentially associates with the Golgi apparatus and regulates stress granule assembly, microRNA activity, and an antiviral response [42]. Intracellular expression of PARP12 increases upon stimulation by type II interferons, thereby leading to increased NF- κ B signaling, implicating PARP12 in cellular immune responses [41]. PARP13, also referred as ZAP (zinc finger antiviral protein), has been so far regarded as a catalytically inactive ART with the roles in the assembly of stress granules and regulation of microRNAs, with consequent implications in innate antiviral defense and cancer [42,43].

PARP9 and PARP14 are believed to act on transcription, especially the transcription of genes required for macrophage activation [24]. PARP9 possesses a unique MARYlating activity

specifically targeting the ubiquitin peptides and participates in the DNA damage response, transcription in lymphocytes, and in antiviral response [42]. PARP14 has been implicated in multiple cellular functions such as survival of B cells, cell migration, assembly of stress granules, transcription during inflammation processes, the DNA damage response, and an antiviral response [42]. PARP14 regulates the class distribution, affinity repertoire, and recall capacity of antibody responses, which require efficient differentiation and interactions among B cells, T helper cells, and dendritic cells [41].

Concurrently with its nuclear pore localization, PARP11 modifies targets involved in the coordination of the nuclear envelope and organization of nuclear pores and nuclear envelope biology [24,42]. PARP15 is a centrosomal PARP involved in stress granule formation, an antiviral response, cytosolic RNA processing, and tumor formation [41,42]. PARP16 is located in the endoplasmic reticulum (ER) and regulates the unfolded protein response [24,42]. Cellular localization of other PARPs (PARP8 and PARP17) and their involvement in biological processes remain unknown.

Moreover, some PARP family members can interact with each other, e.g., PARP1 with PARP2 or PARP3 as well as tankyrase 1 with tankyrase 2 [27]. This type of heterodimers may occur in different subcellular compartments and act on different substrates, which monomeric PARPs could not otherwise target individually. This observation may highlight a new organizational order for PARPs that may greatly diversify their biological responses, via combinatorial interactions.

Excessive ADP-ribosylation can lead to the activation of cell death pathways, including parthanatos, a unique form of programmed cell death that occurs independently of caspases and is distinct from necrosis and apoptosis [44]. Due to its manifold role in cell survival, the protein PARylation process is finely regulated. PAR is rapidly degraded PARG, the main enzyme that specifically hydrolyses ribose–ribose bonds encoded by a single gene in mammals [7]. Disruption of the *PARG* gene in mice causes embryonic lethality, and studies of PARG-deficient cells have shown that accumulation of PARylated macromolecules is highly

toxic to the cell [45,46]. Nevertheless, PARG has rather limited processivity on short PAR polymers and is unable to remove MARylation marks from proteins [47]. A complete reversal of MARylation is performed in human cells by amino acid-specific ADPr-acceptor hydrolases, such as macrodomain-containing proteins MacroD1 and MacroD2, terminal ADP-ribose protein glycohydrolase 1 (TARG1), and ADP-ribosylhydrolase (ARH) family members ARH1 and ARH3 (reviewed in [48]).

Protein acceptors for ADP-ribosylation

Despite PARPs' different biological functions, over decades, little has been known about ADPr acceptors. Starting from the protein PARylation discovery, for ADP-ribosylated proteome analysis, researchers have applied chemical (high pH, hydroxylamine) or enzymatic sensitive methods (based on ARH1, PARG, ARH3, SVP, or NudT16) to quickly release the ADPr groups from modified residues. Hayaishi's group provided one of the first mechanistic insights into PAR synthesis. They demonstrated that in the rat liver, ADPr binds to histone H1 through an ester linkage with either a γ -carboxyl group of glutamic acid residue 2 or 14 or with an α -carboxyl group of C-terminal lysine residue 213 [49]. Linker histones H1 and H5 are known to be primary targets for PARP1-catalyzed PARylation, whereas PARP2 and PARP3 preferentially ADP-ribosylate core histone H2B [50-52]. PARP3 preferentially adds a mono ADPr moiety on Glu2 of histone H2B upon DNA damage [51]. Until 2017, it had been generally thought that PARP-catalyzed auto-PARylation and ADP-ribosylation of other proteins occur predominantly on aspartates, glutamates, and lysines [53-55]. Nonetheless, conventional approaches have to overcome many limitations, such as the dynamic heterogeneous nature of protein ADP-ribosylation, low abundance, lability of some sites, and chemical or enzymatic resistance of other ADPr acceptor sites. The evolution of methods for the detection of MAR/PAR attachment sites has led to the use of mutagenesis assays as well as NAD⁺ analogs, unbiased enrichment strategies, chemotherapeutic PARP inhibitors, advanced mass spectrometry (particularly based on electron-transfer higher-energy collisional dissociation), and quantitative proteomic techniques [56-59]. Investigators have uncovered modification of

more than 7000 ADP-ribosylation sites across more than 2000 ADP-ribosylation target proteins covering over one-third of the nuclear proteome under genotoxic stress conditions [59]. Upon DNA damage, serine (Ser) becomes the major ($\approx 90\%$) ADPr acceptor residue with the most easily identifiable signals related to the modification of histone proteins as well as PARP automodification [57,59]. Histones are MARylated selectively on serine residues of histone H3 (Ser10 and Ser28) and Ser6 of H2B unless the neighboring lysine residues are acetylated [57,60]. Notably, Ser ADP-ribosylation sites strongly overlap with known kinase-regulated sites (Aurora B and others) [59]. ADP-ribosylation and phosphorylation of these serine residues are considered mutually exclusive [60], suggesting a complex interplay between histone marks. The major hydrolase responsible for the reversal of the Ser-ADPr modification is ARH3 [61,62]. ARH3-deficient cells show a dramatic increase of PAR content in response to hydrogen peroxide exposure with induction of an AIF release from mitochondria and parthanatos [62,63]. Moreover, the specificity of ADP-ribosylation is regulated by different factors. HPF1 (histone PARylation factor 1) interacts with PARP1 and PARP2 and guides the ADP-ribosylation of PARP1 and high-mobility group proteins through a serine residue [56]. In HPF1's absence, acidic residues (Asp and Glu) become the main target sites for ADPr in proteins. Hundreds of ADP-ribosylation sites are also located on histidine, arginine, lysine, cysteine, and tyrosine residues [59,60,64]. It is still possible that further development of proteomic tools will allow researchers to detect new types of modifications, such as an acid-labile ADPr adduct of phosphoserine residues. This chimeric modification was noted in histones from the rat liver more than 40 years ago [65], but the enzymes responsible for its formation are still unknown. The diversity of ADPr substrate amino acids has revealed the importance of this PTM in cell signaling and survival and thus the necessity of its regulation.

Readers of ADP-ribosylated targets

ADP-ribosylation is a PTM of proteins: it induces the recruitment of the protein (such as TET [66], TP53 [67], NF- κ B [68]) or modulates its activity by covalent or noncovalent binding. Aside from protein modification, ADP-ribosylation is also involved in signaling as well as protein–

protein or protein–DNA interactions [69]. PARylation as a PTM directly regulates many cellular pathways such as transcription, chromatin modification, and DNA damage and oxidative-stress signaling. Proteins may have a PAR- or MAR-recognizing domains (Figure 2) that bind to PAR polymers or MAR moieties [29]. Depending on the nature of recognition, different proteins have different motifs. For instance, a PAR-binding motif (PBM) is believed to engage in an electrostatic interaction with negatively charged PAR chains [69,70], whereas a PAR-binding zinc finger (PBZ) recognizes two consecutive ADPr moieties although some can also recognize only one ADPr of a PAR chain [71-73]. Similarly to PBZ, WWE requires two consecutive ADPr units for its successful binding; hence, it interacts with iso-ADPr formed by both ADPr units [74]. FHA (fork head–associated) and BRCT (BRCA1 C-terminal) are protein domains that are mostly known to interact with phosphorylated peptides but also have affinity for PAR chains [75]. The latter interaction seems to be similar to that of WWE domain or PBM, respectively. Another class of ADPr-recognizing domains is macrodomains. Unlike other domains, macrodomains interact with mono-ADPr or the terminal ADPr of PAR chains in the case of H2A1.1 [76]. There are also RNA- and DNA-binding motifs that unexpectedly recognize PAR ADPr moieties [77].

The PBM

The consensus sequence of a PBM is ([HKR]-X-X-[AIQVY]-[KR]-[KR]-[AILV]-[FILPV]), i.e., approximately 20 residues. The positively-charged-amino acid content of a PBM allows for an electrostatic interaction with highly negatively charged PAR polymers. PBMs have been detected in more than 800 proteins *in silico*, and >500 hits have been obtained in proteomic analysis [69,70]. PBMs are often found in many DNA damage response proteins and other proteins that are included in the ADPrDB database of ADP-ribosylated proteins [78], suggesting that PAR binding promotes PARylation. For example, tumor protein p53 (p53, TP53) can bind to PAR polymers both in a covalent and in a noncovalent manner. TP53 contains multiple PBMs. Hence, Fishbach *et al.* suggest that TP53 gets covalently PARylated upon a noncovalent interaction between a PBM located in a C-terminal domain of TP53 and

PARylated PARP1 [67]. They demonstrated that noncovalent PAR binding diminishes the sequence-independent DNA-binding capacity of TP53. Nevertheless, simply having a PBM seems to be insufficient for PAR binding. For instance, the entire BRCT domain of XRCC1—rather than a short PBM—is required for its affinity for PAR [75].

The PBZ

The PBZ is a C2H2 zinc finger domain consisting of approximately 30 amino acid residues. The PBZ domain has a consensus sequence of [K/R]-X-X-C-X-[F/Y]-G-X-X-C-X-[K/R]-[K/R]-X-X-X-X-H-X-X-X-[F/Y]-X-H and so far has been discovered in three proteins: APLF (aprataxin and PNK-like factor), CHFR (checkpoint with forkhead-associated and ring domain), and CTCF [77]. Unlike CHFR, APLF contains two PBZ domains. Accordingly, one of the two PBZ domains identified in the APLF protein interacts with two consecutive ADPr units, whereas the second PBZ domain is thought to bind to the 3rd ADPr unit likely on a branched PAR polymer or terminal poly-ADPr. The PAR recognition by APLF induces its histone chaperone activity for the release of histones H3 and H4 and chromatin relaxation [79,80].

Macrodomains

Macrodomains are mono-ADPr-recognizing domains [76]. One of the well-studied macrodomains is histone variant macroH2A1.1. In addition to MAR, macroH2A1.1 can recognize PAR polymers via their terminal ADPr unit. MacroH2A1.1 participates in metabolic regulation and energy production by inhibiting PARP1 activity and decreasing its nuclear NAD⁺ consumption [81]. MacroH2A1.1–PARP1 interaction is also involved in gene regulation, for instance, in response to heat shock stress and during expression regulation of senescence-associated secretory phenotype genes or genes participating in adipocyte differentiation and metabolic regulation during muscle differentiation [82]. Another macrodomain-dependent chromatin-remodeling factor is ALC1. This is an inactive ATPase and one of the chromatin remodelers that activates upon DNA damage. During DSB repair, MacroH2A1.1 [83] and ALC1 [84] take part in chromatin remodeling in a macrodomain-dependent manner. PARP family members PARP9, PARP14, and PARP15 have both the MARYlation activity and a

macrodomain interacting with MAR [76,85,86]. PARG, TARG1, and MACROD1–3 ADPr-hydrolases also contain macrodomains [87].

The WWE domain

This domain contains two conserved tryptophans and a glutamic acid residue, hence its name, and in total is approximately 80–100 residues long [88,89]. It recognizes iso-ADPr moieties between two consecutive ADPr units. The WWE domain is reported to be present mostly in E3 ubiquitin-protein ligases (RNF146, DELTEX1, DELTEX2, DELTEX4, and HUWE1) and in two PARPs (PARP11 and PARP14) [74].

FHA and BRCT domains

These domains play a huge part in cellular responses to DNA damage by recognizing phosphorylated peptides [90,91]. It has also been discovered that FHA and BRCT domains can recognize PAR polymers. Similarly to the WWE domain, the FHA domain binds iso-ADPr of PAR chains by recognizing the two phosphate groups on ADPr moieties, whereas the BRCT domain directly recognizes ADPr of a PAR chain [75]. The latter phenomenon is possibly due to the phosphate groups on ADPr, which mimics the phosphorylated serine residue recognized by the BRCT domain [92]. ADPr recognition by an FHA or BRCT domain facilitates rapid recruitment of DNA damage response proteins: PNKP and aprataxin by the FHA domain and ligase IV, XRCC1, and the BRCA1–BARD1 complex by the BRCT domain [75,92-94].

RNA- and DNA-binding motifs (RRM, SR repeat- and KR-rich motif, OB fold, PIN domain, and GAR domain)

Of note, RNA- and DNA-binding motifs can also bind to PAR. Although this is not very surprising because PAR chains have a structure similar to that of oligonucleotides. NONO, an RNA-binding protein, is believed to increase survival during DSB repair although its function is not yet clear; its recruitment is PARP1 dependent. RRM (RNA recognition motif) of NONO recognizes PAR, thereby facilitating the recruitment of NONO to a DNA damage site [95].

It has been shown that splice factors ASF/SF2, SF3A1, SF3B1, and SF3B2 can recognize PAR chains via their SR (serine/arginine) repeats [96,97]. PAR binding to splicing factor ASF/SF2 inhibits its phosphorylation by TOPI (DNA topoisomerase I) and activity [96], indicating the involvement of PARPs and PAR chains in RNA stability and metabolism [98]. In a similar context, upon heat shock, KR (lysine/arginine)-rich repeats of the *Drosophila* Mi-2 protein bind PAR chains thus leading to Mi-2 recruitment to heat shock–responsive genes [99].

Oligonucleotide/oligosaccharide-binding fold (OB fold) is an ssDNA- and RNA-binding motif. Just as WWE and FHA domains, the OB fold of human ssDNA-binding protein 1 (hSSB1) recognizes iso-ADPr of PAR chains in addition to its ssDNA-binding ability [100].

Proteins with PIN (PiIT N terminus) domains are mostly nucleases cleaving ssDNA or ssRNA [101]. In particular, during DNA damage repair, the PIN domain of exonuclease 1 (EXO1) was found to recognize DNA damage–induced PARs, and this event is rather sufficient for its recruitment to the DNA damage site [102].

GAR (or RG/RGG box) is another PAR-binding domain and consists of a sequence enriched in arginine and glycine. There are several RNA-binding proteins with GAR domains known to recognize PAR chains during DNA damage responses, e.g., FUS/TLS, EWS/EWSR1, TAF15, and CIRBP [77,103].

Reversible ADP-ribosylation of DNA and RNA

The first evidence of DNA ADP-ribosylation was obtained 20 years ago. Watanabe's group demonstrated that a cabbage butterfly toxin, pierisin, induces apoptosis via irreversible MARylation of a guanine base in DNA [104,105]. Later, other examples of DNA MARylation have been demonstrated for different families of toxins: guanine MARylation by CARP-1 from shellfish [11] and by scabin from *Streptomyces scabies* [106] as well as thymine MARylation by DarT from bacterial toxin–antitoxin system DarTG [12].

Recently, *in vitro* studies in our laboratory have uncovered that mammalian DNA-dependent PARPs catalyze reversible modification of DNA via ADP-ribosylation of terminal phosphates at DNA strand breaks [13]. This finding provides novel molecular insights into PARPs' functions in mammalian cells. Taking into account an unsolved challenge (how to distinguish ADPr adducts on proteins and DNA in the cell), DNA ADP-ribosylation studies have been focused on *in vitro* approaches to gain knowledge about the mechanisms and specific requirements for this unusual substrate specificity of PARPs. It has been found that PARP1 preferentially PARylates DSBs containing 5'- and 3'-terminal phosphates in gapped recessed DNA duplexes, whereas PARP2 and PARP3 preferentially act on 5'-terminal phosphates at DSB and SSB termini of DNA containing multiple proximal breaks [13,14,23]. Similarly to protein modification, PARP3 produces a MAR not PAR adduct on DNA substrates, in contrast to PARP1 and PARP2 [14,23]. In addition to phosphate groups, PARP1 can PARylate 2'-OH groups of 3'-deoxynucleotide and ribonucleotides incorporated at the 3' terminus of oligodeoxyribonucleotides [13]. A recent study by Zarkovic G. et al. revealed ADP-ribosylation of ~3 kb plasmid-based DNA constructs, thus indicating DNA size limitlessness of PARP-mediated modifications of DNA break termini [14]. Moreover, PARP2 and PARP3 switch their substrate preference to DNA from protein when acting upon certain configuration of closely spaced DNA strand breaks, preferentially ADP-ribosylating DNA rather than catalyzing auto-ADP-ribosylation. Effectiveness of PARP3- and PARP2-catalyzed DNA ADP-ribosylation depends on the orientation and a distance between DNA strand breaks in a single DNA molecule [14]. According to a proposed mechanistic model, binding of a PARP to one DNA break activates the CAT domain, which in turn targets and ADP-ribosylates an acceptor group at the second breakage site of the same DNA molecule [13,14]. This process necessitates the presence of at least two DNA strand breaks separated by a distance from 1 to 2 helix turns [14]. In a DNA-bound PARP complex, this distance determines the accessibility of the DNA acceptor groups for the activated CAT domain directing ADP-ribosylation to a 5'- or 3'-terminal phosphate. At present, little is known about the mechanisms governing substrate interaction and specificity of PARP1, which accounts for most of cellular PARylation activity. Moreover, it

remains unclear of how can PARPs adopt the conformation that predisposes to DNA ADP-ribosylation activity. According to existing structural data on PARP1 and PARP2 bound to DNA breaks, the PARP's DNA-binding domain is far from its CAT domain, which is not oriented along the DNA helix [35,107,108]. Nevertheless, broad substrate specificity in *trans*, including also auto-modification of different amino acid residues in *cis*, and the multidomain structure of PARPs imply high flexibility of the CAT domain position in DNA–PARP complexes. Therefore, there may be some unexplored abilities to target substrates including formation of oligomeric protein complexes on DNA.

Effective DNA-PAR/MARylation occurs on DNA substrates that mimic intermediate products occurring in various DNA excision repair pathways such as base excision repair (BER), nucleotide excision repair (NER), mismatch repair (MMR), HR, and NHEJ. For example, DNA strand break acceptor sites containing 5'-phosphates can be generated by the action of various DNA exo- and endonucleases, tyrosyl-DNA phosphodiesterase 2 (TDP2), and dRP (5'-deoxyribose phosphate) lyase activity of bifunctional DNA polymerases, whereas 3'-terminal phosphates are produced by certain bifunctional DNA glycosylases, TDP1 and MRE11 [109,110]. DNA duplexes containing a DSB and a proximal SSB can form in HR and NHEJ repair pathways. It has been reported that a stably blocked replication fork can switch the endonuclease activity of MRN–CtIP complex on and produces an internal nick located ~20 nt downstream of 5'-termini of a DSB [111], thus ensuring proximity of activating and acceptor sites required for DNA ADP-ribosylation activity of PARPs.

At present, the physiological relevance of PARP-dependent DNA ADP-ribosylation is a debated issue. Nevertheless, a dramatic substrate switch of PARPs observed *in vitro* assays, the highly efficient PARP1-catalyzed DNA PARylation in human cell-free extracts, and the presence of a PAR signal in purified genomic DNA after genotoxic treatment provide the strong albeit indirect evidence of the presence of PAR–DNA adducts in live cells [14,112]. Furthermore, it has been shown that 1 nt gapped DNA containing a MARylated 5'-phosphate residue is recognized as a 5'-adenylated DNA substrate by DNA ligase I or IIIa or by other

DNA ligases and ligated in the absence of ATP, resulting in the sealed unbroken double-stranded DNA with an aberrant abasic (AP) site-like residue [112]. Such residue can be processed further by apurinic/apyrimidinic endonuclease 1 (APE1) in BER pathway [112]. In line with these results, it has been proposed that PARP2 and PARP3 are involved in the final ligation step of NHEJ, judging by the finding that 5'-phosphorylated nicks are especially efficient activators of the auto-ADP-ribosylation activity of PARP2 and PARP3 but not that of PARP1 [36]. We can hypothesize that DNA ADP-ribosylation can promote retention of the DSB ends either until a complete repair complex is formed or until the ATP concentration required for DNA ligation is restored. Similarly, in case of SSB repair, PARP-mediated ADP-ribosylation can promote the ligation of a gap without polymerase synthesis and ATP. Of note, extensive PARP-mediated PAR synthesis leads to inhibition of hexokinase 1 activity, blockage of glycolysis, and ATP loss [113]. Thus, one of the functions of DNA ADP-ribosylation can be the patching of DNA breaks during bioenergetic collapse avoiding formation or degradation of toxic DSBs.

Recent advances in RNA biology took the phenomenon of ADP-ribosylation to another level. Studies by Shuman's group have revealed that PARP-like tRNA splicing enzymes Tpt1 (KptA) from bacteria and fungi can ADP-ribosylate RNA and DNA at 5'-monophosphate termini [114,115]. Further studies by Ahel's laboratory have shown that Tpt1 homologs in higher organisms TRPT1 (PARP18) as well as human PARP10, PARP11, and PARP15 can MARylate phosphorylated ends of RNA [15]. This 5'-phospho-ADPr modification or "capping" of RNA termini may protect RNA substrates from degradation or dephosphorylation and mediate ADP-ribosylation signaling via recruitment of specific cellular factors. Overall, these RNA related studies provide additional evidence that the phenomenon of ADP-ribosylation of nucleic acids at terminal phosphates is more widespread than previously thought.

ADPr removal from DNA and RNA termini. ADP-ribosylation of DNA and RNA termini is a fully reversible process. We have demonstrated that PARG efficiently restores native DNA structure

by hydrolyzing PAR–DNA or MAR–DNA adducts generated by PARP1, PARP2, or PARP3 [13,14]. Moreover, recently, Ahel's laboratory demonstrated that the MAR moiety that is covalently attached to oligonucleotide termini can also be removed by other cellular hydrolases, such as MACROD1, MACROD2, TARG1, and ARH3, though with much lower efficacy [23,116]. We believe that the half-life of DNA–PAR or DNA–MAR adducts is similar to that of PARylated proteins and may depend on the recruitment of PARG to the sites of ADP-ribosylation. In the absence of PARG, which is the major glycohydrolase in the nucleus, ADP-ribosylated DNA strand break termini would result in persistent DNA damage and is expected to be highly genotoxic as compared to the PARylated proteins: mainly PARPs and histones. Similarly, hydrolases PARG, TARG1, ARH3, and MACROD1 and -2 can restore intact RNA structure after ADP-ribosylation of a 5'-terminal phosphate [15]. The broad substrate specificity of glycohydrolases toward ADP-ribosylated DNA and RNA can be explained by the acid lability of the phosphodiester bond between ADPr and terminal phosphates in nucleic acids, in contrast to the bond between amino acids and ADPr in protein target [14]. Noteworthy, the replacement of a phosphate acceptor group with a thiophosphate residue has little impact on its ADP-ribosylation but makes MAR–DNA adducts resistant to PARG hydrolysis [14].

DNA damage–induced DNA demethylation, ADP-ribosylation, and cell differentiation

DNA damage response and repair proteins play a crucial role in genomic integrity. In addition, these proteins have important functions in gene expression, in particular during organism development and stem cell maintenance and differentiation. For instance, programmed DNA damage and repair are important in the immune response for B- and T-cell development and for generation of the diversity of antigen receptors [117]. In the adaptive immune system, not only DNA repair proteins but also other cell cycle regulators and checkpoint proteins play important roles. They function as regulators of proliferation, of introduction of diversity, and cell cycle arrest during V(D)J recombination and class switch recombination (CSR). Classic NHEJ

is the major pathway repairing the RAG1/RAG2-induced DSBs during V(D)J recombination, whereas in mature B cells, alternative NHEJ and other repair mechanisms such as BER also participate to repair the activation-induced cytidine deaminase (AID)-induced DNA lesions during CSR and somatic hypermutation [118]. In addition to the generation of antigen diversity, during B- and T-cell development, programmed DNA damage is a trigger for the expression of many genes including genes related to cell survival, proliferation, and development [119]. Deamination by AID occurs at the GC-rich transcriptional start sites of heavy-chain and light-chain genes where cytidine is converted into uracil. Uracil-N-glycosylase (UNG), BER, and MMR proteins detect the uracil residues in U•G mispairs. Thereafter, the nick will be introduced into DNA, and subsequent repair of the DNA lesion may lead to deletion, transition, and transversional mutations [120]. Alternatively, the repair of deaminated bases via the nick-initiated long-patch DNA excision-resynthesis mechanism during long-patch BER [121,122], NER [123], and noncanonical MMR [124] leads to replacement of neighboring 5-methylcytidine nucleotides by unmodified nucleotides. Thus, locus-specific AID targeting in transgenic mice has been reported to induce local processive DNA demethylation even ~1 kb beyond its target motif [122]. Activation and regulation of AID are not yet well characterized, although CSR is initiated by AID-induced DNA lesions at least after three cell cycles [120], and AID is more stable in the G1 phase and is regulated by the cell cycle [125]. Accordingly, replication-dependent types of DNA damage may be the prior signal for the initiation of CSR and upregulation of *AID* expression regulated by NF- κ B signaling [126,127]. AID is active on single-stranded DNA (ssDNA), indicating the presence of a secondary structure of DNA (like R-loops) during the initiation of CSR and somatic hypermutation [128]. Indeed, it has been suggested that AID recognizes G4 (quadruplex) DNA structures with at least a 5 nt ssDNA overhang prior to CSR [129].

There are multiple types of stem cells, which exploit endogenous types of DNA damage to regulate their differentiation. Immortalized myoblasts, which follow the fate similar to that of activated skeletal muscle stem cells, need BER factors to differentiate successfully [130]. A

while ago, endogenous DNA damage was observed immediately prior to myotube fusion [131,132]. These DNA lesions have been predicted to be SSBs or DNA nicks, which are some of the major causes of PARP activation [133]. Consistently with these data, Farzaneh *et al.* mentioned the need for PARP activity during terminal differentiation of myoblasts [131]. Later, it was also discovered that these types of DNA damage are induced by caspase-activated DNase (CAD), which in the end leads to changes in gene expression patterns, for instance, upregulation of p21, a cyclin/cyclin-dependent kinase (CDK) inhibitor protein inducing cell cycle arrest [134]. Indeed, these types of CAD-dependent DNA damage may be one of the reasons because they trigger the changes in the DNA methylation pattern of differentiating myoblasts, and these alterations eventually lead to the upregulation of myogenic factors needed for multinucleated myotube fusion [135].

ADP-ribosylation-dependent chromatin remodeling is critical for initiating the expression of genes. For example, neural activation by stimulation of immediate-early-gene expression requires a release of linker histone H1. Accordingly, Azad *et al.* have shown that a release of H1 from the promoter of an immediate early gene requires ADP-ribosylation by PARP1 and phosphorylation of the histone [136]. PARylation-dependent H1 disposition has also been observed in hormone-regulated genes [137]. A growing number of studies have revealed that PARP1 regulates gene expression through PARylation of histone methyltransferases and demethylases [66,138]. This in turn changes the histone H3 and H4 acetylation and methylation statuses and subsequently strongly alters the regulation of gene expression patterns independently of histone ADP-ribosylation, pointing to the critical role of chromatin modifying factors in transcription regulation [28]. Notably, PARylation of epigenetic regulators at DNA damage sites is very important to maintain the histone mark balance to ensure correct spatial and temporal coordination of DNA repair. In this context, ADP-ribosylation may be linked to the repair of DNA damage and chromatin remodeling; however, this mechanism may not be enough to explain the epigenetic regulation of genes responsible for the fate of the cells undergoing either B-cell or T-cell development and during myogenic cell differentiation in the

absence of ADP-ribosylation. Accordingly, ADP-ribosylation may contribute to the signaling cascade during epigenetic regulation since the methylation patterns of the cells are changing at the target sites in related genes and not globally. One of the vivid examples of this phenomenon is the concentration of programmed DNA damage at the promoter site of the *p21* gene during myogenic differentiation [134].

Active DNA demethylation as a source of programmed DNA breaks

Dynamic DNA methylation is one of the major epigenetic regulation mechanisms. DNMTs (DNA methyltransferase enzymes) transfer a methyl group onto the 5' position of cytosine. Methylated cytosine is a signature of repressed gene expression. DNA methylation regulates tissue-specific gene expression, genomic imprinting, and X-chromosome inactivation [139]. Additionally, the majority of gene promoters are located in the proximity of CpG islands, which are CG repeat-rich sequences. Unmethylated and methylated CpG islands are associated with actively transcribed and inactive genes, respectively [140]. Embryonic stem cells have approximately 4% of the CpG islands methylated [141], and this figure increases to 70–80% in somatic cells [142]. This difference can be related to the pluripotency of stem cells or the differentiated or specialized state of somatic cells. To switch pluripotency off, heterochromatinization takes place, followed by DNA methylation. Histones H3 and H4 are methylated. For instance, H3K9 residues get trimethylated by G9a, a histone methyltransferase, and are deacetylated by histone deacetylases. This event is followed by the recruitment and activity of DNA methyltransferases DNMT3 and DNMT3B [143].

DNA methylation can be modulated either for the developmental, differentiated gene expression or to avoid the hypermethylation of CpG islands, which are maintained under hypomethylation state [144]. In vertebrates, the most studied proteins involved in DNA demethylation are activation-induced deaminase/apolipoprotein B mRNA-editing catalytic polypeptide-like (AID/APOBEC) family, which are cytidine deaminases, and the ten-eleven translocation (TET) family of proteins [145]. It has been suggested that AID-catalyzed

deamination of 5-methylcytosine (5mC) to thymine results in the formation of the mismatched base pair G•T, which is repaired by methyl-CpG-binding domain protein 4 (MBD4)-initiated BER [146]. It should be noted that deamination of 5mC may be carried out not only by proteins of the AID/APOBEC family but also by DNA methyltransferases DNMT3A and DNMT3B in the absence of the methyl donor S-adenosylmethionine [147]. The participation of AID/APOBEC families has been extensively reviewed by Rebhandl *et al.*; the authors stated that AID/APOBEC takes part in many different cellular processes mostly by introducing a mutation. These enzymes play a role in B- and T-cell development by mutating immunoglobulin heavy-chain variable genes (IgV), thereby increasing the diversity of generated antibodies. The APOBEC family also participates in immune defense by targeting and mutating viral DNA [148].

TET enzymes belong to the family of 2-oxoglutarate-dependent dioxygenases. There are three members of the TET family in vertebrates: TET1, TET2, and TET3. They are all responsible for the demethylation of 5mC in DNA by oxidizing it into 5-hydroxymethyl-cytosine (5hmC), which can be followed by oxidation into 5-formyl-cytosine or 5-carboxyl-cytosine (5caC) [149,150]. It is believed that each form of oxidized cytosine has specific readers that can bind it, possibly to regulate the expression of genes. During active DNA demethylation, 5-formyl-cytosine and 5caC residues are removed from DNA by thymine-DNA glycosylase (TDG) in the BER pathway [149,151]. An alternative murine demethylation pathway involving 5mC oxidation prior to deamination has been proposed, based on a complex of GADD45A, AID, and TDG detected and the finding that SMUG1, MBD4, or TDG has a glycosylase activity on 5-hydroxymethyl-uracil [145,152].

DNA demethylation of the paternal genome in murine primordial germ cells is mechanistically linked to the emergence of SSBs, high levels of PARP1 expression, and activation of the BER pathway, accompanied by the appearance of γ H2A.X foci and nuclear PARylation [153,154]. Suppression of BER by PARP1- and APE1-specific small-molecule inhibitors increases methylation of the paternal genome both globally and in LINE1 elements [154]. Taken together,

these data indicate that DNA breaks and activation of PARPs are important for active DNA demethylation.

Interplay between PARylation and DNA methylation

PARPs-catalyzed PARylation performs diverse and important functions in the regulation of both DNA methylation and demethylation. Nucleosome-bound PARP1 is enriched in chromatin domains showing lower 5mC content within 1 kb from the transcription start sites of highly expressed genes [155,156]. For example, *Dnmt1*, *p16*, α -SMA (smooth muscle actin alpha), pluripotency-related genes, NF- κ B-dependent genes, peroxisome proliferator activated receptor γ (PPAR γ)-dependent genes, and other genes are regulated by PAR moieties and PARP1 located at the promoter site (for more detailed review see Ciccarone *et al.* [66]). DNMT1 plays an important part in DNA methylation of newly synthesized hemimethylated DNA during replication [157,158]. Zampieri and coauthors demonstrated that PARP1 is colocalized with PAR specifically at one out of the five inferred *Dnmt1* promoter regions [159]. Auto-PARylated PARP1 and PAR polymers interact with both CTCF and DNMT1, thereby preventing their access to DNA and methylation of cytosines [9,160]. DNMT1 contains two PAR-binding domains that render higher affinity of the methyltransferase to PAR polymers than to DNA [159]. Accordingly, overexpression of hydrolase PARG causes increased methylation of the *Dnmt1* promoter and repression of *Dnmt1* expression [159]. The existence of an additional layer of DNMT1 expression control should be noted: through PARP1-catalyzed PARylation of the UHRF1 factor, which mediates ubiquitination of DNMT1, to ensure its timely regulated abundance in S and G2 phases [161]. Competitive PARP inhibition leads to global genomic-DNA hypermethylation mainly concentrated in CGI (CpG island) regions *in vivo*, whereas hyperactivation of PARP1 leads to hypomethylation [159]. In the absence of ADP-ribosylation, a particular gene could also be differently affected as hypermethylated at the CGIs of the promoter site while hypomethylated within the gene body [156]. Finally, PARP1-mediated PARylation of methyl CpG-binding domain protein 2 (MeCP2) impairs its ability to bind 5mCpG sites and reorganize heterochromatin [162]. Overall, these observations suggest

that the dynamic PARylation of target proteins is involved in the crosstalk between PARP1 and DNA methylation.

Nevertheless, the origin of PARP1 activation on those promoter regions remains poorly understood. Based on *in vitro* data, it has been proposed that CTCF directly interacts with PARP1 and induces PARP1 automodification in a DNA-independent manner [9]. Nevertheless, no solid evidence available that this mechanism is responsible for the observed PAR synthesis in the cell. *In vitro* data show that the level of PARP1 activity was ~10-fold higher in the presence of both activated DNA and CTCF as compared to just DNA and CTCF alone [9]. In this regard, the combined action of both DNA breaks and CTCF seems preferable for the induction of PARP1 automodification during PARP1-mediated regulation of gene expression at certain promoter sites in the genome. Moreover, several studies indicate that even though CTCF plays certain roles in the regulation of gene expression, DNMT1 [159] and under certain circumstances p16 can still be expressed in the absence of CTCF but not that of PAR polymers [163]. In the context of genotoxic stress-induced enzymatic modifications of DNA, CTCF is actually recruited to the DNA damage site once there is PAR in the proximity of the lesion. CTCF has 11 zinc finger domains that can bind to DNA and among them zinc finger 4–6 motifs have been reported to recognize and bind PAR chains, which are structurally similar to ssDNA [164]. CTCF can also be PARylated by the PARP proteins. This PARylation seems to be cell-cycle-dependent; proliferating cells hardly contain any ADP-ribosylated CTCF, whereas the cells under cell cycle arrest contain a large amount of modified CTCF. This PARylation also correlates with upregulation of many genes responsible for cell cycle arrest, differentiation, and development [165]. It is noteworthy that Klenova and colleagues have provided evidence that CTCF dissociates from majority of sites on chromatin after PARylation [165]. This idea also supports the notion of CTCF binding to ADPr motifs instead of intact DNA [164].

Moreover, the physical and functional interplays among CTCF, DNMT1, and PARP1 also involve TET proteins. On the one hand, CTCF interacts with and recruits TET proteins to genomic DNA, thus promoting oxidation of 5mC [166]; on the other hand, TET-catalyzed

formation of 5hmC and especially 5caC strengthens CTCF's association with DNA [167,168]. TET expression is positively regulated by the PARylation activity of PARP1, which leads to DNA demethylation [169]. Additionally, covalently PARylated TET enzymes convert 5mC into its oxidized forms more efficiently, although as negative feedback, noncovalent binding of PAR to a TET protein represses its activity [66]. Accordingly, a noncovalent PAR-binding motif has been identified in the catalytic domain of TET1 [170]. It should be emphasized here that 5caC residues can serve as a potential source of SSB and subsequent PARP activation, when they are processed by TDG-dependent BER. Alternatively, TET1 can also activate PARP1 *in vitro* in the absence of nicked DNA [170], making their interactions even more complex. Accordingly, TET1-dependent activation of PARP1 would lead to covalent PARylation of TET1 and induction of its hydroxylase activity, which can be blocked at some point by non covalent interaction of TET1 with PAR. Nevertheless, inactive TET1-PAR complex still can bind DNA, block the access to DNMT1, and act as an anchor for the transcription factors via PAR interaction [170]. Moreover, it was shown that TET1 is recruited by PARP1-dependent PARylation at the PPAR response elements and promotes the local production of 5hmC during adipocyte differentiation [171].

Crosstalk of transcription, DNA breaks, PARylation, and epigenetic regulation

Regardless of exogenous or endogenous DNA-damaging agents, during DNA transcription and replication, different regions of genomic DNA show increased susceptibility to DNA breakage owing to multiple factors such as noncanonical DNA secondary structures (G-quadruplexes, hairpins, or R-loops) or a chromatin context (chromosomal fragile sites) (reviewed in [172,173]). Secondary structures of DNA increase the risk of DNA breaks: either targeted ones such as G4 structures recognized by AID during B-cell development or off-targeted G4s in active gene regions [129]. Another vivid example of transcription-associated DNA damage is the damage due to formation of R-loops: a naturally occurring reannealing of the nascent RNA

transcript with the template DNA strand, with the accompanying displacement of the opposite ssDNA strand. Unscheduled formation of R-loops is associated with DNA breaks, replication fork stalling, and transcription blockage [174]. Notably, aside from transcription pausing, R-loops are also observed in unmethylated CGI sequences in the proximal promoter regions during development, possibly regulating transcription activation and restricting DNA methylation by DNMT3B1 [175]. Formation of R-loops is favored by negative supercoiling behind RNA polymerase II and by a specific sequence context (reviewed in [176]). TOP1 counteracts both positive and negative DNA supercoiling during transcription by introducing SSBs accompanied with the formation of transient TOP1 cleavage complexes (TOP1ccs) at their 3' termini [177]; this event leads to a decrease in the formation of DNA:RNA hybrids [178]. TOP1ccs are readily "trapped" on chromatin and become irreversible covalent adducts, which, if not repaired, can lead to transcription and replication blockage and formation of SSBs and DSBs. It has been reported that cleavage of the ssDNA strand of R-loops by endonucleases, including XPF, XPG, and FEN1, results in TOP1cc-induced DSB production during transcription in nonreplicating cells [179].

Nevertheless, the DNA damage in promoter and enhancer regions upstream of transcription start sites can stimulate transcription instead of blocking it by switching on DNA damage response pathways including PAR signaling (Figure 3). Indeed, activation of estrogen-responsive gene transcription of pS2 is dependent on the β isoform of DNA topoisomerase II (TOP2 β)-induced DSBs in the promoter region [180]. This phenomenon has also been observed in androgen receptor, retinoic acid receptor, and activator protein 1-dependent types of gene transcription [180]. In general, TOP2 has a role of introducing transient DSBs to resolve the concatenated DNA and supercoiling for transcription regulation (TOP2 β) and topological stress during chromosomal segregation and DNA replication (TOP2 α) [181]. The repair of TOP1- and TOP2 β -dependent DSBs is mediated by both NHEJ and HR pathways and is often accompanied by PARP1 recruitment to the DNA damage site and induction of PAR synthesis (reviewed in [182,183]). This leads to modulation of gene expression at different levels

including changes in chromatin structure, DNA methylation, and transcription factor recruitment and regulation of their activity (reviewed in [17,184]). For example, the aforementioned ADP-ribose readers (chromatin remodelers such as ALC1 [84], APLF [79,80]; transcription factors NF- κ B [185] and TAF15 [186]; and DNA damage repair proteins, such as XRCC4, Ligase IV, and MRN [75]) are recruited to the DSB sites by noncovalent PAR binding, frequently becoming a substrate of subsequent PARP1-dependent PARylation as well. Recent research revealed that RNA polymerase II and PARP1-dependent NELF (negative elongation factor) complex recruitment is required for DSB-induced transcriptional repression [187], but concurrently, PARP1-catalyzed PARylation of NELF-E and NELF-A inhibits NELF and promotes transcription elongation [188]. Another example of topoisomerase-dependent and PARP1-dependent gene expression is believed to be *TP53* expression. *TP53* is split into two epigenetic domains depending on its chromatin organization and methylation [189]. Accordingly, the first domain—specifically the promoter region of *TP53*—is hypomethylated, despite being rich in epigenetic histone markers H3K9ac, H3K4me2, H3K4me3, and H4K16ac, which are involved in the regulation of active gene transcription [189]. Furthermore, TOP2, PARP1, HDAC, DNMT1, and CTCF have been found to be localized to this region and additionally with TOP1 and BRG1 (chromatin-remodeling ATPase) in the hypermethylated 2nd domain [189]. One possibility is that the hypomethylated status of the promoter region and epigenetic regulation are maintained by the inhibitory effect of PARP1-dependent ADP-ribosylation on DNMT1 as well as by recruitment of CTCF via its PBZ domain [77] after TOP2-coupled DNA damage [9,160].

Notably, DNA repair and/or processing of transcription and/or topoisomerase-induced DNA damage lead to the formation of terminally phosphorylated DNA breaks that can be targeted for PARP-dependent DNA ADP-ribosylation as discussed earlier. Thus, TOP1cc removal depends primarily on the TDP1-driven excision of the 3'-tyrosine adduct that generates a 3'-phosphorylated terminus [190]. It has been reported that TDP1 directly interacts with PARP1 and that they are epistatic for the repair of Top1ccs [191]. DSB processing during alternative

NHEJ or HR pathways goes through formation of 5' protruding ends also shown to be effective substrates for PARP1-catalyzed PARylation [13,14]. Moreover, PARP1 is activated by DNA secondary structures like DNA hairpins, G4, and stably unpaired regions [192], whose presence at promoter and enhancer sites in the proximity of a DSB will create alternative PARP1 activation or binding sites for the modification of DNA termini. Notably, PARP3-dependent suppression of G4 in response to DNA damage was recently reported [193]. PARP3 deficiency leads to an increase in the content of G4 in G4-rich regions at the sites flanking DSBs, but the molecular mechanism of PARP3 activity at G4 sites remains unknown [193]. It is possible that ADP-ribosylation of DSB termini in these cases will temporarily block their processing or degradation and modulate DNA break signaling, coordinating the choice of a repair mechanism and transcription.

Concluding Remarks

Besides the well-known biological roles of PARPs such as DNA repair, chromatin modification, and gene expression regulation, these enzymes might also be involved in the programmed DNA strand break-dependent regulation of transcription and replication. The majority of genes regulated by PARPs belong to stress-responsive and differentiation-related genes. This observation suggests that DNA strand breaks may be required also for the regulation of expression of some genes among others listed earlier. The recruitment of effectors—whether via nonspecific surface charge binding or through specific interaction with PAR or MAR adducts covalently linked to protein or DNA—may initiate a signaling cascade of epigenetic changes in chromatin, which result in modulation of the patterns of gene expression (Figure 4).

It is tempting to speculate that the PARP-dependent regulation of gene expression involves transient DNA strand breaks at specific promoter sites, which induce ADP-ribosylation of not only of PARPs themselves and other nuclear proteins, but also DNA strand breaks termini, therefore leading to the recruitment of specific DNA repair and transcription factors to the

methylation-free gene promoters. However, this hypothesis awaits confirmation from further technically advanced studies. In the meantime, PARylated DNA along with auto-PARylated PARP1 in proximity may block the access of DNMT1 to DNA and maintain the hypomethylated status, which is prerequisite to gene expression. This idea may also be valid to the regulation of expression of *p16* and *RASSF1A*, which are dependent on the presence of PAR [163]. One of the common features of *DNMT1*, *p16*, and *RASSF1A* is that they are all CTCF target genes [66,163]; in addition, both *p16* and *RASSF1A* take part in cell cycle regulation and arrest during DNA damage response [194-196]. Alternatively, covalent ADP-ribosylation of DNA strand break termini may retard the repair, and this in part may explain the phenomenon of the long-lived DSBs produced by TOP2 in complex with PARP1 at the promoters of genes, which are regulated by the signal-dependent mechanism, such as PSA, RARb, DIO1 and MMP12, and ER α (estrogen receptor- α) target genes [180]. Notably, androgen-induced TOP2 β -mediated DSBs could be detected even 6 h after hormone stimulation [197].

In addition, new roles of PARPs and PARylation in the RNA biology are emerging. Very recently, using RNA immunoprecipitation it was shown that PARP1 binds thousands of mRNAs and long noncoding RNAs as well as hundreds of small nuclear RNAs and small nucleolar RNAs (snoRNAs). PARP1 binding to snoRNAs leads to its activation and autoPARylation, recruitment, and PARylation of DDX21, an RNA helicase, which, in turn, promotes ribosomal DNA transcription when ADP-ribosylated [198]. Noteworthy, activation of PARPs when bound to RNA or DNA substrates creates a possibility that terminal phosphate residue in proximity to their CAT domain can be ADP-ribosylated. Whether noncanonical RNAs are naturally occurring ADPr acceptors in a living cell remains to be examined in future studies.

At present, it is not clear how specificity of PAR and MAR readers is affected by the nature of ADP-ribosylated target protein residue. Similarly, the specific binding factors of DNA–MAR or DNA–PAR adducts are not yet known, but it is tempting to speculate that they should recognize both the DNA/RNA and ADPr-phosphate moiety. One of the possible readers of ADP-ribosylated DNA strand breaks termini could be aprataxin, which recognizes an ADP residue

on 5' termini of a DNA break formed during an abortive DNA ligation reaction and catalyzes the release of the AMP group [199]. Aprataxin interacts with PARP1, which promotes the recruitment of aprataxin to the sites of DNA breaks [200,201]. The PAR-binding affinity of the FHA domain of aprataxin may also contribute to its recruitment to the site of nicked DNA. Hence, due to structural similarities, the MAR unit at a DNA strand break end [14,112] may also be a good substrate for aprataxin activity along with recruitment of XRCC1 or XRCC4, depending on the nature of the DNA strand break, to finalize the repair of DNA damage via BER or NHEJ, respectively [199].

In conclusion, recent biochemical, structural, and cellular studies have expanded our understanding of the diverse roles of ADP-ribosylation. However, new technologies and tools are required for future studies to reliably distinguish ADP-ribosylated proteins and ADP-ribosylated DNA or RNA products in a live cell, to identify target- and site-specific ADPr readers, and to reveal the functional relevance of site-specific ADP-ribosylation on individual targets [14,41,202].

Acknowledgments

This work is supported by funding from French National Research Agency (ANR-18-CE44-0008); Electricité de France ; Fondation ARC (PJA-20181208015). E.M. was supported by doctoral fellowship from ABELA FRERES.

References

- [1] Boyer R. (2006). Posttranslational modification of proteins: Expanding nature's inventory. Christopher T. Walsh, Roberts & Company Publishers, Greenwood Village, CO, 2005, 576 pp., ISBN 0-9747077-3-2, \$98.00. *Biochemistry and Molecular Biology Education*. 34, 461-462. <https://doi.org/10.1002/bmb.2006.494034069996>.
- [2] Klungland A., Robertson A. B. (2017). Oxidized C5-methyl cytosine bases in DNA: 5-Hydroxymethylcytosine; 5-formylcytosine; and 5-carboxycytosine. *Free Radic Biol Med*. 107, 62-68. <https://doi.org/10.1016/j.freeradbiomed.2016.11.038>.
- [3] Dabin J., Fortuny A., Polo S. E. (2016). Epigenome Maintenance in Response to DNA Damage. *Mol Cell*. 62, 712-727. <https://doi.org/10.1016/j.molcel.2016.04.006>.
- [4] Vyas S., Matic I., Uchima L., Rood J., Zaja R., Hay R. T., Ahel I., Chang P. (2014). Family-wide analysis of poly(ADP-ribose) polymerase activity. *Nat Commun*. 5, 4426. <https://doi.org/10.1038/ncomms5426>.

- [5] Hottiger M. O. (2015). Nuclear ADP-Ribosylation and Its Role in Chromatin Plasticity, Cell Differentiation, and Epigenetics. *Annu Rev Biochem.* 84, 227-263. <https://doi.org/10.1146/annurev-biochem-060614-034506>.
- [6] Qi H., Price B. D., Day T. A. (2019). Multiple Roles for Mono- and Poly(ADP-Ribose) in Regulating Stress Responses. *Trends Genet.* 35, 159-172. <https://doi.org/10.1016/j.tig.2018.12.002>.
- [7] Bonicalzi M. E., Haince J. F., Droit A., Poirier G. G. (2005). Regulation of poly(ADP-ribose) metabolism by poly(ADP-ribose) glycohydrolase: where and when? *Cell Mol Life Sci.* 62, 739-750. <https://doi.org/10.1007/s00018-004-4505-1>.
- [8] Yu W., Ginja V., Pant V., Chernukhin I., Whitehead J., Docquier F., Farrar D., Tavoosidana G., Mukhopadhyay R., Kanduri C., Oshimura M., Feinberg A. P., Lobanenko V., Klenova E., Ohlsson R. (2004). Poly(ADP-ribosyl)ation regulates CTCF-dependent chromatin insulation. *Nat Genet.* 36, 1105-1110. <https://doi.org/10.1038/ng1426>.
- [9] Guastafierro T., Cecchinelli B., Zampieri M., Reale A., Riggio G., Sthandier O., Zupi G., Calabrese L., Caiafa P. (2008). CCTC-binding factor activates PARP-1 affecting DNA methylation machinery. *J Biol Chem.* 283, 21873-21880. <https://doi.org/10.1074/jbc.M801170200>.
- [10] Guetg C., Scheifele F., Rosenthal F., Hottiger M. O., Santoro R. (2012). Inheritance of silent rDNA chromatin is mediated by PARP1 via noncoding RNA. *Mol Cell.* 45, 790-800. <https://doi.org/10.1016/j.molcel.2012.01.024>.
- [11] Nakano T., Takahashi-Nakaguchi A., Yamamoto M., Watanabe M. (2015). Pierisins and CARP-1: ADP-ribosylation of DNA by ARTCs in butterflies and shellfish. *Curr Top Microbiol Immunol.* 384, 127-149. https://doi.org/10.1007/82_2014_416.
- [12] Jankevicius G., Ariza A., Ahel M., Ahel I. (2016). The Toxin-Antitoxin System DarTG Catalyzes Reversible ADP-Ribosylation of DNA. *Mol Cell.* 64, 1109-1116. <https://doi.org/10.1016/j.molcel.2016.11.014>.
- [13] Talhaoui I., Lebedeva N. A., Zarkovic G., Saint-Pierre C., Kutuzov M. M., Sukhanova M. V., Matkarimov B. T., Gasparutto D., Saparbaev M. K., Lavrik O. I., Ishchenko A. A. (2016). Poly(ADP-ribose) polymerases covalently modify strand break termini in DNA fragments in vitro. *Nucleic Acids Res.* 44, 9279-9295. <https://doi.org/10.1093/nar/gkw675>.
- [14] Zarkovic G., Belousova E. A., Talhaoui I., Saint-Pierre C., Kutuzov M. M., Matkarimov B. T., Biard D., Gasparutto D., Lavrik O. I., Ishchenko A. A. (2018). Characterization of DNA ADP-ribosyltransferase activities of PARP2 and PARP3: new insights into DNA ADP-ribosylation. *Nucleic Acids Res.* 46, 2417-2431. <https://doi.org/10.1093/nar/gkx1318>.
- [15] Munnur D., Bartlett E., Mikolcevic P., Kirby I. T., Matthias Rack J. G., Mikoc A., Cohen M. S., Ahel I. (2019). Reversible ADP-ribosylation of RNA. *Nucleic Acids Res.* 47, 5658-5669. <https://doi.org/10.1093/nar/gkz305>.
- [16] Schreiber V., Dantzer F., Ame J. C., de Murcia G. (2006). Poly(ADP-ribose): novel functions for an old molecule. *Nat Rev Mol Cell Biol.* 7, 517-528. <https://doi.org/10.1038/nrm1963>.
- [17] Posavec Marjanovic M., Crawford K., Ahel I. (2017). PARP, transcription and chromatin modeling. *Semin Cell Dev Biol.* 63, 102-113. <https://doi.org/10.1016/j.semcdb.2016.09.014>.
- [18] Rodríguez-Vargas J. M., Oliver-Pozo F. J., Dantzer F. (2019). PARP1 and Poly(ADP-ribosyl)ation Signaling during Autophagy in Response to Nutrient Deprivation. *Oxidative Medicine and Cellular Longevity.* 2019, 1-15. <https://doi.org/10.1155/2019/2641712>.
- [19] Hottiger M. O., Hassa P. O., Luscher B., Schuler H., Koch-Nolte F. (2010). Toward a unified nomenclature for mammalian ADP-ribosyltransferases. *Trends Biochem Sci.* 35, 208-219. <https://doi.org/10.1016/j.tibs.2009.12.003>.
- [20] Ame J. C., Spenlehauer C., de Murcia G. (2004). The PARP superfamily. *Bioessays.* 26, 882-893. <https://doi.org/10.1002/bies.20085>.
- [21] Aravind L., Zhang D., de Souza R. F., Anand S., Iyer L. M. (2015). The natural history of ADP-ribosyltransferases and the ADP-ribosylation system. *Curr Top Microbiol Immunol.* 384, 3-32. https://doi.org/10.1007/82_2014_414.
- [22] Burkle A. (2005). Poly(ADP-ribose). The most elaborate metabolite of NAD⁺. *FEBS J.* 272, 4576-4589. <https://doi.org/10.1111/j.1742-4658.2005.04864.x>.

- [23] Munnur D., Ahel I. (2017). Reversible mono-ADP-ribosylation of DNA breaks. *FEBS J.* 284, 4002-4016. <https://doi.org/10.1111/febs.14297>.
- [24] Palazzo L., Mikoc A., Ahel I. (2017). ADP-ribosylation: new facets of an ancient modification. *FEBS J.* 284, 2932-2946. <https://doi.org/10.1111/febs.14078>.
- [25] Shieh W. M., Ame J. C., Wilson M. V., Wang Z. Q., Koh D. W., Jacobson M. K., Jacobson E. L. (1998). Poly(ADP-ribose) polymerase null mouse cells synthesize ADP-ribose polymers. *J. Biol. Chem.* 273, 30069-30072.
- [26] Poirier G. G., de Murcia G., Jongstra-Bilen J., Niedergang C., Mandel P. (1982). Poly(ADP-ribosyl)ation of polynucleosomes causes relaxation of chromatin structure. *Proc Natl Acad Sci U S A.* 79, 3423-3427. <https://doi.org/10.1073/pnas.79.11.3423>.
- [27] Krishnakumar R., Kraus W. L. (2010). The PARP side of the nucleus: molecular actions, physiological outcomes, and clinical targets. *Mol Cell.* 39, 8-24. <https://doi.org/10.1016/j.molcel.2010.06.017>.
- [28] Krishnakumar R., Kraus W. L. (2010). PARP-1 regulates chromatin structure and transcription through a KDM5B-dependent pathway. *Mol Cell.* 39, 736-749. <https://doi.org/10.1016/j.molcel.2010.08.014>.
- [29] Kraus W. L. (2015). PARPs and ADP-Ribosylation: 50 Years ... and Counting. *Mol Cell.* 58, 902-910. <https://doi.org/10.1016/j.molcel.2015.06.006>.
- [30] Hanzlikova H., Kalasova I., Demin A. A., Pennicott L. E., Cihlarova Z., Caldecott K. W. (2018). The Importance of Poly(ADP-Ribose) Polymerase as a Sensor of Unligated Okazaki Fragments during DNA Replication. *Mol Cell.* 71, 319-331 e313. <https://doi.org/10.1016/j.molcel.2018.06.004>.
- [31] Ame J. C., Rolli V., Schreiber V., Niedergang C., Apiou F., Decker P., Muller S., Hoger T., Menissier-de Murcia J., de Murcia G. (1999). PARP-2, A novel mammalian DNA damage-dependent poly(ADP-ribose) polymerase. *J Biol Chem.* 274, 17860-17868.
- [32] Menissier de Murcia J., Ricoul M., Tartier L., Niedergang C., Huber A., Dantzer F., Schreiber V., Ame J. C., Dierich A., LeMeur M., Sabatier L., Chambon P., de Murcia G. (2003). Functional interaction between PARP-1 and PARP-2 in chromosome stability and embryonic development in mouse. *EMBO J.* 22, 2255-2263. <https://doi.org/10.1093/emboj/cdg206>.
- [33] Fouquin A., Guirouilh-Barbat J., Lopez B., Hall J., Amor-Gueret M., Pennaneach V. (2017). PARP2 controls double-strand break repair pathway choice by limiting 53BP1 accumulation at DNA damage sites and promoting end-resection. *Nucleic Acids Res.* 45, 12325-12339. <https://doi.org/10.1093/nar/gkx881>.
- [34] Bai P. (2015). Biology of Poly(ADP-Ribose) Polymerases: The Factotums of Cell Maintenance. *Mol Cell.* 58, 947-958. <https://doi.org/10.1016/j.molcel.2015.01.034>.
- [35] Obaji E., Haikarainen T., Lehtio L. (2016). Characterization of the DNA dependent activation of human ARTD2/PARP2. *Sci Rep.* 6, 34487. <https://doi.org/10.1038/srep34487>.
- [36] Langelier M. F., Riccio A. A., Pascal J. M. (2014). PARP-2 and PARP-3 are selectively activated by 5' phosphorylated DNA breaks through an allosteric regulatory mechanism shared with PARP-1. *Nucleic Acids Res.* 42, 7762-7775. <https://doi.org/10.1093/nar/gku474>.
- [37] Riccio A. A., Cingolani G., Pascal J. M. (2016). PARP-2 domain requirements for DNA damage-dependent activation and localization to sites of DNA damage. *Nucleic Acids Res.* 44, 1691-1702. <https://doi.org/10.1093/nar/gkv1376>.
- [38] Gibson B. A., Kraus W. L. (2012). New insights into the molecular and cellular functions of poly(ADP-ribose) and PARPs. *Nat Rev Mol Cell Biol.* 13, 411-424. <https://doi.org/10.1038/nrm3376>.
- [39] Beck C., Robert I., Reina-San-Martin B., Schreiber V., Dantzer F. (2014). Poly(ADP-ribose) polymerases in double-strand break repair: focus on PARP1, PARP2 and PARP3. *Exp Cell Res.* 329, 18-25. <https://doi.org/10.1016/j.yexcr.2014.07.003>.
- [40] Rouleau M., McDonald D., Gagne P., Ouellet M. E., Droit A., Hunter J. M., Dutertre S., Prigent C., Hendzel M. J., Poirier G. G. (2007). PARP-3 associates with polycomb group bodies and with components of the DNA damage repair machinery. *J Cell Biochem.* 100, 385-401. <https://doi.org/10.1002/jcb.21051>.

- [41] Gupte R., Liu Z., Kraus W. L. (2017). PARPs and ADP-ribosylation: recent advances linking molecular functions to biological outcomes. *Genes Dev.* 31, 101-126. <https://doi.org/10.1101/gad.291518.116>.
- [42] Palazzo L., Ahel I. (2018). PARPs in genome stability and signal transduction: implications for cancer therapy. *Biochem Soc Trans.* 46, 1681-1695. <https://doi.org/10.1042/BST20180418>.
- [43] Martin-Hernandez K., Rodriguez-Vargas J. M., Schreiber V., Dantzer F. (2017). Expanding functions of ADP-ribosylation in the maintenance of genome integrity. *Semin Cell Dev Biol.* 63, 92-101. <https://doi.org/10.1016/j.semcdb.2016.09.009>.
- [44] David K. K., Andrabi S. A., Dawson T. M., Dawson V. L. (2009). Parthanatos, a messenger of death. *Front Biosci (Landmark Ed).* 14, 1116-1128.
- [45] Koh D. W., Lawler A. M., Poitras M. F., Sasaki M., Wattler S., Nehls M. C., Stoger T., Poirier G. G., Dawson V. L., Dawson T. M. (2004). Failure to degrade poly(ADP-ribose) causes increased sensitivity to cytotoxicity and early embryonic lethality. *Proc Natl Acad Sci U S A.* 101, 17699-17704. <https://doi.org/10.1073/pnas.0406182101>.
- [46] Tang J. B., Svilar D., Trivedi R. N., Wang X. H., Goellner E. M., Moore B., Hamilton R. L., Banze L. A., Brown A. R., Sobol R. W. (2011). N-methylpurine DNA glycosylase and DNA polymerase beta modulate BER inhibitor potentiation of glioma cells to temozolomide. *Neuro Oncol.* 13, 471-486. <https://doi.org/10.1093/neuonc/nor011>.
- [47] Hatakeyama K., Nemoto Y., Ueda K., Hayaishi O. (1986). Purification and characterization of poly(ADP-ribose) glycohydrolase. Different modes of action on large and small poly(ADP-ribose). *J Biol Chem.* 261, 14902-14911.
- [48] O'Sullivan J., Tedim Ferreira M., Gagne J. P., Sharma A. K., Hendzel M. J., Masson J. Y., Poirier G. G. (2019). Emerging roles of eraser enzymes in the dynamic control of protein ADP-ribosylation. *Nat Commun.* 10, 1182. <https://doi.org/10.1038/s41467-019-08859-x>.
- [49] Ogata N., Ueda K., Kagamiyama H., Hayaishi O. (1980). ADP-ribosylation of histone H1. Identification of glutamic acid residues 2, 14, and the COOH-terminal lysine residue as modification sites. *J Biol Chem.* 255, 7616-7620.
- [50] Haenni S. S., Hassa P. O., Altmeyer M., Fey M., Imhof R., Hottiger M. O. (2008). Identification of lysines 36 and 37 of PARP-2 as targets for acetylation and auto-ADP-ribosylation. *Int J Biochem Cell Biol.* 40, 2274-2283. <https://doi.org/10.1016/j.biocel.2008.03.008>.
- [51] Grundy G. J., Polo L. M., Zeng Z., Rulten S. L., Hoch N. C., Paomephan P., Xu Y., Sweet S. M., Thorne A. W., Oliver A. W., Matthews S. J., Pearl L. H., Caldecott K. W. (2016). PARP3 is a sensor of nicked nucleosomes and monoribosylates histone H2B(Glu2). *Nat Commun.* 7, 12404. <https://doi.org/10.1038/ncomms12404>.
- [52] Messner S., Altmeyer M., Zhao H., Pozivil A., Roschitzki B., Gehrig P., Rutishauser D., Huang D., Caflisch A., Hottiger M. O. (2010). PARP1 ADP-ribosylates lysine residues of the core histone tails. *Nucleic Acids Res.* 38, 6350-6362. <https://doi.org/10.1093/nar/gkq463>.
- [53] Altmeyer M., Messner S., Hassa P. O., Fey M., Hottiger M. O. (2009). Molecular mechanism of poly(ADP-ribosylation) by PARP1 and identification of lysine residues as ADP-ribose acceptor sites. *Nucleic Acids Res.* 37, 3723-3738. <https://doi.org/10.1093/nar/gkp229>.
- [54] Zhang Y., Wang J., Ding M., Yu Y. (2013). Site-specific characterization of the Asp- and Glu-ADP-ribosylated proteome. *Nat Methods.* 10, 981-984. <https://doi.org/10.1038/nmeth.2603>.
- [55] Martello R., Leutert M., Jungmichel S., Bilan V., Larsen S. C., Young C., Hottiger M. O., Nielsen M. L. (2016). Proteome-wide identification of the endogenous ADP-ribosylome of mammalian cells and tissue. *Nat Commun.* 7, 12917. <https://doi.org/10.1038/ncomms12917>.
- [56] Bonfiglio J. J., Fontana P., Zhang Q., Colby T., Gibbs-Seymour I., Atanassov I., Bartlett E., Zaja R., Ahel I., Matic I. (2017). Serine ADP-Ribosylation Depends on HPF1. *Mol Cell.* 65, 932-940 e936. <https://doi.org/10.1016/j.molcel.2017.01.003>.
- [57] Palazzo L., Leidecker O., Prokhorova E., Dauben H., Matic I., Ahel I. (2018). Serine is the major residue for ADP-ribosylation upon DNA damage. *Elife.* 7, e34334. <https://doi.org/10.7554/eLife.34334>.

- [58] Kalesh K., Lukauskas S., Borg A. J., Snijders A. P., Ayyappan V., Leung A. K. L., Haskard D. O., DiMaggio P. A. (2019). An Integrated Chemical Proteomics Approach for Quantitative Profiling of Intracellular ADP-Ribosylation. *Sci Rep.* 9, 6655. <https://doi.org/10.1038/s41598-019-43154-1>.
- [59] Hendriks I. A., Larsen S. C., Nielsen M. L. (2019). An Advanced Strategy for Comprehensive Profiling of ADP-ribosylation Sites Using Mass Spectrometry-based Proteomics. *Mol Cell Proteomics.* 18, 1010-1026. <https://doi.org/10.1074/mcp.TIR119.001315>.
- [60] Bartlett E., Bonfiglio J. J., Prokhorova E., Colby T., Zobel F., Ahel I., Matic I. (2018). Interplay of Histone Marks with Serine ADP-Ribosylation. *Cell Rep.* 24, 3488-3502.e3485. <https://doi.org/10.1016/j.celrep.2018.08.092>.
- [61] Abplanalp J., Leutert M., Frugier E., Nowak K., Feurer R., Kato J., Kistemaker H. V. A., Filippov D. V., Moss J., Cafilisch A., Hottiger M. O. (2017). Proteomic analyses identify ARH3 as a serine mono-ADP-ribosylhydrolase. *Nat Commun.* 8, 2055. <https://doi.org/10.1038/s41467-017-02253-1>.
- [62] Fontana P., Bonfiglio J. J., Palazzo L., Bartlett E., Matic I., Ahel I. (2017). Serine ADP-ribosylation reversal by the hydrolase ARH3. *Elife.* 6, e28533. <https://doi.org/10.7554/eLife.28533>.
- [63] Mashimo M., Kato J., Moss J. (2013). ADP-ribosyl-acceptor hydrolase 3 regulates poly (ADP-ribose) degradation and cell death during oxidative stress. *Proc Natl Acad Sci U S A.* 110, 18964-18969. <https://doi.org/10.1073/pnas.1312783110>.
- [64] Leslie Pedrioli D. M., Leutert M., Bilan V., Nowak K., Gunasekera K., Ferrari E., Imhof R., Malmstrom L., Hottiger M. O. (2018). Comprehensive ADP-ribosylome analysis identifies tyrosine as an ADP-ribose acceptor site. *EMBO Rep.* 19, e45310. <https://doi.org/10.15252/embr.201745310>.
- [65] Ord M. G., Stocken L. A. (1977). Adenosine diphosphate ribosylated histones. *Biochem J.* 161, 583-592.
- [66] Ciccarone F., Zampieri M., Caiafa P. (2017). PARP1 orchestrates epigenetic events setting up chromatin domains. *Semin Cell Dev Biol.* 63, 123-134. <https://doi.org/10.1016/j.semcdb.2016.11.010>.
- [67] Fischbach A., Kruger A., Hampp S., Assmann G., Rank L., Hufnagel M., Stockl M. T., Fischer J. M. F., Veith S., Rossatti P., Ganz M., Ferrando-May E., Hartwig A., Hauser K., Wiesmuller L., Burkle A., Mangerich A. (2018). The C-terminal domain of p53 orchestrates the interplay between non-covalent and covalent poly(ADP-ribosylation) of p53 by PARP1. *Nucleic Acids Res.* 46, 804-822. <https://doi.org/10.1093/nar/gkx1205>.
- [68] Verheugd P., Forst A. H., Milke L., Herzog N., Feijs K. L., Kremmer E., Kleine H., Luscher B. (2013). Regulation of NF-kappaB signalling by the mono-ADP-ribosyltransferase ARTD10. *Nat Commun.* 4, 1683. <https://doi.org/10.1038/ncomms2672>.
- [69] Pleschke J. M., Kleczkowska H. E., Strohm M., Althaus F. R. (2000). Poly(ADP-ribose) binds to specific domains in DNA damage checkpoint proteins. *J Biol Chem.* 275, 40974-40980. <https://doi.org/10.1074/jbc.M006520200>.
- [70] Gagne J. P., Isabelle M., Lo K. S., Bourassa S., Hendzel M. J., Dawson V. L., Dawson T. M., Poirier G. G. (2008). Proteome-wide identification of poly(ADP-ribose) binding proteins and poly(ADP-ribose)-associated protein complexes. *Nucleic Acids Res.* 36, 6959-6976. <https://doi.org/10.1093/nar/gkn771>.
- [71] Oberoi J., Richards M. W., Crumpler S., Brown N., Blagg J., Bayliss R. (2010). Structural basis of poly(ADP-ribose) recognition by the multizinc binding domain of checkpoint with forkhead-associated and RING Domains (CHFR). *J Biol Chem.* 285, 39348-39358. <https://doi.org/10.1074/jbc.M110.159855>.
- [72] Ahel I., Ahel D., Matsusaka T., Clark A. J., Pines J., Boulton S. J., West S. C. (2008). Poly(ADP-ribose)-binding zinc finger motifs in DNA repair/checkpoint proteins. *Nature.* 451, 81-85. <https://doi.org/10.1038/nature06420>.
- [73] Li G. Y., McCulloch R. D., Fenton A. L., Cheung M., Meng L., Ikura M., Koch C. A. (2010). Structure and identification of ADP-ribose recognition motifs of APLF and role in the DNA damage response. *Proc Natl Acad Sci U S A.* 107, 9129-9134. <https://doi.org/10.1073/pnas.1000556107>.

- [74] Wang Z., Michaud G. A., Cheng Z., Zhang Y., Hinds T. R., Fan E., Cong F., Xu W. (2012). Recognition of the iso-ADP-ribose moiety in poly(ADP-ribose) by WWE domains suggests a general mechanism for poly(ADP-ribosyl)ation-dependent ubiquitination. *Genes Dev.* 26, 235-240. <https://doi.org/10.1101/gad.182618.111>.
- [75] Li M., Lu L. Y., Yang C. Y., Wang S., Yu X. (2013). The FHA and BRCT domains recognize ADP-ribosylation during DNA damage response. *Genes Dev.* 27, 1752-1768. <https://doi.org/10.1101/gad.226357.113>.
- [76] Karras G. I., Kustatscher G., Buhecha H. R., Allen M. D., Pugieux C., Sait F., Bycroft M., Ladurner A. G. (2005). The macro domain is an ADP-ribose binding module. *EMBO J.* 24, 1911-1920. <https://doi.org/10.1038/sj.emboj.7600664>.
- [77] Teloni F., Altmeyer M. (2016). Readers of poly(ADP-ribose): designed to be fit for purpose. *Nucleic Acids Res.* 44, 993-1006. <https://doi.org/10.1093/nar/gkv1383>.
- [78] Vivelto C. A., Wat R., Agrawal C., Tee H. Y., Leung A. K. (2017). ADPRiboDB: The database of ADP-ribosylated proteins. *Nucleic Acids Res.* 45, D204-D209. <https://doi.org/10.1093/nar/gkw706>.
- [79] Rulten S. L., Fisher A. E., Robert I., Zuma M. C., Rouleau M., Ju L., Poirier G., Reina-San-Martin B., Caldecott K. W. (2011). PARP-3 and APLF function together to accelerate nonhomologous end-joining. *Mol Cell.* 41, 33-45. <https://doi.org/10.1016/j.molcel.2010.12.006>.
- [80] Chen Q., Kassab M. A., Dantzer F., Yu X. (2018). PARP2 mediates branched poly ADP-ribosylation in response to DNA damage. *Nat Commun.* 9, 3233. <https://doi.org/10.1038/s41467-018-05588-5>.
- [81] Posavec Marjanovic M., Hurtado-Bages S., Lassi M., Valero V., Malinverni R., Delage H., Navarro M., Corujo D., Guberovic I., Douet J., Gama-Perez P., Garcia-Roves P. M., Ahel I., Ladurner A. G., Yanes O., Bouvet P., Suelves M., Teperino R., Pospisilik J. A., Buschbeck M. (2017). MacroH2A1.1 regulates mitochondrial respiration by limiting nuclear NAD(+) consumption. *Nat Struct Mol Biol.* 24, 902-910. <https://doi.org/10.1038/nsmb.3481>.
- [82] Hurtado-Bages S., Guberovic I., Buschbeck M. (2018). The MacroH2A1.1 - PARP1 Axis at the Intersection Between Stress Response and Metabolism. *Front Genet.* 9, 417. <https://doi.org/10.3389/fgene.2018.00417>.
- [83] Xu C., Xu Y., Gursoy-Yuzugullu O., Price B. D. (2012). The histone variant macroH2A1.1 is recruited to DSBs through a mechanism involving PARP1. *FEBS Lett.* 586, 3920-3925. <https://doi.org/10.1016/j.febslet.2012.09.030>.
- [84] Singh H. R., Nardoza A. P., Moller I. R., Knobloch G., Kistemaker H. A. V., Hassler M., Harrer N., Blessing C., Eustermann S., Kotthoff C., Huet S., Mueller-Planitz F., Philippov D. V., Timinszky G., Rand K. D., Ladurner A. G. (2017). A Poly-ADP-Ribose Trigger Releases the Auto-Inhibition of a Chromatin Remodeling Oncogene. *Mol Cell.* 68, 860-871.e867. <https://doi.org/10.1016/j.molcel.2017.11.019>.
- [85] Feijs K. L., Forst A. H., Verheugd P., Luscher B. (2013). Macrodomein-containing proteins: regulating new intracellular functions of mono(ADP-ribosyl)ation. *Nat Rev Mol Cell Biol.* 14, 443-451. <https://doi.org/10.1038/nrm3601>.
- [86] Forst A. H., Karlberg T., Herzog N., Thorsell A. G., Gross A., Feijs K. L., Verheugd P., Kursula P., Nijmeijer B., Kremmer E., Kleine H., Ladurner A. G., Schuler H., Luscher B. (2013). Recognition of mono-ADP-ribosylated ARTD10 substrates by ARTD8 macrodomains. *Structure.* 21, 462-475. <https://doi.org/10.1016/j.str.2012.12.019>.
- [87] Rosenthal F., Feijs K. L., Frugier E., Bonalli M., Forst A. H., Imhof R., Winkler H. C., Fischer D., Caflisch A., Hassa P. O., Luscher B., Hottiger M. O. (2013). Macrodomein-containing proteins are new mono-ADP-ribosylhydrolases. *Nat Struct Mol Biol.* 20, 502-507. <https://doi.org/10.1038/nsmb.2521>.
- [88] DaRosa P. A., Wang Z., Jiang X., Pruneda J. N., Cong F., Klevit R. E., Xu W. (2015). Allosteric activation of the RNF146 ubiquitin ligase by a poly(ADP-ribosyl)ation signal. *Nature.* 517, 223-226. <https://doi.org/10.1038/nature13826>.
- [89] Aravind L. (2001). The WWE domain: a common interaction module in protein ubiquitination and ADP ribosylation. *Trends Biochem Sci.* 26, 273-275.
- [90] Durocher D., Jackson S. P. (2002). The FHA domain. *FEBS Lett.* 513, 58-66. [https://doi.org/10.1016/s0014-5793\(01\)03294-x](https://doi.org/10.1016/s0014-5793(01)03294-x).

- [91] Yu X., Chini C. C., He M., Mer G., Chen J. (2003). The BRCT domain is a phospho-protein binding domain. *Science*. 302, 639-642. <https://doi.org/10.1126/science.1088753>.
- [92] Li M., Yu X. (2013). Function of BRCA1 in the DNA damage response is mediated by ADP-ribosylation. *Cancer Cell*. 23, 693-704. <https://doi.org/10.1016/j.ccr.2013.03.025>.
- [93] Breslin C., Hornyak P., Ridley A., Rulten S. L., Hanzlikova H., Oliver A. W., Caldecott K. W. (2015). The XRCC1 phosphate-binding pocket binds poly (ADP-ribose) and is required for XRCC1 function. *Nucleic Acids Res*. 43, 6934-6944. <https://doi.org/10.1093/nar/gkv623>.
- [94] Polo L. M., Xu Y., Hornyak P., Garces F., Zeng Z., Hailstone R., Matthews S. J., Caldecott K. W., Oliver A. W., Pearl L. H. (2019). Efficient Single-Strand Break Repair Requires Binding to Both Poly(ADP-Ribose) and DNA by the Central BRCT Domain of XRCC1. *Cell Rep*. 26, 573-581.e575. <https://doi.org/10.1016/j.celrep.2018.12.082>.
- [95] Krietsch J., Caron M. C., Gagne J. P., Ethier C., Vignard J., Vincent M., Rouleau M., Hendzel M. J., Poirier G. G., Masson J. Y. (2012). PARP activation regulates the RNA-binding protein NONO in the DNA damage response to DNA double-strand breaks. *Nucleic Acids Res*. 40, 10287-10301. <https://doi.org/10.1093/nar/gks798>.
- [96] Malanga M., Czuby A., Girstun A., Staron K., Althaus F. R. (2008). Poly(ADP-ribose) binds to the splicing factor ASF/SF2 and regulates its phosphorylation by DNA topoisomerase I. *J Biol Chem*. 283, 19991-19998. <https://doi.org/10.1074/jbc.M709495200>.
- [97] Bock F. J., Todorova T. T., Chang P. (2015). RNA Regulation by Poly(ADP-Ribose) Polymerases. *Mol Cell*. 58, 959-969. <https://doi.org/10.1016/j.molcel.2015.01.037>.
- [98] Ke Y., Zhang J., Lv X., Zeng X., Ba X. (2019). Novel insights into PARPs in gene expression: regulation of RNA metabolism. *Cell Mol Life Sci*. 76, 3283-3299. <https://doi.org/10.1007/s00018-019-03120-6>.
- [99] Murawska M., Hassler M., Renkawitz-Pohl R., Ladurner A., Brehm A. (2011). Stress-induced PARP activation mediates recruitment of Drosophila Mi-2 to promote heat shock gene expression. *PLoS Genet*. 7, e1002206. <https://doi.org/10.1371/journal.pgen.1002206>.
- [100] Zhang F., Chen Y., Li M., Yu X. (2014). The oligonucleotide/oligosaccharide-binding fold motif is a poly(ADP-ribose)-binding domain that mediates DNA damage response. *Proc Natl Acad Sci U S A*. 111, 7278-7283. <https://doi.org/10.1073/pnas.1318367111>.
- [101] Senissar M., Manav M. C., Brodersen D. E. (2017). Structural conservation of the PIN domain active site across all domains of life. *Protein Sci*. 26, 1474-1492. <https://doi.org/10.1002/pro.3193>.
- [102] Zhang F., Shi J., Chen S. H., Bian C., Yu X. (2015). The PIN domain of EXO1 recognizes poly(ADP-ribose) in DNA damage response. *Nucleic Acids Res*. 43, 10782-10794. <https://doi.org/10.1093/nar/gkv939>.
- [103] Chen J. K., Lin W. L., Chen Z., Liu H. W. (2018). PARP-1-dependent recruitment of cold-inducible RNA-binding protein promotes double-strand break repair and genome stability. *Proc Natl Acad Sci U S A*. 115, E1759-e1768. <https://doi.org/10.1073/pnas.1713912115>.
- [104] Watanabe M., Kono T., Matsushima-Hibiya Y., Kanazawa T., Nishisaka N., Kishimoto T., Koyama K., Sugimura T., Wakabayashi K. (1999). Molecular cloning of an apoptosis-inducing protein, pierisin, from cabbage butterfly: possible involvement of ADP-ribosylation in its activity. *Proc Natl Acad Sci U S A*. 96, 10608-10613. <https://doi.org/10.1073/pnas.96.19.10608>.
- [105] Takamura-Enya T., Watanabe M., Totsuka Y., Kanazawa T., Matsushima-Hibiya Y., Koyama K., Sugimura T., Wakabayashi K. (2001). Mono(ADP-ribosyl)ation of 2'-deoxyguanosine residue in DNA by an apoptosis-inducing protein, pierisin-1, from cabbage butterfly. *Proc Natl Acad Sci U S A*. 98, 12414-12419. <https://doi.org/10.1073/pnas.221444598>.
- [106] Lyons B., Ravulapalli R., Lanoue J., Lugo M. R., Dutta D., Carlin S., Merrill A. R. (2016). Scabin, a Novel DNA-acting ADP-ribosyltransferase from *Streptomyces scabies*. *J Biol Chem*. 291, 11198-11215. <https://doi.org/10.1074/jbc.M115.707653>.
- [107] Eustermann S., Wu W. F., Langelier M. F., Yang J. C., Easton L. E., Riccio A. A., Pascal J. M., Neuhaus D. (2015). Structural Basis of Detection and Signaling of DNA Single-Strand Breaks by Human PARP-1. *Mol Cell*. 60, 742-754. <https://doi.org/10.1016/j.molcel.2015.10.032>.

- [108] Dawicki-McKenna J. M., Langelier M. F., DeNizio J. E., Riccio A. A., Cao C. D., Karch R., McCauley M., Steffen J. D., Black B. E., Pascal J. M. (2015). PARP-1 Activation Requires Local Unfolding of an Autoinhibitory Domain. *Mol Cell*. 60, 755-768. <https://doi.org/10.1016/j.molcel.2015.10.013>.
- [109] Sacho E. J., Maizels N. (2011). DNA repair factor MRE11/RAD50 cleaves 3'-phosphotyrosyl bonds and resects DNA to repair damage caused by topoisomerase 1 poisons. *J Biol Chem*. 286, 44945-44951. <https://doi.org/10.1074/jbc.M111.299347>.
- [110] Kawale A. S., Povirk L. F. (2018). Tyrosyl-DNA phosphodiesterases: rescuing the genome from the risks of relaxation. *Nucleic Acids Res*. 46, 520-537. <https://doi.org/10.1093/nar/gkx1219>.
- [111] Anand R., Ranjha L., Cannavo E., Cejka P. (2016). Phosphorylated CtIP Functions as a Co-factor of the MRE11-RAD50-NBS1 Endonuclease in DNA End Resection. *Mol Cell*. 64, 940-950. <https://doi.org/10.1016/j.molcel.2016.10.017>.
- [112] Belousova E. A., Ishchenko A. A., Lavrik O. I. (2018). DNA is a New Target of PARP3. *Sci Rep*. 8, 4176. <https://doi.org/10.1038/s41598-018-22673-3>.
- [113] Fouquerel E., Goellner E. M., Yu Z., Gagne J. P., Barbi de Moura M., Feinstein T., Wheeler D., Redpath P., Li J., Romero G., Migaud M., Van Houten B., Poirier G. G., Sobol R. W. (2014). ARTD1/PARP1 negatively regulates glycolysis by inhibiting hexokinase 1 independent of NAD⁺ depletion. *Cell Rep*. 8, 1819-1831. <https://doi.org/10.1016/j.celrep.2014.08.036>.
- [114] Munir A., Banerjee A., Shuman S. (2018). NAD⁺-dependent synthesis of a 5'-phospho-ADP-ribosylated RNA/DNA cap by RNA 2'-phosphotransferase Tpt1. *Nucleic Acids Res*. 46, 9617-9624. <https://doi.org/10.1093/nar/gky792>.
- [115] Banerjee A., Munir A., Abdullahu L., Damha M. J., Goldgur Y., Shuman S. (2019). Structure of tRNA splicing enzyme Tpt1 illuminates the mechanism of RNA 2'-PO₄ recognition and ADP-ribosylation. *Nat Commun*. 10, 218. <https://doi.org/10.1038/s41467-018-08211-9>.
- [116] Agnew T., Munnur D., Crawford K., Palazzo L., Mikoc A., Ahel I. (2018). MacroD1 Is a Promiscuous ADP-Ribosyl Hydrolase Localized to Mitochondria. *Front Microbiol*. 9, 20. <https://doi.org/10.3389/fmicb.2018.00020>.
- [117] Bednarski J. J., Sleckman B. P. (2019). At the intersection of DNA damage and immune responses. *Nat Rev Immunol*. 19, 231-242. <https://doi.org/10.1038/s41577-019-0135-6>.
- [118] Dudley D. D., Chaudhuri J., Bassing C. H., Alt F. W. (2005). Mechanism and control of V(D)J recombination versus class switch recombination: similarities and differences. *Adv Immunol*. 86, 43-112. [https://doi.org/10.1016/s0065-2776\(04\)86002-4](https://doi.org/10.1016/s0065-2776(04)86002-4).
- [119] Bednarski J. J., Sleckman B. P. (2012). Lymphocyte development: integration of DNA damage response signaling. *Adv Immunol*. 116, 175-204. <https://doi.org/10.1016/b978-0-12-394300-2.00006-5>.
- [120] Keim C., Kazadi D., Rothschild G., Basu U. (2013). Regulation of AID, the B-cell genome mutator. *Genes Dev*. 27, 1-17. <https://doi.org/10.1101/gad.200014.112>.
- [121] Santos F., Peat J., Burgess H., Rada C., Reik W., Dean W. (2013). Active demethylation in mouse zygotes involves cytosine deamination and base excision repair. *Epigenetics Chromatin*. 6, 39. <https://doi.org/10.1186/1756-8935-6-39>.
- [122] Franchini D. M., Chan C. F., Morgan H., Incorvaia E., Rangam G., Dean W., Santos F., Reik W., Petersen-Mahrt S. K. (2014). Processive DNA demethylation via DNA deaminase-induced lesion resolution. *PLoS One*. 9, e97754. <https://doi.org/10.1371/journal.pone.0097754>.
- [123] Barreto G., Schafer A., Marhold J., Stach D., Swaminathan S. K., Handa V., Doderlein G., Maltry N., Wu W., Lyko F., Niehrs C. (2007). Gadd45a promotes epigenetic gene activation by repair-mediated DNA demethylation. *Nature*. 445, 671-675. <https://doi.org/10.1038/nature05515>.
- [124] Grin I., Ishchenko A. A. (2016). An interplay of the base excision repair and mismatch repair pathways in active DNA demethylation. *Nucleic Acids Res*. 44, 3713-3727. <https://doi.org/10.1093/nar/gkw059>.

- [125] Le Q., Maizels N. (2015). Cell Cycle Regulates Nuclear Stability of AID and Determines the Cellular Response to AID. *PLoS Genet.* 11, e1005411. <https://doi.org/10.1371/journal.pgen.1005411>.
- [126] Endo Y., Marusawa H., Kinoshita K., Morisawa T., Sakurai T., Okazaki I. M., Watashi K., Shimotohno K., Honjo T., Chiba T. (2007). Expression of activation-induced cytidine deaminase in human hepatocytes via NF-kappaB signaling. *Oncogene.* 26, 5587-5595. <https://doi.org/10.1038/sj.onc.1210344>.
- [127] Duan Z., Zheng H., Liu H., Li M., Tang M., Weng X., Yi W., Bode A. M., Cao Y. (2016). AID expression increased by TNF-alpha is associated with class switch recombination of Igalpha gene in cancers. *Cell Mol Immunol.* 13, 484-491. <https://doi.org/10.1038/cmi.2015.26>.
- [128] Chaudhuri J., Tian M., Khuong C., Chua K., Pinaud E., Alt F. W. (2003). Transcription-targeted DNA deamination by the AID antibody diversification enzyme. *Nature.* 422, 726-730. <https://doi.org/10.1038/nature01574>.
- [129] Qiao Q., Wang L., Meng F. L., Hwang J. K., Alt F. W., Wu H. (2017). AID Recognizes Structured DNA for Class Switch Recombination. *Mol Cell.* 67, 361-373 e364. <https://doi.org/10.1016/j.molcel.2017.06.034>.
- [130] Al-Khalaf M. H., Blake L. E., Larsen B. D., Bell R. A., Brunette S., Parks R. J., Rudnicki M. A., McKinnon P. J., Jeffrey Dilworth F., Megeney L. A. (2016). Temporal activation of XRCC1-mediated DNA repair is essential for muscle differentiation. *Cell Discov.* 2, 15041. <https://doi.org/10.1038/celldisc.2015.41>.
- [131] Farzaneh F., Zalin R., Brill D., Shall S. (1982). DNA strand breaks and ADP-ribosyl transferase activation during cell differentiation. *Nature.* 300, 362-366. <https://doi.org/10.1038/300362a0>.
- [132] Dawson B. A., Lough J. (1988). Immunocytochemical localization of transient DNA strand breaks in differentiating myotubes using in situ nick-translation. *Dev Biol.* 127, 362-367.
- [133] Eustermann S., Videler H., Yang J. C., Cole P. T., Gruszka D., Veprintsev D., Neuhaus D. (2011). The DNA-binding domain of human PARP-1 interacts with DNA single-strand breaks as a monomer through its second zinc finger. *J Mol Biol.* 407, 149-170. <https://doi.org/10.1016/j.jmb.2011.01.034>.
- [134] Larsen B. D., Rampalli S., Burns L. E., Brunette S., Dilworth F. J., Megeney L. A. (2010). Caspase 3/caspase-activated DNase promote cell differentiation by inducing DNA strand breaks. *Proc Natl Acad Sci U S A.* 107, 4230-4235. <https://doi.org/10.1073/pnas.0913089107>.
- [135] Carrio E., Suelves M. (2015). DNA methylation dynamics in muscle development and disease. *Front Aging Neurosci.* 7, 19. <https://doi.org/10.3389/fnagi.2015.00019>.
- [136] Azad G. K., Ito K., Sailaja B. S., Biran A., Nissim-Rafinia M., Yamada Y., Brown D. T., Takizawa T., Meshorer E. (2018). PARP1-dependent eviction of the linker histone H1 mediates immediate early gene expression during neuronal activation. *J Cell Biol.* 217, 473-481. <https://doi.org/10.1083/jcb.201703141>.
- [137] Vicent G. P., Wright R. H., Beato M. (2016). Linker histones in hormonal gene regulation. *Biochim Biophys Acta.* 1859, 520-525. <https://doi.org/10.1016/j.bbagr.2015.10.016>.
- [138] Huang X., LeDuc R. D., Fornelli L., Schunter A. J., Bennett R. L., Kelleher N. L., Licht J. D. (2019). Defining the NSD2 interactome: PARP1 PARylation reduces NSD2 histone methyltransferase activity and impedes chromatin binding. *J Biol Chem.* 294, 12459-12471. <https://doi.org/10.1074/jbc.RA118.006159>.
- [139] Moore L. D., Le T., Fan G. (2013). DNA methylation and its basic function. *Neuropsychopharmacology.* 38, 23-38. <https://doi.org/10.1038/npp.2012.112>.
- [140] Deaton A. M., Bird A. (2011). CpG islands and the regulation of transcription. *Genes Dev.* 25, 1010-1022. <https://doi.org/10.1101/gad.2037511>.
- [141] Ross S. E., Bogdanovic O. (2019). TET enzymes, DNA demethylation and pluripotency. *Biochem Soc Trans.* 47, 875-885. <https://doi.org/10.1042/BST20180606>.
- [142] Gavin D. P., Chase K. A., Sharma R. P. (2013). Active DNA demethylation in post-mitotic neurons: a reason for optimism. *Neuropharmacology.* 75, 233-245. <https://doi.org/10.1016/j.neuropharm.2013.07.036>.
- [143] Cedar H., Bergman Y. (2009). Linking DNA methylation and histone modification: patterns and paradigms. *Nat Rev Genet.* 10, 295-304. <https://doi.org/10.1038/nrg2540>.

- [144] Lang Z., Lei M., Wang X., Tang K., Miki D., Zhang H., Mangrauthia S. K., Liu W., Nie W., Ma G., Yan J., Duan C. G., Hsu C. C., Wang C., Tao W. A., Gong Z., Zhu J. K. (2015). The methyl-CpG-binding protein MBD7 facilitates active DNA demethylation to limit DNA hypermethylation and transcriptional gene silencing. *Mol Cell*. 57, 971-983. <https://doi.org/10.1016/j.molcel.2015.01.009>.
- [145] Bochtler M., Kolano A., Xu G. L. (2017). DNA demethylation pathways: Additional players and regulators. *Bioessays*. 39, 1-13. <https://doi.org/10.1002/bies.201600178>.
- [146] Rai K., Huggins I. J., James S. R., Karpf A. R., Jones D. A., Cairns B. R. (2008). DNA demethylation in zebrafish involves the coupling of a deaminase, a glycosylase, and gadd45. *Cell*. 135, 1201-1212. <https://doi.org/10.1016/j.cell.2008.11.042>.
- [147] Chen C. C., Wang K. Y., Shen C. K. (2013). DNA 5-methylcytosine demethylation activities of the mammalian DNA methyltransferases. *J Biol Chem*. 288, 9084-9091. <https://doi.org/10.1074/jbc.M112.445585>.
- [148] Rebhandl S., Huemer M., Greil R., Geisberger R. (2015). AID/APOBEC deaminases and cancer. *Oncoscience*. 2, 320-333. <https://doi.org/10.18632/oncoscience.155>.
- [149] He Y. F., Li B. Z., Li Z., Liu P., Wang Y., Tang Q., Ding J., Jia Y., Chen Z., Li L., Sun Y., Li X., Dai Q., Song C. X., Zhang K., He C., Xu G. L. (2011). Tet-mediated formation of 5-carboxylcytosine and its excision by TDG in mammalian DNA. *Science*. 333, 1303-1307. <https://doi.org/10.1126/science.1210944>.
- [150] Ito S., Shen L., Dai Q., Wu S. C., Collins L. B., Swenberg J. A., He C., Zhang Y. (2011). Tet proteins can convert 5-methylcytosine to 5-formylcytosine and 5-carboxylcytosine. *Science*. 333, 1300-1303. <https://doi.org/10.1126/science.1210597>.
- [151] Maiti A., Drohat A. C. (2011). Thymine DNA glycosylase can rapidly excise 5-formylcytosine and 5-carboxylcytosine: potential implications for active demethylation of CpG sites. *J Biol Chem*. 286, 35334-35338. <https://doi.org/10.1074/jbc.C111.284620>.
- [152] Cortellino S., Xu J., Sannai M., Moore R., Caretti E., Cigliano A., Le Coz M., Devarajan K., Wessels A., Soprano D., Abramowitz L. K., Bartolomei M. S., Rambow F., Bassi M. R., Bruno T., Fanciulli M., Renner C., Klein-Szanto A. J., Matsumoto Y., Kobi D., Davidson I., Alberti C., Larue L., Bellacosa A. (2011). Thymine DNA glycosylase is essential for active DNA demethylation by linked deamination-base excision repair. *Cell*. 146, 67-79. <https://doi.org/10.1016/j.cell.2011.06.020>.
- [153] Wossidlo M., Arand J., Sebastiano V., Lepikhov K., Boiani M., Reinhardt R., Scholer H., Walter J. (2010). Dynamic link of DNA demethylation, DNA strand breaks and repair in mouse zygotes. *EMBO J*. 29, 1877-1888. <https://doi.org/10.1038/emboj.2010.80>.
- [154] Hajkova P., Jeffries S. J., Lee C., Miller N., Jackson S. P., Surani M. A. (2010). Genome-wide reprogramming in the mouse germ line entails the base excision repair pathway. *Science*. 329, 78-82. <https://doi.org/10.1126/science.1187945>.
- [155] Krishnakumar R., Gamble M. J., Frizzell K. M., Berrocal J. G., Kininis M., Kraus W. L. (2008). Reciprocal binding of PARP-1 and histone H1 at promoters specifies transcriptional outcomes. *Science*. 319, 819-821. <https://doi.org/10.1126/science.1149250>.
- [156] Nalabothula N., Al-jumaily T., Eteleeb A. M., Flight R. M., Xiaorong S., Moseley H., Rouchka E. C., Fondufe-Mittendorf Y. N. (2015). Genome-Wide Profiling of PARP1 Reveals an Interplay with Gene Regulatory Regions and DNA Methylation. *PLoS One*. 10, e0135410. <https://doi.org/10.1371/journal.pone.0135410>.
- [157] Qin W., Wolf P., Liu N., Link S., Smets M., La Mastra F., Forne I., Pichler G., Horl D., Fellingner K., Spada F., Bonapace I. M., Imhof A., Harz H., Leonhardt H. (2015). DNA methylation requires a DNMT1 ubiquitin interacting motif (UIM) and histone ubiquitination. *Cell Res*. 25, 911-929. <https://doi.org/10.1038/cr.2015.72>.
- [158] Loo S. K., Ab Hamid S. S., Musa M., Wong K. K. (2018). DNMT1 is associated with cell cycle and DNA replication gene sets in diffuse large B-cell lymphoma. *Pathol Res Pract*. 214, 134-143. <https://doi.org/10.1016/j.prp.2017.10.005>.
- [159] Zampieri M., Passananti C., Calabrese R., Perilli M., Corbi N., De Cave F., Guastafierro T., Bacalini M. G., Reale A., Amicosante G., Calabrese L., Zlatanova J., Caiafa P. (2009). Parp1 localizes within the Dnmt1 promoter and protects its unmethylated state by its enzymatic activity. *PLoS One*. 4, e4717. <https://doi.org/10.1371/journal.pone.0004717>.

- [160] Zampieri M., Guastafierro T., Calabrese R., Ciccarone F., Bacalini M. G., Reale A., Perilli M., Passananti C., Caiafa P. (2012). ADP-ribose polymers localized on Ctcf-Parp1-Dnmt1 complex prevent methylation of Ctcf target sites. *Biochem J.* 441, 645-652. <https://doi.org/10.1042/bj20111417>.
- [161] De Vos M., El Ramy R., Quenet D., Wolf P., Spada F., Magroun N., Babbio F., Schreiber V., Leonhardt H., Bonapace I. M., Dantzer F. (2014). Poly(ADP-ribose) polymerase 1 (PARP1) associates with E3 ubiquitin-protein ligase UHRF1 and modulates UHRF1 biological functions. *J Biol Chem.* 289, 16223-16238. <https://doi.org/10.1074/jbc.M113.527424>.
- [162] Becker A., Zhang P., Allmann L., Meilinger D., Bertulat B., Eck D., Hofstaetter M., Bartolomei G., Hottiger M. O., Schreiber V., Leonhardt H., Cardoso M. C. (2016). Poly(ADP-ribosylation) of Methyl CpG Binding Domain Protein 2 Regulates Chromatin Structure. *J Biol Chem.* 291, 4873-4881. <https://doi.org/10.1074/jbc.M115.698357>.
- [163] Witcher M., Emerson B. M. (2009). Epigenetic silencing of the p16(INK4a) tumor suppressor is associated with loss of CTCF binding and a chromatin boundary. *Mol Cell.* 34, 271-284. <https://doi.org/10.1016/j.molcel.2009.04.001>.
- [164] Han D., Chen Q., Shi J., Zhang F., Yu X. (2017). CTCF participates in DNA damage response via poly(ADP-ribosylation). *Sci Rep.* 7, 43530. <https://doi.org/10.1038/srep43530>.
- [165] Pavlaki I., Docquier F., Chernukhin I., Kita G., Gretton S., Clarkson C. T., Teif V. B., Klenova E. (2018). Poly(ADP-ribosylation) associated changes in CTCF-chromatin binding and gene expression in breast cells. *Biochim Biophys Acta Gene Regul Mech.* 1861, 718-730. <https://doi.org/10.1016/j.bbagr.2018.06.010>.
- [166] Dubois-Chevalier J., Oger F., Dehondt H., Firmin F. F., Gheeraert C., Staels B., Lefebvre P., Eeckhoutte J. (2014). A dynamic CTCF chromatin binding landscape promotes DNA hydroxymethylation and transcriptional induction of adipocyte differentiation. *Nucleic Acids Res.* 42, 10943-10959. <https://doi.org/10.1093/nar/gku780>.
- [167] Marina R. J., Sturgill D., Bailly M. A., Thenoz M., Varma G., Prigge M. F., Nanan K. K., Shukla S., Haque N., Oberdoerffer S. (2016). TET-catalyzed oxidation of intragenic 5-methylcytosine regulates CTCF-dependent alternative splicing. *EMBO J.* 35, 335-355. <https://doi.org/10.15252/embj.201593235>.
- [168] Nanan K. K., Sturgill D. M., Prigge M. F., Thenoz M., Dillman A. A., Mandler M. D., Oberdoerffer S. (2019). TET-Catalyzed 5-Carboxylcytosine Promotes CTCF Binding to Suboptimal Sequences Genome-wide. *iScience.* 19, 326-339. <https://doi.org/10.1016/j.isci.2019.07.041>.
- [169] Ciccarone F., Valentini E., Bacalini M. G., Zampieri M., Calabrese R., Guastafierro T., Mariano G., Reale A., Franceschi C., Caiafa P. (2014). Poly(ADP-ribosylation) is involved in the epigenetic control of TET1 gene transcription. *Oncotarget.* 5, 10356-10367. <https://doi.org/10.18632/oncotarget.1905>.
- [170] Ciccarone F., Valentini E., Zampieri M., Caiafa P. (2015). 5mC-hydroxylase activity is influenced by the PARylation of TET1 enzyme. *Oncotarget.* 6, 24333-24347. <https://doi.org/10.18632/oncotarget.4476>.
- [171] Fujiki K., Shinoda A., Kano F., Sato R., Shirahige K., Murata M. (2013). PPARgamma-induced PARylation promotes local DNA demethylation by production of 5-hydroxymethylcytosine. *Nat Commun.* 4, e2262. <https://doi.org/10.1038/ncomms3262>.
- [172] Puget N., Miller K. M., Legube G. (2019). Non-canonical DNA/RNA structures during Transcription-Coupled Double-Strand Break Repair: Roadblocks or Bona fide repair intermediates? *DNA Repair (Amst).* 81, e102661. <https://doi.org/10.1016/j.dnarep.2019.102661>.
- [173] Feng W., Chakraborty A. (2017). Fragility Extraordinaire: Unsolved Mysteries of Chromosome Fragile Sites. *Adv Exp Med Biol.* 1042, 489-526. https://doi.org/10.1007/978-981-10-6955-0_21.
- [174] Aguilera A., Garcia-Muse T. (2012). R loops: from transcription byproducts to threats to genome stability. *Mol Cell.* 46, 115-124. <https://doi.org/10.1016/j.molcel.2012.04.009>.
- [175] Ginno P. A., Lott P. L., Christensen H. C., Korf I., Chedin F. (2012). R-loop formation is a distinctive characteristic of unmethylated human CpG island promoters. *Mol Cell.* 45, 814-825. <https://doi.org/10.1016/j.molcel.2012.01.017>.

- [176] Drolet M. (2006). Growth inhibition mediated by excess negative supercoiling: the interplay between transcription elongation, R-loop formation and DNA topology. *Mol Microbiol.* 59, 723-730. <https://doi.org/10.1111/j.1365-2958.2005.05006.x>.
- [177] Pommier Y., Sun Y., Huang S. N., Nitiss J. L. (2016). Roles of eukaryotic topoisomerases in transcription, replication and genomic stability. *Nat Rev Mol Cell Biol.* 17, 703-721. <https://doi.org/10.1038/nrm.2016.111>.
- [178] El Hage A., French S. L., Beyer A. L., Tollervey D. (2010). Loss of Topoisomerase I leads to R-loop-mediated transcriptional blocks during ribosomal RNA synthesis. *Genes Dev.* 24, 1546-1558. <https://doi.org/10.1101/gad.573310>.
- [179] Cristini A., Ricci G., Britton S., Salimbeni S., Huang S. N., Marinello J., Calsou P., Pommier Y., Favre G., Capranico G., Gromak N., Sordet O. (2019). Dual Processing of R-Loops and Topoisomerase I Induces Transcription-Dependent DNA Double-Strand Breaks. *Cell Rep.* 28, 3167-3181 e3166. <https://doi.org/10.1016/j.celrep.2019.08.041>.
- [180] Ju B. G., Lunyak V. V., Perissi V., Garcia-Bassets I., Rose D. W., Glass C. K., Rosenfeld M. G. (2006). A topoisomerase IIbeta-mediated dsDNA break required for regulated transcription. *Science.* 312, 1798-1802. <https://doi.org/10.1126/science.1127196>.
- [181] Soubeyrand S., Pope L., Hache R. J. (2010). Topoisomerase IIalpha-dependent induction of a persistent DNA damage response in response to transient etoposide exposure. *Molecular Oncology.* 4, 38-51. <https://doi.org/10.1016/j.molonc.2009.09.003>.
- [182] Puc J., Aggarwal A. K., Rosenfeld M. G. (2017). Physiological functions of programmed DNA breaks in signal-induced transcription. *Nat Rev Mol Cell Biol.* 18, 471-476. <https://doi.org/10.1038/nrm.2017.43>.
- [183] D'Alessandro G., d'Adda di Fagagna F. (2017). Transcription and DNA Damage: Holding Hands or Crossing Swords? *J Mol Biol.* 429, 3215-3229. <https://doi.org/10.1016/j.jmb.2016.11.002>.
- [184] Jubin T., Kadam A., Gani A. R., Singh M., Dwivedi M., Begum R. (2017). Poly ADP-ribose polymerase-1: Beyond transcription and towards differentiation. *Semin Cell Dev Biol.* 63, 167-179. <https://doi.org/10.1016/j.semcdb.2016.07.027>.
- [185] Stilmann M., Hinz M., Arslan S. C., Zimmer A., Schreiber V., Scheidereit C. (2009). A nuclear poly(ADP-ribose)-dependent signalosome confers DNA damage-induced IkappaB kinase activation. *Mol Cell.* 36, 365-378. <https://doi.org/10.1016/j.molcel.2009.09.032>.
- [186] Izhar L., Adamson B., Ciccica A., Lewis J., Pontano-Vaites L., Leng Y., Liang A. C., Westbrook T. F., Harper J. W., Elledge S. J. (2015). A Systematic Analysis of Factors Localized to Damaged Chromatin Reveals PARP-Dependent Recruitment of Transcription Factors. *Cell Rep.* 11, 1486-1500. <https://doi.org/10.1016/j.celrep.2015.04.053>.
- [187] Awwad S. W., Abu-Zhayia E. R., Guttmann-Raviv N., Ayoub N. (2017). NELF-E is recruited to DNA double-strand break sites to promote transcriptional repression and repair. *EMBO Rep.* 18, 745-764. <https://doi.org/10.15252/embr.201643191>.
- [188] Gibson B. A., Zhang Y., Jiang H., Hussey K. M., Shrimp J. H., Lin H., Schwede F., Yu Y., Kraus W. L. (2016). Chemical genetic discovery of PARP targets reveals a role for PARP-1 in transcription elongation. *Science.* 353, 45-50. <https://doi.org/10.1126/science.aaf7865>.
- [189] Su C. H., Shann Y. J., Hsu M. T. (2009). p53 chromatin epigenetic domain organization and p53 transcription. *Mol Cell Biol.* 29, 93-103. <https://doi.org/10.1128/mcb.00704-08>.
- [190] Interthal H., Chen H. J., Champoux J. J. (2005). Human Tdp1 cleaves a broad spectrum of substrates, including phosphoamide linkages. *J Biol Chem.* 280, 36518-36528. <https://doi.org/10.1074/jbc.M508898200>.
- [191] Das B. B., Huang S. Y., Murai J., Rehman I., Ame J. C., Sengupta S., Das S. K., Majumdar P., Zhang H., Biard D., Majumder H. K., Schreiber V., Pommier Y. (2014). PARP1-TDP1 coupling for the repair of topoisomerase I-induced DNA damage. *Nucleic Acids Res.* 42, 4435-4449. <https://doi.org/10.1093/nar/gku088>.
- [192] Lonskaya I., Potaman V. N., Shlyakhtenko L. S., Oussatcheva E. A., Lyubchenko Y. L., Soldatenkov V. A. (2005). Regulation of poly(ADP-ribose) polymerase-1 by DNA structure-specific binding. *J Biol Chem.* 280, 17076-17083. <https://doi.org/10.1074/jbc.M413483200>.
- [193] Day T. A., Layer J. V., Cleary J. P., Guha S., Stevenson K. E., Tivey T., Kim S., Schinzel A. C., Izzo F., Doench J., Root D. E., Hahn W. C., Price B. D., Weinstock D. M. (2017). PARP3

is a promoter of chromosomal rearrangements and limits G4 DNA. *Nat Commun.* 8, 15110. <https://doi.org/10.1038/ncomms15110>.

[194] Liu Y., Sharpless N. E. (2009). Tumor suppressor mechanisms in immune aging. *Curr Opin Immunol.* 21, 431-439. <https://doi.org/10.1016/j.coi.2009.05.011>.

[195] Shivakumar L., Minna J., Sakamaki T., Pestell R., White M. A. (2002). The RASSF1A tumor suppressor blocks cell cycle progression and inhibits cyclin D1 accumulation. *Mol Cell Biol.* 22, 4309-4318. <https://doi.org/10.1128/mcb.22.12.4309-4318.2002>.

[196] Donninger H., Clark J., Rinaldo F., Nelson N., Barnoud T., Schmidt M. L., Hobbing K. R., Vos M. D., Sils B., Clark G. J. (2015). The RASSF1A tumor suppressor regulates XPA-mediated DNA repair. *Mol Cell Biol.* 35, 277-287. <https://doi.org/10.1128/mcb.00202-14>.

[197] Haffner M. C., Aryee M. J., Toubaji A., Esopi D. M., Albadine R., Gurel B., Isaacs W. B., Bova G. S., Liu W., Xu J., Meeker A. K., Netto G., De Marzo A. M., Nelson W. G., Yegnasubramanian S. (2010). Androgen-induced TOP2B-mediated double-strand breaks and prostate cancer gene rearrangements. *Nat Genet.* 42, 668-675. <https://doi.org/10.1038/ng.613>.

[198] Kim D. S., Camacho C. V., Nagari A., Malladi V. S., Challa S., Kraus W. L. (2019). Activation of PARP-1 by snoRNAs Controls Ribosome Biogenesis and Cell Growth via the RNA Helicase DDX21. *Mol Cell.* 75, 1270-1285 e1214. <https://doi.org/10.1016/j.molcel.2019.06.020>.

[199] Rass U., Ahel I., West S. C. (2007). Actions of aprataxin in multiple DNA repair pathways. *J Biol Chem.* 282, 9469-9474. <https://doi.org/10.1074/jbc.M611489200>.

[200] Harris J. L., Jakob B., Taucher-Scholz G., Dianov G. L., Becherel O. J., Lavin M. F. (2009). Aprataxin, poly-ADP ribose polymerase 1 (PARP-1) and apurinic endonuclease 1 (APE1) function together to protect the genome against oxidative damage. *Hum Mol Genet.* 18, 4102-4117. <https://doi.org/10.1093/hmg/ddp359>.

[201] Gueven N., Becherel O. J., Kijas A. W., Chen P., Howe O., Rudolph J. H., Gatti R., Date H., Onodera O., Taucher-Scholz G., Lavin M. F. (2004). Aprataxin, a novel protein that protects against genotoxic stress. *Hum Mol Genet.* 13, 1081-1093. <https://doi.org/10.1093/hmg/ddh122>.

[202] Crawford K., Bonfiglio J. J., Mikoc A., Matic I., Ahel I. (2018). Specificity of reversible ADP-ribosylation and regulation of cellular processes. *Crit Rev Biochem Mol Biol.* 53, 64-82. <https://doi.org/10.1080/10409238.2017.1394265>.

FIGURE LEGENDS

Fig. 1. An overview of substrates, sites and products of ADP-ribosyltransferases.

Fig. 2. ADPr recognizing domains

Fig. 3. Schematic representation of the DNA damage–induced ADP-ribosylation and transcription. Prior to transcriptional initiation, DNA is nicked by topoisomerases and/or nucleases introducing SSBs and DSBs. Upon DNA damage, PARP1 (possibly PARP2, PARP3, or other PARPs) will be activated and recruited to the damage site. PARPs ADP-ribosylate themselves, potentially DNA termini, histones, and other proteins, block DNMT1 activity, and recruit DNA repair proteins and transcription factors to the DNA damage sites in the promoter or enhancer region. Then, the affected chromatin decondenses, DNA gets demethylated, and transcription starts. After restoration of DNA integrity and potentially of the methylation pattern, transcription can be blocked again.

Fig. 4. Schematic representation of the cellular responses to programmed and random DNA strand breaks.

Figure 1
[Click here to download high resolution image](#)

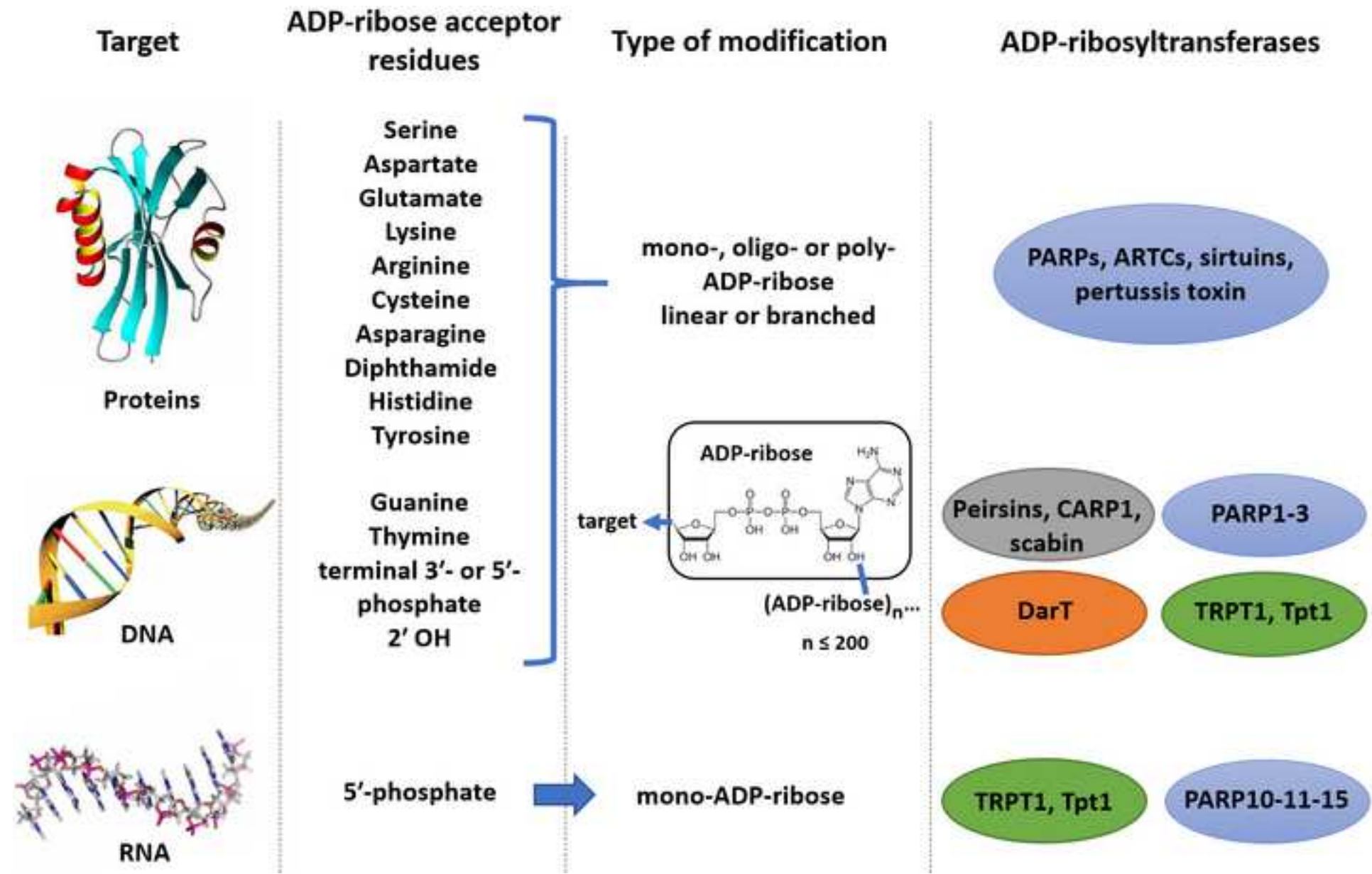


Figure 2

[Click here to download high resolution image](#)

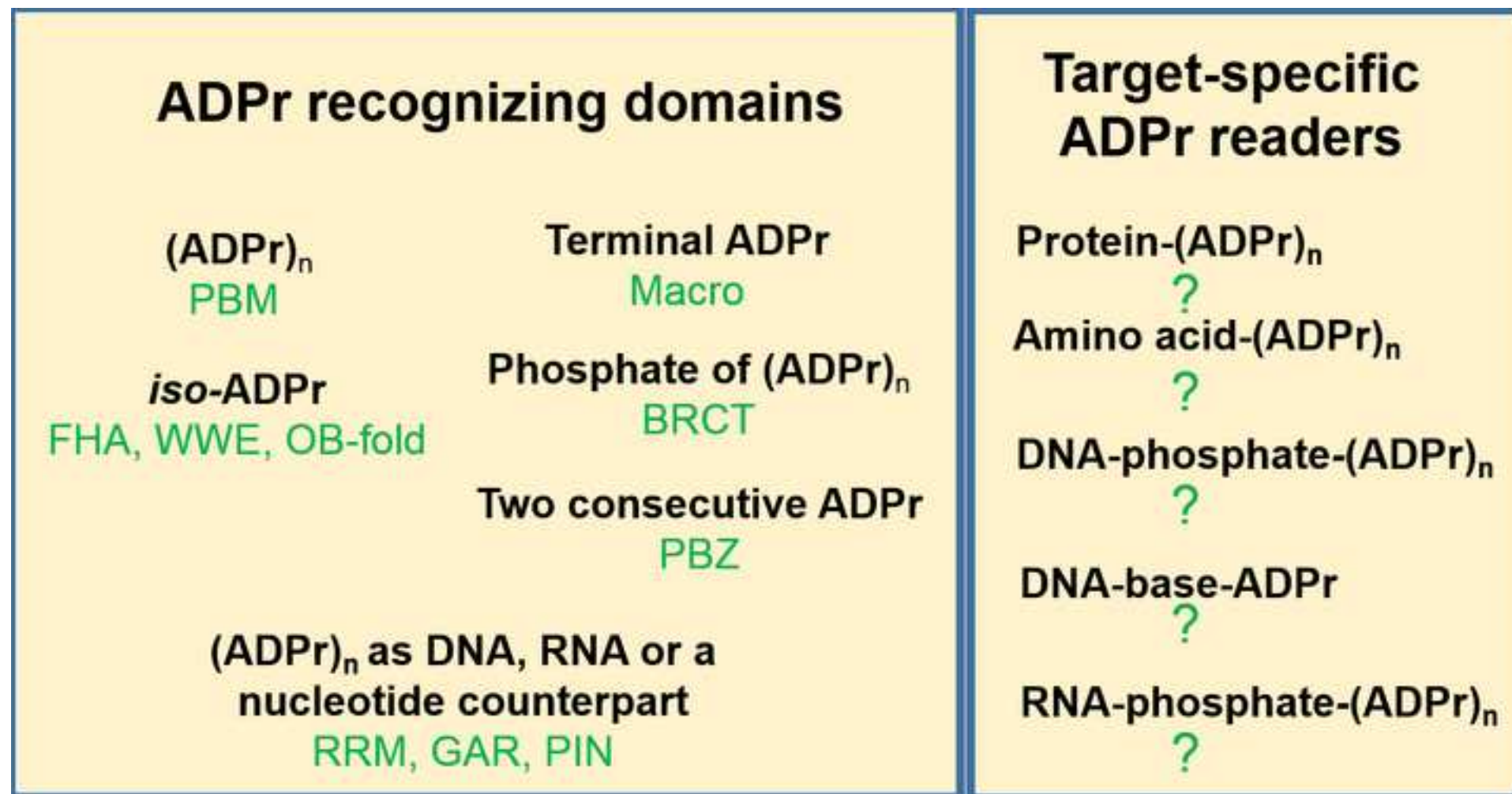


Figure 3

[Click here to download high resolution image](#)

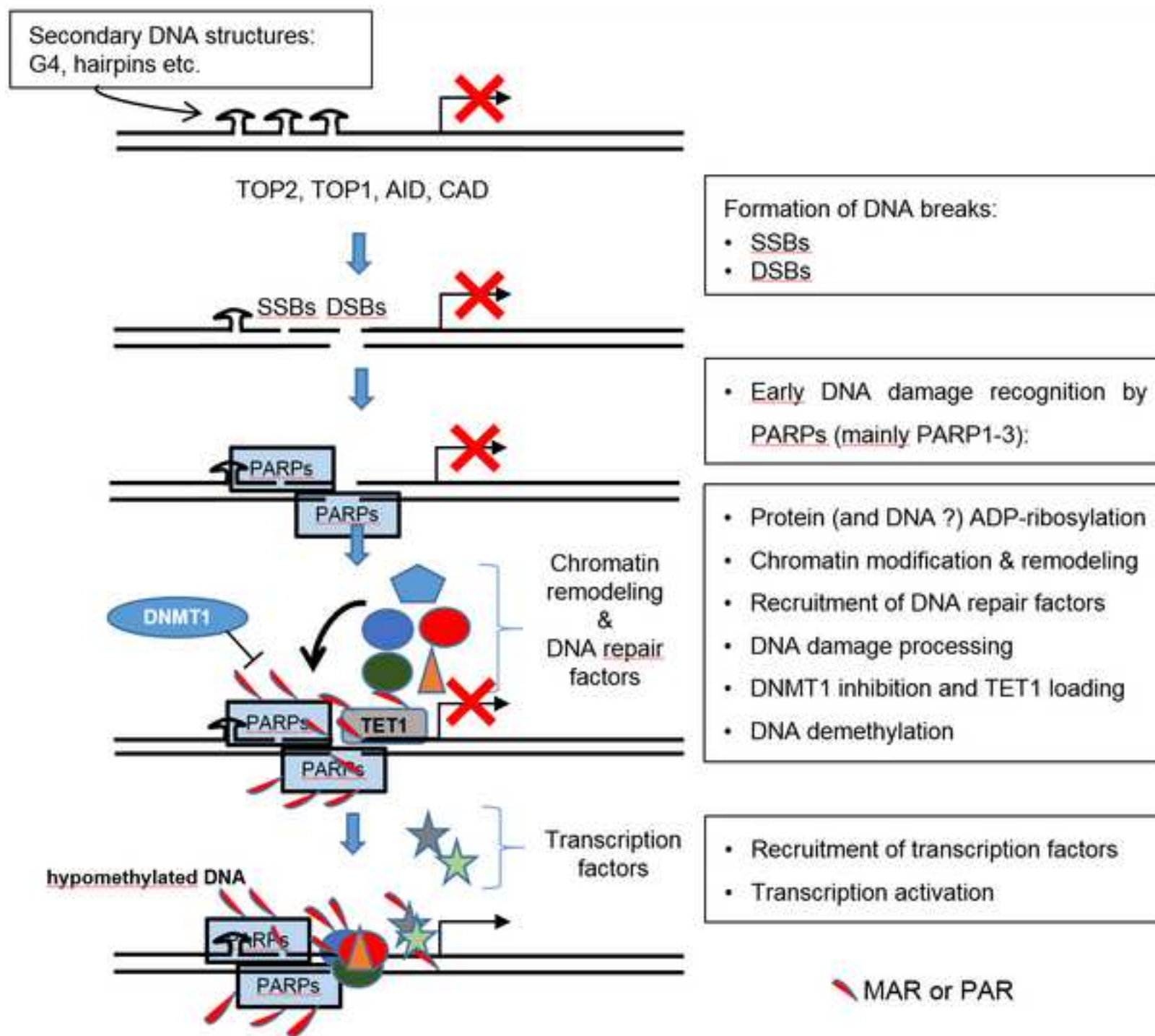
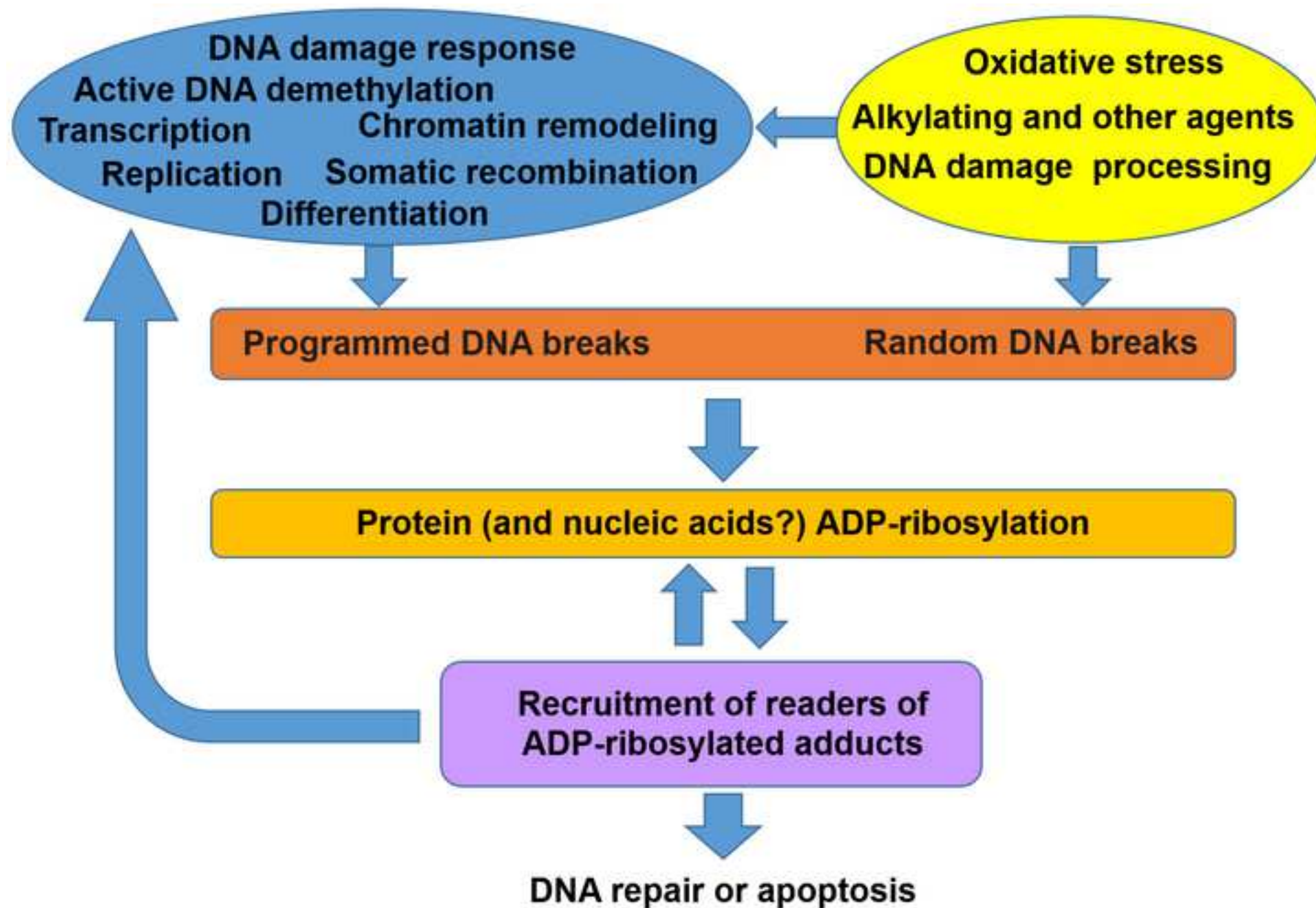


Figure 4
[Click here to download high resolution image](#)



Insight into DNA substrate specificity of PARP1-catalysed DNA poly(ADP-ribosyl)ation

Elie Matta^{1,2,†}, Assel Kiribayeva^{3,4,†}, Bekbolat Khassenov³, Bakhyt T. Matkarimov⁵, Alexander A. Ishchenko^{1,2}

¹Laboratoire «Intégrité du Génome et Cancers» CNRS, UMR9019, Université Paris-Saclay, F-94805 Villejuif, France

²Gustave Roussy, Université Paris-Saclay, F-94805 Villejuif, France

³National Center for Biotechnology, Nur-Sultan, 010000, Kazakhstan.

⁴L.N. Gumilyov Eurasian National University, Nur-Sultan, 010000, Kazakhstan.

⁵National Laboratory Astana, Nazarbayev University, Nur-Sultan, 010000, Kazakhstan.

[†]E.M. and A.K. contributed equally. Correspondence and requests for materials should be addressed to A.A.I. (email: Alexander.Ishchenko@gustaveroussy.fr)

DNA-dependent poly(ADP-ribose) polymerases (PARPs) PARP1, PARP2 and PARP3 act as DNA break sensors signalling DNA damage. Upon detecting DNA damage, these PARPs use nicotinic adenine dinucleotide as a substrate to synthesise a monomer or polymer of ADP-ribose (MAR or PAR, respectively) covalently attached to the acceptor residue of target proteins. Recently, it was demonstrated that PARP1–3 proteins can directly ADP-ribosylate DNA breaks by attaching MAR and PAR moieties to terminal phosphates. Nevertheless, little is still known about the mechanisms governing substrate recognition and specificity of PARP1, which accounts for most of cellular PARylation activity. Here, we characterised PARP1-mediated DNA PARylation of DNA duplexes containing various types of breaks at different positions. The 3'-terminal phosphate residue at double-strand DNA break ends served as a major acceptor site for PARP1-catalysed PARylation depending on the orientation and distance between DNA strand breaks in a single DNA molecule. A preference for ADP-ribosylation of DNA molecules containing 3'-terminal phosphate over PARP1 auto-ADP-ribosylation was observed, and a model of DNA modification by PARP1 was proposed. Similar results were obtained with purified recombinant PARP1 and HeLa cell-free extracts. Thus, the biological effects of PARP-mediated ADP-ribosylation may strongly depend on the configuration of complex DNA strand breaks.

Introduction

One of the earliest DNA damage response events in the cell is the recruitment of DNA-dependent poly(ADP-ribose) polymerases 1, 2 and 3 (PARP1–3) to the sites of DNA strand breaks^{1–3}. PARPs 1–3 are catalytically activated through interaction with DNA strand discontinuities and catalyse poly(ADP-ribosyl)ation (PARylation) or mono(ADP-ribosyl)ation (MARylation, in case of PARP3) of nuclear acceptor proteins including auto-ADP-ribosylation using NAD⁺ as the ADP-ribose donor^{4–6}. Protein ADP-ribosylation provides a scaffold for the recruitment of other proteins, which also become potential targets for PARP-dependent ADP-ribosylation altering the function of the modified proteins and coordinating the choice of DNA break processing and repair pathways. PARP1 is one of the most abundant nuclear proteins and accounts for ~80–90% of the PARylation activity in the cell induced by DNA damage^{7,8}. PARP1 is recruited to damage sites in genomic DNA within a few seconds after laser micro-irradiation³ and modulates multiple pathways involved in DNA strand break repair: base excision repair, nucleotide excision repair, homologous recombination and non-homologous end-joining^{4,9}. Depletion of PARP1 results in hypersensitivity to ionising radiation, to oxidative stress, and to alkylating agents¹⁰.

Recently, the previously unknown phenomenon of post-replicative reversible ADP-ribosylation of DNA strand break termini catalysed by mammalian PARP1–3 was uncovered. These PARPs catalyse covalent addition of ADP-ribose units to 5'- and 3'-terminal phosphates and to 2'-OH termini of modified nucleotides at DNA strand breaks, thereby producing a covalent MAR–DNA or PAR–DNA adduct^{11–13}. This discovery provides novel molecular insights into PARPs' functions. Previously, we have partially characterised these activities *in vitro* and obtained the first indirect evidence of the presence of PAR–DNA adducts in human cells after a genotoxic treatment¹². We have demonstrated that PARP2- and PARP3-catalysed DNA ADP-ribosylation proceeds in a nick/gap-oriented manner and necessitates the presence of at least two DNA strand breaks separated by a distance of 1–2 helix turns.

The protein PARylation activity of PARP1 has been found to be activated by different types of lesions and DNA structures including single- and double-strand DNA breaks (SSBs and DSBs, respectively), DNA crosslinks, stalled replication forks, DNA hairpins, cruciforms, stably unpaired regions and other non-B-conformations of DNA¹⁴, but the mechanism governing substrate recognition and specificity of PARP1-dependent DNA PARylation is still undetermined. Here we further characterised the mechanism and optimal configuration of DNA structures and breaks for PARP1-catalysed ADP-ribosylation of DNA. We proposed a model of DNA break-oriented binding of PARP1 and demonstrated that PARP1 can catalyse ADP-ribosylation of 3'-phosphorylated DSB termini of the DNA molecules mimicking DSB and SSB breaks even more effectively than auto-PARylation. Possible functional interactions between PARP1-mediated PARylation and formation of 3'-phosphorylated breaks are discussed.

Results

Preferential PARylation of 3'-terminal phosphate at a DSB site by PARP1. Previously, we have demonstrated that PARP1 preferentially ADP-ribosylates 5'-terminal phosphates of single-stranded (ss) oligonucleotides and of 5'-overhangs of a DSB in recessed DNA duplexes^{11,12}. Notably, the 2'-hydroxyl group of cordycepin at the 3' end of a recessed DNA is also targeted by PARP1 for covalent PARylation¹¹. Nevertheless, PARP1-mediated DNA ADP-ribosylation of DNA substrates tested until now is still much less effective than PARP2- or PARP3-catalysed PARylation of their preferred DNA substrates^{11,12}. In the present study, we further characterised PARP1 DNA substrate specificity and the mechanism of its DNA PARylation activity. It has been demonstrated elsewhere that PARP2- and PARP3-catalysed DNA ADP-ribosylation is strongly dependent on the distance between breaks in DNA substrates¹². Thus, for optimisation of PARP1 DNA PARylation activity we performed an *in vitro* assay at a saturating concentration of NAD⁺ (1 mM) with the human PARP1 enzyme and various ³²P-radiolabelled Dbait-based DNA structures (Supplementary Table S1) containing a one-nucleotide (nt) gap for PARP1 activation and 5'- or 3'-terminal phosphates as acceptor groups of various overhangs at a unique DSB end (the opposite DSB terminus ended with a hexaethyleneglycol loop). The reaction products were analysed by denaturing PAGE. As shown in Figure 1, in case of a 1-nt gap situated 13 nt downstream of the 5' DSB terminus, effective PARylation of the 5'-terminal phosphate started when 5'-overhangs were ≥ 7 nt, resulting in a 24–34% yield of PARylated products (S1ⁿ DNA substrates, $n \geq 7$; Fig. 1A and B). Similar results were obtained in the presence of a physiological non-saturating concentration of NAD⁺ (50 μ M) and a 2.5-fold-increased concentration of PARP1 (Supplementary Fig. S1) suggesting that speed of PARP1-catalysed PAR formation does not significantly affect DNA substrate specificity. Notably, HPF1 (histone PARylation factor 1), a PARP1's interacting partner that is known for modulation of target specificity of PARP1 to serine residues, did not affect PARP1 activity towards the S1⁷ substrate or its profile towards S1ⁿ DNA substrates (Supplementary Fig. S2). Substrates S0ⁿ mimicking substrates S1ⁿ but containing a gap on the opposite strand were less effectively PARylated than S1ⁿ were; however, S0ⁿ showed a similar profile of the PARylation dependence on the length of 5' overhangs (Fig. 1B). In contrast to S0ⁿ and S1ⁿ, 3'-phosphorylated protruding termini in DNA substrates S2ⁿ and S3ⁿ were not effectively PARylated by PARP1 even at $n = 21$ (Fig. 1C). By contrast, surprisingly, we found that an S2 (S2⁰) DNA substrate containing 3'-phosphate at the blunt DSB terminus was PARylated very effectively (72% of the product; Fig. 1C). Notably, we did not observe significant modification of 3'-phosphorylated termini when the 1-nt gap was placed on the same, 3'-terminus-containing strand of the duplex (S3ⁿ substrates, Fig. 1C). Furthermore, we compared PARP1 activity towards substrates S2, S2¹, S2⁻¹ and S2⁻³ (Fig. 2A) to verify how sensitive PARP1 is towards the

position of the 3'-phosphate in S2-based DNA duplexes. The results revealed drastic inhibition of DNA PARylation in case of substrates with a 1-nt 3'-overhang or 3-nt recessed 3' terminus (S2¹ and S2⁻³, respectively; Fig. 2A). Only substrate S2⁻¹ was as effective as substrate S2 was (Fig. 2A and B), suggesting strict necessity of PARP1 for a 3'-phosphorylated blunt or 1-nt recessed DSB terminus when the gap is positioned on the opposite strand of the DNA duplex 13 nt downstream from the 5' terminus of DSB. Modification of an unlabelled 3'-terminal phosphate and not of a 5'-[³²P]labelled terminus in the S2 molecule was confirmed by calf intestinal alkaline phosphatase (CIP) treatment of the reaction products (Fig. 2C). PARP1 kinetic experiments uncovered rapid 3'-phosphate modification with a majority of S2 and S2⁻¹ DNA substrates PARylated already after the first minute of the reaction (Fig. 2B) and continued to be effective at low (down to 2 μM) concentrations of NAD⁺ (Fig. 2D).

An SSB-oriented mechanism of PARP DNA PARylation. It has been demonstrated that the accessibility of terminal phosphates of a DSB for PARP2 and PARP3 catalytic sites depends on the distance from a downstream nick¹². Here, we assessed the dependence of PARP1-catalysed 3'-terminal phosphate PARylation on the distance between a gap and a blunt DSB end in Dbait-based DNA structures of different lengths. As presented in Figure 3, among substrates tested in columns 1–10, only DNA substrates containing a gap at a 13- or 23-nt distance from DSB termini (substrates S2 and S15 or S10 and S18, respectively) were PARylated effectively. Notably, the extent of DNA-PARylation was very sensitive to the distance between the DSB and the 3' end of the SSB because attachment of a single nucleotide to the S7 substrate resulted in a strong reduction of DNA PARylation in comparison to the S2 substrate. Taking into account that the 10-nt difference in the distance represents one turn of the DNA helix, these data suggest that the position of the acceptor phosphate relative to SSB in the DNA helix plays a discriminating role for PARP1-dependent modification, as observed previously in the case of PARP2 and PARP3 enzymes. This conclusion was confirmed by significant PARylation of a 5'-terminal phosphate observed at a blunt-ended DSB in the S14 substrate (Fig. 3, column 14) but not in the S1⁰ substrate (Fig. 1), which feature a half-DNA helix difference in the positions of their gaps (18 and 13 nt downstream from the DSB end, respectively). The increased size of gaps in substrates S11, S12, and S13 (3, 7 and 11 nt, respectively) resulted in a significantly lower DNA PARylation yield (17–48 %) as compared to the S2 substrate (77%) containing a 1-nt gap (Fig. 3, columns 11–13 versus 2). Modification of an unlabelled 3'-terminal phosphate at DSB end in substrates S10–13 was confirmed by CIP treatment of the reaction products (Supplementary Fig. S3). These results indicated that PARP1-dependent DNA PARylation of the 3'-terminal phosphate at the DSB terminus is not restricted to DNA duplexes with short gaps although the 1-nt gap apparently better coordinates PARP1 binding and activation for subsequent PARylation of such DNA substrates.

The monomeric mode of PARP1 binding to Dbait-based molecules prone to PARylation. DNA molecules prone to ADP-ribosylation contain at least two proximal breaks for PARP activation and terminal phosphate modification. It has been suggested that PARP affinity for the modification site should be relatively low to prevent the binding of a second PARP molecule, which can sterically protect this site from modification^{11,12}. Taking into account that both DSB blunt ends and an SSB have high affinities for PARP1^{15,16}, the effective PARylation of DNA substrates S2 and S14 raises a question: Does PARP1 bind to blunt-ended DSB termini of such substrates? A gel electromobility shift assay (EMSA) of 5'-[³²P]labelled DNA substrates S2, S4, S5 and S15 in the presence of various PARP1 concentrations showed that PARP1 complexes with S2 and control ungapped S4 migrated as single bands and had similar electromobility (Fig. 4A, lanes 8, 9 and 2, 3, respectively). On the contrary, PARP1 complexes with substrate S5 (the same as S2 but the 3'-phosphate is absent) and S16 (contains the 3'-phosphate but at a position not prone to PARylation) migrated notably more slowly as diffuse doublets (Fig. 4A, lanes 6 and 12, respectively) indicating a binding of an additional PARP1 molecule. Previously, formation of 1:1 or 2:1 PARP1–DNA complexes on EMSA gels has been demonstrated with 53-bp blunt-ended DNA duplexes¹⁷. These data are suggestive of the monomeric mode of PARP1 binding to the S2 DNA substrate (Fig. 4B). Intramolecular accommodation of the phosphorylated DSB terminus of the S2 substrate in the catalytic site of PARP1 bound to the gap on the same DNA molecule, in our opinion, could explain the observed “hiding” of the DSB terminus of the S2 substrate from the binding of an additional PARP1 molecule and consequently its effective PARylation.

A 3'-phosphorylated DSB terminus is a major acceptor site of PARylation as compared to PARP1 auto-ADP-ribosylation. Previously, we demonstrated preferential DNA break modifications by enzymes PARP2 (~5-fold) and PARP3 (~50-fold) as compared to their auto-ADP-ribosylation if the DNA substrates are prone to ADP-ribosylation¹². Nevertheless, PARP1 modification of DNA breaks in our *in vitro* assays has always been at least 10-fold less effective than simultaneous auto-ADP-ribosylation^{11,12}. Here, we incubated unlabelled DNA substrates S2, S4 and S5 with PARP1 in the presence of a low concentration of [adenylate-³²P]NAD⁺ and separated both types of ADP-ribosylation products by SDS-PAGE (Fig. 5). The results indicated that PARP1 was efficiently auto-ADP-ribosylated in the presence of any DNA substrates tested, but a DNA ADP-ribosylation product was observed only in case of the S2 construct containing the 3'-phosphate at the DSB terminus. The yield of S2 DNA ADP-ribosylation was ~5-fold higher as compared to PARP1 auto-ADP-ribosylation in the same reaction mixture (Fig. 5, lane 4), suggesting that PARP1-catalysed DNA ADP-ribosylation can be even more effective than its auto-ADP-ribosylation in case of an optimal configuration of proximal DNA strand breaks.

3'-Phosphorylated DNA substrates are PARylated in human cell-free extracts. To test the possibility of the 3'-terminal phosphate ADP-ribosylation at a DSB site in extracts of human cells, we used DNA substrates S19 and S20 mimicking constructs S4 and S2, respectively, but containing several internucleotide thiophosphate linkages for protection against nuclease degradation (Supplementary Table S1). As depicted in Figure 6, the 5'-[³²P]labelled S19 control substrate without a gap and 3'-terminal phosphate group was not effectively PARylated in HeLa PARG^{KD} cell-free extracts and partially degraded (lanes 3–5). In contrast, the 5'-[³²P]labelled S20 substrate with a 1-nt gap, 3'-terminal phosphate, and an additional thiophosphate linkage at the site of the hexaethyleneglycol loop was effectively PARylated and not degraded in the condition tested (lanes 9, 10 and 15). PARylation of the 3'- but not 5'-[³²P]labelled phosphate in the S20 substrate was confirmed by additional CIP treatment that completely removed the unprotected [³²P]labelled phosphate of PARylated products (lanes 14 and 16). These results are in agreement with the data obtained in our previous work showing effective PARP1-dependent PARylation of a 5'-terminal phosphate in a 5'-overhang of an S1⁷-like DNA molecule in human cell-free extracts¹². Altogether, these results suggest that the DNA PARylation activity in the HeLa cell-free extracts can be efficient towards both 3'- and 5'-terminal phosphates depending on the structure of DNA breaks.

Discussion

PARP1 is an abundant, ubiquitously expressed nuclear protein that has long been regarded as a central DNA damage-responsive factor in mammalian cells that is required for the maintenance of genome integrity^{3,18}. It is generally accepted that PARP-dependent PARylation of chromatin results in chromatin remodelling facilitating the assembly of repair complexes at SSBs and DSBs^{4,19}. PARylation and other PARP1-mediated events are critically involved not only in DNA damage repair but also in a wide array of other biological processes, including replication, epigenetic regulation, transcription, apoptosis, inflammation, RNA metabolism, autophagy and proteasomal activation²⁰⁻²³. Other DNA-dependent proteins, PARP2 and PARP3, have their specific and partially redundant functions relative to PARP1, and all three enzymes often act synergistically in response to genotoxic stress^{2,10}. The number of known PARP functions in the cell continues to grow. For example, recent work from Caldecott's laboratory indicates that in unperturbed cells, PARP1 is a sensor of unligated Okazaki fragments during DNA replication and facilitates their repair²⁴. Other functions still need to be clarified, including the roles of reversible ADP-ribosylation of DNA catalysed by PARP1–3 and MARYlation of 5'-phosphorylated termini of RNA molecules by PARP10, PARP11, PARP15 and TRPT1 recently demonstrated in *in vitro* studies^{11-13,25}.

Despite prior insights into PARP1 DNA PARylation activity, there remain key questions regarding the regulation of PARP1 activity, including the mechanism and specific requirements for its

unusual substrate specificity towards DNA breaks. PARP1 activity towards previously tested DNA substrates is relatively slow and not very effective as compared to the DNA ADP-ribosylation activity of enzymes PARP2 and PARP3^{11,12}, thus casting a reasonable doubt on the biological relevance of this PARP1 activity. Here, we show that PARP1 very effectively PARylates a 3'-terminal phosphate at a DSB site of gapped DNA duplexes thereby producing more than 50% of PARylated DNA products already after 1 min of incubation at relatively low (20 nM) enzyme concentrations (Fig. 2B). This activity is effective in a wide range (2–1000 μM) of NAD^+ concentrations (Fig. 2D). Taking into account that the NAD^+ concentrations in the nucleus and cytoplasm are estimated to be $\sim 100 \mu\text{M}$ ²⁶, these results support the potency of PARP1-dependent PARylation of specific DNA breaks in the cell. This notion is also supported by the PARylation of 3'-phosphorylated DNA breaks in cell-free extracts (Fig. 6) and by the results of the parallel measurement of PARP1-mediated auto- and DNA PARylation, revealing even more efficient modification of the 3'-phosphate of the S2 DNA substrate prone to PARylation as compared to simultaneous PARP1 auto-PARylation (Fig. 5). A similar observation has been made previously regarding PARP2-mediated and PARP3-mediated ADP-ribosylation of a 5'-terminal phosphate at a DSB site of nicked DNA duplexes¹², suggesting that all three DNA-dependent PARPs can preferentially target proximal DNA breaks.

PARP1 is a modular protein and has six distinct folded domains, where three N-terminal zinc finger domains and a tryptophan-glycine-arginine (WGR) domain have been reported to be essential for DNA break binding and DNA-dependent activation of the C-terminal catalytic (CAT) domain²⁷⁻³⁰. Interdomain contacts play a primary role in the allosteric mechanism of catalytic activation of all three DNA-dependent PARPs via local destabilisation of the auto-inhibitory helical subdomain of CAT³¹. In contrast to PARP1, PARP2 and PARP3 do not have zinc finger domains and PARPs 1–3 are differently activated by a variety of damaged DNA structures³²⁻³⁴. Notably, PARP2 and PARP3 are preferentially activated by an SSB harbouring a 5'-terminal phosphate, in contrast to PARP1, which is activated regardless of the phosphorylation status of the DNA ends³⁴. Previously, we proposed a mechanistic model where PARP3-catalysed and PARP2-catalysed DNA ADP-ribosylation depends on the orientations and distances between DNA strand breaks in a single DNA molecule¹². Accordingly, PARP3 and PARP2 ADP-ribosylate the 5' DSB terminus of the same nicked strand if these breaks are separated by a distance of one or two turns of the DNA helix and less effectively ADP-ribosylate the 3'-DSB terminus of opposite strands if the breaks are separated by a distance of 1.5 helix turns¹². The present study shows that PARP1 has different DNA substrate requirements for PARylation of terminal phosphates (1.3 or 2.3 and 1.8 helix turns for 3'- and 5'-DSB blunt termini, respectively) but shows similar dependence on DNA helicity and on the orientations of strand breaks (Figs. 1 and 3). Taken together, these findings suggest that effective DNA ADP-ribosylation depends on an interplay between the activation of a DNA-bound PARPs and accessibility of the DNA acceptor group for their CAT domain. According to these results, we propose a model of PARP1-mediated DNA ADP-

ribosylation (Fig. 7) where the binding of PARP1 to an SSB (1-nt gap) activates its catalytic domain, which in turn starts to ADP-ribosylate all sterically accessible acceptor groups in the same DNA–enzyme complex. This model is supported by the observed monomeric mode of PARP1 binding to the S2 DNA substrate prone to effective PARylation despite the presence of two breaks on the same DNA molecule (Fig. 4). Structural studies conducted in Pascal’s and Neuhaus’s laboratories have revealed that PARP1 binds SSBs with directional selectivity, where zinc fingers 1 and 2 bind to 5’ and 3’ stems, respectively, and the distance between a DNA break (DSB or SSB)-binding site and the catalytic site in PARP1–DNA complexes is $\sim 45 \text{ \AA}$, which corresponds to ~ 1.3 turns (≈ 13 bp) of a B-DNA helix^{27,29}. This observation may explain the strong preference of PARP1 for the S2 substrate, in which the distance between a protein-binding SSB and the PAR-accepting DSB termini is 13 bp. Nevertheless, it should be stressed that other DNA substrates with a greater distance between two strand break sites can still be modified by PARP1. We can hypothesise that the efficient ADP-ribosylation of S2, S10, S14 and other DNA substrates is due to (i) the position of their acceptor phosphates, which is on the same side of the DNA helix exposed to the active site of the PARP1 CAT domain; (ii) the highly dynamic nature of the multi-domain proteins and (iii) the flexibility of ss overhangs in substrates S0ⁿ and S1ⁿ (with $n \geq 7$), which might enable 5’ termini to reach the CAT site. The latter notion is supported by effective ADP-ribosylation of 5’ overhangs in S1ⁿ duplexes (with $n \geq 3$ nt) – but not that of the blunt S1⁰ duplex – catalysed by PARP2 or PARP3 (Supplementary Fig. S4) relaxing the necessity of a 10 or 20 bp distance between a blunt DSB and an SSB for effective ADP-ribosylation of a 5’ DSB terminus¹². The absence of PARylation of the S21 substrate (Figure 3), which mimics S1²¹ but lacks a gap, rules out that PARP1 is activated on ds-ssDNA transitions at 5’ overhangs when it PARylates S1²¹ and other S1ⁿ structures. The absence of DNA PARylation of substrates S2ⁿ and S3ⁿ with 3’ overhangs (Figure 1) suggests that other structural elements of the acceptor DNA terminus are required for accommodation of the terminal phosphate residue in the active site of the PARP1 CAT domain. Given the strong flexibility of both PARP1 and SSB-containing DNA polymers, it is tempting to speculate that with DNA molecules prone to PARylation, PARP1 will preferentially form structurally different complexes stabilised by interactions with both proximal breaks including the CAT domain interaction with an upstream phosphorylated terminus. Further studies are needed to test this hypothesis.

According to the evidence collected so far, DNA ADP-ribosylation activity of PARPs strongly depends on the type and position of DNA breaks. Proximal DNA breaks can be generated directly by genotoxic agents or during processing of the initial DNA damage by DNA repair and DNA replication machineries. In this study, we demonstrate that PARP1 preferentially PARylates a 3’-phosphate of DSB sites in proximity to an SSB. It should be noted that 3’-phosphate termini can be generated endogenously as an intermediate of the action of bi-functional DNA glycosylases or as a product of a tyrosyl-DNA phosphodiesterase 1 (TDPI) reaction, which can remove a variety of 3’ adducts from an

SSB and DSB during DNA repair and leave a 3'-terminal phosphate^{35,36}. It has been reported that PARP1 plays a critical part in TDP1-mediated repair of trapped topoisomerase I (TOP1) cleavage complexes³⁷. PARP1 directly binds to the N-terminal domain of TDP1 and PARylates TDP1 without blocking its catalytic activity. Multiple studies show that PARP inhibitors are sensitise cells to TOP1 poisoning by camptothecin³⁸⁻⁴⁰. Moreover, genetic evidence indicates that PARP1 and TDP1 are epistatic for the repair of TOP1-induced DNA damage³⁷. We suggest that the PARP1-dependent PARylation of 3'-phosphorylated DNA breaks observed here may further enhance the functional interactions between the PARP1 and TDP1. Additional studies are warranted to elucidate how PARP1-dependent DNA PARylation can perform its specific function in a cellular response to DNA damage.

Materials and Methods

Proteins, chemicals and reagents. Proteinase K from *Tritirachium album* and deoxyribonuclease I from bovine pancreas (DNase I) were purchased from Sigma–Aldrich (France), whereas CIP and TdT (terminal deoxynucleotidyl transferase) from New England Biolabs France (Evry, France). Human poly(ADP-ribose) polymerase 1 (PARP1; EC 2.4.2.30) and bovine PARG were bought from Trevigen (Gaithersburg, MD, USA).

Oligonucleotides and Dbait molecules. Sequences of the oligonucleotides and their duplexes used in this work are shown in [Supplementary Table S1](#). Regular oligonucleotides, oligonucleotides with thiophosphates as well as Dbait molecules containing a hexaethyleneglycol linker [(CH₂-CH₂-O)₆] tethering two complementary DNA strands were acquired from Eurogentec (Seraing, Belgium). Prior to enzymatic assays, the oligonucleotides were labelled at the 5'-OH end using T4 polynucleotide kinase (Thermo Scientific) in the presence of [γ -³²P]ATP (3000 Ci·mmol⁻¹, PerkinElmer) as described previously¹¹. Cold ATP at 0.1 mM was added to phosphorylate the remaining non-labelled oligonucleotides. After the labelling reactions, the radioactively labelled oligonucleotides were desalted on a Sephadex G-25 column, equilibrated with water and then annealed with a corresponding complementary strand for 3 min at 65°C in the following buffer: 20 mM HEPES-KOH (pH 7.6) and 50 mM KCl.

DNA ADP-ribosylation assay. PARP-dependent DNA ADP-ribosylation activity was measured as described previously¹¹. Briefly, one of 20 nM [³²P]labelled oligonucleotide duplexes was combined with 20 nM PARP1 in the presence of 1 mM NAD⁺ in ADPR buffer (20 mM HEPES-KOH pH 7.6, 50 mM KCl, 2 mM MgCl₂, 1 mM DTT and 100 μ g/ml BSA). The mixture was incubated for 30 min at 37°C, unless stated otherwise. After the reaction, the samples were incubated with 50 ng/ μ l proteinase K and 0.15% of SDS for 30 min at 50°C followed by the addition of 4 M urea and incubation for 10 s at 95°C. The reaction products were analysed by electrophoresis in denaturing 20% (w/v)

polyacrylamide gels (PAGE; 7 M Urea, 0.5× TBE, 42°C). A Fuji FLA-3000 Phosphor Screen was exposed to the gels and was then scanned with Typhoon FLA-9500, and the image was analysed in the Image Gauge 4.0 software.

Simultaneous evaluation of the efficiency of PARP1-catalysed auto- and DNA ADP-ribosylation.

This assay was carried out as described previously¹² with minor modifications. 320 nM PARP1 was added to cold 1 μM oligonucleotide duplex and incubated in ADPR buffer but without BSA in the presence of 0.5 μM [adenylate-³²P]NAD⁺ (800 Ci·mmol⁻¹, PerkinElmer) for 30 min at 37°C. The reaction products were treated with 10.5 U of DNase I for 30 min at 37°C in the presence of 0.5 mM CaCl₂. After heating for 1 min at 95°C in 1× LDS sample buffer (Invitrogen), the products of the reaction were separated by SDS-PAGE on precast 10% gels (Invitrogen).

The cell line, culture conditions, and preparation of nuclear extracts. Stable PARG knockdown (shPARG/PARG^{KD}) and control (shCTL/BD650) HeLa cell lines have been described elsewhere⁴¹. The cells were grown in DMEM (Dulbecco's modified Eagle's medium) supplemented with penicillin/streptomycin (Gibco, Gaithersburg, USA) and 10% of foetal bovine serum in a humidified atmosphere containing 5% of CO₂. After harvesting, the cells were washed twice in cold phosphate-buffered saline (PBS). All the procedures were conducted at 4°C. The cell pellets were resuspended in 3 volumes (w/v) of cytoplasmic extract buffer (10 mM HEPES-KOH pH 7.6, 10 mM KCl, 0.1 mM EDTA, 0.15 mM spermine, 0.7 mM spermidine, 1× cOmplete protease inhibitors EDTA-free [Roche] and 1 mM DTT); 0.1% of NP-40 was added immediately after cell resuspension. The cells were allowed to swell on ice for 5 min. Nuclei were collected by centrifugation (500 × g, 5 min), then resuspended in 1 volume of nuclear extract buffer (20 mM HEPES-KOH pH 7.6, 0.4 M NaCl, 1 mM EDTA, 25% of glycerol, 1× cOmplete protease inhibitors EDTA-free [Roche] and 1 mM DTT). After 10-min incubation on ice, the samples were centrifuged at 13 000 × g for 5 min. The nuclear extracts (supernatants) were stored at -20°C if not used immediately.

Data availability

The raw and processed data are available from the corresponding author on reasonable request.

References

- 1 Mortusewicz, O., Ame, J. C., Schreiber, V. & Leonhardt, H. Feedback-regulated poly(ADP-ribosyl)ation by PARP-1 is required for rapid response to DNA damage in living cells. *Nucleic acids research* **35**, 7665-7675, doi:10.1093/nar/gkm933 (2007).
- 2 Boehler, C. *et al.* Poly(ADP-ribose) polymerase 3 (PARP3), a newcomer in cellular response to DNA damage and mitotic progression. *Proceedings of the National Academy of Sciences of the United States of America* **108**, 2783-2788, doi:10.1073/pnas.1016574108 (2011).
- 3 Haince, J. F. *et al.* PARP1-dependent kinetics of recruitment of MRE11 and NBS1 proteins to multiple DNA damage sites. *The Journal of biological chemistry* **283**, 1197-1208, doi:10.1074/jbc.M706734200 (2008).

- 4 Martin-Hernandez, K., Rodriguez-Vargas, J. M., Schreiber, V. & Dantzer, F. Expanding functions of ADP-ribosylation in the maintenance of genome integrity. *Seminars in cell & developmental biology* **63**, 92-101, doi:10.1016/j.semcdb.2016.09.009 (2017).
- 5 Wei, H. & Yu, X. Functions of PARylation in DNA Damage Repair Pathways. *Genomics, proteomics & bioinformatics* **14**, 131-139, doi:10.1016/j.gpb.2016.05.001 (2016).
- 6 Pascal, J. M. & Ellenberger, T. The rise and fall of poly(ADP-ribose): An enzymatic perspective. *DNA repair* **32**, 10-16, doi:10.1016/j.dnarep.2015.04.008 (2015).
- 7 Huber, A., Bai, P., de Murcia, J. M. & de Murcia, G. PARP-1, PARP-2 and ATM in the DNA damage response: functional synergy in mouse development. *DNA repair* **3**, 1103-1108, doi:10.1016/j.dnarep.2004.06.002 (2004).
- 8 Yamanaka, H., Penning, C. A., Willis, E. H., Wasson, D. B. & Carson, D. A. Characterization of human poly(ADP-ribose) polymerase with autoantibodies. *The Journal of biological chemistry* **263**, 3879-3883 (1988).
- 9 Gupte, R., Liu, Z. & Kraus, W. L. PARPs and ADP-ribosylation: recent advances linking molecular functions to biological outcomes. *Genes & development* **31**, 101-126, doi:10.1101/gad.291518.116 (2017).
- 10 Menissier de Murcia, J. *et al.* Functional interaction between PARP-1 and PARP-2 in chromosome stability and embryonic development in mouse. *The EMBO journal* **22**, 2255-2263, doi:10.1093/emboj/cdg206 (2003).
- 11 Talhaoui, I. *et al.* Poly(ADP-ribose) polymerases covalently modify strand break termini in DNA fragments in vitro. *Nucleic acids research* **44**, 9279-9295, doi:10.1093/nar/gkw675 (2016).
- 12 Zarkovic, G. *et al.* Characterization of DNA ADP-ribosyltransferase activities of PARP2 and PARP3: new insights into DNA ADP-ribosylation. *Nucleic acids research* **46**, 2417-2431, doi:10.1093/nar/gkx1318 (2018).
- 13 Munnur, D. & Ahel, I. Reversible mono-ADP-ribosylation of DNA breaks. *The FEBS journal* **284**, 4002-4016, doi:10.1111/febs.14297 (2017).
- 14 Lonskaya, I. *et al.* Regulation of poly(ADP-ribose) polymerase-1 by DNA structure-specific binding. *The Journal of biological chemistry* **280**, 17076-17083, doi:10.1074/jbc.M413483200 (2005).
- 15 D'Silva, I. *et al.* Relative affinities of poly(ADP-ribose) polymerase and DNA-dependent protein kinase for DNA strand interruptions. *Biochimica et biophysica acta* **1430**, 119-126 (1999).
- 16 Clark, N. J., Kramer, M., Muthurajan, U. M. & Luger, K. Alternative modes of binding of poly(ADP-ribose) polymerase 1 to free DNA and nucleosomes. *The Journal of biological chemistry* **287**, 32430-32439, doi:10.1074/jbc.M112.397067 (2012).
- 17 Lilyestrom, W., van der Woerd, M. J., Clark, N. & Luger, K. Structural and biophysical studies of human PARP-1 in complex with damaged DNA. *Journal of molecular biology* **395**, 983-994, doi:10.1016/j.jmb.2009.11.062 (2010).
- 18 Liu, C., Vyas, A., Kassab, M. A., Singh, A. K. & Yu, X. The role of poly ADP-ribosylation in the first wave of DNA damage response. *Nucleic acids research* **45**, 8129-8141, doi:10.1093/nar/gkx565 (2017).
- 19 Rouleau, M., Aubin, R. A. & Poirier, G. G. Poly(ADP-ribosyl)ated chromatin domains: access granted. *Journal of cell science* **117**, 815-825, doi:10.1242/jcs.01080 (2004).
- 20 Schreiber, V., Dantzer, F., Ame, J. C. & de Murcia, G. Poly(ADP-ribose): novel functions for an old molecule. *Nature reviews. Molecular cell biology* **7**, 517-528, doi:10.1038/nrm1963 (2006).
- 21 Hottiger, M. O. Nuclear ADP-Ribosylation and Its Role in Chromatin Plasticity, Cell Differentiation, and Epigenetics. *Annual review of biochemistry* **84**, 227-263, doi:10.1146/annurev-biochem-060614-034506 (2015).

- 22 Posavec Marjanovic, M., Crawford, K. & Ahel, I. PARP, transcription and chromatin modeling. *Seminars in cell & developmental biology*, doi:10.1016/j.semcdb.2016.09.014 (2016).
- 23 Rodríguez-Vargas, J. M., Oliver-Pozo, F. J. & Dantzer, F. PARP1 and Poly(ADP-ribose)ation Signaling during Autophagy in Response to Nutrient Deprivation. *Oxidative Medicine and Cellular Longevity* **2019**, 1-15, doi:10.1155/2019/2641712 (2019).
- 24 Hanzlikova, H. *et al.* The Importance of Poly(ADP-Ribose) Polymerase as a Sensor of Unligated Okazaki Fragments during DNA Replication. *Molecular cell* **71**, 319-331 e313, doi:10.1016/j.molcel.2018.06.004 (2018).
- 25 Munnur, D. *et al.* Reversible ADP-ribosylation of RNA. *Nucleic acids research* **47**, 5658-5669, doi:10.1093/nar/gkz305 (2019).
- 26 Sallin, O. *et al.* Semisynthetic biosensors for mapping cellular concentrations of nicotinamide adenine dinucleotides. *eLife* **7**, doi:10.7554/eLife.32638 (2018).
- 27 Langelier, M. F., Planck, J. L., Roy, S. & Pascal, J. M. Structural basis for DNA damage-dependent poly(ADP-ribose)ation by human PARP-1. *Science* **336**, 728-732, doi:10.1126/science.1216338 (2012).
- 28 Ikejima, M. *et al.* The zinc fingers of human poly(ADP-ribose) polymerase are differentially required for the recognition of DNA breaks and nicks and the consequent enzyme activation. Other structures recognize intact DNA. *The Journal of biological chemistry* **265**, 21907-21913 (1990).
- 29 Eustermann, S. *et al.* Structural Basis of Detection and Signaling of DNA Single-Strand Breaks by Human PARP-1. *Molecular cell* **60**, 742-754, doi:10.1016/j.molcel.2015.10.032 (2015).
- 30 Steffen, J. D., McCauley, M. M. & Pascal, J. M. Fluorescent sensors of PARP-1 structural dynamics and allosteric regulation in response to DNA damage. *Nucleic acids research* **44**, 9771-9783, doi:10.1093/nar/gkw710 (2016).
- 31 Dawicki-McKenna, J. M. *et al.* PARP-1 Activation Requires Local Unfolding of an Autoinhibitory Domain. *Molecular cell* **60**, 755-768, doi:10.1016/j.molcel.2015.10.013 (2015).
- 32 Ame, J. C. *et al.* PARP-2, A novel mammalian DNA damage-dependent poly(ADP-ribose) polymerase. *J. Biol. Chem.* **274**, 17860-17868 (1999).
- 33 Kutuzov, M. M. *et al.* Interaction of PARP-2 with DNA structures mimicking DNA repair intermediates and consequences on activity of base excision repair proteins. *Biochimie* **95**, 1208-1215, doi:10.1016/j.biochi.2013.01.007 (2013).
- 34 Langelier, M. F., Riccio, A. A. & Pascal, J. M. PARP-2 and PARP-3 are selectively activated by 5' phosphorylated DNA breaks through an allosteric regulatory mechanism shared with PARP-1. *Nucleic acids research* **42**, 7762-7775, doi:10.1093/nar/gku474 (2014).
- 35 Krokan, H. E. & Bjoras, M. Base excision repair. *Cold Spring Harbor perspectives in biology* **5**, a012583, doi:10.1101/cshperspect.a012583 (2013).
- 36 Interthal, H., Chen, H. J. & Champoux, J. J. Human Tdp1 cleaves a broad spectrum of substrates, including phosphoamide linkages. *The Journal of biological chemistry* **280**, 36518-36528, doi:10.1074/jbc.M508898200 (2005).
- 37 Das, B. B. *et al.* PARP1-TDP1 coupling for the repair of topoisomerase I-induced DNA damage. *Nucleic acids research* **42**, 4435-4449, doi:10.1093/nar/gku088 (2014).
- 38 Zhang, Y. W. *et al.* Poly(ADP-ribose) polymerase and XPF-ERCC1 participate in distinct pathways for the repair of topoisomerase I-induced DNA damage in mammalian cells. *Nucleic acids research* **39**, 3607-3620, doi:10.1093/nar/gkq1304 (2011).
- 39 Patel, A. G. *et al.* Enhanced killing of cancer cells by poly(ADP-ribose) polymerase inhibitors and topoisomerase I inhibitors reflects poisoning of both enzymes. *The Journal of biological chemistry* **287**, 4198-4210, doi:10.1074/jbc.M111.296475 (2012).
- 40 Znojek, P., Willmore, E. & Curtin, N. J. Preferential potentiation of topoisomerase I poison cytotoxicity by PARP inhibition in S phase. *British journal of cancer* **111**, 1319-1326, doi:10.1038/bjc.2014.378 (2014).

41 Ame, J. C. *et al.* Radiation-induced mitotic catastrophe in PARG-deficient cells. *Journal of cell science* **122**, 1990-2002, doi:10.1242/jcs.039115 (2009).

Acknowledgements

This work is supported by funding from the French National Research Agency (ANR-18-CE44-0008), Electricité de France, and Fondation ARC (PJA-20181208015) to A.A.I.; by the Science Committee of the Ministry of Education and Science of the Republic of Kazakhstan, program 0115RK02473, grant 3755/GF4, and NU ORAU to B.T.M and grant AP05133470 to B.K. E.M. was supported by a doctoral fellowship from ABELA FRERES.

Author Contributions

E.M. conducted the experiments, participated in the experimental design, performed statistical analysis and participated in drafting the manuscript. A.K. conducted the experiments, acquired imaging data and performed annotations and statistical analysis. B.K. participated in analysing results and the preparation of this manuscript. B.T.M. contributed to the conception, data analyses and the preparation of the manuscript. A.A.I. designed the study and wrote and edited the manuscript. All the authors read and approved the final manuscript.

Additional Information

Supplementary information accompanies this paper at <http://>

Competing Interests: The authors declare no competing interests.

FIGURE LEGENDS

Figure 1. Effects of the type and size of protruding ends in Dbait-based DNA structures containing a 1-nt gap on the PARP1-catalysed formation of PAR–DNA adducts. Twenty-nanomolar PARP1 was incubated with 20 nM 5'-[³²P]labelled oligonucleotide and 1 mM NAD⁺ for 15 min at 37°C under standard reaction conditions. (A) Denaturing PAGE analysis of PARP1-generated products of PARylation of [³²P]labelled DNA substrates S1ⁿ. (B) and (C) Comparison of DNA PARylation activities of PARP1 towards DNA substrates containing 5'-overhangs (S0ⁿ and S1ⁿ) or 3'-overhangs (S2ⁿ and S3ⁿ), respectively. The data on PARP-catalysed formation of PAR-DNA products are presented as mean ± SD from three independent experiments.

Figure 2. PARP1-catalysed PARylation of S3ⁿ DNA structures with a 3'-phosphate terminus at the DBS end. (A) [³²P]labelled DNA substrates S2ⁿ (50 nM) were incubated with 40 nM PARP1 for 10 min 37°C. (B) Time dependence of PARP1-driven PARylation of substrates S2 and S2⁻¹. DNA substrates (50 nM) were incubated with 20 nM PARP1 for the indicated period under standard reaction conditions. (C) CIP-induced dephosphorylation of 5'-[³²P]labelled PAR-S2 products. After

incubation with PARP1, the S2 samples were heated for 10 min at 85°C, and the resulting [³²P]labelled DNA PARylation products were further incubated with 10 U of CIP for 30 min at 37°C. **(D)** The dependence of S2 DNA (40 nM) PARylation by PARP1 (20 nM) on NAD⁺ concentration. The data in panels C and D are presented as mean ± SD from three independent experiments.

Figure 3. Gap–DSB distance dependence of PARP1-catalysed PARylation of the 3' phosphate at a DSB end of DNA duplexes. The data on PARP-catalysed formation of PAR-DNA products are presented as mean ± SD from three independent experiments performed under standard reaction conditions.

Figure 4. The monomeric mode of PARP1 binding to DNA molecules prone to PARylation. **(A)** The EMSA. Each of 20 nM DNA duplexes was incubated with 0, 50 or 100 nM PARP1 in a buffer consisting of 20 mM Tris-HCl pH 7.6, 50 mM KCl and 1 mM DTT for 10 min at room temperature. The DNA–protein complexes were analysed by electrophoresis in a 4–12% Tris-Glycine polyacrylamide gel (Novex) under non-denaturing conditions at 4°C after addition of 10 % glycerol. **(B)** The putative model of PARP1 complexes with DNA substrates prone (S2) or not prone (S5) to DNA break PARylation.

Figure 5. Comparison of the efficiency of PARP1-catalysed auto- and DNA ADP-ribosylation. The denaturing SDS-PAGE analysis of the products of PARP1 incubation with cold oligonucleotide duplexes in the presence of [adenylate-³²P]NAD⁺. For details see Materials and Methods.

Figure 6. Formation of PAR–3' phosphate–DNA adducts in nuclear extracts from HeLa PARG^{KD} cells. Fifty-nanomolar [³²P]labelled S19 or S20 Dbait-based molecules were incubated with 2.5 µg/µl HeLa extracts or 40 nM PARP1 in the presence of 67 mM KCl, 10 mM HEPES-KOH pH 8.0 and 500 µM NAD⁺ for 20 min at 37°C. The reactions were stopped by heating the samples for 10 min at 80°C, and the resulting DNA PARylation products were next incubated with 20 pg/µl PARG (lanes 5 and 10) or after phenol-chloroform extraction with 10 U of CIP for 30 min at 37°C (lanes 12, 14 and 16). The reaction products were analysed by denaturing PAGE.

Figure 7. Schematic representation of the putative model of DNA modification by PARP1 activated on a 1-nt gap.

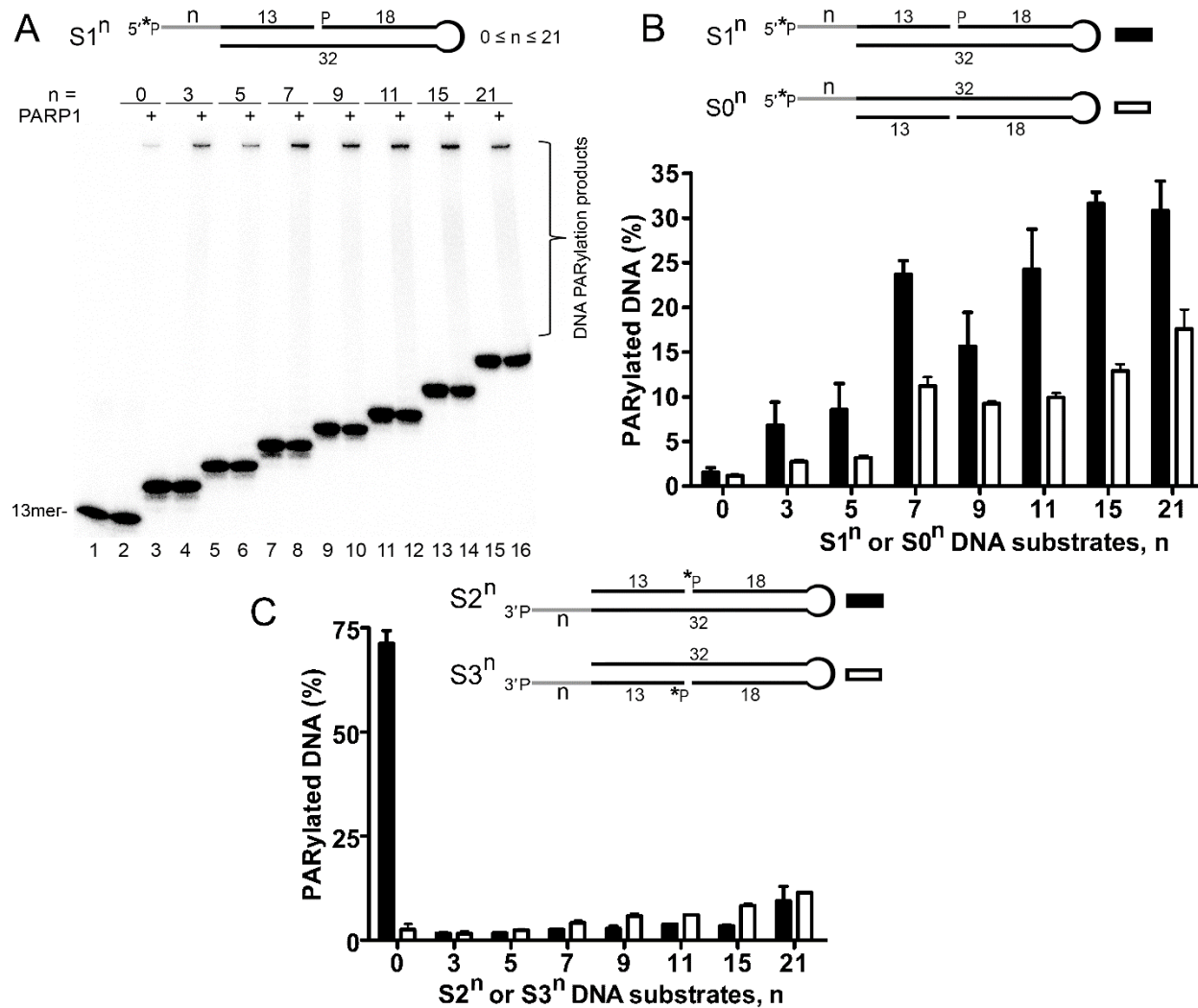


Figure 1. Effects of the type and size of protruding ends in Dbait-based DNA structures containing a 1-nt gap on the PARP1-catalysed formation of PAR–DNA adducts. Twenty-nanomolar PARP1 was incubated with 20 nM 5'-[³²P]labelled oligonucleotide and 1 mM NAD⁺ for 15 min at 37°C under standard reaction conditions. **(A)** Denaturing PAGE analysis of PARP1-generated products of PARylation of [³²P]labelled DNA substrates $S1^n$. **(B)** and **(C)** Comparison of DNA PARylation activities of PARP1 towards DNA substrates containing 5'-overhangs ($S0^n$ and $S1^n$) or 3'-overhangs ($S2^n$ and $S3^n$), respectively. The data on PAR-catalysed formation of PAR-DNA products are presented as mean ± SD from three independent experiments.

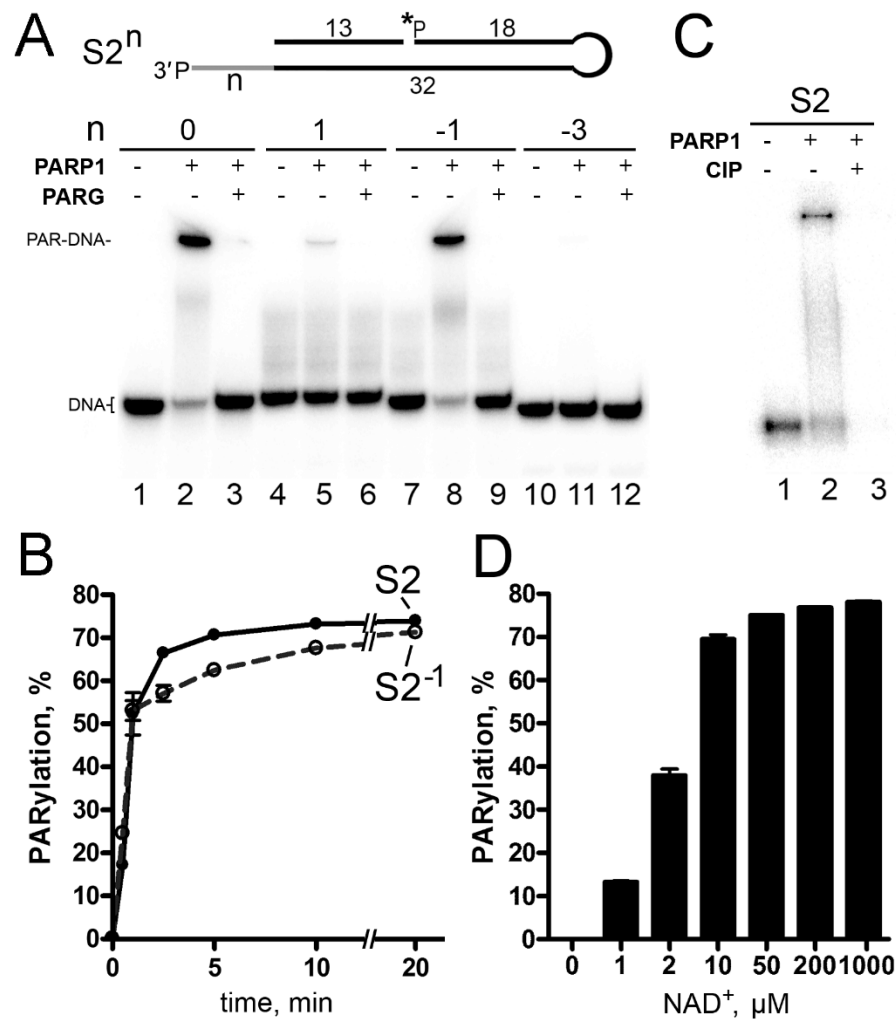


Figure 2. PARP1-catalysed PARylation of S3ⁿ DNA structures with a 3'-phosphate terminus at the DBS end. (A) [³²P]labelled DNA substrates S2ⁿ (50 nM) were incubated with 40 nM PARP1 for 10 min 37°C. (B) Time dependence of PARP1-driven PARylation of substrates S2 and S2⁻¹. DNA substrates (50 nM) were incubated with 20 nM PARP1 for the indicated period under standard reaction conditions. (C) CIP-induced dephosphorylation of 5'-[³²P]labelled PAR-S2ⁿ products. After incubation with PARP1, the S2 samples were heated for 10 min at 85°C, and the resulting [³²P]labelled DNA PARylation products were further incubated with 10 U of CIP for 30 min at 37°C. (D) The dependence of S2 DNA (40 nM) PARylation by PARP1 (20 nM) on NAD⁺ concentration. The data in panels C and D are presented as mean ± SD from three independent experiments.

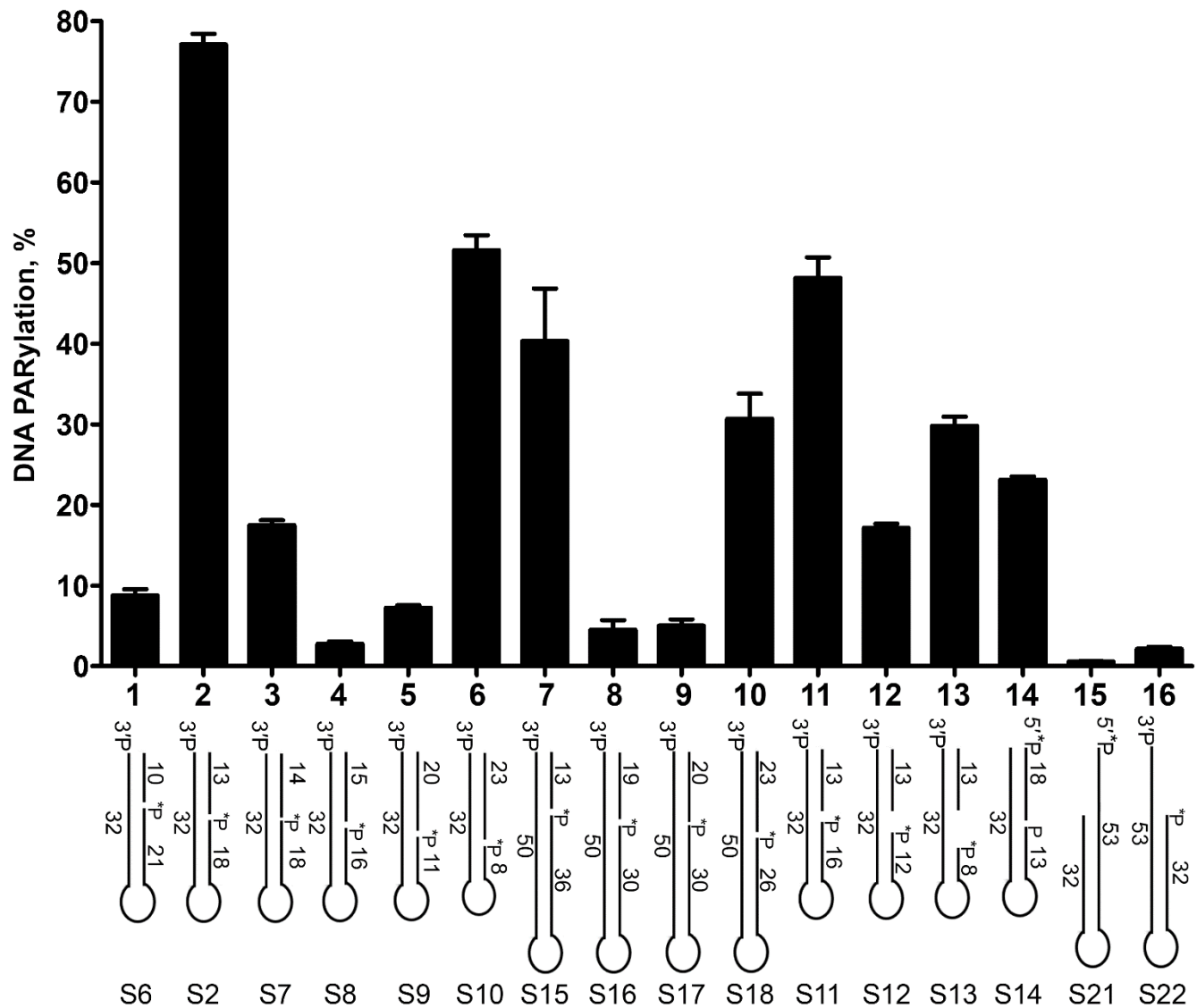


Figure 3. Gap–DSB distance dependence of PARP1-catalysed PARylation of the 3' phosphate at a DSB end of DNA duplexes. The data on PARP-catalysed formation of PAR-DNA products are presented as mean \pm SD from three independent experiments performed under standard reaction conditions.

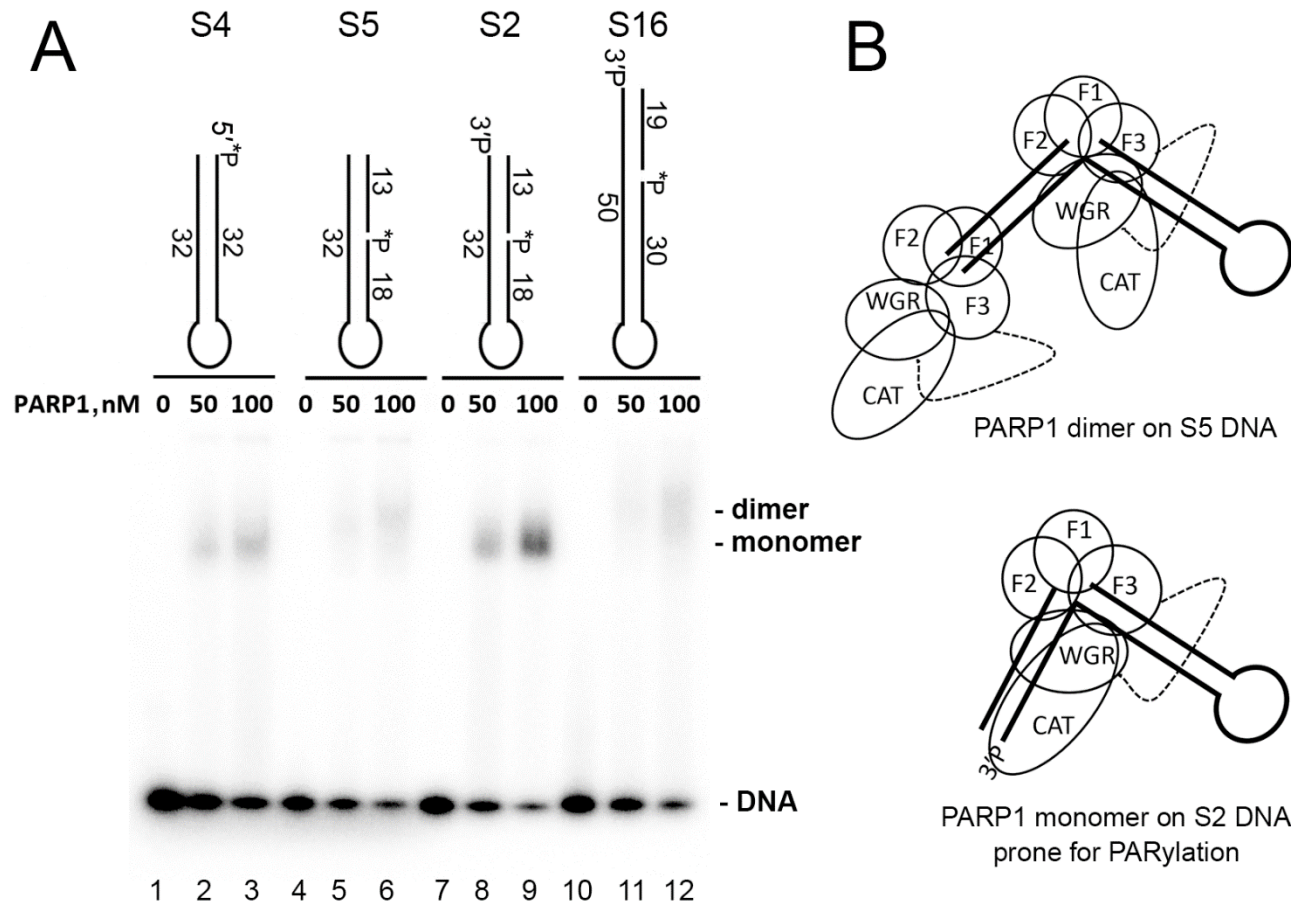


Figure 4. The monomeric mode of PARP1 binding to DNA molecules prone to PARylation. (A) The EMSA. Each of 20 nM DNA duplexes was incubated with 0, 50 or 100 nM PARP1 in a buffer consisting of 20 mM Tris-HCl pH 7.6, 50 mM KCl and 1 mM DTT for 10 min at room temperature. The DNA–protein complexes were analysed by electrophoresis in a 4–12% Tris-Glycine polyacrylamide gel (Novex) under non-denaturing conditions at 4°C after addition of 10 % glycerol. **(B)** The putative model of PARP1 complexes with DNA substrates prone (S2) or not prone (S5) to DNA break PARylation.

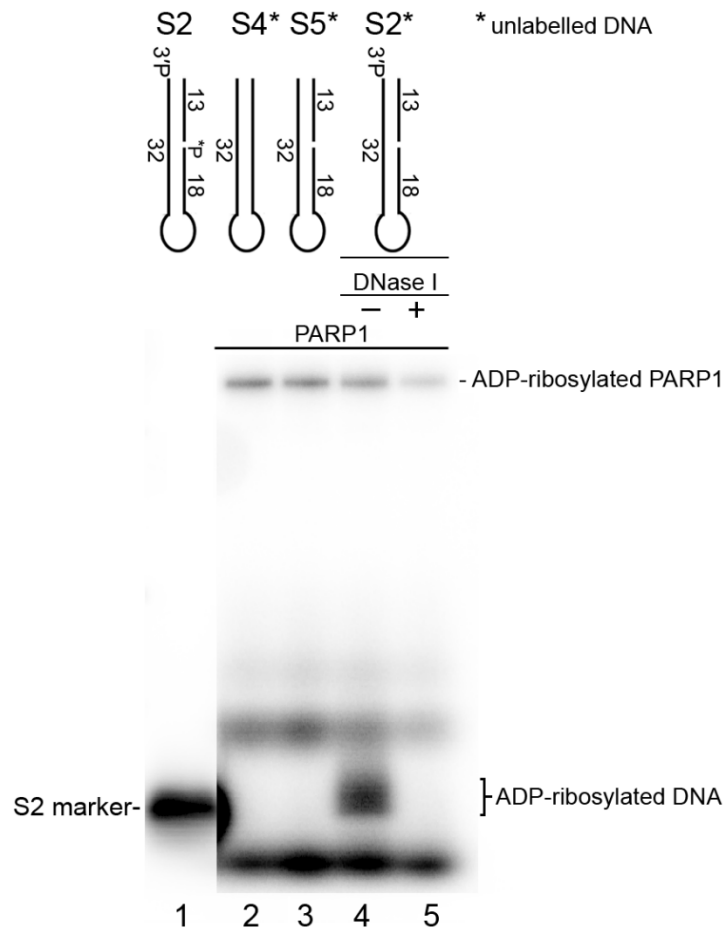


Figure 5. Comparison of the efficiency of PARP1-catalysed auto- and DNA ADP-ribosylation. The denaturing SDS-PAGE analysis of the products of PARP1 incubation with cold oligonucleotide duplexes in the presence of [adenylate- ^{32}P]NAD $^{+}$. For details see Materials and Methods.

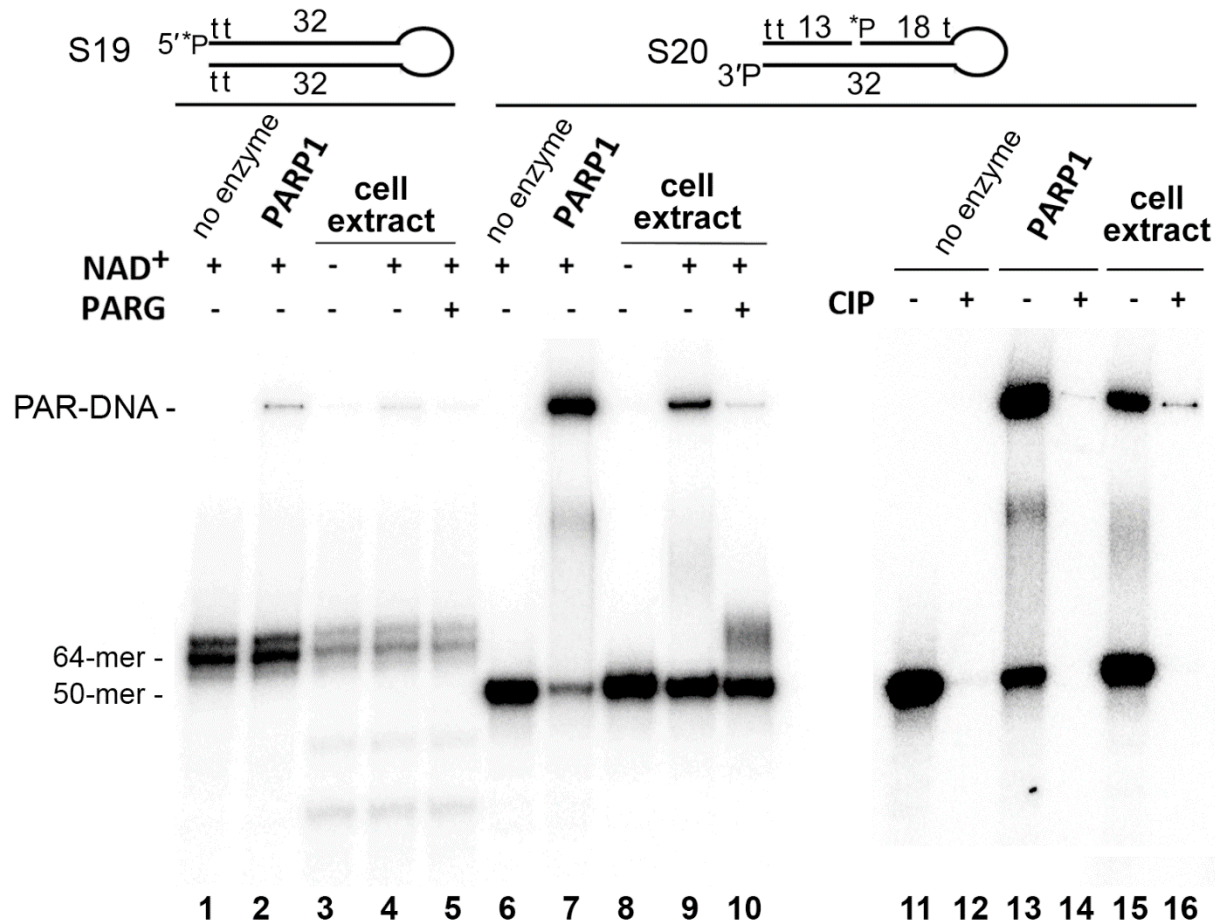


Figure 6. Formation of PAR-3' phosphate-DNA adducts in nuclear extracts from HeLa PARG^{KD} cells. Fifty-nanomolar [³²P]labelled S19 or S20 Dbait-based molecules were incubated with 2.5 µg/µl HeLa extracts or 40 nM PARP1 in the presence of 67 mM KCl, 10 mM HEPES-KOH pH 8.0 and 500 µM NAD⁺ for 20 min at 37°C. The reactions were stopped by heating the samples for 10 min at 80°C, and the resulting DNA PARylation products were next incubated with 20 pg/µl PARG (lanes 5 and 10) or after phenol-chloroform extraction with 10 U of CIP for 30 min at 37°C (lanes 12, 14 and 16). The reaction products were analysed by denaturing PAGE.

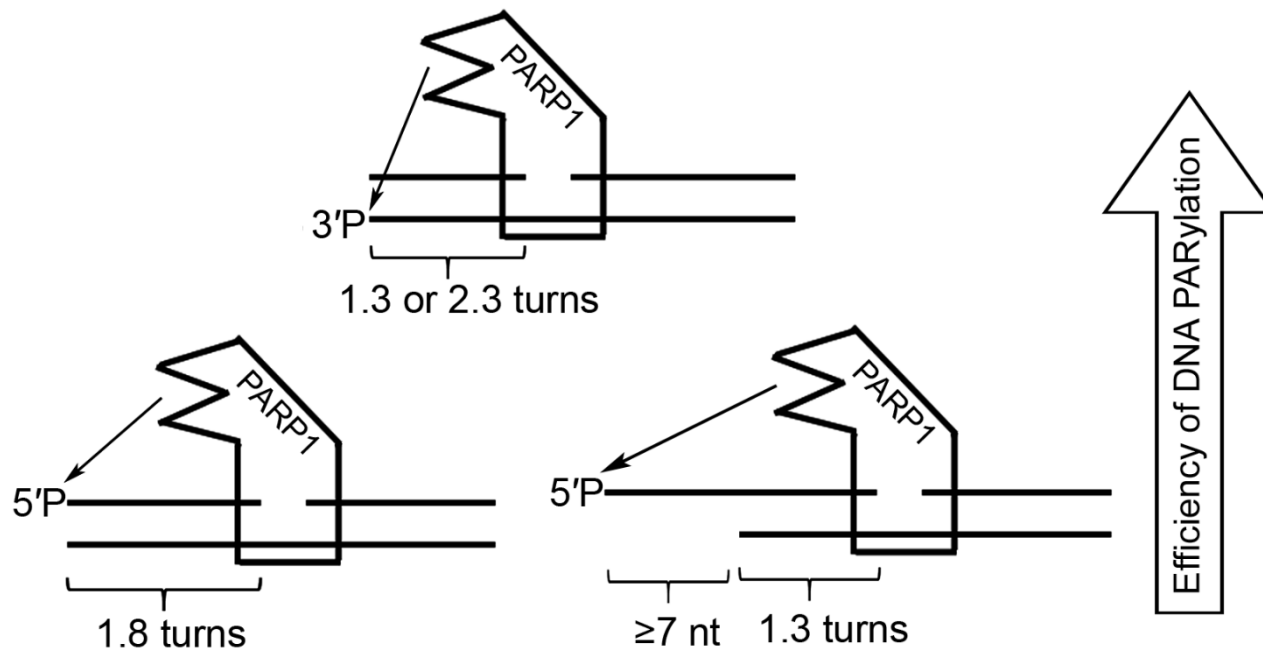


Figure 7. Schematic representation of the putative model of DNA modification by PARP1 activated on a 1-nt gap.

Insight into DNA substrate specificity of PARP1 catalyzed DNA poly(ADP-ribosylation)

Elie Matta^{1,2,†}, Assel Kiribayeva^{3,4,†}, Bekbolat Khassenov³, Bakhyt T. Matkarimov⁵, Alexander A. Ishchenko^{1,2}

¹Laboratoire «Intégrité du Génome et Cancers» CNRS, UMR9019, Université Paris-Saclay, F-94805 Villejuif, France

²Gustave Roussy, Université Paris-Saclay, F-94805 Villejuif, France

³National Center for Biotechnology, Nur-Sultan, 010000, Kazakhstan.

⁴L.N. Gumilyov Eurasian National University, Nur-Sultan, 010000, Kazakhstan.

⁵National Laboratory Astana, Nazarbayev University, Nur-Sultan, 010000, Kazakhstan.

Table S1. Sequences of the oligonucleotides and their duplexes used in this study.

Name	Oligonucleotides sequences and structures
S0 ⁿ	$ \begin{array}{l} \text{5' } \overset{32\text{P}}{\text{TCATAGGCTTAGTCGTCATT}}\overset{n}{\text{C}}\text{GCTGTGCCCTCAACCGAATTCACAAGCCTAGA} \\ \text{3' } \text{CGACACGGGAGTT GCTTAAAGTGTTCCGGATCT} \end{array} $
S1 ⁿ	$ \begin{array}{l} \text{5' } \overset{32\text{P}}{\text{TCATAGGCTTAGTCGTCATT}}\overset{n}{\text{C}}\text{GCTGTGCCCTCAA } \overset{\text{P}}{\text{CGAATTCACAAGCCTAGA}} \\ \text{3' } \text{CGACACGGGAGTTGGCTTAAAGTGTTCCGGATCT} \end{array} $
S2 ⁿ	$ \begin{array}{l} \text{5' } \text{GCTGTGCCCTCAA } \overset{32\text{P}}{\text{CGAATTCACAAGCCTAGA}} \\ \text{3' } \overset{\text{P}}{\text{CTTACTGCTGATTCGGATACT}}\text{CGACACGGGAGTTGGCTTAAAGTGTTCCGGATCT} \end{array} $
S2 (S2 ⁰)	$ \begin{array}{l} \text{5' } \text{GCTGTGCCCTCAA } \overset{32\text{P}}{\text{CGAATTCACAAGCCTAGA}} \\ \text{3' } \overset{\text{P}}{\text{CGACACGGGAGTTGGCTTAAAGTGTTCCGGATCT}} \end{array} $
S2 ⁻¹	$ \begin{array}{l} \text{5' } \text{GCTGTGCCCTCAA } \overset{32\text{P}}{\text{CGAATTCACAAGCCTAGA}} \\ \text{3' } \overset{\text{P}}{\text{GACACGGGAGTTGGCTTAAAGTGTTCCGGATCT}} \end{array} $
S2 ⁻³	$ \begin{array}{l} \text{5' } \text{GCTGTGCCCTCAA } \overset{32\text{P}}{\text{CGAATTCACAAGCCTAGA}} \\ \text{3' } \overset{\text{P}}{\text{CACGGGAGTTGGCTTAAAGTGTTCCGGATCT}} \end{array} $
S3 ⁿ	$ \begin{array}{l} \text{5' } \text{GCTGTGCCCTCAACCGAATTCACAAGCCTAGA} \\ \text{3' } \overset{\text{P}}{\text{CTTACTGCTGATTCGGATACT}}\text{CGACACGGGAGTT GCTTAAAGTGTTCCGGATCT} \end{array} $
S4	$ \begin{array}{l} \text{5' } \overset{32\text{P}}{\text{GCTGTGCCCTCAACCGAATTCACAAGCCTAGA}} \\ \text{3' } \text{CGACACGGGAGTTGGCTTAAAGTGTTCCGGATCT} \end{array} $
S5	$ \begin{array}{l} \text{5' } \text{GCTGTGCCCTCAA } \overset{32\text{P}}{\text{CGAATTCACAAGCCTAGA}} \\ \text{3' } \text{CGACACGGGAGTTGGCTTAAAGTGTTCCGGATCT} \end{array} $
S6	$ \begin{array}{l} \text{5' } \text{GCTGTGCCCT } \overset{32\text{P}}{\text{AAGCGAATTCACAAGCCTAGA}} \\ \text{3' } \text{CGACACGGGAGTTGGCTTAAAGTGTTCCGGATCT} \end{array} $
S7	$ \begin{array}{l} \text{5' } \text{GCTGTGCCCTCAAC } \overset{32\text{P}}{\text{CGAATTCACAAGCCTAGA}} \\ \text{3' } \overset{\text{P}}{\text{CGACACGGGAGTTG-GCTTAAAGTGTTCCGGATCT}} \end{array} $
S8	$ \begin{array}{l} \text{5' } \text{GCTGTGCCCTCAACC } \overset{32\text{P}}{\text{AATTCACAAGCCTAGA}} \\ \text{3' } \overset{\text{P}}{\text{CGACACGGGAGTTGGCTTAAAGTGTTCCGGATCT}} \end{array} $
S9	$ \begin{array}{l} \text{5' } \text{GCTGTGCCCTCAACCGAATT } \overset{32\text{P}}{\text{ACAAGCCTAGA}} \\ \text{3' } \overset{\text{P}}{\text{CGACACGGGAGTTGGCTTAAAGTGTTCCGGATCT}} \end{array} $
S10	$ \begin{array}{l} \text{5' } \text{GCTGTGCCCTCAACCGAATTCAC } \overset{32\text{P}}{\text{AGCCTAGA}} \\ \text{3' } \overset{\text{P}}{\text{CGACACGGGAGTTGGCTTAAAGTGTTCCGGATCT}} \end{array} $
S11	$ \begin{array}{l} \text{5' } \text{GCTGTGCCCTCAA } \overset{32\text{P}}{\text{AATTCACAAGCCTAGA}} \\ \text{3' } \overset{\text{P}}{\text{CGACACGGGAGTTGGCTTAAAGTGTTCCGGATCT}} \end{array} $
S12	$ \begin{array}{l} \text{5' } \text{GCTGTGCCCTCAA } \overset{32\text{P}}{\text{CACAAGCCTAGA}} \\ \text{3' } \overset{\text{P}}{\text{CGACACGGGAGTTGGCTTAAAGTGTTCCGGATCT}} \end{array} $
S13	$ \begin{array}{l} \text{5' } \text{GCTGTGCCCTCAA } \overset{32\text{P}}{\text{AGCCTAGA}} \\ \text{3' } \overset{\text{P}}{\text{CGACACGGGAGTTGGCTTAAAGTGTTCCGGATCT}} \end{array} $
S14	$ \begin{array}{l} \text{5' } \text{GCTGTGCCCTCAACCGAA } \overset{\text{P}}{\text{TCACAAGCCTAGA}} \\ \text{3' } \overset{32\text{P}}{\text{CGACACGGGAGTTGGCTTAAAGTGTTCCGGATCT}} \end{array} $
S15	$ \begin{array}{l} \text{5' } \text{GCTGTGCCCTCAA } \overset{32\text{P}}{\text{CGAATTCACAAGCCTAGAGTTACATTAGCAGATACG}} \\ \text{3' } \overset{\text{P}}{\text{CGACACGGGAGTTGGCTTAAAGTGTTCCGGATCTCAATGTAATCGTCTATGC}} \end{array} $
S16	$ \begin{array}{l} \text{5' } \text{GCTGTGCCCTCAACCGAAT } \overset{32\text{P}}{\text{CACAAGCCTAGAGTTACATTAGCAGATACG}} \\ \text{3' } \overset{\text{P}}{\text{CGACACGGGAGTTGGCTTAAAGTGTTCCGGATCTCAATGTAATCGTCTATGC}} \end{array} $
S17	$ \begin{array}{l} \text{5' } \text{GCTGTGCCCTCAACCGAATT } \overset{32\text{P}}{\text{CACAAGCCTAGAGTTACATTAGCAGATACG}} \\ \text{3' } \overset{\text{P}}{\text{CGACACGGGAGTTGGCTTAA-GTGTTCGGATCTCAATGTAATCGTCTATGC}} \end{array} $
S18	$ \begin{array}{l} \text{5' } \text{GCTGTGCCCTCAACCGAATTCAC } \overset{32\text{P}}{\text{AGCCTAGAGTTACATTAGCAGATACG}} \\ \text{3' } \overset{\text{P}}{\text{CGACACGGGAGTTGGCTTAAAGTGTTCCGGATCTCAATGTAATCGTCTATGC}} \end{array} $
S19	$ \begin{array}{l} \text{5' } \overset{32\text{P}}{\text{GCTGTGCCCTCAACCGAATTCACAAGCCTAGA}} \\ \text{3' } \overset{\text{tt}}{\text{CGACACGGGAGTTGGCTTAAAGTGTTCCGGATCT}} \end{array} $
S20	$ \begin{array}{l} \text{5' } \overset{\text{tt}}{\text{GCTGTGCCCTCAA}} \overset{32\text{P}}{\text{CGAATTCACAAGCCTAGA}} \\ \text{3' } \overset{\text{t}}{\text{CGACACGGGAGTTGGCTTAAAGTGTTCCGGATCT}} \end{array} $
S21	$ \begin{array}{l} \text{5' } \overset{32\text{P}}{\text{TCATAGGCTTAGTCGTCATT}}\text{CGCTGTGCCCTCAACCGAATTCACAAGCCTAGA} \\ \text{3' } \text{CGACACGGGAGTTGGCTTAAAGTGTTCCGGATCT} \end{array} $
S22	$ \begin{array}{l} \text{5' } \overset{32\text{P}}{\text{GCTGTGCCCTCAACCGAATTCACAAGCCTAGA}} \\ \text{3' } \overset{\text{P}}{\text{CTTACTGCTGATTCGGATACTCGACACGGGAGTTGGCTTAAAGTGTTCCGGATCT}} \end{array} $

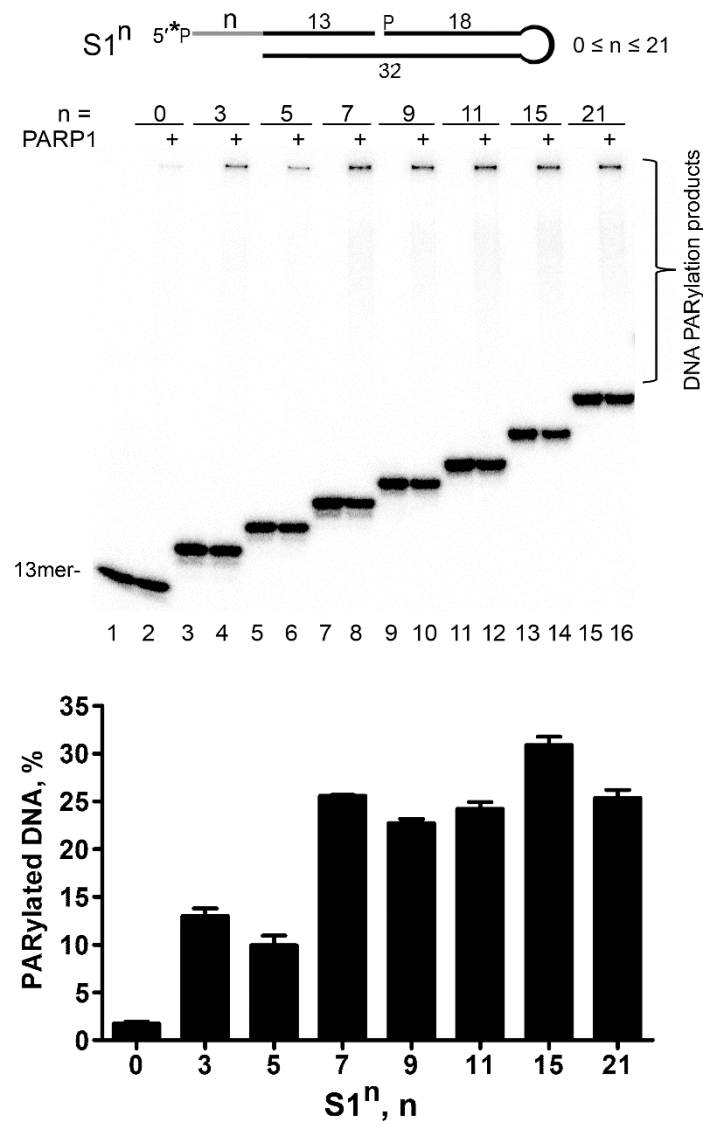


Figure S1. ADP-ribosylation of S1ⁿ DNA duplexes containing 5'-otherhangs by PARP1 at a non-saturating concentration of NAD⁺. [³²P]labelled S1ⁿ DNA duplexes (20 nM) were combined with 50 nM PARP1 in the presence of 50 μM NAD⁺ for 15 min at 37°C under standard reaction conditions. The data on PARP-catalysed formation of DNA ADP-ribosylation products are presented as mean ± SD from three independent experiments.

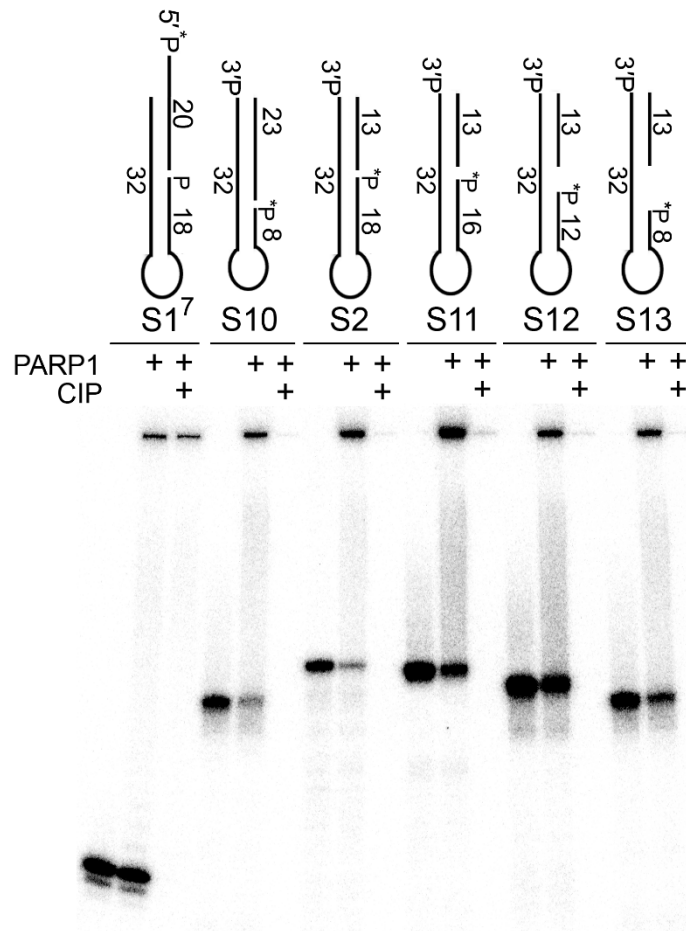


Figure S3. Validation of PARP1-dependent PARylation of 3'-phosphorylated DSB termini of DNA substrates S2 and S10-13 by CIP-induced dephosphorylation. After incubation with PARP1, the 5'-[³²P]labelled DNA samples were heated for 10 min at 85°C, and the resulting [³²P]labelled DNA PARylation products were further incubated with 10 U of CIP for 30 min at 37°C.

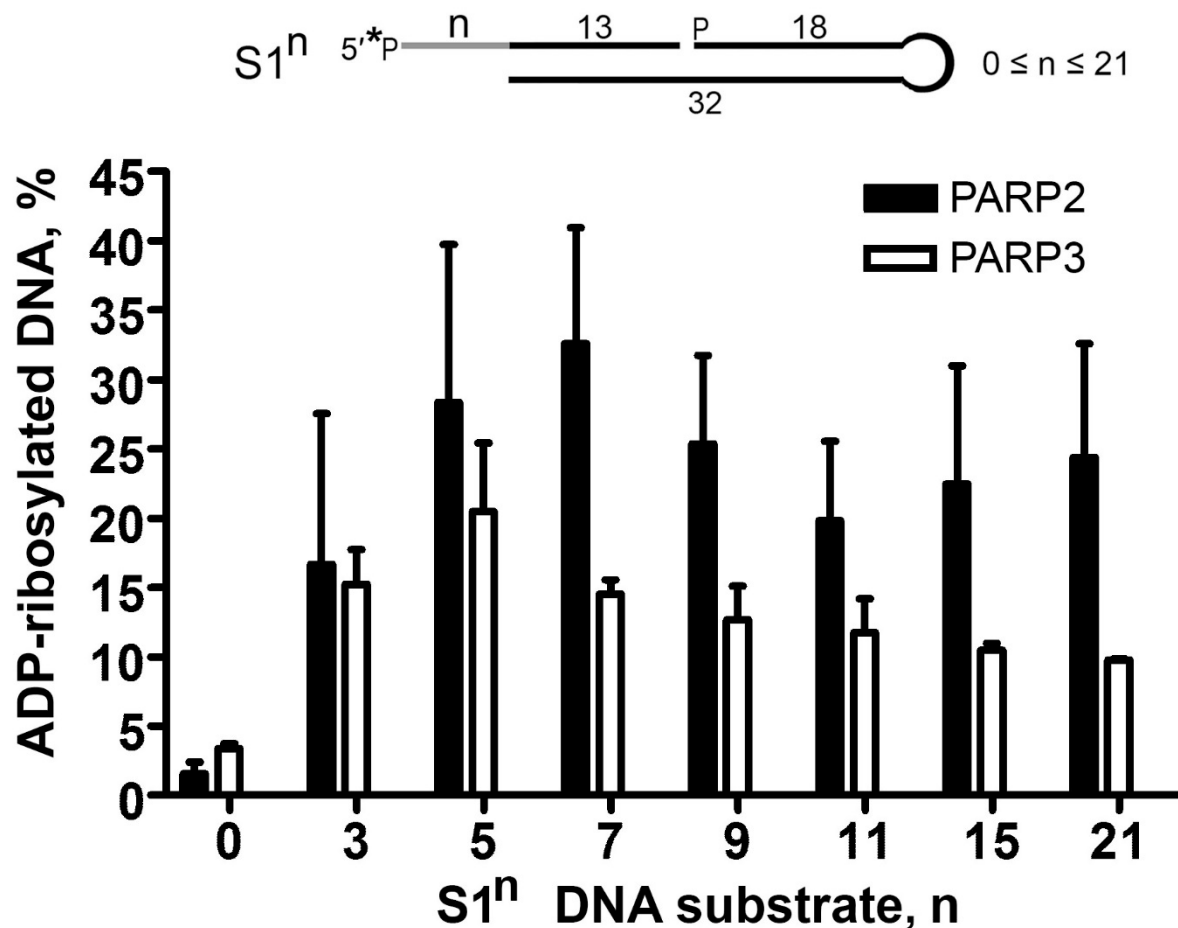


Figure S4. ADP-ribosylation of $S1^n$ DNA duplexes containing 5'-otherhangs by PARP2 and PARP3. [^{32}P]labelled $S1^n$ DNA duplexes (20 nM) were combined with 50 nM PARP3 or PARP2 in the presence of 1 mM NAD^+ in ADPR buffer (20 mM HEPES-KOH pH 7.6, 50 mM KCl, 5 mM $MgCl_2$, 1 mM DTT and 100 μ g/mL BSA). The mixture was incubated for 10 min (PARP3) or 30 min (PARP2) at 37°C. The data on PARP-catalysed formation of DNA ADP-ribosylation products are presented as mean \pm SD from three independent experiments.

Titre : Caractérisation des mécanismes d'ADP-ribosylation de l'ADN et son rôle dans la signalisation des dommages à l'ADN

Mots clés : ADP-ribosylation de l'ADN, PARPs, Spécificité du substrat PARP, NHEJ, Réparation des cassures double brins.

Résumé :

L'ADN cellulaire est constamment endommagé par des facteurs exogènes et endogènes entraînant des cassures d'ADN simple ou double brin (SSB ou DSB). Les mécanismes de réparation de l'ADN jouent un rôle essentiel dans la sensibilité et la résistance des cellules tumorales pendant et après les traitements anticancéreux. Les poly (ADP-ribose) polymérase ADP-dépendantes (PARP) PARP1, PARP2 et PARP3 agissent comme des capteurs de cassure d'ADN signalant des dommages à l'ADN. Il est généralement admis que l'ADP-ribosylation des protéines médiée par le PARP joue un rôle important dans la réparation des cassures des brins d'ADN et la létalité synthétique. Nos études récentes ont montré un nouveau type d'activité des protéines PARP de mammifères qui peuvent attacher directement des oligomères mono- ou poly (ADP-ribose) (MAR ou PAR, respectivement) non seulement aux protéines mais aussi aux extrémités de l'ADN,

mais leur mécanismes sont encore peu clairs. Nous pensons que la situation actuelle du terrain nécessite un recours urgent à des approches originales sur les mécanismes d'action des PARP. Ici, un modèle de modification de l'ADN par PARP1 a été proposé. De plus, nous avons élaboré une nouvelle technique protéomique et environ 90 lecteurs potentiels d'adduits MAR-ADN ont été identifiés. Enfin, le rôle de l'ADP-ribosylation de l'ADN dans la voie (NHEJ) de réparation des cassures double brin a été partiellement caractérisé. En perspective, les nouvelles connaissances sur le rôle et les mécanismes des actions des PARPs dans la signalisation des dommages à l'ADN identifieront de nouvelles cibles thérapeutiques ou diagnostiques dans le cancer et d'autres maladies liées à l'âge.

Title : Characterization of DNA ADP-ribosylation mechanism and its role in DNA damage signaling

Keywords : PARP substrate specificity, DNA ADP-ribosylation, PARPs, NHEJ, DSB repair

Abstract :

Cellular DNA is constantly damaged by exogenous and endogenous factors resulting in single- or double-strand DNA breaks (SSB or DSB). DNA repair mechanisms play critical roles in sensitivity and resistance of tumor cells during and after anticancer treatments. DNA-dependent poly(ADP-ribose) polymerases (PARPs) PARP1, PARP2 and PARP3 act as DNA break sensors signaling DNA damage. It is generally accepted that PARP-mediated ADP-ribosylation of proteins play important role in DNA strand breaks repair and synthetic lethality. Our recent studies showed novel type of activity of mammalian PARPs proteins that can directly attach mono- or poly(ADP-ribose) (MAR or PAR, respectively) moieties not only to proteins but also to the DNA termini at the sites of DNA strand breaks but their mechanisms are still elusive.

We believe that current situation in the field requires an urgent employment of original approaches and new-look at mechanisms of PARPs action. Here a mechanistic model of DNA modification by PARP1 was proposed. Moreover, we elaborated new proteomic technique and about 90 potential MAR-DNA adduct readers were identified. Finally, the role of DNA ADP-ribosylation in Non-Homologous End-Joining (NHEJ) pathway of DNA double strand break repair was partially characterized. In perspective, the new knowledge about the role and mechanisms of PARPs actions in DNA damage signaling will identify novel therapeutic or diagnostic targets in cancer and other age-related diseases.

